KU Leuven
Biomedical Sciences Group
Faculty of Kinesiology and Rehabilitation Sciences
Department of Kinesiology

RELATING KNEE JOINT MOTION AND LOADING TO CARTILAGE STRUCTURE AND MRI-BASED MATRIX COMPOSITION

Sam VAN ROSSOM

Jury:

Promoter:	Prof. dr. I. Jonkers
Co-promoter:	Prof. dr. B. Vanwanseele
	Prof. dr. D. Van Assche
Chair:	Prof. dr. W. Helsen
Jury members:	Prof. dr. F. Luyten
	Prof. dr. G. Vanderschueren
	Prof. dr. W. Dankaerts
	Prof. dr. Ir. C. Stewart

Dissertation presented in partial fulfilment of the requirements for the degree of Doctor in Biomedical Sciences

October 2017

"Promise me you'll always remember:
You're braver than you believe,
stronger than you seem,
and smarter than you think."

—Winnie The Pooh, A.A. Milne

Table of contents

Chapter 1

Summary

Abstract

Articular cartilage is a highly complex tissue at the ends of the diarthrodial joints and is essential for optimal joint function. Thanks to its specialized composition, articular cartilage provides a smooth interface between the moving bones and distributes joint loading onto the subchondral bone. The mechanosensitive chondrocytes maintain extracellular matrix homeostasis under physiological loading. However when physiological loading is disturbed, homeostasis can be disturbed as well, resulting in an imbalance between anabolic and catabolic processes. Consequently, matrix loss and cartilage degeneration can be accelerated, ultimately leading to osteoarthritis (OA). Therefore, loading during daily life has the potential to affect cartilage homeostasis. Chronic loading patterns were found to dominate the biologic response of the knee cartilage, by increasing its thickness, as well as its proteoglycan and collagen content, which can be interpreted as a protective adaptation to the imposed chronic loading. However, to better understand the role of mechanical signals on either cartilage homeostasis or degenerative cartilage diseases, such as OA, the influence of mechanical factors and joint loading in particular on cartilage homeostasis in-vivo is required.

Therefore, the aim of this PhD was to evaluate the relation between movement, knee loading and structural and matrix properties of the cartilage in the knee joint of healthy asymptomatic controls as well as in the presence of OA predisposing factors, more specific altered knee joint alignment and geometry as well as in the presence of isolated cartilage defects. This resulted in three different research goals: 1) Evaluate cartilage loading during different functional activities in a cohort of healthy adults (study I). 2) Evaluate the relation between local cartilage loading and cartilage structural and matrix properties determined on MRI (study II and III). 3) Evaluate cartilage loading in the presence of OA-predisposing factors (study IV and V).

Firstly, we evaluated cartilage loading during different functional activities in a cohort of healthy adults (study I). Muscle forces, knee contact forces and shear forces were calculated using a musculoskeletal model during frequently performed activities of daily life and rehabilitation exercises (more specific: walking, stair ascending and descending, stand-up, sit down, squat, forward and sideward lunge and single leg hop). This allowed quantification of knee loading during these exercises, based on which more biomechanically informed rehabilitation programs can be conceptualized. Except for sit down, stand up and even stair ascent, descent and squatting, all exercises imposed higher tibiofemoral contact forces compared to gait. As all exercises required more knee extensor muscle force production, these exercises could be included early in rehabilitation without exposing the knee to high contact forces. Furthermore, the distribution of loading over the medial and lateral condyle was sensitive to the performed exercise, with increased compartmental contact forces being accompanied by increased compartmental shear forces. Therefore, high compartmental contact forces as well as shear forces on the injured zone can be avoided by careful selecting exercises. Based on the results, a graded exercise program can be conceptualized, which accounts for progressive knee loading to protect the knee structures from increased loading, while simultaneously providing sufficient stimuli to regain muscle control and strength to restore normal knee function.

Secondly, we evaluated the relation between local cartilage loading during gait and cartilage structural and matrix properties determined on MRI (study II and III) in a control population. In study II, we investigated the relation between knee contact forces and pressures during walking and cartilage thickness, $T1\rho$ and T2 relaxation times (as an estimation of proteoglycan and collagen content, respectively) in the central zone of the femur condyles. We found significant correlations between cartilage thickness in the central zone and total knee loading across subjects. In addition, a relation between compartmental cartilage loading and

cartilage thickness in the central zone of the condyles was observed, with thicker cartilage being related to increased loading. Furthermore, proteoglycan and collagen content, estimated by $T1\rho$ and T2 relaxation time mapping, respectively were related to cartilage loading during walking. Increased proteoglycan and collagen content (indicated by a decreased $T1\rho$ and T2 relaxation time, respectively) were related to higher compressive forces, whereas a decreased proteoglycan concentration was related to higher shear forces. This suggests that in subjects who experience higher loads in the tibiofemoral joint during walking thicker cartilage and an increased proteoglycan and collagen content were present as a protective adaptation to the cyclic loads during walking.

In study III, we investigated the local variation in cartilage thickness, $T1\rho$ and T2 relaxation times over the femoral condyle in healthy adults and related this to local differences in loading during walking. The distribution of cartilage thickness and relaxation times over the articular cartilage surface was investigated. The weight-bearing and non-weight-bearing zones during walking were determined by the contact force impulse and MRI-based cartilage properties were compared between the weight-bearing and non-weight-bearing zones. A strong correlation between the location of loading and the local thickness of the medial condyle cartilage was observed, indicating that the location of thickest cartilage coincides with the location of highest cumulative loading on the articular cartilage surface during waking. Lower $T1\rho$ relaxation time, indicative of increased proteoglycan content, and a higher T2 relaxation time, indicative of a lower collagen content, was observed in the weight-bearing zone of the medial condyle compared to the non-weight-bearing zone. This indicates that the weight-bearing zone of the medial condyle has a less dense collagen network with a higher proteoglycan concentration. This implies an increased capacity of the extracellular matrix to sustain compressive loads as this would increase the capacity to deform under compression. Therefore, we could confirm that the weight-bearing zone of the medial condyle as a whole is adapted to the cumulative loading perceived during the stance phase of the gait cycle as this zone has superior biochemical properties in terms of proteoglycan content and is therefore better suited to withstand the high loading experienced during walking.

Based on study II and III, we could conclude that long-term cartilage adaptations were present in the knee complex and especially in the medial condyle cartilage and that these adaptations were related to chronic loading imposed during walking.

Finally, we evaluated cartilage loading in the presence of factors that were previously related to an increased incidence of OA. Indeed, subject- and joint-related risk factors were identified that contribute to knee OA initiation and progression by affecting physiological joint loading and therefore initiating degenerative pathways. More specific, the effect of variation in tibiofemoral joint geometry and alignment as well as the presence of an isolated articular cartilage defect on knee joint loading were investigated in study IV and V.

In study IV, the isolated effect of altered joint geometry and alignment was studied using musculoskeletal modelling. The geometry and alignment of the tibiofemoral joint was systematically changed between $\pm 15^\circ$ in steps of 2° from its neutral position in the coronal and transverse plane. Subsequently, changes in load distribution at peak loading and peak ligament strains were analyzed. The medial-lateral tibiofemoral load distribution and ligament strains during walking were sensitive to both joint geometry and alignment in the coronal plane, but were less sensitive to changes in joint geometry and alignment in the transverse plane. Varus alignment as well as a more elevated medial tibia plateau increased loading on the medial condyle, while valgus and a more elevated lateral tibia plateau resulted in increased loading on the lateral condyle. Simultaneously, a load reduction on the opposite condyle was observed. Alterations in joint geom-

etry and alignment in the transverse plane had a less pronounced effect on the load distribution compared to alterations in the coronal plane. In addition, altered coronal tibial slope strongly affected peak strains of the collateral ligaments, which could introduce joint laxity on the long term. Therefore, coronal plane knee laxity likely adds to a vicious circle, initiated by knee instability and consequent knee malalignment, which could induce altered joint loading and increased articular cartilage breakdown. Furthermore, our findings confirm the role of varus malalignment in medial compartment overloading with a consequent increased risk of medial knee OA initiation and progression.

In study V, we investigated the effect of an isolated articular cartilage defect on knee joint loading. Experimental motion data was collected in fifteen patients with isolated cartilage defects and compared to data collected in nineteen asymptomatic healthy controls. Patients were further subdivided based on defect location, i.e. patients presenting medial- vs lateral-involvement. Contact forces and pressures were calculated and analyzed to see whether changes in the loading pattern were present. Additionally, the contact pressure distribution was investigated to evaluate the effect on contact locations. Although the patients with lateral compartment involvement group walked significantly slower compared to the healthy controls, no adaptations in the movement pattern resulting in decreased loading of the injured condyle as well as no changes in contact location were observed. The current results suggest that isolated cartilage defects do not induce changes in the knee joint loading pattern. Consequently, a similar force magnitude should be distributed over the remaining cartilage surrounding the articular cartilage defect. Consequently, the stress on the cartilage surrounding the defect will be increased and this may initiate local degenerative changes in the cartilage matrix. This in combination with tissue reactivity might play a key role in the progression from articular cartilage defect to a more severe OA phenotype.

Based on study IV and V, we can conclude that both alignment and the presence of an isolated articular cartilage defect have a distinct role in altered articular cartilage loading, therefore affecting cartilage homeostasis and initiating degenerative pathways that may ultimately lead to OA initiation.

Overall, this PhD contributed to a better understanding of the role of knee loading to cartilage tissue adaptation and factors affecting the cartilage load distribution.

Samenvatting

Gewrichtskraakbeen is een complex weefsel in de gewrichten en is essentieel voor een optimale werking van het gewricht. Dankzij zijn gespecialiseerde samenstelling vormt gewrichtskraakbeen een glad oppervlak tussen twee bewegende botstukken en verdeelt het de belasting over het subchondrale bot. Onder fysiologische gewrichtsbelasting behouden de mechanosensitieve chondrocyten homeostase in de extracellulaire matrix. Wanneer de fysiologische belasting echter verstoord wordt, kan de homeostase in het kraakbeen verstoord worden wat kan resulteren in een disbalans tussen anabolische en catabolische processen. Dit leidt tot verlies van extracellulaire matrixcomponenten en kan leiden tot degeneratie van het kraakbeen en uiteindelijk osteoarthrose (OA). Aangezien de chondrocyten mechanosensitief zijn, kan belasting in het dagelijks leven de homeostase in het kraakbeen beïnvloeden. Hierbij kan een chronisch belastingpatroon de biologische en structurele respons van het kraakbeen domineren, waarbij een verdikking en een verhoging van het proteoglycaan- en collageengehalte beschouwd kunnen worden als een beschermende aanpassing aan de chronische belasting van kraakbeen. Kennis van de rol van mechanische factoren en gewrichtsbelasting op de homeostase in het kraakbeen in vivo is noodzakelijk om de rol van mechanische signalen in degeneratieve aandoeningen zoals OA en homeostase van kraakbeen beter te begrijpen.

Daarom was het doel van dit doctoraat om de relatie tussen beweging, kniebelasting en structurele en matrixeigenschappen van het kraakbeen na te gaan in het kniegewricht van gezonde, asymptomatische controlesubjecten alsook in de aanwezigheid van factoren die de kans op OA verhogen, namelijk een afwijkende gewrichtsuitlijning en -geometrie en de aanwezigheid van geïsoleerde kraakbeenletsels. Dit resulteerde in drie afzonderlijke onderzoeksdoelstellingen: 1) Nagaan van de belasting van het kraakbeen tijdens verschillende functionele activiteiten in een groep gezonde controlepersonen (Studie I). 2) Nagaan van de relatie tussen lokale belasting en de structurele en matrixeigenschappen van het kraakbeen, bepaald door middel van MRI (Studie II en III). 3) Nagaan van de belasting op het kraakbeen in het bijzijn van risicofactoren voor OA (Studie IV en V).

Eerst werd de belasting van het kraakbeen tijdens verschillende functionele bewegingen nagegaan in een groep gezonde controlepersonen (Studie I). Spierkrachten, knie-contactkrachten en schuifkrachten werden berekend aan de hand van een musculoskeletaal model tijdens frequent uitgevoerde activiteiten die zowel in het dagelijks leven als in de revalidatie gebruikt worden (wandelen, op- en afgaan van een trap, rechtstaan uit een stoel en weer gaan zitten, squat, voorwaartse en een zijwaartse uitvalspas en springen op één been). Hierdoor konden we de kniebelasting tijdens deze bewegingen kwantificeren en op basis hiervan kan een revalidatie-protocol opgesteld worden dat meer rekening houdt met de belasting op de knie. Uitgezonderd van het gaan zitten, rechtstaan uit een stoel en zelfs traplopen en squat zorgden alle oefeningen voor significant hogere contactkrachten in het tibiofemorale gewricht in vergelijking tot wandelen. Aangezien voor alle oefeningen meer spierkracht in de knie-extensoren nodig was, kunnen deze oefeningen dus vroeg in een revalidatieprogramma geïncludeerd worden zonder de knie bloot te stellen aan hoge contactkrachten. Verder was de verdeling van de belasting over de mediale en laterale femurcondyl afhankelijk van de uitgevoerde oefening, waarbij hoge contactkrachten op een bepaald compartiment samengingen met hoge schuifkrachten op hetzelfde compartiment. Dit toont aan dat hoge contactkrachten en schuifkrachten op de gekwetste zone vermeden kunnen worden door een zorgvuldige selectie van oefeningen. Op basis van onze resultaten is het mogelijk om een revalidatieprotocol op te stellen, waarin de belasting stelselmatig opgebouwd kan worden om de verschillende structuren in de knie te beschermen tegen overmatige belasting, terwijl voldoende prikkels gegeven worden om spiercontrole en spierkracht en uiteindelijk het normaal functioneren terug te winnen.

In een tweede deel werd de relatie tussen de belasting tijdens wandelen en de dikte en matrixeigenschappen van het kraakbeen nagegaan in een gezonde controlepopulatie (studie II en III). In studie II werd de relatie tussen de contactkracht en contactdruk in de knie tijdens wandelen en de kraakbeendikte, $T1\rho$- en T2-relaxatietijd (respectievelijk als maat voor de proteoglycaan- en collageenconcentratie) van de centrale zone van de femurcondyl bestudeerd. Significante correlaties tussen de kraakbeendikte in de centrale regio en de totale kniecontactkracht werden gevonden, alsook significante correlaties tussen de belasting in een specifiek compartiment en de kraakbeendikte in het bijhorende compartiment. Hierbij was dikker kraakbeen steeds gerelateerd aan hogere belasting. Daarnaast vonden we ook dat het proteoglycaan- en collageengehalte (op basis van $T1\rho$- en T2-relaxatietijden) gerelateerd was aan de belasting tijdens wandelen. Hierbij was een hoger proteoglycaan- en collageengehalte (gezien als lagere $T1\rho$- en T2-relaxatietijd) gerelateerd aan hogere compressieve belasting, terwijl een lager proteoglycaangehalte gerelateerd was aan hogere schuifkrachten. Dit suggereert dat bij personen die hogere tibiofemorale belasting ondervinden tijdens wandelen, het kraakbeen dikker is en een hoger proteoglycaan- en collageengehalte heeft. Dit kan geïnterpreteerd worden als een beschermende aanpassing aan de cyclische belasting tijdens wandelen.

In studie III werd de lokale variatie in kraakbeendikte en de $T1\rho$- en T2-relaxatietijd over de femurcondyllen bij gezonde personen nagegaan en werd dit verder gerelateerd aan lokale verschillen in belasting tijdens wandelen. De verdeling van kraakbeendikte en relaxatiewaardes over het gewrichtskraakbeen werd bepaald op basis van MRI en op basis van de impuls van de contactkracht werd de gewichtsdragende zone tijdens wandelen afgebakend. Vervolgens werden de op basis van MRI bepaalde eigenschappen van het kraakbeen vergeleken tussen de gewichtsdragende en niet-gewichtsdragende zone. We vonden een sterke correlatie tussen de locatie van belasting en de lokale kraakbeendikte van de mediale femurcondyl. Dit toont aan dat de locatie van het dikste kraakbeen samenvalt met de locatie met de hoogste cumulatieve belasting op het kraakbeenoppervlak tijdens wandelen. Een lagere $T1\rho$-relaxatietijd, een maat voor een hoger proteoglycaangehalte, en een hogere T2-relaxatietijd, een maat voor een lager collageengehalte, werd gevonden in de gewichtsdragende zone van de mediale femurcondyl in vergelijking tot de niet-gewichtsdragende zone. Dit toont aan dat de gewichtsdragende zone van de mediale femurcondyl een minder gebonden collageen netwerk heeft met een hoger gehalte proteoglycaan. Dit wijst op een verhoogde capaciteit van de extracellulaire matrix om te vervormen onder compressie, wat de capaciteit om belasting op te vangen verhoogt. Op basis van deze studie kunnen we besluiten dat de gehele gewichtsdragende zone van de mediale femurcondyl aangepast is aan de cumulatieve belasting tijdens de standfase van de gangcyclus aangezien deze zone superieure biochemische eigenschappen heeft, meer bepaald een hoger proteoglycaangehalte en daardoor een verhoogde capaciteit om de hoge belasting tijdens wandelen op te vangen.

Op basis van studie II en III kunnen we besluiten dat lange-termijn aanpassingen aanwezig waren in het kraakbeen van de knie, dit was vooral terug te vinden in het kraakbeen van de mediale femurcondyl en kan gerelateerd worden aan de chronische en cyclische belasting tijdens wandelen.

Als laatste zijn we de belasting van het kraakbeen nagegaan in aanwezigheid van factoren die eerder al gerelateerd waren aan een hogere incidentie van OA. Zowel persoons- als gewrichtgebonden risicofactoren die bijdragen tot initiatie en progressie van OA door de fysiologische gewrichtsbelasting aan te tasten en degeneratieve pathways te initiëren zijn gevonden. Meer bepaald zijn we het effect van variatie in kniegeometrie en -uitlijning en van geïsoleerde kraakbeenletsels op de kniebelasting nagegaan in studie IV en V.

In studie IV werd het effect van een gewijzigde gewrichtsgeometrie en -uitlijning bestudeerd aan de hand van musculoskeletaal modelleren. De geometrie en uitlijning van het tibiofemorale gewricht was systematisch aangepast in zowel het coronale als het transversale vlak tussen $\pm 15°$ van zijn neutrale positie in stappen van $2°$. Vervolgens werd de verandering in belasting op het mediale en laterale compartiment op moment van piekbelasting geanalyseerd en werd de piekspanning in de ligamenten geanalyseerd. De verdeling van de belasting over de mediale en laterale condyl en ligamentspanning was gevoelig aan wijzigingen in zowel gewrichtsgeometrie als aan de uitlijning in het coronale vlak, maar was minder sensitief aan wijzigingen in het transversale vlak. Zowel varus uitlijning als een verhoogd mediaal tibiaplateau resulteerde in toegenomen belasting op de mediale femurcondyl, terwijl valgus uitlijning en verhoogd lateraal tibiaplateau resulteerden in toegenomen belasting op de laterale femurcondyl. Tegelijkertijd werd een verlaging in belasting op de tegenoverliggende femurcondyl waargenomen. Veranderingen in gewrichtsgeometrie en -uitlijning in het transversale vlak hadden een minder uitgesproken effect op de verdeling van de belasting in vergelijking met het effect van wijzigingen in het coronale vlak. Daarnaast had een wijziging in coronale tibia slope een sterk effect op de piekspanning in de collaterale ligamenten, wat op lange termijn gewrichtslaxiteit kan induceren. Hierdoor kan laxiteit in het coronale vlak bijdragen tot een vicieuze cirkel, waarbij knie-instabiliteit geïnitieerd wordt en vervolgens kniemalalignement, wat veranderingen in gewrichtsbelasting kan induceren, met een verhoogde afbraak van het kraakbeen als gevolg. Onze resultaten bevestigen een rol van varus malalignement in overbelasting van het mediale compartiment en vervolgens een toegenomen risico op initiatie en progressie van OA in de mediale knie.

In studie V zijn we het effect van een geïsoleerd kraakbeenletsel op de kniebelasting nagegaan. Bewegingsdata werden verzameld bij vijftien patiënten met een geïsoleerd letsel en vergeleken met de opgemeten data bij negentien asymptomatische controlepersonen. Patiënten werden verder opgedeeld op basis van letsellocatie, meer bepaald patiënten met een letsel op de mediale of laterale femurcondyl. Contactkrachten en -drukken werden vergeleken met controlepersonen om het effect op het belastingspatroon na te gaan. Verder werd de drukverdeling geanalyseerd om het effect op contactlocatie na te gaan. Hoewel de patiënten met een lateraal letsel trager wandelden in vergelijking met de controles, werden geen aanpassingen in het gangpatroon gevonden die leidden tot een verminderde belasting op de aangedane femurcondyl of een aanpassing in contactlocatie. Deze resultaten suggereren dat geïsoleerde kraakbeenletsels geen verandering in belastingspatroon induceren. Bijgevolg moet een even grote kracht verdeeld worden over het overgebleven kraakbeen rond het letsel. Dit zal de stress in het omliggende kraakbeen verhogen, wat lokaal degeneratieve veranderingen in de kraakbeenmatrix kan initiëren. Dit in combinatie met inflammatie heeft mogelijk een belangrijke bijdrage in de progressie van kraakbeendefect naar OA.

Op basis van studie IV en V kunnen we concluderen dat zowel uitlijning als een kraakbeendefect een afzonderlijke rol hebben in veranderde kraakbeenbelasting en daarom de homeostase in het kraakbeen kunnen aantasten, wat degeneratieve pathways en uiteindelijk OA kan initiëren.

In het algemeen droeg dit doctoraat bij aan een betere kennis van de rol van kniebelasting in kraakbeenaanpassingen en factoren die de kraakbeenbelasting kunnen aanpassen.

Chapter 2

General introduction

During daily life, the human body is constantly in motion and experiences external forces (e.g. ground reaction forces and gravity). These forces impose enormous stress on the joints and their surrounding tissues. Currently, the loading magnitude and its impact on the load-transmitting tissues, in particular the articular cartilage, is not well documented. This despite the fact that nowadays, joint loading can be quantified in-vivo by combining integrated motion capture and dynamic simulations of motion.

Quantification of knee joint loading

Using computer-based motion capture, three-dimensional segment positions can be measured and consequent joint angles can be calculated. By combining the measured joint pose with ground reaction forces, external joint moments can be calculated[1]. These external joint moments provide information on the resultant action at the joint in terms of joint moments that need to be balanced by the muscles forces. However, these external moments do not fully capture the internal load on the joints. Indeed, internal joint loading is determined by both the external (e.g. ground reaction forces and joint moments) and the internal (e.g. muscle forces) forces[2–4]. Nevertheless, external joint moments are often used to estimate non-invasively internal joint loading in a clinical setting.

Therefore, external joint moments have been used to investigate the relation between joint loading and the pathomechanics of degenerative joint diseases in which excessive loading is thought to be an important contributor to disease initiation and progression (e.g. Osteoarthritis (OA), see section osteoarthritis). The most often reported parameter in the context of knee OA is the external knee adduction moment (KAM). The knee adduction moment during walking is often used to evaluate the medial-lateral load distribution in the knee joint[5]. More specific, an increased knee adduction moment is seen as indicative of higher medial than lateral condyle loading. As OA mainly affects the medial condyle, the knee adduction moment was identified as a potential biomarker to evaluate the role of overloading in OA initiation and progression. This way, increased KAM was related to OA disease progression, state and severity of cartilage loss[6–9].

Knee contact forces (i.e. the forces acting in the knee due to the joint reaction, muscle and ligament forces) are a more direct and comprehensive representation of knee joint loading, but can only be directly measured using instrumented implants[10–13]. Although, instrumented implants provide a valuable measurement of knee contact forces, they are limited to patients treated with a total knee prosthesis. In general, this patient population is older, with movement dynamics likely being different from a healthy young population. As a consequence, the measured contact forces may have limited generalizability.

Alternatively, musculoskeletal modelling in combination with dynamic simulations of motion can be used to calculate joint contact forces non-invasively[3,14–16]. A musculoskeletal model is a mathematical description of the human body, more specific the body segments, muscles and joints. In combination with simulations of motion, it can be used to estimate the muscle forces, reaction forces and the consequent joint contact forces[3,14]. The segments are defined by their mass, center of mass and inertia, whereas joints describe the relative motion of two adjacent segments along their degrees of freedom. Muscles are represented as a line of action running from origin to insertion, with a Hill-type muscle model being used to describe their force-generating capacities[17,18]. A simulation workflow typically holds the following steps: First, the generic model is scaled to the anthropometry of the subject to account for the subject-specific dimensions and mass. Next, joint angles are calculated based on a least-square fitting of the measured marker trajectories and

model markers[19,20]. By combining joint angles and the external forces, joint moments are calculated by solving the dynamic equations of motion of the system[1,14]. Subsequently, muscle forces that are required to counteract the external joint moments are calculated using either optimization methods that solve the muscle redundancy problem (e.g. static optimization[21], computed muscle control[22] and physiologic inverse analysis[23]). Lastly, contact forces in the knee are calculated using the vector sum of the estimated muscle forces and reaction forces in the joint (a more detailed overview of the musculoskeletal modelling workflow is provided in the methods section – *dynamic simulations of motion*)[15].

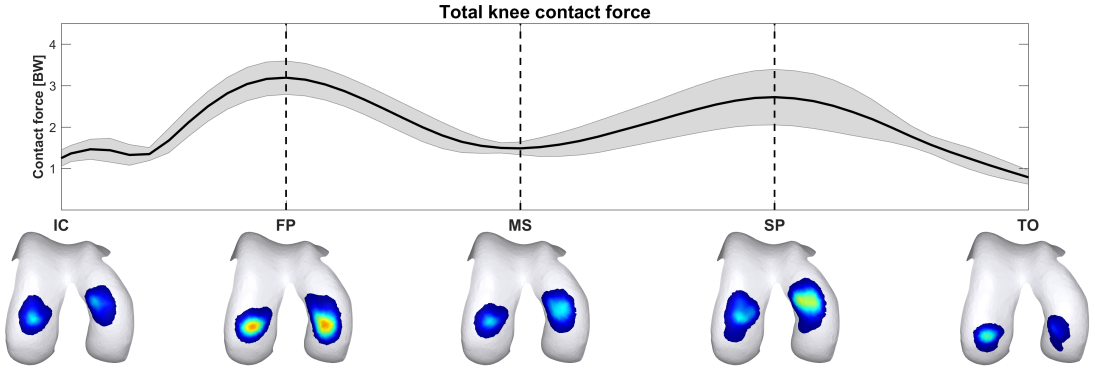

Figure 2.1: **Total knee contact force.**
Average resultant total knee contact force ($\pm 1SD$) during the stance phase of the gait cycle. Average pressure distributions at initial contact (IC), first peak (FP), midstance (MS), second peak (SP) and toe-off (TO) are shown.

Typically, the total knee contact force during the stance phase of the gait cycle shows a double bump profile, with a first peak in contact force at initial double support (FP) and a second peak in contact force at terminal double support (SP) (Figure 2.1). During walking, peak contact forces around 2.5 times bodyweight (BW) were previously measured using instrumented implants[10,12,13,24–26]. Contact forces were found to vary between movements with higher contact forces being observed during stair ascent and descent (2.8BW and 3.5BW, respectively) as well as during fast walking (3BW) and jogging (4BW)[24]. Using musculoskeletal modelling, knee contact forces during walking were slightly higher in healthy adults (2.7-4.4BW vs 2.5BW measured)[3,27,28]. Both measured and calculated contact forces increased during more demanding tasks, although the observed increase differed (e.g. stair ascent 5.4BW vs 2.8BW measured)[29]. However, these measured contact forces (obtained with instrumented implants) cannot be generalized to healthy control subjects given the different movement dynamics in both groups.

Articular cartilage adapts to loading

The load-transmitting tissues in the human body such as bone, tendons, skeletal muscles and articular cartilage are exquisitely tuned to their mechanical and biochemical environment[30]. This indicates that their structure and composition will change in response to an altered mechanical environment, in order to be capable of withstanding the altered loading conditions. For example, bone quantity and quality can be increased after a period of increased exercise as described by Wolff's law[31,32]. A period of increased loading was found to induce muscle adaptations showing increased neural activation, muscle size and muscle strength[33]. In addition, tendon stiffness and cross-sectional area increased in response to a period of

increased loading[34]. Likewise, articular cartilage is known to adapt to overloading and underloading.

Articular cartilage is a highly complex tissue located at the end of the diarthrodial joints and is essential for optimal joint function. Articular cartilage provides a smooth friction-free interface between the moving bones of a joint and distributes loading onto the subchondral bone. Thanks to its specialized composition, it is able to maintain this function and to cope with the high forces experienced during human locomotion.

Articular cartilage is composed of a dense extracellular matrix (95%) in which chondrocytes (5%) are dispersed. The extracellular matrix is mainly composed of collagen type II fibers (45% of the dry weight), proteoglycans (35% of the dry weight) and water (65%)[35,36]. This complex network of collagen fibers and proteoglycans provide the cartilage with resistance against both compressive and shear forces[36,37]: The negatively charged glycosaminoglycan molecules (GAG) attract and bind water molecules into the extracellular matrix. Due to the low porosity of the cartilage extracellular matrix, the interaction between water and proteoglycans provides resistance against compressive forces[36,38]. On the other hand, the complex structure and typical orientation of the collagen type II fibers gives the cartilage its main resistance against superficial shear forces, whereas towards the deep cartilage layer the oblique orientation of collagen type II fibers provides solid anchoring in the calcified layer of the subchondral bone[39].

A complex interaction of growth factors, hormones, joint mechanics and mechanical loading regulates the extracellular matrix homeostasis[40,41]. Under physiological loading, chondrocyte homeostasis is maintained resulting in a balance of anabolic and catabolic processes in the extracellular matrix[37,38]. Since chondrocytes are mechanosensitive, mechanical signals are known to affect cartilage homeostasis[40]. Therefore, alterations to the physiological loading conditions affect cartilage homeostasis, eventually causing a local deterioration of the extracellular matrix[42]. As articular cartilage is an avascular and aneural tissue, the self-regenerative capacities of the cartilage are limited. Furthermore, articular cartilage lacks undifferentiated cells, limiting its repair capacities even more[43]. Consequently, once damaged, cartilage will not regenerate and catabolic events will induce inflammation and further damage the extracellular matrix, ultimately initiating osteoarthritis.

During locomotion, the articular cartilage distributes the loading transmitted through the long bones, over the joint surface and the subchondral bone. This loading, in combination with the internal fluid flow inside the articular cartilage, provokes an internal stress-strain distribution dependent on the local cartilage curvature and its local mechanical properties[40]. The resulting cartilage stresses and strains determine the mechanical environment of the chondrocytes and consequently affect the mechanosensitive pathways of the chondrocytes and therefore cartilage homeostasis. Consequently, loading during daily life will affect cartilage homeostasis, with chronic loading patterns dominating the biologic response of the cartilage, more specific by increasing its thickness, as well as its proteoglycan and collagen content and improved collagen fiber orientation[37,40,44].

Indeed, increased knee cartilage volume was found in healthy children that were more involved in physical activity compared to their inactive peers, as well as in healthy adults who presented with increased muscle cross-sectional area[45,46]. On the other hand, femoral cartilage volumes were found not to be significantly different in elite-triathletes compared to healthy controls[47]. This suggests that childhood physical activity may be an important determinant for the development of larger cartilage volumes. On the other hand, unloading due to paralysis was found to result in thinning of the cartilage[48,49]. In healthy adults,

the ratio of the medial and lateral condyle cartilage thickness in the knee was found to be related to the knee adduction moment during walking[44,50,51]. This suggests that healthy cartilage responds positively to load by thickening and that thicker cartilage may be a long-term protective response to the higher loading during walking. Moreover, the anterior-posterior thickness distribution on the medial condyle was found to be affected by the kinematic pattern during walking[52–54]. In this, the location of thickest cartilage was found to coincide with the contacting region at heel strike. The authors hypothesized that the thicker cartilage in this area developed in response to the high loading occurring at heel strike

In addition to the thickness adaptations, studies described changes in cartilage constitution evaluated using magnetic resonance imaging (MRI). T2 relaxation times (see Section *Imaging of cartilage*) were decreased after a standardized training period, which is indicative of an increased collagen content [55,56]. On the other hand, a period of unloading, resulted in increased $T1\rho$ and T2 relaxation times, indicative for a decreased proteoglycan and collagen content[57]. This shows that articular cartilage is responsive to changes in mechanical environment.

Likewise, numerous in-vitro studies using cartilage explants demonstrated that the biosynthetic activity of the chondrocytes can either be promoted or inhibited by mechanical loading[58–67]. Furthermore, mechanical stimulation was required to maintain a stable articular cartilage phenotype[68,69]. Compressive loading to in-vitro explants influenced cartilage extracellular matrix quality, quantity and spatial distribution[67,70,71]. Besides the biochemical constitution, in-vitro loading was found to influence the biomechanical properties of the cartilage explants (i.e. stiffness and friction coefficient). Furthermore, both compression and sliding motion are required to optimize biomechanical properties of the cartilage[72].

These insights obtained from in-vitro studies in cartilage explants are also reflected in the region-dependent distribution of the knee cartilage extracellular matrix composition[38,40,41,73–75]. The weight-bearing zones of the knee cartilage were found to have higher GAG content compared to the non-weight-bearing zones of the cartilage[76,77]. Furthermore, chondrocytes from the weight-bearing zone of the tibia cartilage were found to respond differently to compressive loading compared to chondrocytes obtained from less-weight-bearing zones[78]. The role of mechanical loading in the development of this topographical variation is further supported by the fact that the topographical variation was present in adult ovine cartilage, whereas this was not present in neonatal ovine cartilage. This suggests that the topographical variation in proteoglycan concentration is caused by the topographical variation in weight-bearing stress as the neonatal cartilage was not exposed to any weight-bearing stress[73]. Furthermore, the mechanical properties of cartilage were found to show a topographical variation, that can be related to local differences in mechanical loading[79–81].

The topographical variation in cartilage structure and composition in the weight-bearing zone indicates that the cartilage has superior biomechanical and biochemical properties, increasing its capacity to withstand high cyclic loading[75,79,82,83]. Therefore, factors that affect the physiological load distribution may cause increased loading on a specific zone or cause a shift in contact location. If these changes are sufficient to cause a shift in contact location to regions of cartilage that have less weight-bearing capacity, normal cartilage homeostasis may be disrupted by activation of catabolic pathways, ultimately leading to OA initiation[40,84].

Imaging of articular cartilage

Magnetic resonance imaging has been proposed as a powerful tool to non-invasively evaluate cartilage morphology, by assessing cartilage thickness, volume, surface and subchondral bone integrity[85–88]. Additionally, the whole-organ MRI scoring (WORMS) has been used to evaluate the cartilage integrity and detect risk factors for the development of structural knee OA[85]. For this purpose, fast spin-echo (FSE) or fat-suppressed gradient-echo (GRE) acquisitions are most commonly used[89]. Furthermore, these sequences were used to evaluate success of cartilage repair surgery using the magnetic resonance observation of cartilage repair tissue (MOCART) scoring system[90,91]. More recently, advanced quantitative MRI-methods were proposed that reflect the articular cartilage extracellular matrix composition[92–96]. Since the interaction between water molecules and the surrounding matrix molecules determines the MRI relaxation times, these sequences allow estimating and visualizing the cartilage extracellular matrix composition in-vivo in a whole joint complex. Therefore, these techniques have a high potential to detect early degenerative changes in the cartilage extracellular matrix components. These techniques are therefore a non-invasive alternative for Delayed Gadolinium enhanced MRI of cartilage (dGEMERIC) that was previously used to investigate GAG concentration[97]. After intravenous administration of a contrast agent and a period of standardized loading, the contrast agent enters the cartilage. Due to the anionic nature of the contrast agent, it will accumulate in places with a relatively low concentration of GAG. Therefore, depletion of GAG can be visualized by an accumulation of the contrast agent (reflected in decreased T1 values). Using relaxometry, $T1\rho$ relaxation time mapping can be used to investigate proteoglycan content without the need for intravenous contrast agent administration and T2 mapping can be used to study collagen content and organization[96]. Increased $T1\rho$ relaxation time is associated with a decreased proteoglycan concentration, which is one of the early degenerative changes in the cartilage extracellular matrix[95,98]. Whereas increased T2 relaxation time is related to increased collagen anisotropy and collagen loss[93,99].

Apart from monitoring biochemical composition of the cartilage extracellular matrix, the spatial distribution of the relaxation times also reflects variation in biomechanical properties. Indeed, specific biomechanical properties of the cartilage such as Young's modulus, aggregate modulus and dynamic modulus could be correlated to the $T1\rho$ and T2 relaxation time, with a decreased relaxation time being related to an increased tissue stiffness[100–102].

Joint loading adapations contribute to the onset and progression of osteoarthritis

Osteoarthritis is one of the most prevalent chronic joint disorders that affects millions of people worldwide. It is a chronic, multifactorial disease, that mostly affects the knee joint[103–105]. Incidence rate for knee OA is 6.5/1000 person/year, whereas this is only 2.1/1000 person/year for hip osteoarthritis[106]. Osteoarthritis will ultimately end in irreversible structural and functional failure of the joint[107]. Age, gender and obesity were previously identified as person-related risk factors[108–110]. Furthermore, a major genetic contribution to OA disease initiation was previously observed in epidemiologic studies[111,112]. In addition, previous knee injuries, knee laxity, variations in joint geometry and static as well as dynamic joint alignment were identified as joint-related risk factors causing aberrant mechanical loading (both alterations in loading magnitude and location) compared to the physiological loading to which the cartilage is adapted[84,108–110,113–122].

Therefore, OA should be considered as a disease of the whole person, initiated by multiple factors. Following-up retrospective patient studies confirming a potential key role of aberrant mechanical loading in disease initiation in people that are already genetically disposed for OA, the present thesis, however studied OA from a merely mechanical perspective[104,123]. Consequently, the influencing effect of other known risk factors, such as genetic predisposition as well as the psychosocial environment of the person (i.e. pain mechanisms, maladaptive beliefs, socioeconomics and environment) are neglected, although these factors may be as important determinants of the overall level of disability of the subjects[124].

Knee joint geometry and malalignment contribute to knee OA initiation

In a healthy knee joint, knee stability is provided by the shape of the condyles and menisci and passively supported by the ligaments[125]. In addition, the muscles crossing the knee joint provide stability during dynamic situations. Injury to or weakness of one of these structures can potentially hamper knee stability and therefore affect the loading distribution. Factors that influence knee load distribution, have been suggested to increase stress on the different knee structures, more specifically the ligaments, menisci, articular cartilage and subchondral bone, and may consequently contribute to OA initiation. In a neutrally aligned knee joint, the medial condyle is loaded more during walking compared to the lateral condyle[5]. Aberrant joint alignment, more specific varus and valgus malalignment ($> 3°$ deviation from neutral alignment) was previously related to an increased risk for bone marrow lesions and cartilage loss in the medial and lateral condyle, respectively[126–130]. Consequently, varus malalignment was previously identified as risk factor for medial knee OA[113,131]. In a healthy population, physiological varus alignment ($1,3°$) is normally observed however, more extreme deviations might be detrimental for the articular cartilage by increasing compartmental loading[132].

Many studies indicate knee alignment to be a major source of altered medial-lateral loading balance in the knee, therefore introducing compartmental overloading. The knee adduction moment, as an indirect measure of medial condyle loading was found to be directly proportional to the degree of varus alignment, suggesting that varus alignment increases loading on the medial condyle[7,133–135]. In agreement with this, in vitro studies showed that varus alignment resulted in increased medial condyle pressure under static loading[136,137]. Additionally, lateral condyle pressure was decreased after correcting for valgus malalignment[138]. Furthermore, musculoskeletal modelling studies observed that coronal plane alignment of the prosthetic components during a total knee replacement had a substantial influence on the medial-lateral force distribution, whereas the total knee contact force was not significantly affected[28,139–142]. In contrast, no effect of component rotation in the transverse plane was found on the force distribution[142,143]. Based on the results obtained using instrumented implants, it could be concluded that knee alignment in the coronal plane significantly affects knee load distribution, and could therefore contribute to OA initiation and progression[6,113,144–147]. Besides static joint malalignment, dynamic malalignment during walking, more specific the so called 'varus thrust' in which the tibia abducts during the stance phase of gait, was previously identified as a possible risk factor for OA initiation[120–122,148]. This dynamic knee instability may cause an increase in medial condyle loading during each step. This cyclic occurring event may increase dynamic medial compartment loading and may therefore be more detrimental for the articular cartilage than the static malalignment[149].

Besides joint alignment, joint geometry has the potential to affect knee medial-lateral load distribution. Variations in joint geometry, more specific an increased elevation of the lateral tibia plateau, width of the femoral condyles and tibia plateau and an increased coronal tibial slope were previously related to an increased risk for OA initiation[115,150,151]. Furthermore, increased internal tibial torsion was hypothesized to increase compressive and shear loading on the medial condyle and was previously identified as a risk factor for knee OA[152–155]. These variations in joint geometry might affect the knee joint congruity and could therefore influence the medial-lateral knee load distribution[129]. This could cause excessive loading on the cartilage and therefore disturb cartilage homeostasis. In support of this, OA patients with internal tibial torsion, were found to walk with an increased knee adduction moment, suggesting increased loading on the medial condyle[156]. Furthermore, aberrant joint geometry was suggested to induce joint malalignment at a later stage, ultimately accelerating OA progression[151].

Knee injury contribute to OA initiation

Apart from constitutional factors such as joint geometry and alignment, a history of knee injury was identified as potential risk factor for knee OA development[108]. Indeed, the majority of isolated cartilage defects (patients older >40 years) were found to progress to OA within 2 years and even 30% of this population required a total knee replacement within 10 years[157–159]. Articular cartilage defects are highly prevalent in the active population, with approximately 36% of all athletes presenting full-thickness chondral defects[160]. Healthy cartilage is essential for an optimal distribution of loading over the subchondral bone, to reduce friction between the articulating bones and therefore an articular cartilage defect might hamper joint function[161–163]. However, a better understanding of cartilage loading or movement behavior in presence of an articular cartilage defect is needed, since aberrant mechanical loading of the cartilage is known to contribute to the development of OA.

Knee injuries e.g. ACL-ruptures are known to alter knee joint kinematics and consequently alter the contact areas in the knee[164–167]. However, alterations in knee joint kinematics following an isolated articular cartilage defect are less well documented. Previously, three months after surgical treatment for articular cartilage defects using autologous chondrocyte implantation, patients were found to walk with increased knee flexion at heel strike and decreased knee flexion and knee adduction moments, suggesting that patients with an articular cartilage defect do adapt their movement pattern to unload the involved knee joint [168,169]. As muscle forces are a substantial contributor of the knee joint loading, the role of altered muscle coordination as a potential contributing factor in altering knee joint loading needs to be evaluated[170,171]. To date, muscle co-contraction was found to be unaffected in patients with an articular cartilage defect in the knee[172]. Additionally, no changes in joint reaction forces were observed in patients with an articular cartilage defect compared to healthy controls, when accounting for gait speed and quadriceps strength[173]. However, joint reaction forces do not comprise the effect of muscle forces and do not allow a separate evaluation of medial and lateral condyle loading. To date, no studies provide an analysis of knee loading in terms of knee contact forces that do account for the muscle, ligament and joint reaction forces. Furthermore, musculoskeletal modelling has the unique potential to evaluate the medial and lateral condyle loading separately, which could provide additional insight in the compensatory mechanisms to unload the involved compartment.

Objectives

The aim of this PhD is to evaluate the relation between movement, knee loading and structural and matrix properties of the cartilage in a healthy tibiofemoral joint as well in the presence of OA predisposing factors such as altered knee alignment and isolated cartilage defects.

In order to address this overarching goal, three main objectives were defined: 1) Evaluate cartilage loading during different functional activities in a cohort of healthy adults. 2) Evaluate the relation between local cartilage loading and cartilage structural and matrix properties determined on MRI. 3) Evaluate cartilage loading in presence of factors that were previously related to an increased incidence of OA, as these factors might affect the relation between joint movement and cartilage loading (figure 2.2). In this work, the effect of altered joint geometry and alignment as well as the effect of an isolated articular cartilage defect on the medial-lateral load distribution is explored.

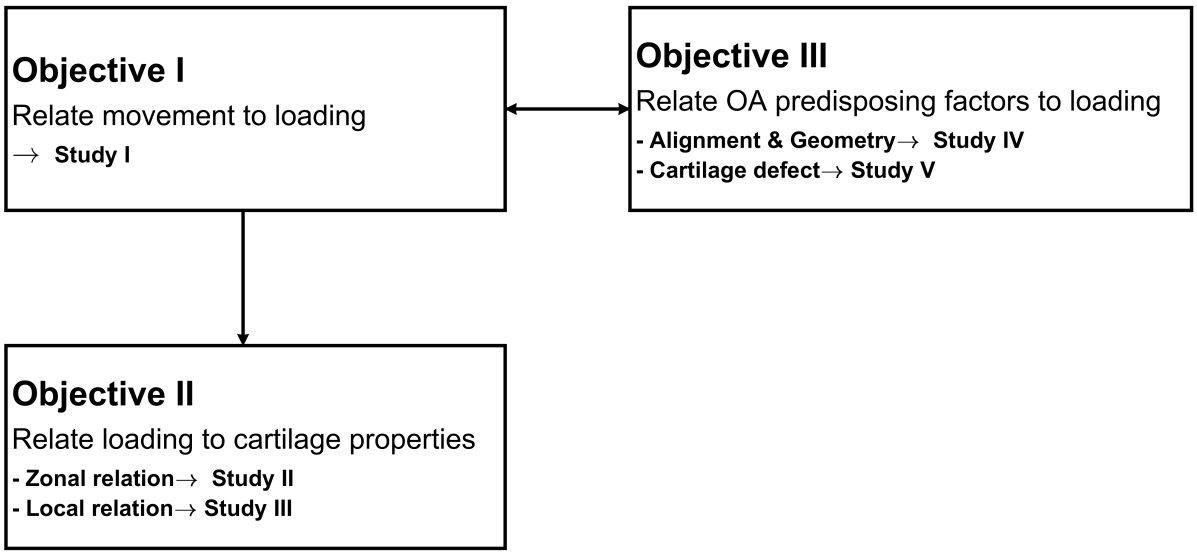

Figure 2.2: General overview of the three main objectives of this PhD.

Objective I: Evaluation of knee loading during different clinically relevant tasks and its relevance for rehabilitation after knee injury

Study I aimed to analyze cartilage loading and muscle forces during different activities of daily life (i.e. walking, stair negotiation and chair rise) and during different therapeutic exercises (i.e. lunging, squatting and single leg hopping). This would allow physiotherapist to design more staged rehabilitation programs in which contact forces are minimized to prevent (re-) injury, while maximizing muscle forces to regain muscle strength[174]. Therefore, experimental motion data was collected in fifteen healthy adults and processed using musculoskeletal modelling. The magnitude, type (i.e. shear and compression) and location of the contact force in the medial and lateral as well as patellofemoral compartment were evaluated.

Hypothesis study I: Quantification of knee joint loading can support a grading in exercise intensity and allow for the design of more evidence-based rehabilitation programs.

Objective II: Investigate cartilage structure and matrix-composition using MRI and its relation to knee joint loading in healthy adults

Cartilage loading is partially regulated by mechanical factors and therefore chronic loading patterns could dominate the biologic and structural response of the cartilage[37,40,44]. Indeed, indirect estimates of cartilage loading, more specific increased KAM during walking was previously related to thicker cartilage[44,50,51]. Currently, novel musculoskeletal modelling techniques could be used to provide a more specific measure of knee joint loading that account for the muscle and ligament forces and could be used to further investigate the relation between loading and cartilage thickness. It was hypothesized that the topographical variation in cartilage thickness and matrix composition was caused by differences in localized mechanical loading. Indeed, topographical variation in cartilage thickness and $T1\rho$ and T2 relaxation times were previously only investigated separately and never related to the location and magnitude (i.e. cartilage pressure and contact forces) of internal loading during walking.

Hypothesis study II: Higher cartilage loading in the central zone of the medial and lateral condyle is expected to relate to increased thickness and to lower $T1\rho$ and T2 relaxation times, indicative of a higher proteoglycan and collagen concentration and orientation.

Study III investigated the variation in cartilage thickness and $T1\rho$ and T2 relaxation times over the femoral articular cartilage surface and compared these measures between weight-bearing and non-weight-bearing zones of the femoral condyle.

Hypothesis study III: Local variation in loading during walking relates to increased thickness and lower $T1\rho$ and T2 relaxation times, indicative of higher proteoglycan and collagen concentration and therefore increased weight-bearing capacities compared to the non-weight-bearing zone.

Objective III: Analyze the effect of osteoarthritis predisposing factors on the knee load distribution

Several person- and joint-related risk factors were previously identified to contribute to OA initiation and progression. Alterations in mechanical loading may disrupt cartilage homeostasis and initiate degenerative pathways[104]. Therefore, the effect of different joint-related OA risk factors, specifically knee joint geometry and alignment and previous knee injuries on joint loading was investigated in study IV and V, as each of these factors was previously hypothesized to induce aberrant joint loading[84,108–110,113–119].

Study IV investigated the effect of altered knee joint geometry and alignment in both the transverse and frontal plane on the knee load distribution as well as on the ligament elongation. To do so, a sensitivity study was conducted in which the alignment and geometry of the knee joint was systematically changed between $\pm 15^{\circ}$ from its normal position in the frontal and transverse plane and its effect on cartilage load distribution and ligament elongation was quantified. This analysis might contribute to a better understanding of the isolated effect of each of these mechanical factors on cartilage loading and therefore a better understanding of their potential role in the onset and progression of degenerative cartilage diseases.

Hypothesis study IV: Altered tibiofemoral geometry and alignment will result in increased compartmental loading, indicative for increased OA initiation risk.

Study V investigated the effect of isolated articular cartilage defects on the knee contact force and pressure distribution. Isolated cartilage defects are known to cause pain and dysfunction[161,163,175,176]. Furthermore, articular cartilage defects are known to be associated with clinical impairments that were previously related to adaptations in the movement pattern (e.g. swelling, reduced range of motion)[168,176,177]. However, the effect of an isolated articular cartilage defect on the movement pattern and the according joint loading pattern is not yet documented in-vivo. Therefore, patients with isolated articular cartilage defects were measured using integrated 3D motion capture and knee contact forces and pressures were calculated and compared to contact forces and pressures obtained in healthy asymptomatic control subjects.

Hypothesis study V: Patients with isolated articular cartilage defects in an otherwise healthy knee joint will present kinematic adaptations, inducing a loading avoidance strategy that decreases the loading on the injured site.

Methodology

Subjects

In the current project, subjects were recruited at the University of Leuven and at Cardiff University. For study I-IV, only healthy control subjects recruited in Leuven were included, whereas for study V data from Cardiff and Leuven were pooled and used together.

Table 2.1: Subject characteristics

	Controls	Patients
	Average ± standard deviation	Average ± standard deviation
Mass (kg)	72.07 ± 8.03	81.08 ± 12.87
Height (cm)	175.71 ± 6.68	174.77 ± 4.65
BMI (kg/m^2)	22.35 ± 2.38	26.52 ± 3.91
Age (Years)	30.05 ± 5.36	35.67 ± 9.47
Gender (M/F)	11/9	12/3
KOOS QDL	96.94 ± 4.30	58.13 ± 25.64
KOOS ADL	99.21 ± 1.63	72.77 ± 20.16
KOOS Symptoms	99.79 ± 2.07	58.41 ± 25.41
KOOS pain	98.21 ± 3.88	62.22 ± 24.31

QDL: quality of daily live, ADL: activities of daily life

Fifteen healthy asymptomatic control subjects were recruited in Leuven. Inclusion criteria were: BMI 35 <kg/m^2, age between 18 and 50 years and no history of previous major lower limb and knee injuries. Control subjects were recruited based on verbal screening and after completing the Knee Osteoarthritis Outcome Score (KOOS) to examine the absence of pain and symptoms. No frontal plane radiographs were taken of the control subjects to assess OA symptoms. Additional, five subjects with isolated focal cartilage defects in the tibiofemoral joint were recruited in Leuven and assessed at the Movement and posture Analysis Laboratory Leuven (KU Leuven). Inclusion criteria were the same as control subjects, except for the presence of an isolated cartilage defect ($> 1cm^2$ and ICRS-grade ≥ 3), and irrespective of KOOS scoring. Subjects with co-morbidities that may have affected gait were not included.

Five additional healthy control subjects and ten subjects with isolated focal cartilage defects in the tibiofemoral joint were recruited from the Cardiff & Vale University Health Board and assessed at the Arthritis Research UK Biomechanics and Bioengineering Centre (Cardiff University). The same inclusion criteria as for the subjects recruited in Leuven were used for the subjects in Cardiff. Subject characteristics are reported in table 2.1.

Data collection

Experimental motion analysis, Leuven

During experimental motion analysis, three-dimensional marker position were captured using 10 infrared Vicon cameras (VICON, Oxford Metrics, Oxford, UK, 100Hz). Simultaneously, ground reaction forces were

recorded using three force plates embedded in the ground (AMTI, Watertown, MA, USA, 1000Hz). Retroreflective markers were attached to the body according to a full-body Plug-in-Gait markerset, which was extended with additional markers, resulting in 65 markers in total[178]. Additional, three-marker clusters were attached to the upper and lower arms and legs, replacing the single markers from the original Plug-in-Gait markerset. Furthermore, additional anatomical markers were placed on the sacrum, medial femur epicondyles and the medial malleoli (figure 2.3).

After a static calibration trial, participants performed the following exercises at their preferred execution speed: level walking, ascending and descending a standardized four-step staircase, stand-up from a chair without using the arms, sit-down on a chair, squat, forward and sideward lunge and single leg hop. For stand-up and sit down a backless chair was used and chair height was standardized to the height of the lateral knee markers. During squat and single leg hop, the arms were fixed in the loin, whereas during the lunges, arms were held in scapular plane. Step length of the lunges was standardized to 80% of the leg length. For study II-V, only the walking trials were used, whereas for study I all exercises were included. Participants performed at least three valid trials that were retained for further processing.

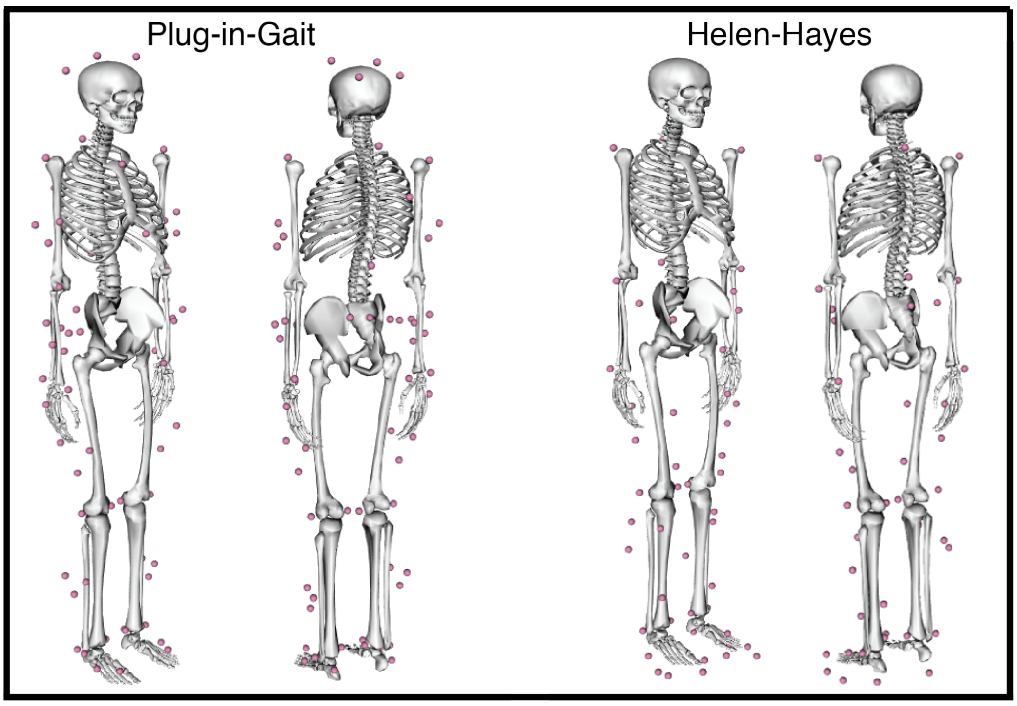

Figure 2.3: **Marksets used for the different studies.**
Left, extended Plug-in-Gait markerset. Right, extended Helen-Hayes markerset.

Experimental motion analysis, Cardiff

Participants assessed at Cardiff University were measured using a nine-camera Qualisys system (Qualisys, Qualisys Medical AB, Sweden, 120Hz). Ground reaction forces were recorded using four ground-embedded force plates (Bertec, Columbus, USA, 1080Hz). Retroreflective markers were attached to the body according to a full-body Helen-Hayes markerset, with additional markers, resulting in 54 markers in total[179]. Additional, four markers were attached to the upper and lower legs and additional markers on the midfoot and toe, as well as anatomical markers placed on the greater trochanter, medial femur epicondyles and medial

malleoli (figure 2.3).

After a static calibration trial, participants were measured during level walking at self-selected speed. Participants performed at least three valid trials that were retained for further processing.

Medical imaging, Leuven

At the same day of the experimental motion analysis, magnetic resonance images were acquired from the dominant knee of the fifteen control subjects measured in Leuven. Imaging was performed on a 3T Ingenia scanner after one hour standardized rest, to minimize the effect of prior movement (Philips Healthcare, Best, The Netherlands). Participants were positioned in supine position, with the knee in full extension and neutral rotation. The knee was fixed to minimize movement. The following scanning sequences were acquired: 1) A high resolution 3D-fast spin echo acquisition (3D-FSE), 2) $T1\rho$ relaxation time sequence and 3) T2 relaxation time sequence. A more detailed overview of the scanning parameters is provided in table 2.2. MR-images were only processed for study II and III.

Table 2.2: Overview of the MRI sequence parameters.

	3D-FSE	$T1\rho$	T2
TR (ms) / TE (ms)	1800/120	5.9587/3.082	4000/11-22-33-44-55-66-77-88
Field of view (cm)	16	16	16
Matrix	268 x 268	292 x 256	160 x 160
Slice thickness (mm)	1	4	4
Echo train length	85	64	12
Bandwidth (kHz)	562	522	367
Number of excitations	2	1	1
Number of slices	320	20	20
Acquisition time (min)	5.94	17.20	5.24
Time of recovery (ms)	/	2000	/
Time of spinlock (ms)	/	0/10/20/40/60	/
Frequency of spinlock (Hz)	/	500	/

Data processing

Musculoskeletal model

A generic musculoskeletal model was used to calculate muscle and knee contact forces[180]. In this model, a customized and validated knee model was implemented[181]. The customized knee joint allows six degrees of freedom (DoF) in the tibiofemoral and patellofemoral joint. The model included 44 musculotendon actuators, representing the lower leg muscles. Additionally, 14 bundles of non-linear springs were incorporated to represent the main knee ligaments and posterior capsule. Last, a non-linear elastic foundation contact model was implemented in the knee to calculate the cartilage contact pressure[181–183]. The cartilage was modelled with a uniformly distributed cartilage thickness, with a combined thickness of 4mm in the tibiofemoral joint and 7mm in the patellofemoral joint[46,184,185]. An elastic modulus of 10MPa and Poisson's ratio of 0.45 was defined for the cartilage[186–188]. This model therefore uses an implicit formulation to describe the effect of the meniscus on cartilage contact pressure. The model was implemented in SIMM with the Dynamics

Pipeline (Musculographics Inc., Santa Rosa, CA) and SD/Fast (Parametric Technology Corp., Needham, MA) used to generate the multibody equations of motion. This generic model was used for all studies.

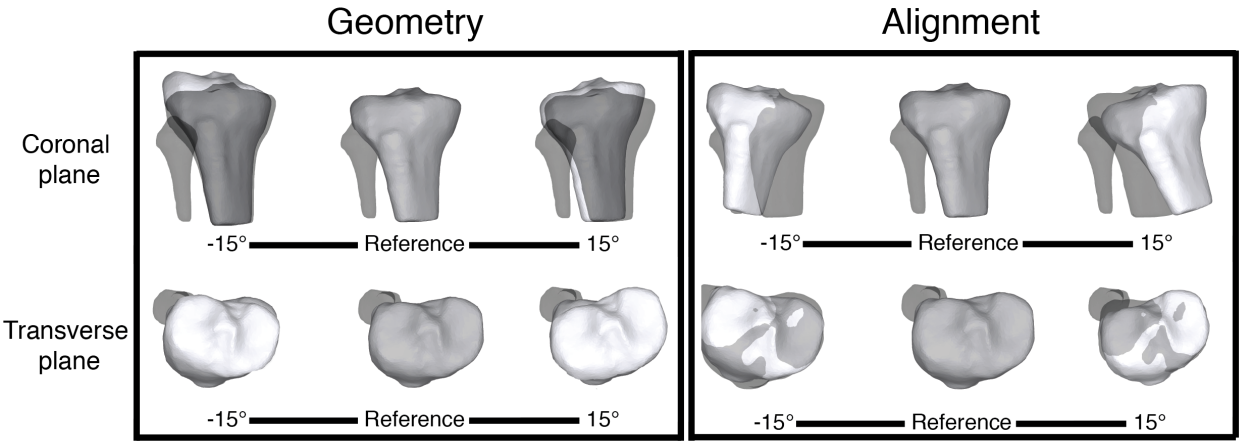

Figure 2.4: **Model adaptations in study IV.**
Geometry was changed in the coronal plane to simulate coronal tibial slope and in the transverse plane to simulate tibial torsion. Alignment in the coronal plane was changed to simulate varus-valgus alignment and in the transverse plane to simulate tibial rotation. Black represents the original model, whereas white is the adapted model.

For study IV, changes in the knee alignment and geometry were introduced to reflect the effect of variations in joint geometry and alignment. Variation in joint geometry was simulated by altering the orientation of the tibia plateau in the coronal and transverse plane. For this purpose, the orientation of the tibia component of the contact model was systematically changed in the coronal and transverse plane. This way, knee geometries with a more elevated medial or lateral tibia plateau were created, mimicking coronal tibial slope as well as tibias with a higher or lower degree of tibial torsion. The effect of varying the knee alignment in the coronal and transverse plane was investigated by changing the orientation of the tibia relative to the femur in the coronal and transverse plane. For this purpose, both the orientation of the tibial component of the contact model as well as the tibia were systematically altered. This resulted in a more varus or valgus aligned knee or a more internally or externally rotated knee. Each parameter was systematically changed from $\pm 1°$ till $\pm 15°$ from its normal position in steps of $2°$[113,143](figure 2.4).

These modified musculoskeletal models were subsequently used to generate simulations with the reference input kinematics and ground reaction forces using the standard workflow as described below (see *dynamic simulations of motion*, figure 2.5). This resulted in a dataset containing 765 simulations for each type of modification (in total 3060 simulations, 51 simulations for each subject for each type of modification). Given that the location of the foot with respect to the measured application point of the ground reaction force vector is changed for the simulations with an altered knee alignment, the point of application of the ground reaction force was expressed in the local reference frame of the foot. This ensures that for these simulations the location of the ground reaction force was identical to the reference simulation. To account for any dynamic inconsistency, compensations were assumed to occur in the trunk[189].

Dynamic simulations of motion

Knee contact forces for all studies, irrespective of inclusion location, were calculated using the following standard workflow (Figure 2.6). First, the generic model was scaled to the participants' anthropometry

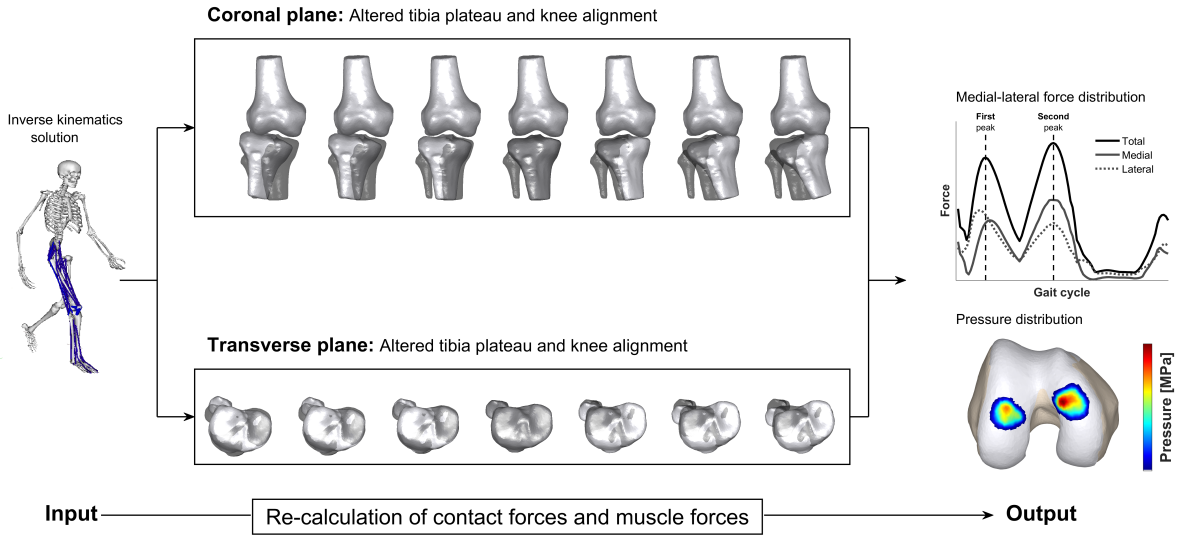

Figure 2.5: **Overview of the workflow used in study IV.**
A scaled musculoskeletal model was used to calculate the kinematics during walking. Next the muscle forces and contact forces were calculated with models in which the alignment of the knee or the position of the tibia plateau to simulate a deviating joint geometry was systematically changed from 1° to 15° from its reference position in the coronal and transverse plane in steps of 2°. Subsequently, the effect on the contact force and pressure distribution was analyzed and compared with the reference loading pattern obtained with the original model.

using the relative distances between the model markers and the markers measured during a calibration trial and using the mass of the participant. Subsequently, pelvis rotations and translations, hip angles, knee flexion angle and ankle angle were calculated at each frame of the gait cycle using a global optimization method for inverse kinematics that minimized the weighted sum of squared differences between experimental and model marker positions[19]. Next, the concurrent optimization of muscle forces and kinematics algorithm was used to calculate the muscle activation required to reproduce the measured primary hip, knee (i.e. only knee flexion) and ankle accelerations, while minimizing the weighted sum of squared muscle activations and contact energy[140,183]. Only the knee flexion angle was prescribed during the optimization, while the kinematics in the secondary tibiofemoral and all patellofemoral DoF evolved as a function of muscle, ligament and contact forces[140,181,183].

Cartilage segmentation and relaxation time mapping

The femoral cartilage and distal part of the femur were semi-automatically segmented from the high-resolution images (3D-FSE) for study II and III. From the segmented masks, 3D triangulated surfaces were created (Mimics, Innovation Suite, Materialise, Leuven, Belgium). These surfaces were used to calculate the subject-specific cartilage thickness distribution. Cartilage thickness was calculated based on the minimal distance between the subchondral bone surface (represented by the femur mesh) and the cartilage surface for each vertex of the cartilage surface separately[185]. For study II, the subject-specific mesh was used to calculate the thickness distribution, whereas for study III, the subject-specific mesh was first transformed to the generic cartilage mesh used in the musculoskeletal model using an advanced non-rigid deformation procedure (Mimics Innovation Suite, Materialise, Leuven, Belgium). Next, the transformed mesh was used

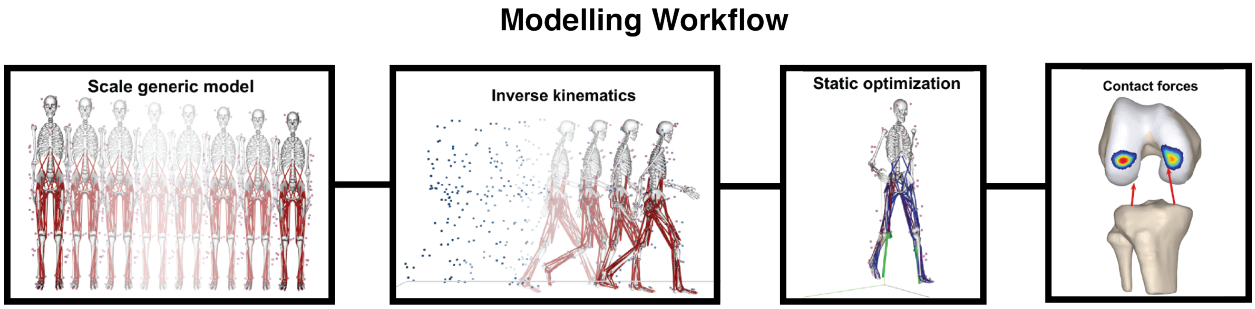

Figure 2.6: **Standard modelling workflow used in the different studies.**
First, the generic model is scaled to subjects' anthropometry, next marker positions are recalculated to joint angles. Subsequently, muscle force required to reproduce the measured joint accelerations and joint moments are calculated using static optimization. Last, joint reaction forces are calculated as well as the contact pressure based on the penetration depth of the rigid bodies in the spring layer of the elastic foundation contact model.

to calculate the cartilage thickness.

Relaxation time maps of the $T1\rho$ and T2 images were generated by a pixel-by-pixel evaluation of the mono-exponential Levenberg-Marquardt fitting algorithm[190]:

$$M(TSL) \propto e^{-\frac{TSL}{T1\rho}}$$
$$M(TE) \propto e^{-\frac{TE}{T2}}$$

Only relaxation times between 1 and 100ms were used to avoid outliers caused by a bad fit (0ms) or by synovial fluid and chemical shift artifact ($>$ 100ms)[191,192].

For study II, volumetric cartilage meshes were registered on the $T1\rho$ and T2 relaxation time maps to outline the region of interest. Next, the average relaxation time in the central part of the condyles was determined. The central part (representing the weight-bearing area) was defined as the area between the intercondylar notch and 60% of the distance to the most posterior point of the femoral condyles[193,194]. Furthermore, the average and peak cartilage thickness of the central part of the condyles was calculated. The peak thickness was calculated as the mean of the top 10% of all thickness values in the central region, whereas the mean thickness was calculated using all thickness values of the central region[185].

For study III, $T1\rho$ and T2 relaxation time profiles were registered on the generic cartilage mesh to evaluate the anterior-posterior distribution over the femoral cartilage. To do so, the morphed cartilage surfaces were rigidly registered on the relaxation time maps and the relaxation time values were assigned to the corresponding surface vertices. Subsequently, the angle-dependent profile of the thickness, $T1\rho$ and T2 relaxation time was evaluated by partitioning the cartilage into angular segments over the length of the cartilage surface. To do so, a sphere was fitted on the vertices of the medial and lateral condyle separately, using a least-squares fitting algorithm and assuming a circular cartilage shape. Next, from the vertical line (angle 0°), the cartilage was divided in angular segments with 5° increments clockwise and counter-clockwise (figure 2.7). Lastly, the average thickness, $T1\rho$ and T2 relaxation time was calculated for each angular segment.

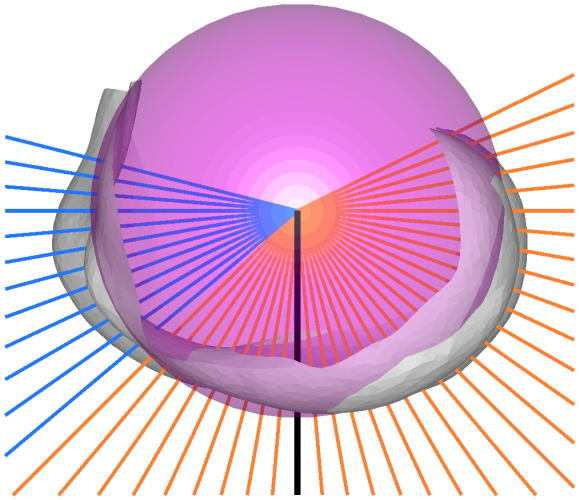

Figure 2.7: **Angular division of femur cartilage.**
Dark gray: trochlear cartilage, Light gray: tibiofemoral cartilage. Black line represents the vertical, 0°

References

1. Winter DA. The biomechanics and motor control of human gait: normal, elderly and pathological. Waterloo, Ontario: University of Waterloo Press. 1991.
2. Sritharan P, Lin Y-C, Pandy MG. Muscles that do not cross the knee contribute to the knee adduction moment and tibiofemoral compartment loading during gait. J Orthop Res. 2012;30: 1586–95.
3. Winby CR, Lloyd DG, Besier TF, Kirk TB. Muscle and external load contribution to knee joint contact loads during normal gait. J Biomech. Elsevier; 2009;42: 2294–300.
4. Giarmatzis G, Jonkers I, Wesseling M, Van Rossom S, Verschueren S. Loading of Hip Measured by Hip Contact Forces at Different Speeds of Walking and Running. J Bone Miner Res. 2015;30: 1431–1440.
5. Schipplein OD, Andriacchi TP. Interaction between active and passive knee stabilizers during level walking. J Orthop Res. 1991;9: 113–119.
6. Miyazaki T, Wada M, Kawahara H, Sato M, Baba H, Shimada S. Dynamic load at baseline can predict radiographic disease progression in medial compartment knee osteoarthritis. Ann Rheum Dis. 2002;61: 617–622.
7. Hurwitz DE, Ryals AB, Case JP, Block JA, Andriacchi TP. The knee adduction moment during gait in subjects with knee osteoarthritis is more closely correlated with static alignment than radiographic disease severity, toe out angle and pain. J Orthop Res. 2002;20: 101–107.
8. Andriacchi TP, Mündermann A. The role of ambulatory mechanics in the initiation and progression of knee osteoarthritis. Curr Opin Rheumatol. 2006;18: 514–518.
9. Baliunas AJ, Hurwitz DE, Ryals AB, Karrar A, Case JP, Block JA, et al. Increased knee joint loads during walking are present in subjects with knee osteoarthritis. Osteoarthr Cartil. 2002;10: 573–579.
10. D'Lima DD, Fregly BJ, Patil S, Steklov N, Colwell CW. Knee joint forces: prediction, measurement, and significance. Proc Inst Mech Eng H. 2012;226: 95–102.
11. D'Lima DD, Steklov N, Fregly BJ, Banks S a., Colwell CW. In vivo contact stresses during activities of daily living after knee arthroplasty. J Orthop Res. 2008;26: 1549–1555.

12. Kutzner I, Heinlein B, Graichen F, Bender a., Rohlmann a., Halder a., et al. Loading of the knee joint during activities of daily living measured in vivo in five subjects. J Biomech. Elsevier; 2010;43: 2164–2173.

13. Fregly BJ, Besier TF, Lloyd DG, Delp SL, Banks S a, Pandy MG, et al. Grand challenge competition to predict in vivo knee loads. J Orthop Res. 2012;30: 503–13.

14. Delp SL, Anderson FC, Arnold AS, Loan P, Habib A, John CT, et al. OpenSim: open-source software to create and analyze dynamic simulations of movement. IEEE Trans Biomed Eng. 2007;54: 1940–50.

15. Steele KM, Demers MS, Schwartz MH, Delp SL. Compressive tibiofemoral force during crouch gait. Gait Posture. Elsevier B.V.; 2012;35: 556–60.

16. Fregly BJ, D'Lima DD, Colwell CW. Effective gait patterns for offloading the medial compartment of the knee. J Orthop Res. 2009;27: 1016–1021.

17. Zajac FE. Muscle and tendon: properties, models, scaling, and application to biomechanics and motor control. Crit Rev Biomed Eng. 1989;17: 359–411.

18. Thelen DG. Adjustment of Muscle Mechanics Model Parameters to Simulate Dynamic Contractions in Older Adults. J Biomech Eng. 2003;125: 70.

19. Lu TW, O'Connor JJ. Bone position estimation from skin marker co-ordinates using global optimisation with joint constraints. J Biomech. 1999;32: 129–134.

20. De Groote F, De Laet T, Jonkers I, De Schutter J. Kalman smoothing improves the estimation of joint kinematics and kinetics in marker-based human gait analysis. J Biomech. 2008;41: 3390–3398.

21. Anderson FC, Pandy MG. Static and dynamic optimization solutions for gait are practically equivalent. J Biomech. 2001;34: 153–161.

22. Thelen DG, Anderson FC, Delp SL. Generating dynamic simulations of movement using computed muscle control. J Biomech. 2003;36: 321–328.

23. De Groote F, Demeulenaere B, Swevers J, De Schutter J, Jonkers I, Groote F De, et al. A physiology-based inverse dynamic analysis of human gait using sequential convex programming: a comparative study. Comput Methods Biomech Biomed Engin. 2012;15: 1093–102.

24. D'Lima DD, Steklov N, Patil S, Colwell CW. The Mark Coventry award: In vivo knee forces during recreation and exercise after knee arthroplasty. Clin Orthop Relat Res. 2008;466: 2605–2611.

25. D'Lima DD, Patil S, Steklov N, Slamin JE, Colwell CW. Tibial forces measured in vivo after total knee arthroplasty. J Arthroplasty. 2006;21: 255–262.

26. Zhao D, Banks SA, Lima DDD, Jr CWC, Fregly BJ. In Vivo Medial and Lateral Tibial Loads during Dynamic and High Flexion Activities. J Orthop Res. 2007; 593–602.

27. Shelburne KB, Torry MR, Pandy MG. Contributions of Muscles , Ligaments , and the Ground-Reaction Force to Tibiofemoral Joint Loading During Normal Gait. 2006; 1983–1990.

28. Heller MO, Taylor WR, Perka C, Duda GN. The influence of alignment on the musculo-skeletal loading conditions at the knee. Langenbeck's Arch Surg. 2003;388: 291–297.

29. Taylor WR, Heller MO, Bergmann G, Duda GN. Tibio-femoral loading during human gait and stair climbing. J Orthop Res. 2004;22: 625–632.

30. Zernicke RF, Judex S, Lorincz C. Adaptation of biological materials to exercise, disuse, and aging. Biomechanics of the musculo-skeletal system. 2006. pp. 226–243.

31. Frost H. From Wolff's law to the Utah paradigm: insights about bone physiology and its clinical applications. Anat Rec. 2001;262: 398–419.

32. Frost HM. Bone's mechanostat: A 2003 update. Anat Rec Part a. 2003;275A: 1081–1101.

33. Blazevich AJ. Effects of physical training and detraining, immobilisation, growth and aging on human fascicle geometry. Sport Med. 2006;36: 1003–1017.

34. Bohm S, Mersmann F, Arampatzis A. Human tendon adaptation in response to mechanical loading: a systematic review and meta-analysis of exercise intervention studies on healthy adults. Sport Med - Open. 2015;1: 7.

35. Sophia Fox AJ, Bedi A, Rodeo S a. The basic science of articular cartilage: structure, composition, and function. Sports Health. 2009;1: 461–8.

36. Triche R, Mandelbaum BR. Overview of cartilage biology and new trends in cartilage stimulation. Foot and Ankle Clinics. 2013. pp. 1–12.

37. Chen C, Tambe DT, Deng L, Yang L. Biomechanical properties and mechanobiology of the articular chondrocyte. Am J Physiol Cell Physiol. 2013;305: C1202-8.

38. Carter DR, Beaupré GS, Wong M, Smith RL, Andriacchi TP, Schurman DJ. The Mechanobiology of Articular Cartilage Development and Degeneration. Clin Orthop Relat Res. 2004;427: S69–S77.

39. Koláčná L, Bakešová J, Varga F, Koštáková E, Plánka L, Nečas A, et al. Biochemical and biophysical aspects of collagen nanostructure in the extracellular matrix. Physiol Res. 2007;56.

40. Andriacchi TP, Favre J. The Nature of In Vivo Mechanical Signals That Influence Cartilage Health and Progression to Knee Osteoarthritis. Curr Rheumatol Rep. 2014;16: 463–470.

41. Lee H, Salter DM. Biomechanics of Cartilage and Osteoarthritis. Osteoarthr - Prog Basic Res Treat. 2015;

42. Chaudhari AMW, Briant PL, Bevill SL, Koo S, Andriacchi TP. Knee kinematics, cartilage morphology, and osteoarthritis after ACL injury. Med Sci Sports Exerc. 2008;40: 215–22.

43. Stubbs AJ, Potter HG. Section VII: Chondral lesions. J Bone Joint Surg Am. 2009;91 Suppl 1: 119.

44. Koo S, Andriacchi TP. A comparison of the influence of global functional loads vs. local contact anatomy on articular cartilage thickness at the knee. J Biomech. 2007;40: 2961–2966.

45. Jones G, Ding C, Glisson M, Hynes K, Ma D, Cicuttini F. Knee articular cartilage development in children: A longitudinal study of the effect of sex, growth, body composition, and physical activity. Pediatr Res. 2003;54: 230–236.

46. Hudelmaier M, Glaser C, Englmeier K-H, Reiser M, Putz R, Eckstein F. Correlation of knee-joint cartilage morphology with muscle cross-sectional areas vs. anthropometric variables. Anat Rec Part A. 2003;270: 175–184.

47. Eckstein F, Faber S, Mühlbauer R, Hohe J, Englmeier KH, Reiser M, et al. Functional adaptation of human joints to mechanical stimuli. Osteoarthr Cartil. 2002;10: 44–50.

48. Vanwanseele B, Eckstein F, Hadwighorst H, Knecht H, Spaepen A, Stüssi E. In Vivo Precision of Quantitative Shoulder Cartilage Measurements, and Changes after Spinal Cord Injury. Magn Reson Med. 2004;51: 1026–1030.

49. Vanwanseele B, Eckstein F, Knecht H, Spaepen A, Stüssis E. Longitudinal Analysis of Cartilage Atrophy in the Knees of Patients with Spinal Cord Injury. Arthritis Rheum. 2003;48: 3377–3381.

50. Blazek K, Favre J, Asay J, Erhart-Hledik J, Andriacchi T. Age and obesity alter the relationship between femoral articular cartilage thickness and ambulatory loads in individuals without osteoarthritis. J Orthop Res. 2014;32: 394–402.

51. Andriacchi TP, Mündermann A, Smith RL, Alexander EJ, Dyrby CO, Koo S. A framework for the in vivo pathomechanics of osteoarthritis at the knee. Ann Biomed Eng. 2004;32: 447–457.

52. Koo S, Rylander JH, Andriacchi TP. Knee joint kinematics during walking influences the spatial cartilage thickness distribution in the knee. J Biomech. Elsevier; 2011;44: 1405–1409.

53. Scanlan SF, Favre J, Andriacchi TP. The relationship between peak knee extension at heel-strike of walking and the location of thickest femoral cartilage in ACL reconstructed and healthy contralateral knees. J Biomech. Elsevier; 2013;46: 849–854.

54. Li G, Park SE, DeFrate LE, Schutzer ME, Ji L, Gill TJ, et al. The cartilage thickness distribution in the tibiofemoral joint and its correlation with cartilage-to-cartilage contact. Clin Biomech. 2005;20: 736–744.

55. Koli J, Multanen J, Kujala UM, Häkkinen A, Nieminen MT, Kautiainen H, et al. Effects of Exercise on Patellar Cartilage in Women with Mild Knee Osteoarthritis. Med Sci Sports Exerc. 2015;47: 1767–1774.

56. Munukka M, Waller B, Rantalainen T, Häkkinen A, Nieminen MT, Lammentausta E, et al. Efficacy of progressive aquatic resistance training for tibiofemoral cartilage in postmenopausal women with mild knee osteoarthritis: A randomised controlled trial. Osteoarthr Cartil. 2016;24: 1708–1717.

57. Souza RB, Baum T, Wu S, Feeley BT, Kadel N, Li X, et al. Effects of unloading on knee articular cartilage T1rho and T2 magnetic resonance imaging relaxation times: a case series. J Orthop Sports Phys Ther. 2012;42: 511–20.

58. Ackermann B, Steinmeyer J. Collagen biosynthesis of mechanically loaded articular cartilage explants. Osteoarthr Cartil. 2005;13: 906–914.

59. Bleuel J, Zaucke F, Brüggemann G-P, Niehoff A. Effects of Cyclic Tensile Strain on Chondrocyte Metabolism: A Systematic Review. PLoS One. 2015;10: e0119816.

60. Thibault M, Poole AR, Buschmann MD. Cyclic compression of cartilagdbone explants in vitro leads to physical weakening , mechanical breakdown of collagen and release of matrix fragments. J Orthop Res. 2002;20: 1265–1273.

61. Chen C, Bhargava M, Lin PM, Torzilli PA. Time , stress , and location dependent chondrocyte death and collagen damage in cyclically loaded articular cartilage. 2003;21: 888–898.

62. Chen C, Lust NBG, Bank RA, Iekoppele JM. Compositional and Metabolic Changes in Damaged Cartilage are Peak-Stress, Stress-Rate, and Loading-Duration Dependent. J Orthop Res. 1999;17: 870–879.

63. Quinn TM, Maung AA, Grodzinsky AJ. Physical and Biological Regulation of Proteoglycan Turnover around Chondrocytes in Cartilage Explants: Implications for Tissue Degradation and Repair. Ann New York Acad Sci. 1999;878: 420–441.

64. Steinmeyer J, Knue S, Raiss RX, Pelzer I. Effects of intermittently applied cyclic loading on proteoglycan metabolism and swelling behaviour of articular cartilage explants. Osteoarthr Cartil. 1999;7: 155–164.

65. Wolf A, Raiss RX, Steinmeyer J. Fibronectin metabolism of cartilage explants in response to the frequency of intermittent loading. 2003;21: 1081–1089.

66. Sauerland K, Raiss RX, Steinmeyer J. Proteoglycan metabolism and viability of articular cartilage explants as modulated by the frequency of intermittent loading. Osteoarthr Cartil. 2003;11: 343–350.

67. Grad S, Eglin D, Alini M, Stoddart MJ. Physical stimulation of chondrogenic cells in vitro: A review. Clin Orthop Relat Res. 2011;469: 2764–2772.

68. Haugh MG, Ph D, Meyer EG, Ph D, Thorpe SD. Temporal and Spatial Changes in Cartilage-Matrix-Specific Gene Expression in Mesenchymal Stem Cells in Response to Dynamic Compression. TISSUE Eng Part A. 2011;17: 23–25.

69. Bian L, Zhai DY, Zhang EC, Mauck RL, Burdick JA. Matrix Synthesis and Distribution and Suppresses. TISSUE Eng Part A. 2012;18.

70. Wu P, Delassus E, Patra D, Liao W, Sandell LJ. Effects of Serum and Compressive Loading on the Cartilage Matrix Synthesis and Spatiotemporal Deposition Around Chondrocytes in 3D Culture. TISSUE Eng Part A. 2013;19: 13–15.

71. Bian L, Fong J, Lima EG, Stoker AM, Ateshian G a, Ph D, et al. Dynamic Mechanical Loading Enhances Functional Properties of Tissue-Engineered Cartilage Using Mature Canine Chondrocytes. 2010;16: 17–20.

72. Grad S, Loparic M, Peter R, Stolz M, Aebi U, Alini M. Sliding motion modulates stiffness and friction coefficient at the surface of tissue engineered cartilage. Osteoarthr Cartil. Elsevier Ltd; 2012;20: 288–295.

73. Little CB, Ghosh P. Variation in proteoglycan metabolism by articular chondrocytes in different joint regions is determined by post-natal mechanical loading. Osteoarthr Cartil. 1997;5: 49–62.

74. Stenhamre H, Slynarski K, Petrén C, Tallheden T, Lindahl A. Topographic variation in redifferentiation capacity of chondrocytes in the adult human knee joint. Osteoarthr Cartil. 2008;16: 1356–1362.

75. Shepherd DE, Seedhom BB. Thickness of human articular cartilage in joints of the lower limb. Ann Rheum Dis. 1999;58: 27–34.

76. Rogers BA, Murphy CL, Cannon SR, Briggs TWR. Topographical variation in glycosaminoglycan content in human articular cartilage. J Bone Jt Surg [Br]. 2006;88: 1670–4.

77. Mayerhoefer ME, Welsch GH, Mamisch TC, Kainberger F, Weber M, Nemec S, et al. The in vivo effects of unloading and compression on T1-Gd (dGEMRIC) relaxation times in healthy articular knee cartilage at 3.0 Tesla. Eur Radiol. 2010;20: 443–449.

78. Bevill SL, Briant PL, Levenston ME, Andriacchi TP. Central and peripheral region tibial plateau chondrocytes respond differently to in vitro dynamic compression. Osteoarthr Cartil. Elsevier Ltd; 2009;17: 980–987.

79. Jurvelin JS, Arokoski JPA, Hunziker EB, Helminen HJ. Topographical variation of the elastic properties of articular cartilage in the canine knee. J Biomech. 2000;33: 669–675.

80. Franz T, Hasler EM, Hagg R, Weiler C, Jakob RP, Mainil-Varlet P. In situ compressive stiffness, biochemical composition, and structural integrity of articular cartilage of the human knee joint. Osteoarthr Cartil. 2001;9: 582–592.

81. Espino DM, Shepherd DET, Hukins DWL. Viscoelastic properties of bovine knee joint articular cartilage: dependency on thickness and loading frequency. BMC Musculoskelet Disord. 2014;15: 205.

82. Kurkijärvi JE, Nissi MJ, Kiviranta I, Jurvelin JS, Nieminen MT. Delayed gadolinium-enhanced MRI of cartilage (dGEMRIC) and T2 characteristics of human knee articular cartilage: Topographical variation and relationships to mechanical properties. Magn Reson Med. 2004;52: 41–46.

83. Silverberg JL, Dillavou S, Bonassar L, Cohen I. Anatomic variation of depth-dependent mechanical properties in neonatal bovine articular cartilage. J Orthop Res. 2013;31: 686–691.

84. Andriacchi TP, Favre J, Erhart-Hledik JC, Chu CR. A Systems View of Risk Factors for Knee Osteoarthritis Reveals Insights into the Pathogenesis of the Disease. Ann Biomed Eng. 2015;43: 376–387.

85. Peterfy CG, Guermazi a., Zaim S, Tirman PFJ, Miaux Y, White D, et al. Whole-organ magnetic resonance imaging score (WORMS) of the knee in osteoarthritis. Osteoarthr Cartil. 2004;12: 177–190.

86. Burstein D, Bashir A, Gray ML. MRI techniques in early stages of cartilage disease. Invest Radiol. 2000;35: 622–38.

87. Braun HJ, Gold GE. Advanced MRI of articular cartilage. Imaging Med. 2011;3: 541–555.

88. Chan DD, Neu CP. Probing articular cartilage damage and disease by quantitative magnetic resonance imaging. J R Soc Interface. 2013;10: 20120608.

89. Trattnig S, Winalski CS, Marlovits S, Jurvelin JS, Welsch GH, Potter HG. Magnetic Resonance Imaging of Cartilage Repair: A Review. Cartilage. 2010;2: 5–26.

90. Marlovits S, Singer P, Zeller P, Mandl I, Haller J, Trattnig S. Magnetic resonance observation of cartilage repair tissue (MOCART) for the evaluation of autologous chondrocyte transplantation: determination of interobserver variability and correlation to clinical outcome after 2 years. Eur J Radiol. 2006;57: 16–23.

91. Marlovits S, Striessnig G, Resinger CT, Aldrian SM, Vecsei V, Imhof H, et al. Definition of pertinent parameters for the evaluation of articular cartilage repair tissue with high-resolution magnetic resonance imaging. Eur J Radiol. 2004;52: 310–9.

92. Li X, Cheng J, Lin K, Saadat E, Bolbos RI, Jobke B, et al. Quantitative MRI using T1ρ and T2 in human osteoarthritic cartilage specimens: Correlation with biochemical measurements and histology. Magn Reson Imaging. Elsevier Inc.; 2011;29: 324–334.

93. Stahl R, Luke A, Li X, Carballido-Gamio J, Ma CB, Majumdar S, et al. T1rho, T2 and focal knee cartilage abnormalities in physically active and sedentary healthy subjects versus early OA patients–a 3.0-Tesla MRI study. Eur Radiol. 2009;19: 132–43.

94. Keenan KE, Besier TF, Pauly JM, Han E, Rosenberg J, Smith RL, et al. Prediction of glycosaminoglycan content in human cartilage by age, T1ρ and T2 MRI. Osteoarthr Cartil. Elsevier Ltd; 2011;19: 171–9.

95. Wheaton AJ, Dodge GR, Elliott DM, Nicoll SB, Reddy R. Quantification of cartilage biomechanical and biochemical properties via T1rho magnetic resonance imaging. Magn Reson Med. 2005;54: 1087–93.

96. Crema MD, Frank W, Marra MD, Burstein D, Gold GE, Eckstein MF, et al. Articular Cartilage in the Knee: Current MR Imaging Techniques and Applications in Clinical. Radiographics. 2011;31: 37–61.

97. Bashir a., Gray ML, Hartke J, Burstein D. Nondestructive imaging of human cartilage glycosaminoglycan concentration by MRI. Magn Reson Med. 1999;41: 857–865.

98. Akella SVS, Regatte RR, Gougoutas AJ, Borthakur A, Shapiro EM, Kneeland JB, et al. Proteoglycan-Induced Changes in T 1ρ -Relaxation of Articular Cartilage at 4T. 2001;423: 419–423.

99. Matzat SJ, van Tiel J, Gold GE, Oei EHG. Quantitative MRI techniques of cartilage composition. Quant Imaging Med Surg. 2013;3: 162–74.

100. Hatcher CC, Collins AT, Kim SY, Michel LC, Mostertz WC, Ziemian SN, et al. Relationship between T1rho magnetic resonance imaging, synovial fluid biomarkers, and the biochemical and biomechanical properties of cartilage. J Biomech. Elsevier Ltd; 2017;55: 18–26.

101. Nissi MJ, Rieppo J, Töyräs J, Laasanen MS, Kiviranta I, Nieminen MT, et al. Estimation of mechanical properties of articular cartilage with MRI - dGEMRIC, T2 and T1 imaging in different species with variable stages of maturation. Osteoarthr Cartil. 2007;15: 1141–1148.

102. Lammentausta E, Kiviranta P, Nissi MJ, Laasanen MS, Kirivanta I, Nieminen MT, et al. T2 relaxation time and delayed gadolinium-enhanced MRI of cartilage (dGEMRIC) of human patellar cartilage at 1.5 T and 9.4 T: Relationships with tissue mechanical properties. J Orthop Res. 2006;24: 366–74.

103. Felson DT, Lawrence RC, Dieppe PA, Hirsch R, Helmick CG, Jordan JM, et al. Osteoarthritis: New insights - Part 1: The disease and its risk factors. Annals of Internal Medicine. 2000. pp. 635–646.

104. Hunter DJ, Felson DT. Osteoarthritis. BMJ. 2006;332: 639–42.

105. Lories RJ, Luyten FP. The bone–cartilage unit in osteoarthritis. Nat Rev Rheumatol. Nature Publishing Group; 2011;7: 43–49.

106. Prieto-Alhambra D, Judge A, Javaid MK, Cooper C, Diez-Perez A, Arden NK. Incidence and risk factors for clinically diagnosed knee, hip and hand osteoarthritis: influences of age, gender and osteoarthritis affecting other joints. Ann Rheum Dis. 2014;73: 1659–64.

107. Nuki G. Osteoarthritis: a problem of joint failure. Z Rheumatol. 1999;58(3): 142–7.

108. Palazzo C, Nguyen C, Lefevre-Colau MM, Rannou F, Poiraudeau S. Risk factors and burden of osteoarthritis. Ann Phys Rehabil Med. 2016;59: 134–138.

109. Johnson VL, Hunter DJ. The epidemiology of osteoarthritis. Best Pract Res Clin Rheumatol. Elsevier Ltd; 2014;28: 5–15.

110. Allen KD, Golightly YM. Epidemiology of osteoarthritis: state of the evidence. Rheumatol, Curr Opin. 2015;27: 276–283.

111. Peach CA, Carr AJ, Loughlin J. Recent advances in the genetic investigation of osteoarthritis. Trends Mol Med. 2005;11: 186–191.

112. Warner S, Valdes A. The Genetics of Osteoarthritis: A Review. J Funct Morphol Kinesiol. 2016;1: 140–153.

113. Brouwer GM, Van Tol AW, Bergink AP, Belo JN, Bernsen RMD, Reijman M, et al. Association between valgus and varus alignment and the development and progression of radiographic osteoarthritis of the knee. Arthritis Rheum. 2007;56: 1204–1211.

114. Baker-LePain JC, Lane NE. Role of bone architecture and anatomy in osteoarthritis. Bone. Elsevier Inc.; 2012;51: 197–203.

115. Hunter D, Nevitt M, Lynch J, Kraus VB, Katz JN, Collins JE, et al. Longitudinal validation of periarticular bone area and 3D shape as biomarkers for knee OA progression? Data from the FNIH OA Biomarkers Consortium. Ann Rheum Dis. 2015; annrheumdis-2015-207602.

116. Felson D, Lawrence R, Dieppe P, Hirsch R, Helmick C, Jordan J, et al. Osteoarthritis: New Insights. Part 1: The Disease and Its Risk Factors. Ann Intern Med. 2000;133: 637–639.

117. Lewek MD, Rudolph KS, Snyder-Mackler L. Control of frontal plane knee laxity during gait in patients with medial compartment knee osteoarthritis. Osteoarthr Cartil. 2004;12: 745–751.

118. Lewek MD, Ramsey DK, Snyder-mackler L, Rudolph KS. Knee Stabilization in Patients With Medial Compartment Knee Osteoarthritis. Arthritis Rheum. 2005;52: 2845–2853.

119. Sharma L, Lou C, Felson DT, Dunlop DD, Kirwan-Mellis G, Hayes KW, et al. Laxity in healthy and osteoarthritic knees. Arthritis Rheum. 1999;42: 861–870.

120. Wink AE, Gross KD, Brown CA, Guermazi A, Roemer F, Niu J, et al. Varus thrust during walking and the risk of incident and worsening medial tibiofemoral MRI lesions: the Multicenter Osteoarthritis Study. Osteoarthr Cartil. Elsevier Ltd; 2017;25: 839–845.

121. Sharma L.;, Chang A, Jackson RD., Nevitt M, Moisio KC., Hochberg M, et al. Varus Thrust and Incident and Progressive Knee Osteoarthritis. Arthritis Rheumatol. 2016;17: 2045–2054.

122. Mahmoudian A, van Dieen JH, Bruijn SM, Baert IA, Faber GS, Luyten FP, et al. Varus thrust in women with early medial knee osteoarthritis and its relation with the external knee adduction moment. Clin Biomech. Elsevier Ltd; 2016;39: 109–114.

123. Roos EM, Arden NK. Strategies for the prevention of knee osteoarthritis. Nat Rev Rheumatol. Nature Publishing Group; 2016;12: 92–101.

124. Baert IAC, Meeus M, Mahmoudian A, Luyten FP, Nijs J, Verschueren SMP. Do Psychosocial Factors Predict Muscle Strength, Pain, or Physical Performance in Patients With Knee Osteoarthritis? JCR J Clin Rheumatol. 2017;23: 308–316.

125. Kakarlapudi TK, Bickerstaff DR. Knee instability: isolated and complex. West J Med. 2001;174: 266–272.

126. Moyer R, Wirth W, Duryea J, Eckstein F. Anatomical alignment, but not goniometry, predicts femorotibial cartilage loss as well as mechanical alignment: Data from the Osteoarthritis Initiative. Osteoarthr Cartil. Elsevier Ltd; 2016;24: 254–261.

127. Hayashi D, Englund M, Roemer FW, Niu J, Sharma L, Felson DT, et al. Knee malalignment is associated with an increased risk for incident and enlarging bone marrow lesions in the more loaded compartments: The MOST study. Osteoarthr Cartil. Elsevier Ltd; 2012;20: 1227–1233. 0

128. Moisio K, Chang A, Eckstein F, Chmiel JS, Wirth W, Almagor O, et al. Varus-valgus alignment reduced risk of subsequent cartilage loss in the less loaded compartment. Arthritis Rheum. 2011;63: 1002–1009.

129. Neogi T, Bowes MA, Niu J, De Souza KM, Vincent GR, Goggins J, et al. Magnetic resonance imaging-based three-dimensional bone shape of the knee predicts onset of knee osteoarthritis: Data from the osteoarthritis initiative. Arthritis Rheum. 2013;65: 2048–2058.

130. Williams TG, Vincent G, Bowes M, Cootes T, Balamoody S, Hutchinson C, et al. Automatic segmentation of bones and inter-image anatomical correspondence by volumetric statistical modelling of knee MRI. 2010 7th IEEE Int Symp Biomed Imaging From Nano to Macro, ISBI 2010 - Proc. 2010; 432–435.

131. Foroughi N, Smith R, Vanwanseele B. The association of external knee adduction moment with biomechanical variables in osteoarthritis: a systematic review. Knee. Elsevier B.V.; 2009;16: 303–9.

132. Bellemans J, Colyn W, Vandenneucker H, Victor J. The chitranjan ranawat award: Is Neutral Mechanical Alignment Normal for All Patients? Clin Orthop Relat Res. 2012;470: 45–53.

133. Turcot K, Armand S, Lübbeke A, Fritschy D, Hoffmeyer P, Suvà D. Does knee alignment influence gait in patients with severe knee osteoarthritis? Clin Biomech. Elsevier Ltd; 2013;28: 34–39.

134. van Egmond N, Stolwijk N, van Heerwaarden R, van Kampen A, Keijsers NLW. Gait analysis before and after corrective osteotomy in patients with knee osteoarthritis and a valgus deformity. Knee Surgery, Sport Traumatol Arthrosc. Springer Berlin Heidelberg; 2016; 1–10.

135. Weidenhielm L, Svensson OK, Broström LÅ, Rudberg U. Change in adduction moment about the knee after high tibial osteotomy and prosthetic replacement in osteoarthrosis of the knee. Clin Biomech. 1992;7: 91–96.

136. Agneskirchner JD, Hurschler C, Wrann CD, Lobenhoffer P. The Effects of Valgus Medial Opening Wedge High Tibial Osteotomy on Articular Cartilage Pressure of the Knee: A Biomechanical Study. Arthrosc - J Arthrosc Relat Surg. 2007;23: 852–861.

137. Riegger-Krugh C, Gerhart TN, Powers WR, Hayes WC. Tibiofemoral Contact Pressures in Degenerative Joint Disease. Clin Orthop Relat Res. 1998;348: 233–245.

138. Quirno M, Campbell KA, Singh B, Hasan S, Jazrawi L, Kummer F, et al. Distal femoral varus osteotomy for unloading valgus knee malalignment: a biomechanical analysis. Knee Surgery, Sport Traumatol Arthrosc. Springer Berlin Heidelberg; 2015;

139. Smith CR, Vignos MF, Lenhart RL, Kaiser J, Thelen DG. The Influence of Component Alignment and Ligament Properties on Tibiofemoral Contact Forces in Total Knee Replacement. J Biomech Eng. 2016;138: 1–10.

140. Thelen DG, Won Choi K, Schmitz AM. Co-simulation of neuromuscular dynamics and knee mechanics during human walking. J Biomech Eng. 2014;136: 21033.

141. Lerner ZF, DeMers MS, Delp SL, Browning RC. How tibiofemoral alignment and contact locations affect predictions of medial and lateral tibiofemoral contact forces. J Biomech. Elsevier; 2015;48: 644–650.

142. Chen Z, Wang L, Liu Y, He J, Lian Q, Li D, et al. Effect of component mal-rotation on knee loading in total knee arthroplasty using multi-body dynamics modeling under a simulated walking gait. J Orthop Res. 2015;33: 1287–1296.

143. Thompson JA, Hast MW, Granger JF, Piazza SJ, Siston RA. Biomechanical effects of total knee arthroplasty component malrotation: A computational simulation. J Orthop Res. 2011;29: 969–975.

144. Sharma L, Song J, Felson DT, Cahue S, Shamiyeh E, Dunlop DD. The role of knee alignment in disease progression and functional decline in knee osteoarthritis. JAMA. 2001;286: 188–195.

145. Cicuttini F, Wluka A, Hankin J, Wang Y. Longitudinal study of the relationship between knee angle and tibiofemoral cartilage volume in subjects with knee osteoarthritis. Rheumatology. 2004;43: 321–324.

146. Huizinga MR, Gorter J, Demmer A, Bierma-Zeinstra SMA, Brouwer RW. Progression of medial compartmental osteoarthritis 2–8 years after lateral closing-wedge high tibial osteotomy. Knee Surgery, Sport Traumatol Arthrosc. Springer Berlin Heidelberg; 2016;

147. Tanamas S, Hanna FS, Cicuttini FM, Wluka AE, Berry P, Urquhart DM. Does knee malalignment increase the risk of development and progression of knee osteoarthritis? A systematic review. Arthritis Care Res. 2009;61: 459–467.

148. Chang A, Hayes K, Dunlop D, Hurwitz D, Song J, Cahue S, et al. Thrust during ambulation and the progression of knee osteoarthritis. Arthritis Rheum. 2004;50: 3897–3903.

149. Chang AH, Chmiel JS, Moisio KC, Almagor O, Zhang Y, Cahue S, et al. Varus thrust and knee frontal plane dynamic motion in persons with knee osteoarthritis. Osteoarthr Cartil. Elsevier Ltd; 2013;21: 1668–1673.

150. Driban JB, Stout AC, Duryea J, Lo GH, Harvey WF, Price LL, et al. Coronal tibial slope is associated with accelerated knee osteoarthritis: data from the Osteoarthritis Initiative. BMC Musculoskelet Disord. BMC Musculoskeletal Disorders; 2016;17: 1–8.

151. Haverkamp DJ, Schiphof D, Bierma-Zeinstra SM, Weinans H, Waarsing JH. Variation in joint shape of osteoarthritic knees. Arthritis Rheum. 2011;63: 3401–3407.

152. Duparc F, Thomine JM, Simonet J, Biga N. Femoral and tibial bone torsions associated with medial femoro-tibial osteoarthritis. Index of cumulative torsions. Orthop Traumatol Surg Res. Elsevier Masson SAS; 2014;100: 69–74.

153. Eckhoff DG. Effect of limb malrotation on malalignment and osteoarthritis. Orthop Clin North Am. 1994;25: 405–415.

154. Eckhoff DG, Johnston RJ, Stamm ER, Kilcoyne RF, Wiedel JD. Version of the osteoarthritic knee. J Arthroplasty. 1994;9: 73–79.

155. Turner MS. The association between tibial torsion and knee joint pathology. Clin Orthop Relat Res. 1994; 47–51.

156. Krackow KA, Mandeville DS, Rachala SR, Bayers-Thering M, Osternig LR. Torsion deformity and joint loading for medial knee osteoarthritis. Gait Posture. Elsevier B.V.; 2011;33: 625–629.

157. Davies-Tuck ML, Wluka AE, Wang Y, Teichtahl AJ, Jones G, Ding C, et al. The natural history of cartilage defects in people with knee osteoarthritis. Osteoarthr Cartil. 2008;16: 337–342.

158. Spahn G, Hofmann G. Focal cartilage defects within the medial knee compartment. predictors for osteoarthritis progression. Z Orthop Unfall. 2014;152: 480–488.

159. Wang Y, Ding C, Wluka AE, Davis S, Ebeling PR, Jones G, et al. Factors affecting progression of knee cartilage defects in normal subjects over 2 years. Rheumatology. 2006;45: 79–84.

160. Flanigan DC, Harris JD, Trinh TQ, Siston RA, Brophy RH. Prevalence of chondral defects in Athletes' Knees: A systematic review. Med Sci Sports Exerc. 2010;42: 1795–1801.

161. Heir S, Nerhus TK, Røtterud JH, Løken S, Ekeland A, Engebretsen L, et al. Focal cartilage defects in the knee impair quality of life as much as severe osteoarthritis: a comparison of knee injury and osteoarthritis outcome score in 4 patient categories scheduled for knee surgery. Am J Sports Med. 2010;38: 231–7.

162. Wondrasch B, Arøen A, Røtterud JH, Høysveen T, Bølstad K, Risberg MA. The feasibility of a 3-month active rehabilitation program for patients with knee full-thickness articular cartilage lesions: the Oslo Cartilage Active Rehabilitation and Education Study. J Orthop Sports Phys Ther. 2013;43: 310–24.

163. Engelhart L, Nelson L, Lewis S, Mordin M, Demuro-Mercon C, Uddin S, et al. Validation of the Knee Injury and Osteoarthritis Outcome Score subscales for patients with articular cartilage lesions of the knee. Am J Sports Med. 2012;40: 2264–72.

164. Yamaguchi S, Gamada K, Sasho T, Kato H, Sonoda M, Banks S a. In vivo kinematics of anterior cruciate ligament deficient knees during pivot and squat activities. Clin Biomech (Bristol, Avon). Elsevier Ltd; 2009;24: 71–6.

165. Georgoulis AD, Papadonikolakis A, Papageorgiou CD, Mitsou A, Stergiou N. Three-dimensional tibiofemoral kinematics of the anterior cruciate ligament-deficient and reconstructed knee during walking. Am J Sports Med. 2003;31: 75–9.

166. Andriacchi TP, Dyrby CO. Interactions between kinematics and loading during walking for the normal and ACL deficient knee. J Biomech. 2005;38: 293–8.

167. Van De Velde SK, Bingham JT, Hosseini A, Kozanek M, DeFrate LE, Gill TJ, et al. Increased tibiofemoral cartilage contact deformation in patients with anterior cruciate ligament deficiency. Arthritis Rheum. 2009;60: 3693–3702.

168. Ebert JR, Robertson WB, Lloyd DG, Zheng MH, Wood DJ, Ackland T. Traditional vs accelerated approaches to post-operative rehabilitation following matrix-induced autologous chondrocyte implantation (MACI): comparison of clinical, biomechanical and radiographic outcomes. Osteoarthritis Cartilage. 2008;16: 1131–40.

169. Ebert JR, Lloyd DG, Ackland T, Wood DJ. Knee biomechanics during walking gait following matrix-induced autologous chondrocyte implantation. Clin Biomech. Elsevier Ltd; 2010;25: 1011–7.

170. Sasaki K, Neptune RR. Individual muscle contributions to the axial knee joint contact force during normal walking. J Biomech. Elsevier; 2010;43: 2780–4.

171. Winby CR, Gerus P, Kirk TB, Lloyd DG. Correlation between EMG-based co-activation measures and medial and lateral compartment loads of the knee during gait. Clin Biomech. Elsevier Ltd; 2013;28: 1014–9.

172. Thoma LM, McNally MP, Chaudhari AM, Flanigan DC, Best TM, Siston RA, et al. Muscle co-contraction during gait in individuals with articular cartilage defects in the knee. Gait Posture. 2016;48: 68–73.

173. Thoma LM, McNally MP, Chaudhari AM, Best TM, Flanigan DC, Siston RA, et al. Differential knee joint loading patterns during gait for individuals with tibiofemoral and patellofemoral articular cartilage defects in the knee. Osteoarthr Cartil. Elsevier Ltd; 2017; 1–9.

174. Mithoefer K, Hambly K, Logerstedt D, Ricci M, Silvers H, Della Villa S. Current concepts for rehabilitation and return to sport after knee articular cartilage repair in the athlete. J Orthop Sports Phys Ther. 2012;42: 254–73.

175. Wondrasch B, Zak L, Welsch GH, Marlovits S. Effect of accelerated weightbearing after matrix-associated autologous chondrocyte implantation on the femoral condyle on radiographic and clinical outcome after 2 years: a prospective, randomized controlled pilot study. Am J Sports Med. 2009;37 Suppl 1: 88S–96S.

176. Løken S, Ludvigsen TC, Høysveen T, Holm I, Engebretsen L, Reinholt FP. Autologous chondrocyte implantation to repair knee cartilage injury: ultrastructural evaluation at 2 years and long-term follow-up including muscle strength measurements. Knee Surg Sports Traumatol Arthrosc. 2009;17: 1278–88.

177. Van Assche D, Staes F, Van Caspel D, Vanlauwe J, Bellemans J, Saris DB, et al. Autologous chondrocyte implantation versus microfracture for knee cartilage injury: a prospective randomized trial, with 2-year follow-up. Knee Surg Sports Traumatol Arthrosc. 2010;18: 486–95.

178. Davis RB, Ounpuu S, Tyburski D, Gage JR. A gait analysis data collection and reduction technique. Hum Mov Sci. 1991;10: 575–587.

179. Kadaba MP, Ramakrishnan HK, Wootten ME. Measurement of lower extremity kinematics during level walking. J Orthop Res. 1990;8: 383–92.

180. Arnold EM, Ward SR, Lieber RL, Delp SL. A model of the lower limb for analysis of human movement. Ann Biomed Eng. 2010;38: 269–79.

181. Lenhart RL, Kaiser J, Smith CR, Thelen DG. Prediction and Validation of Load-Dependent Behavior of the Tibiofemoral and Patellofemoral Joints During Movement. Ann Biomed Eng. 2015;43: 2675–2685.

182. Bei Y, Fregly BJ. Multibody dynamic simulation of knee contact mechanics. Med Eng Phys. 2004;26: 777–789.

183. Smith RC, Choi KW, Negrut D, Thelen DG. Efficient Computation of Cartilage Contact Pressures within Dynamic Simulations of Movement. Comput Methods Biomech Biomed Eng Imaging Vis. 2016;

184. Eckstein F, Winzheimer M, Hohe J, Englmeier KH, Reiser M. Interindividual variability and correlation among morphological parameters of knee joint cartilage plates: Analysis with three-dimensional MR imaging. Osteoarthr Cartil. 2001;9: 101–111.

185. Draper CE, Besier TF, Gold GE, Fredericson M, Fiene A, Beaupre GS, et al. Is cartilage thickness different in young subjects with and without patellofemoral pain? Osteoarthr Cartil. 2006;14: 931–937.

186. Adouni M, Shirazi-Adl A. Partitioning of Knee Joint Internal Forces in Gait Is Dictated By the Knee Adduction Angle and Not By the Knee Adduction Moment. J Biomech. Elsevier; 2014;47: 1696–703.

187. Blankevoort L, Kuiper JH, Huiskes R, Grootenboer HJ. Articular contact in a three-dimensional model of the knee. J Biomech. 1991;24: 1019–1031.

188. Li G, Lopez O, Rubash H. Variability of a Three-Dimensional Finite Element Model Constructed Using Magnetic Resonance Images of a Knee for Joint Contact Stress Analysis. J Biomech Eng. 2001;123: 341–346.

189. Wesseling M, De Groote F, Meyer C, Corten K, Simon JP, Desloovere K, et al. Gait alterations to effectively reduce hip contact forces. J Orthop Res. 2015;33: 1094–1102.

190. Li X, Benjamin Ma C, Link TM, Castillo D-D, Blumenkrantz G, Lozano J, et al. In vivo T1rho and T2 mapping of articular cartilage in osteoarthritis of the knee using 3 T MRI. Osteoarthr Cartil. 2007;15: 789–97.

191. Kaneko Y, Nozaki T, Yu H, Chang A, Kaneshiro K, Schwarzkopf R, et al. Normal T2 map profile of the entire femoral cartilage using an angle/layer-dependent approach. J Magn Reson Imaging. 2015;42: 1507–1516.

192. Kumar D, Kothari A, Souza RB, Wu S, Benjamin Ma C, Li X. Frontal plane knee mechanics and medial cartilage MR relaxation times in individuals with ACL reconstruction: A pilot study. Knee. Elsevier B.V.; 2014;21: 881–885.

193. Erhart-Hledik JC, Favre J, Andriacchi TP. New insight in the relationship between regional patterns of knee cartilage thickness, osteoarthritis disease severity, and gait mechanics. J Biomech. Elsevier; 2015;48: 3868–3875.

194. Eckstein F, Hudelmaier M, Wirth W, Kiefer B, Jackson R, Yu J, et al. Double echo steady state magnetic resonance imaging of knee articular cartilage at 3 Tesla: a pilot study for the Osteoarthritis Initiative. Ann Rheum Dis. 2006;65: 433–441.

Chapter 3

Knee joint loading in healthy adults during functional exercises: implications for rehabilitation guidelines

Sam Van Rossom, Colin R Smith, Darryl G Thelen, Benedicte Vanwanseele, Dieter Van Assche, Ilse Jonkers

Accepted for publication in *Journal of Orthopaedic and Sports Physical Theraphy*

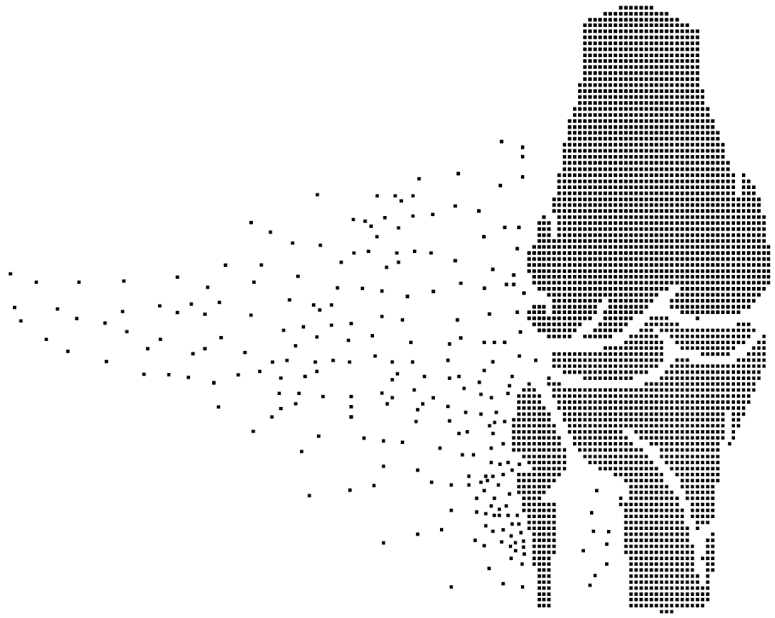

Abstract

Study design: Controlled Laboratory Study

Background: Inclusion of specific exercises in rehabilitation after knee injury is currently expert-based as a thorough description of the knee contact forces during different exercises is lacking.

Objective: To quantify knee loading during frequently used activities such as squat, lunges, single leg hop, walking stairs, standing up and gait in order to define grading in knee joint loading during these activities.

Methods: 3D-motion analysis data of 15 healthy adults were acquired during 9 standardized activities used in rehabilitation. Experimental motion data was processed using musculoskeletal modeling to calculate contact and shear force on the different knee compartments (tibiofemoral and patellofemoral). Using repeated-measures ANOVAs, contact and shear forces were compared between compartments and exercises whereas muscle and average maximum femoral forces were compared between exercises.

Results: Apart from squat, all therapeutic exercises imposed higher forces to the tibiofemoral joint compared to gait. Likewise, patellofemoral forces were increased during all exercises. Increased compartmental contact forces were accompanied by increased compartmental shear forces. Furthermore, force distribution over the medial and lateral compartment was sensitive to the performed exercise. With increased knee flexion, more force was imposed on the posterior part of the condyles.

Conclusion: By carefully selecting exercises, forces on the injured zone can be avoided, as the force distribution differs strongly between exercises. Consequently, compartmental forces can be diminished, resulting in a reduction of shear forces on the involved compartment. Based on the results, a graded exercise program for progressive knee loading during rehabilitation can be conceptualized.

Keywords: Knee · Contact forces · Cartilage pressure · Motion analysis · Rehabilitation exercises

Introduction

Primary goals for physical therapy after knee injury and surgery comprise the return to full range of motion (ROM), full weight-bearing, recovery of neuromuscular control, restoration of muscle strength and ultimately the return to the pre-operative activity level and function[1,2]. A gradual progression of joint loading is one of the key elements during the rehabilitation. Therefore, the use of appropriate exercises to achieve the treatment goals while not overloading the injured joint is a balancing act for the physical therapists.

The selection and timing of specific rehabilitation exercises is currently more expert than evidence-based[1,3,4]. An example of this is the selection of open versus closed kinetic chain (OKC and CKC) exercises. CKC exercises are believed to induce compressive forces on the knee joint, which increase joint stability and decrease ligament strain[5,6]. Contrary, OKC exercises are believed to reduce joint proprioception and synergistic muscle activation, consequently exposing the knee to increased shear forces[5,7–11]. However, to date the magnitude of knee loading during rehabilitation exercises is not well documented[12,13]. Current rehabilitation protocols following cartilage repair surgery aim to account for the graft maturation by gradually incorporating exercises based on perceived joint load and to minimize shear stimuli that have been related to catabolic pathways in the cartilage tissue and undermine cartilage homeostasis[1,4]. Likewise, in the early stages of rehabilitation following ACL-injury and repair surgery, rehabilitation protocols aim to avoid excessive ligament strain [14,15]. However, analysis of loading in terms of contact force (CF) magnitude and location during individual exercises is currently missing[4].

Strengthening thigh musculature is essential for optimal rehabilitation outcome after knee injury[16]. After rehabilitation, strength deficits persist and negatively affect self-reported function and return to sport[17–19]. Consequently, knee stability and the ability to adequately dampen the impact forces is diminished, increasing the long term risk for knee osteoarthritis (OA)[17]. Inclusion of rehabilitation exercises that specifically promote quadriceps musculature is therefore required since even following accelerated weight-bearing protocols, strength deficits persist[20].

In-vivo measurements of knee CFs during functional activities are available, but limited to patients who underwent total knee arthroplasty with an instrumented implant. So far, CFs were documented during specific activities of daily living such as gait, stair climbing, kneeling and lunging[21,22]. Integrated motion capture in combination with musculoskeletal modeling allow to estimate the muscle, ligament and knee CFs during functional activities such as gait and showed good agreement with data measured using instrumented implants[23]. Applying this methodology to other functional activities and especially rehabilitation exercises would allow for quantifying the compartmental forces and their shear components in the knee joint.

Therefore, the present study aims to evaluate: 1) the magnitude of the CF and shear forces in medial and lateral tibiofemoral and patellofemoral compartment, 2) knee muscle forces (i.e., knee flexors and extensors) and 3) femoral force in different locations (i.e., anterior, mid, and posterior zones) during 9 CKC exercises in a cohort of healthy adults. A better understanding of the knee CFs during different exercises may allow physical therapists to design more staged rehabilitation programs designed to minimize CFs and their shear components to prevent cartilage and ligament injury while maximizing muscle strengthening[24].

Methods

Data collection

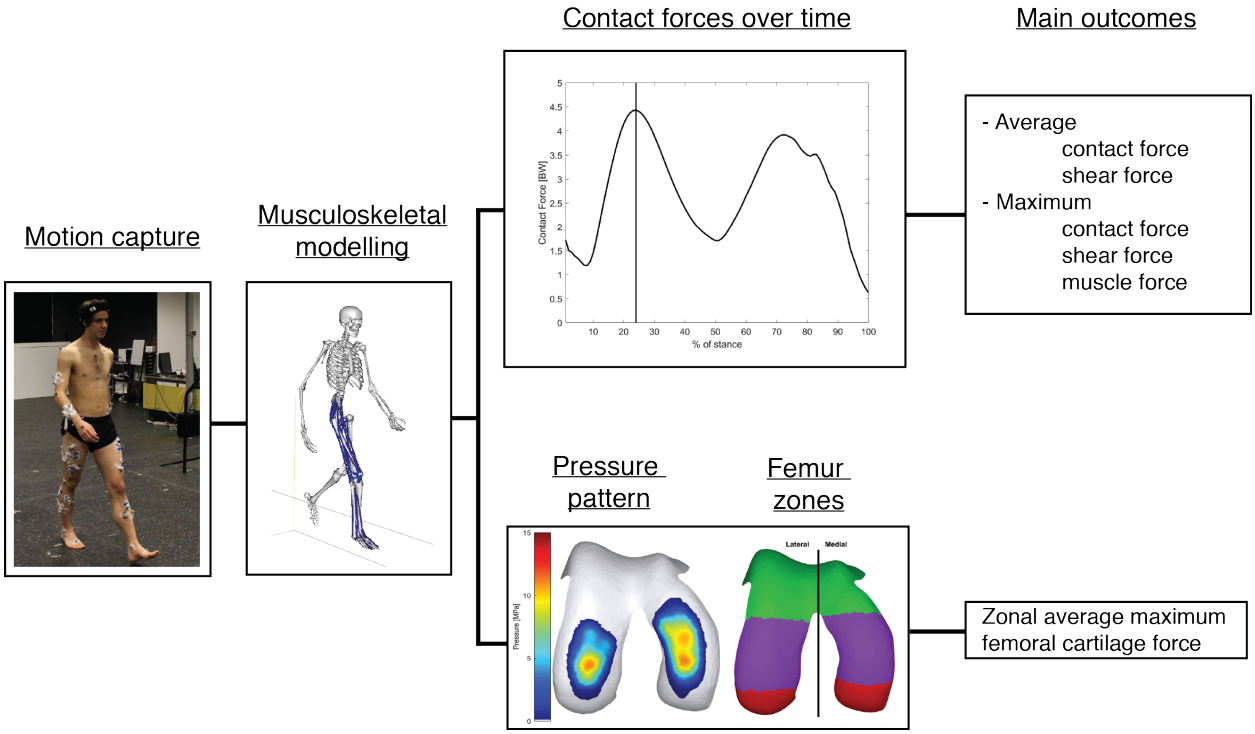

Figure 3.1: **Schematic overview of the workflow.**
Experimental motion data was collected and processed using musculoskeletal modelling in order to calculate the cartilage loading. Contact forces were calculated and the average and peak contact force and shear force was determined. The maximum contact pressure distribution was recalculated to the force distribution and was analyzed by determining the average maximum force in each zone. Loading variables were compared between exercises and compartments using repeated-measures ANOVA.

Fifteen healthy adults (8 males, 7 females, mean age = 31 ± 6 years and body mass index of 22.35 ± 1.54 kg/m^2) with no history of lower limb injury were included in the study. The university hospital Leuven ethics committee approved all study procedures (s56093) and all participants provided informed written consent. After a calibration trial, participants performed five repetitions of the following exercises: Gait at self-selected speed; ascending and descending a standard four step staircase at self-selected speed; stand up from a chair without using the arms; sit down on a chair from full standing without using the arms; squat to 90° self-perceived knee flexion with the arms fixed in the waist; forward and sideward lunge with the arms in scapular plane and step length standardized to 80% of the leg length; single leg hop from upright standing with the arms fixed in the waist. A detailed description of exercises as well as animations are provided in supplementary material (S1 and S4). Exercises were executed barefoot to avoid confounding effects of shoes wear. Three-dimensional marker trajectories were recorded using a 10-camera VICON system (Vicon, Oxford Metrics 100Hz) along with ground reaction forces using three ground-embedded force plates (AMTI, Watertown, USA, 1000Hz). Markers were placed according to a full-body Plug-in-Gait markerset, extended with three-marker clusters on the upper and lower arms and legs and anatomical markers on the sacrum, medial femur epicondyles and the medial malleoli, resulting in 65 markers[25].

Musculoskeletal modelling

Muscle and knee CFs were calculated using a scaled knee model, containing 6 degrees of freedom (DoF) patellofemoral and tibiofemoral joints that was previously validated[26]. This customized knee model was implemented into a generic lower extremity model[27]. The model included 44 musculotendon actuators spanning the hip, knee and ankle, and 14 bundles of non-linear springs, representing the major knee ligaments and posterior capsule. Cartilage contact pressures were calculated using a non-linear elastic foundation formulation based on the penetration depth between overlapping cartilage surface meshes[28]. A combined uniformly distributed thickness of 4mm and 7mm was assumed in the tibiofemoral and patellofemoral joint, respectively[29–31]. An elastic modulus of 10MPa and a Poisson's ratio of 0.45 was assumed for cartilage[32–34]. The lower extremity model was implemented in SIMM, using the Dynamics Pipeline (Musculographics Inc., Santa Rosa, CA) and SD/Fast (Parametric Technology Corp., Needham, MA) to generate the multibody equations of motion. This model was found to be accurate for estimating contact forces measured using instrumented implants with a root-mean-square (RMS) error below 0.33BW[23].

The generic model was scaled to the subjects' anthropometry and mass. Subsequently, pelvic translations, pelvic rotations, hip angles, knee flexion angle and ankle angle were calculated at each frame of the movement cycle using inverse kinematics that minimized the weighted sum of squared differences between experimental and model marker positions[35]. Next, muscle forces required to generate the measured accelerations in the primary DoFs (i.e. hip flexion, hip adduction, hip rotation, knee flexion and ankle flexion) were calculated using the concurrent optimization of muscle activations and kinematics algorithm, that simultaneously solves for the secondary knee kinematics (11DoF), while minimizing the weighted sum of squared muscle activations and contact energy[28]. This algorithm allows the kinematics in the secondary tibiofemoral and patellofemoral DoF to evolve as function of muscle, ligament and CFs[26,28,36]. The resultant CF was calculated based on the contact pressure and the contact area. The resultant CFs on the medial and lateral tibiofemoral compartments and patellofemoral joint were decomposed to estimate the net shear component. This calculation used the curvature information, based on the average mesh face normal of an area of $60mm^2$ around the application point of the CF to define a local coordinate system used for the decomposition.

Data analysis

For each exercise, the maximum and average magnitude of the resultant CF and shear force of the total knee as well as the medial, and lateral tibiofemoral and patellofemoral compartment were determined during the load-bearing phase. A detailed description of the analyzed phases as well as the average trunk angles is provided in supplementary material (S1 and S3). The contact pressure distribution was recalculated to contact force distribution accounting for the area of individual mesh elements. Subsequently, the force distribution over the femur was analyzed by dividing the cartilage mesh in an anterior, mid and posterior zone(figure 3.1, S2 figure 3.9). For the tibiofemoral force, the maximum force on each element of the femoral condyle contacting the tibial surface during the exercise was determined and then averaged over the anterior, mid and posterior zone of the medial and lateral condyle separately to obtain the average maximum tibiofemoral force in the respective zone[37]. For the patellofemoral force, the maximum force on each element of the femoral condyle contacting the patellar surface during the exercise was determined during the exercise and then averaged over the anterior, mid and posterior zone of the femoral cartilage to obtain the average maximum patellofemoral force[37]. Likewise, the average maximum pressure for each zone was analyzed and reported in supplementary material (S5 figure 3.11). The maximum summed muscle force of the knee

extensors (rectus femoris and vastus lateralis, medialis and intermedius) and knee flexors (medial and lateral gastrocnemii, biceps femoris long head and short head, semimembranosus and semitendinosus) throughout the load-bearing phase was determined. Data were averaged over three trials of each participants' right leg. To account for subject-specific mass, muscle forces, CFs and shear forces were normalized to bodyweight (BW).

Statistical analysis

Maximum and average resultant contact and shear force on the medial, lateral tibiofemoral and patellofemoral compartment were compared between exercises and compartments using two-way repeated measures ANOVA. When a significant interaction effect was found, differences in contact and shear forces were evaluated between compartments and exercises using dependent t-tests. To evaluate between exercises, contact and shear forces were compared to gait, since gait was considered a milestone for progression towards more demanding exercises[1,24]. The average maximum tibiofemoral and patellofemoral force in each zone was compared between zones and exercises using two-way repeated-measures ANOVA. When a significant interaction effect was found, exercises were compared for each zone to gait using dependent t-tests. A one-way repeated measures ANOVA compared total knee CF and muscle forces between exercises, using dependent t-tests to compare each exercise to gait when a significant effect for exercise was found. Significance level was set at 0.05, but Bonferroni-corrected to compensate for the effect of multiple testing (α_{bc}). All statistical tests were performed in SPPS (SPSS24, SPSS Inc. Chicago, IL).

Results

Animations of all exercises, with the corresponding contact pressure patterns are provided in supplementary material for a representative subject (S4 Video).

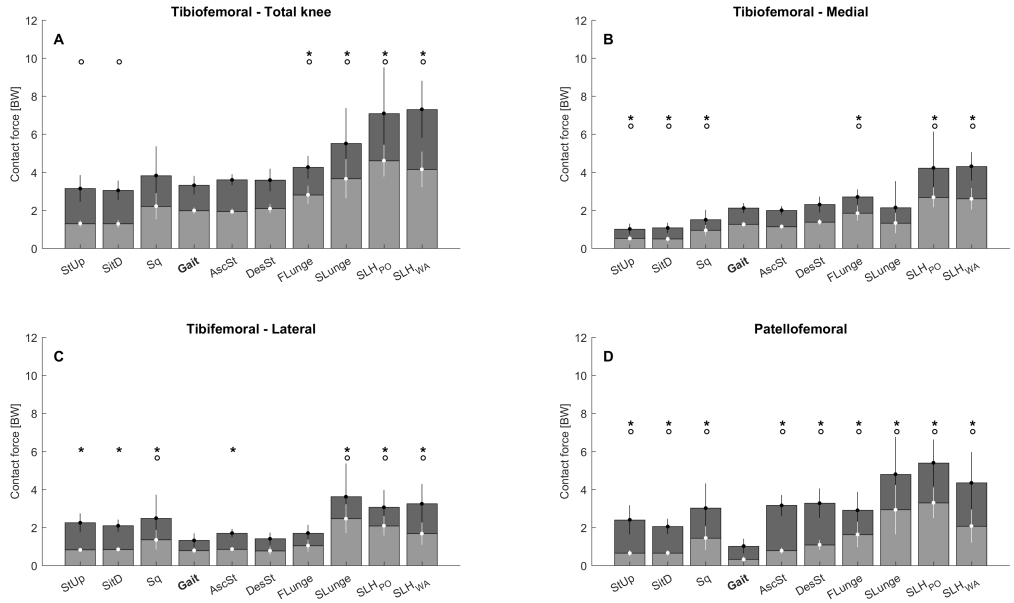

Figure 3.2: The magnitude of the maximum (dark gray) and average (light gray) total tibiofemoral (A), medial tibiofemoral (B), lateral tibiofemoral (C) and patellofemoral (D) contact force during the nine exercises. * indicates a significant difference in maximum contact force and ∘ indicates a significant difference in average contact force compared to gait (α_{bc}=0.0056). SitD: sit down, StUp: stand up, AscSt: ascending stairs, DesSt: descending stairs, Sq: squat, FLunge: forward lunge, SLunge: sideward lunge, SLHwa: single leg hop weight acceptance, SLHpo: single leg hop push-off.

Contact forces

For total maximum and average tibiofemoral CF, a significant main effect for exercise was observed ($p = 0.003$ and $p < 0.001$). For maximum and average compartmental CF, a significant main effect for exercise (both $p < 0.001$) and compartment ($p < 0.001$ and $p = 0.006$, respectively) was observed, with a significant interaction effect for both maximum and average CF ($p < 0.001$).

Post hoc comparison between exercises

For the total tibiofemoral CF, maximum and average total tibiofemoral CF were lowest during sit down, with average total tibiofemoral CF being significantly lower during sit down and stand up compared to gait. They were highest during single leg hop (push-off and weight-acceptance). Both lunges (forward and sideward lunge) and single leg hop had higher maximum and average total tibiofemoral CF than gait (figure 3.2A).

In the medial compartment, maximum and average CF were lowest during stand up and sit down and similar to squat, significantly lower than gait. They were highest during single leg hop and similar to forward lunge, significantly higher than gait (figure 3.2B).

In the lateral compartment, maximum and average CF were lowest during gait and stair descent respectively and highest during sideward lunge. Compared to gait, maximum CF was significantly higher during stair ascent, sit down, stand up, squat, single leg hop and sideward lunge, whereas average CF was higher during squat, single leg hop and sideward lunge (figure 3.2C). In the patellofemoral compartment, maximum and average CF were lowest during gait and was compared to all other exercises significantly lower, with single leg hop push-off having highest maximum and average CF (figure 3.2D).

Post hoc comparison between compartments

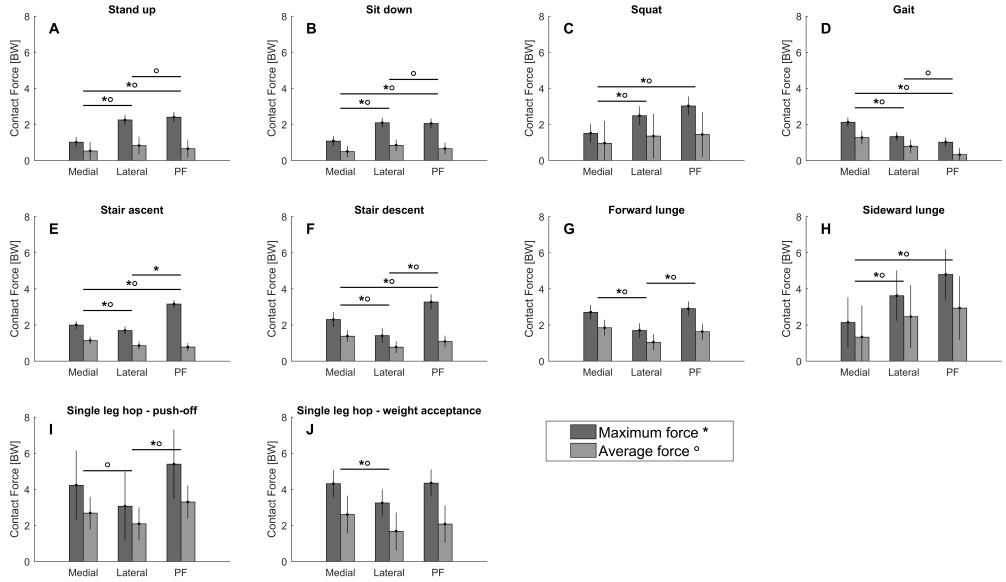

Figure 3.3: Distribution of the maximum (dark gray) and average (light gray) contact force over the different knee compartments. * Indicates a significant difference between the maximum contact forces of two compartments and ∘ indicates a significant difference between the average contact forces of two compartments (α_{bc}=0.0125). A) StUp: stand up, B) SitD: sit down C) Sq: squat, D) Gait, E) AscSt: ascending stairs, F) DesSt: descending stairs, G) FLunge: forward lunge, H) SLunge: sideward lunge, I) SLHpo: single leg hop push-off, J) SLHwa: single leg hop weight acceptance.

During gait, stair ascent and descent, forward lunge and single leg hop weight-acceptance maximum and average CF were significantly higher on the medial than the lateral condyle, whereas this was only confirmed for the average CF during single leg hop push-off only. Maximum and average CF were significantly lower in the medial than the lateral compartment during stand up, sit down, squat and sideward lunge (figure 3.3).

Shear forces

For maximum and average shear force a significant main effect for exercise ($p < 0.001$) and compartment ($p < 0.001$) was observed, with a significant interaction effect for both maximum and average shear force ($p < 0.001$).

Post hoc comparison between exercises

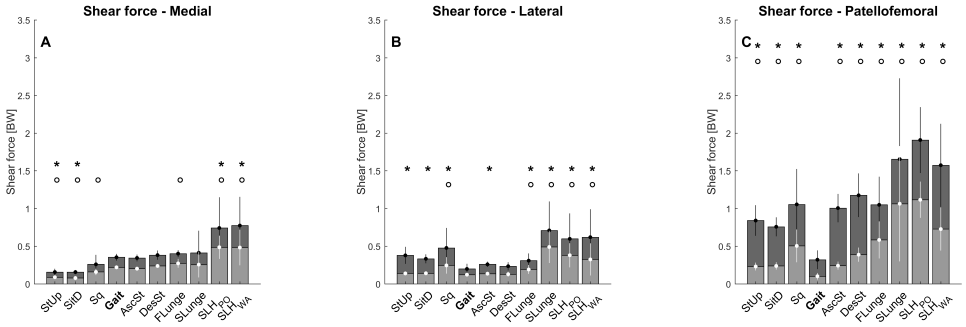

Figure 3.4: The magnitude of the maximum (dark gray) and average (light gray) medial tibiofemoral (A), lateral tibiofemoral (B) and patellofemoral (C) shear force during the nine exercises. * indicates a significant difference in maximum shear force and ∘ indicates a significant difference in average shear force compared to gait (α_{bc}=0.0056). SitD: sit down, StUp: stand up, AscSt: ascending stairs, DesSt: descending stairs, Sq: squat, FLunge: forward lunge, SLunge: sideward lunge, SLHwa: single leg hop weight acceptance, SLHpo: single leg hop push-off.

In the medial compartment, maximum and average shear force was lowest during stand up and sit down respectively, and significantly lower than gait. They were highest during single leg hop and significantly higher than gait. Average shear force was significantly lower during squat and was significantly higher during forward lunge than gait (figure 3.4A).

In the lateral compartment, maximum and average shear force was lowest during gait and highest during sideward lunge. Maximum and average shear force was significantly higher than gait during forward lunge, squat, single leg hop and sideward lunge. Maximum force was significantly higher during stair ascending, sit down and stand up than gait (figure 3.4B).

In the patellofemoral compartment, maximum and average shear force was lowest during gait and highest during single leg hop push-off. All exercises had significantly higher maximum and average patellofemoral shear force compared to gait (figure 3.4C).

Post hoc comparison between compartments

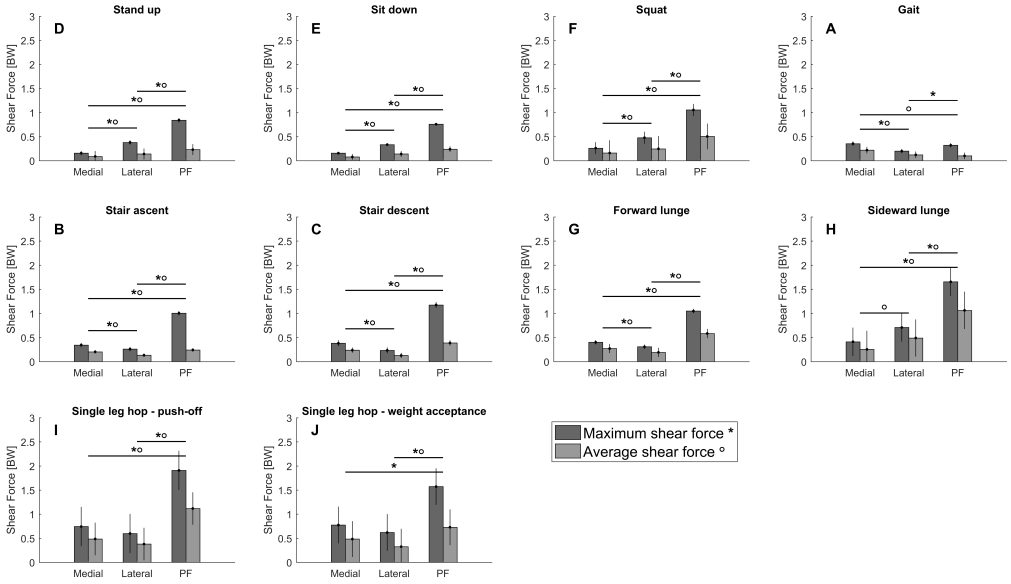

Figure 3.5: Distribution of the maximum (dark gray) and average (light gray) shear force over the different knee compartments. * Indicates a significant difference between the maximum shear forces of two compartments and ∘ indicates a significant difference between the average shear forces of two compartments (α_{bc}=0.0125). A) StUp: stand up, B) SitD: sit down C) Sq: squat, D) Gait, E) AscSt: ascending stairs, F) DesSt: descending stairs, G) FLunge: forward lunge, H) SLunge: sideward lunge, I) SLHpo: single leg hop push-off, J) SLHwa: single leg hop weight acceptance.

Maximum and average shear forces in the medial compartment were significantly higher than the lateral compartment during gait, stair ascent, stair descent and forward lunge. During single leg hop shear forces were not significantly different between medial and lateral compartment. Maximum and average shear forces in the medial compartment were significantly lower than the lateral compartment during stand up, sit down and squat, whereas during sideward lunge only the average shear forces were significantly lower in the medial than the lateral compartment (figure 3.5).

During gait, average shear forces were significantly higher in the patellofemoral compartment than the medial compartment. Average and maximum shear forces were significantly higher in the patellofemoral than the medial compartment during stand up, sit down, squat, stair ascent and descent, lunges and single leg hop push-off, whereas this was only confirmed for the maximum shear forces during single leg hop weight-acceptance. During all exercises, maximum patellofemoral shear forces were significantly higher than the shear forces in the lateral compartment. Average patellofemoral shear forces were significantly higher than the shear forces in the lateral compartment during all exercises, except during gait (figure 3.5).

Average maximum tibiofemoral and patellofemoral force in the different zones

A significant main effect for exercise ($p < 0.001$) and zone ($p < 0.001$) was observed for average maximum tibiofemoral force on the medial and lateral condyle and for the average maximum patellofemoral force, with all showing a significant interaction effect ($p < 0.001$).

Post hoc comparison between exercises

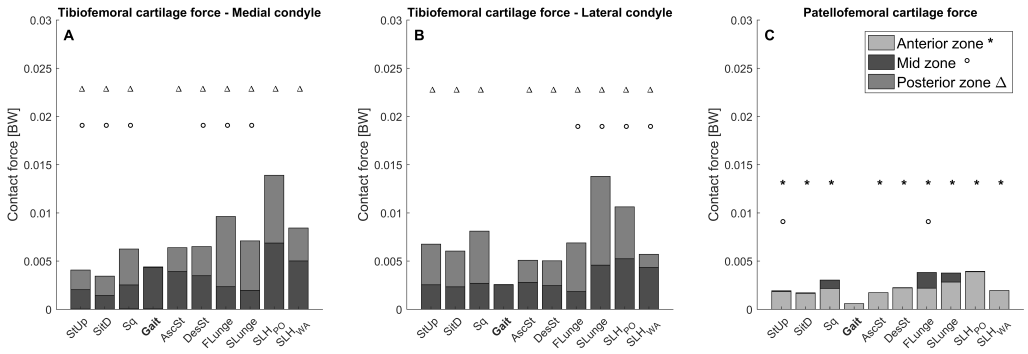

Figure 3.6: The average maximum tibiofemoral force on the anterior (light gray), mid (dark gray) and posterior (gray) zone of the medial condyle (A) and lateral condyle (B). The average maximum patellofemoral force on the anterior (green), mid (purple) and posterior (red) zone of the femur. *, ∘ and Δ indicates a significant difference in anterior, mid or posterior zone pressure, respectively compared to gait (α_{bc}=0.0056). SitD: sit down, StUp: stand up, AscSt: ascending stairs, DesSt: descending stairs, Sq: squat, FLunge: forward lunge, SLunge: sideward lunge, SLHwa: single leg hop weight acceptance, SLHpo: single leg hop push-off.

The mid zone of the medial and lateral condyle experienced lowest average maximum tibiofemoral force during sit down and forward lunge, whereas this zone was most loaded during single leg hop push-off. Compared to gait, the mid zone of the medial condyle presented significantly less average maximum tibiofemoral force during sit down, stand up, stair descent, sideward lunge, forward lunge and squat. Compared to gait, the mid zone of the lateral condyle experienced significantly less average maximum tibiofemoral force during forward lunge and significantly higher average maximum tibiofemoral force during single leg hop and sideward lunge than gait (figure 3.6A and B). The posterior zone of the medial and lateral condyle experienced least average maximum tibiofemoral force during gait, whereas they experienced most average maximum tibiofemoral force during forward and sideward lunge, respectively. All exercises imposed significantly more medial and lateral average maximum tibiofemoral force on the posterior zones than gait (figure 3.6A and B).

The anterior zone of the femur experienced lowest average maximum patellofemoral force during gait. Average maximum patellofemoral force was significantly higher than gait during all exercises (figure 3.6C). The mid zone experienced almost no average maximum patellofemoral force during gait, stair ascent and descent, and single leg hop whereas the highest average maximum patellofemoral force was experienced during forward lunge. Significantly higher average maximum patellofemoral force was imposed on the mid zone during stand up and forward lunge than gait (figure 3.6C).

Muscle forces

A significant main effect for exercise was observed for both flexor ($p = 0.009$) and extensor ($p < 0.001$) summed muscle force.

Post hoc comparison between exercises

Summed knee extensor muscle force was highest during single leg hop push-off and lowest during gait. Summed knee flexor muscle force was highest during single leg hop push-off, but lowest during sit down.

During all exercises, knee extensor muscle forces were significantly higher than during gait, whereas knee flexor muscle force was significantly lower during sit down, stand up and stair descent (figure 3.7A and B).

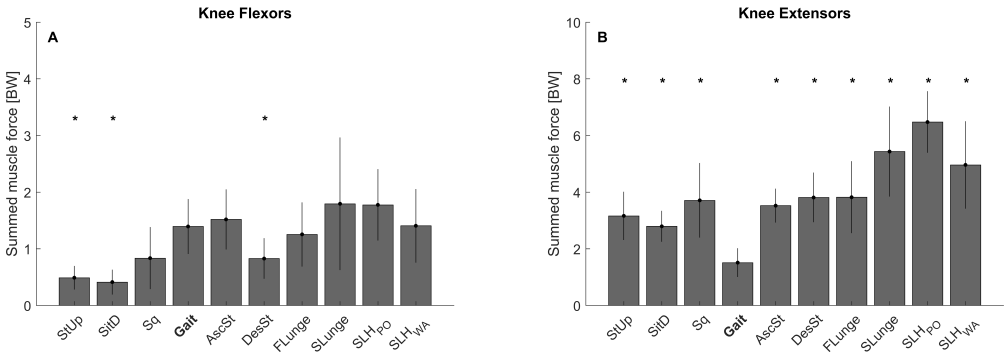

Figure 3.7: Summed muscle force of the knee flexors (A) and knee extensors (B) during each exercise. * Indicates a significant difference between the muscle forces compared to gait (α_{bc}=0.0056). SitD: sit down, StUp: stand up, AscSt: ascending stairs, DesSt: descending stairs, Sq: squat, FLunge: forward lunge, SLunge: sideward lunge, SLHwa: single leg hop weight acceptance, SLHpo: single leg hop push-off.

Discussion

This study evaluated knee loading, in terms of contact forces (CF) and shear forces during nine CKC exercises. Most of the studied functional exercises are commonly used in lower-limb rehabilitation. Estimated loading on the tibiofemoral and patellofemoral joints can then be used to grade different exercises and provide insights for the staging of rehabilitation programs following knee injury or surgical intervention. During rehabilitation, the challenge is to protect the joint structures from excessive forces, while providing sufficient stimuli to regain muscle control and strength to restore normal function.

Tibiofemoral CFs were higher during all exercises compared to gait, except for sit down, stand up and even stair ascent, descent and squatting. Interestingly, although these exercises required higher knee flexion ROM, tibiofemoral CFs equal or lower compared to gait were observed. A similar finding was previously observed using instrumented implants and can be explained by the bilateral support, distributing the bodyweight over both legs, during these exercises and by the lack of foot-floor impact[21,38,39]. Consequently, these exercises can be used to train quadriceps muscle early in rehabilitation without exposing high CF to the tibiofemoral joint. All exercises imposed higher patellofemoral CFs compared to gait. As all exercises required deeper knee flexion and therefore resulted in more quadriceps involvement, higher compression of the patella against the femur by the quadriceps resulted in higher patellofemoral CFs (figure 3.8)[40–42].

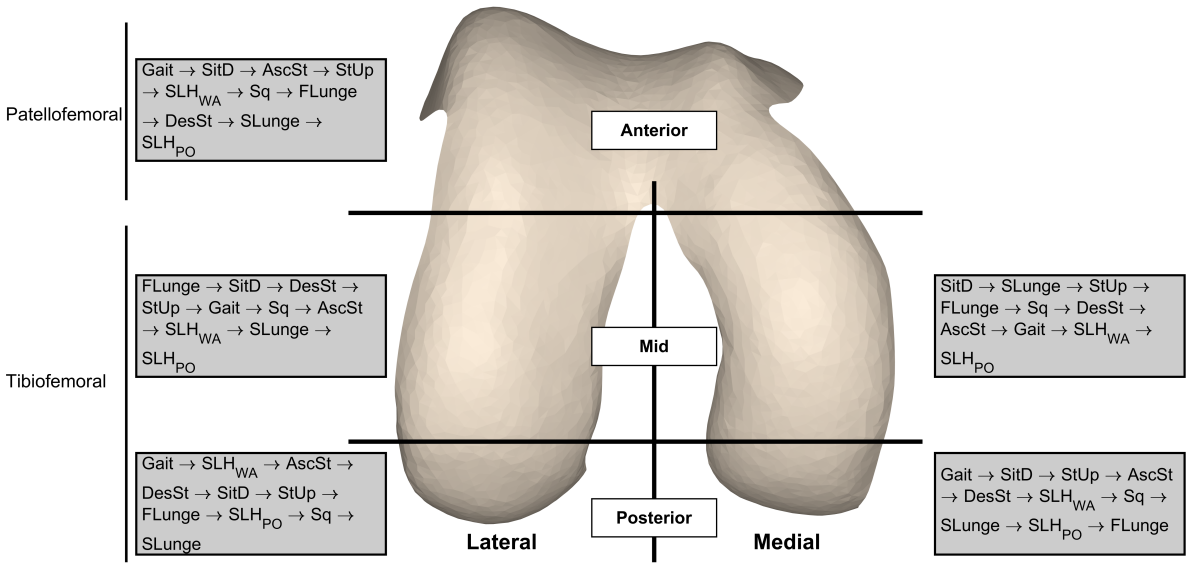

Figure 3.8: Graded exercise sequences dependent on compartment involvement based on local loading (i.e. average maximum zonal femoral force). SitD: sit down, StUp: stand up, AscSt: ascending stairs, DesSt: descending stairs, Sq: squat, FLunge: forward lunge, SLunge: sideward lunge, SLHwa: single leg hop weight acceptance, SLHpo: single leg hop push-off.

A redistribution of CFs over the condyles was observed between exercises. During gait, the majority of the CF passes through the medial condyle [38,43,44], comparable to stair ascent and descent, forward lunge and single leg hop. In contrast, CFs were higher on the lateral than medial condyle during stand up, sit down, squat and sideward lunge. These observations confirm that, in our healthy cohort with uncorrected movement behavior, differential loading of a specific compartment can be achieved by careful and selective exercise selection. Consequently, shear forces on a specific compartment could also be diminished. For instance, for patients with unicompartmental tibiofemoral blunt trauma, strengthening exercises should be selected that avoid overloading the injured condyle. More specifically, forward lunges and walking stairs reduced forces on the lateral compartment and squat and sideward lunges to reduced forces on the medial compartment (figure 3.8). Furthermore, in exercises with more knee flexion (e.g. lunging and squat), the average maximum femoral force was distributed more towards the posterior zone of the condyles, than the mid zone, whereas the mid zone represents the weight-bearing zone of the femoral condyle[37]. Similar findings were previously measured in knee kinematics using fluoroscopy showing more posteriorly located tibiofemoral contact points during deep knee flexion[45–47].

As the repair site is most vulnerable in the first months after surgical intervention (e.g. ACL reconstruction or cartilage repair), it is advisable to initially avoid excessive shear forces[1,2,48,49]. Therefore, exercises presenting high shear forces, should be incorporated wisely in a rehabilitation program. During all therapeutic exercises, shear forces on the lateral condyle were significantly higher than during gait, due to the increased CFs in the lateral compartment. Only forward lunge and single leg hop presented increased medial and lateral shear forces, compared to gait due to the increased medial and lateral CFs. Therefore, inclusion these exercises characterized by high CFs and accompanying shear forces in both compartments should be carefully timed in rehabilitation.

Restoration of muscle strength is one of the key elements for successful rehabilitation, requiring exercises that appropriately recruit the knee musculature[1,2,16]. All exercises resulted in significantly higher knee extensor force production and consequently can be used to train the quadriceps muscles. On the other hand, none of the exercises increased knee flexor muscle force production, indicating that other exercises need to be included to train the knee flexor musculature.

While these results provide important insights into knee loading during several exercises, they should be interpreted with respect to several limitations. First, healthy persons were studied during unconstrained motion. In reality, a physical therapist will control the movement execution or patients may adapt movement patterns to avoid pain and therefore influence knee loading. Secondly, the elastic foundation model did not allow for the direct calculation of local shear forces. Instead, the components of the resultant force on each compartment were interpreted in relation to the cartilage curvature. Therefore, the effect of friction or tissue deformation is neglected by which the estimated magnitude of the shear forces may be underestimated. The presented approach assumes that geometry is the major contributor to shear and therefore, the relative comparison between exercises will not be affected. Third, neutral joint alignment was assumed for all participants. In patients with severe deformities or suffering from gross knee instability, this assumption may no longer be valid and could affect the force distribution over the medial and lateral condyle. Lastly, the model used in the current study comprises a generic knee model, with a uniformly distributed cartilage thickness. Therefore, the effect of physiologic variation in cartilage thickness on contact pressures and forces is not included in the current analysis given the use of a generic uniform mesh. Despite these limitations, the estimated CFs were in line with the previously reported CFs measured with instrumented implants[21,22,39,47]. The higher CFs compared to other studies could possibly be explained by the inclusion of healthy young adults compared to the total knee replacement population used as a reference in the other studies[22,47,50].

The results of this study have the potential to contribute to biomechanically informed rehabilitation programs and can be used for conceptualizing an individualized rehabilitation program in which several factors as rehabilitation goal, injury location, surgical intervention and tissue repair status can be accounted for. A comprehensive overview of exercise grading based on the loading of different zones is proposed in figure 3.8. All exercises can be used to train knee extensor musculature, as they resulted in higher knee extensor muscle force production compared to gait. However, to account jointly for the status of the repair tissue and to optimally train the knee extensor muscles, squat, stand up and sit down can be introduced already early in rehabilitation. Since, these exercises result in CFs lower than gait while providing an adequate training stimulus for the knee extensors. This in contrast to the clinicians' perception that squatting results in high knee loading, therefore being mostly included after full weight-bearing is allowed[1,4]. Furthermore, careful exercise selection allows avoiding the location of the injured or repaired site as differential compartment loading can be achieved through careful selection of exercises. Indeed, forward lunges resulted in more medial loading compared to lateral loading, whereas the opposite was found during squat or sideward lunge. Consequently, individual exercises can be introduced depending on injury location rather than a clinical appreciation of loading. Likewise, in case of lesions or repair surgery to the posterior part of the femoral condyles, the amount of knee flexion during lunges and squats should be restricted as high knee flexion angles impose excessive forces and detrimental shear forces. Furthermore, in the case of patellofemoral lesions or repair surgery, exercises should only gradually be introduced as they all resulted in increased patellofemoral CFs and accompanying shear forces.

Conclusion

The present study analyzed cartilage loading during functional activities and exercises and provide useful insight for the design of evidence based rehabilitation programs. By thoughtful selection of functional exercises, loading and shear forces in particular can be reduced at a knee specific location or within a full knee compartment. Consequently, inclusion of strengthening exercises can be scheduled more easily and may result in less knee joint reactivity.

References

1. Hambly K, Bobic V, Wondrasch B, Van Assche D, Marlovits S. Autologous chondrocyte implantation postoperative care and rehabilitation: science and practice. Am J Sports Med. 2006;34: 1020–38.
2. Hirschmüller A, Baur H, Braun S, Kreuz PC, Südkamp NP, Niemeyer P. Rehabilitation after autologous chondrocyte implantation for isolated cartilage defects of the knee. Am J Sports Med. 2011;39: 2686–96.
3. Assche D Van, Caspel D Van, Staes F, Saris DB, Bellemans J, Vanlauwe J, et al. Implementing one standardized rehabilitation protocol following autologous chondrocyte implantation or microfracture in the knee results in comparable physical therapy management. Physiother Theory Pract. 2011;27: 125–36.
4. Edwards PK, Ackland T, Ebert JR. Clinical Rehabilitation Guidelines for Matrix-induced Autologous Chondrocyte Implantation (MACI) on the Tibiofemoral Joint. J Orthop Sports Phys Ther. 2013;44: 102–119.
5. Stuart MJ, Meglan D a, Lutz GE, Growney ES, An KN. Comparison of intersegmental tibiofemoral joint forces and muscle activity during various closed kinetic chain exercises. Am J Sports Med. 1996;24: 792–799.
6. McGinty G, Irrgang JJ, Pezzullo D. Biomechanical considerations for rehabilitation of the knee. Clin Biomech. 2000;15: 160–166.
7. Edwards PK, Ackland TR, Ebert JR. Accelerated weightbearing rehabilitation after matrix-induced autologous chondrocyte implantation in the tibiofemoral joint: early clinical and radiological outcomes. Am J Sports Med. 2013;41: 2314–24.
8. Escamilla RF, Macleod TD, Wilk KE, Paulos L, Andrews JR. ACL strain and tensile forces for weight bearing and non—weight-bearing exercises after ACL reconstruction: A guide to exercise selection. J Orthop Sport Phys Ther. 2012;42: 208–220.
9. Ackermann B, Steinmeyer J. Collagen biosynthesis of mechanically loaded articular cartilage explants. Osteoarthr Cartil. 2005;13: 906–914.
10. Moger CJ, Arkill KP, Barrett R, Bleuet P, Ellis RE, Green EM, et al. Cartilage collagen matrix reorientation and displacement in response to surface loading. J Biomech Eng. 2009;131: 31008.
11. Cavanaugh JT, Killian SE. Rehabilitation following meniscal repair. Curr Rev Musculoskelet Med. 2012;5: 46–58.
12. Kvist J, Gillquist J. Sagittal plane knee translation and electromyographic activity during closed and open kinetic chain exercises in anterior cruciate ligament-deficient patients and control subjects. Am J Sports Med. 2001;29: 72–82.
13. Norouzi S, Esfandiarpour F, Shakourirad A, Salehi R, Akbar M, Farahmand F. Rehabilitation after ACL injury: A fluoroscopic study on the effects of type of exercise on the knee sagittal plane arthrokinematics. Biomed Res Int. 2013;2013.
14. van Grinsven S, van Cingel REH, Holla CJM, van Loon CJM. Evidence-based rehabilitation following anterior cruciate ligament reconstruction. Knee Surgery, Sport Traumatol Arthrosc. 2010;18: 1128–1144.
15. Yabroudi MA, Irrgang JJ. Rehabilitation and Return to Play After Anatomic Anterior Cruciate Ligament Reconstruction. Clin Sports Med. 2013;32: 165–175.
16. Begalle RL, Distefano LJ, Blackburn T, Padua D a. Quadriceps and hamstrings coactivation during common therapeutic exercises. J Athl Train. 2012;47: 396–405.
17. Eitzen I, Grindem H, Nilstad A, Moksnes H, Risberg MA. Quantifying Quadriceps Muscle Strength in Patients With ACL Injury, Focal Cartilage Lesions, and Degenerative Meniscus Tears: Differences and Clinical Implications. Orthop J Sport Med. 2016;4: 1–10.
18. Ebert JR, Lloyd DG, Wood DJ, Ackland TR. Isokinetic knee extensor strength deficit following matrix-induced autologous chondrocyte implantation. Clin Biomech (Bristol, Avon). 2012;27: 588–94.
19. Løken S, Ludvigsen TC, Høysveen T, Holm I, Engebretsen L, Reinholt FP. Autologous chondrocyte implantation to repair knee cartilage injury: ultrastructural evaluation at 2 years and long-term follow-up including muscle strength measurements. Knee Surg Sports Traumatol Arthrosc. 2009;17: 1278–88.
20. Ebert JR, Fallon M, Zheng MH, Wood DJ, Ackland TR. A randomized trial comparing accelerated and traditional approaches to postoperative weightbearing rehabilitation after matrix-induced autologous chondrocyte implantation: findings at 5 years. Am J Sports Med. 2012;40: 1527–37.
21. D'Lima DD, Patil S, Steklov N, Slamin JE, Colwell CW. Tibial forces measured in vivo after total knee arthroplasty. J Arthroplasty. 2006;21: 255–262.

22. Fregly BJ, Besier TF, Lloyd DG, Delp SL, Banks S a, Pandy MG, et al. Grand challenge competition to predict in vivo knee loads. J Orthop Res. 2012;30: 503–13.

23. Smith CR, Vignos MF, Lenhart RL, Kaiser J, Thelen DG. The Influence of Component Alignment and Ligament Properties on Tibiofemoral Contact Forces in Total Knee Replacement. J Biomech Eng. 2016;138: 1–10.

24. Mithoefer K, Hambly K, Logerstedt D, Ricci M, Silvers H, Della Villa S. Current concepts for rehabilitation and return to sport after knee articular cartilage repair in the athlete. J Orthop Sports Phys Ther. 2012;42: 254–73.

25. Davis RB, Ounpuu S, Tyburski D, Gage JR. A gait analysis data collection and reduction technique. Hum Mov Sci. 1991;10: 575–587.

26. Lenhart RL, Kaiser J, Smith CR, Thelen DG. Prediction and Validation of Load-Dependent Behavior of the Tibiofemoral and Patellofemoral Joints During Movement. Ann Biomed Eng. 2015;43: 2675–2685.

27. Arnold EM, Ward SR, Lieber RL, Delp SL. A model of the lower limb for analysis of human movement. Ann Biomed Eng. 2010;38: 269–79.

28. Smith RC, Choi KW, Negrut D, Thelen DG. Efficient Computation of Cartilage Contact Pressures within Dynamic Simulations of Movement. Comput Methods Biomech Biomed Eng Imaging Vis. 2016;

29. Hudelmaier M, Glaser C, Englmeier K-H, Reiser M, Putz R, Eckstein F. Correlation of knee-joint cartilage morphology with muscle cross-sectional areas vs. anthropometric variables. Anat Rec Part A. 2003;270: 175–184.

30. Eckstein F, Reiser M, Englmeier KH, Putz R. In vivo morphometry and functional analysis of human articular cartilage with quantitative magnetic resonance imaging–from image to data, from data to theory. Anat Embryol (Berl). 2001;203: 147–73.

31. Draper CE, Besier TF, Gold GE, Fredericson M, Fiene A, Beaupre GS, et al. Is cartilage thickness different in young subjects with and without patellofemoral pain? Osteoarthr Cartil. 2006;14: 931–937.

32. Blankevoort L, Kuiper JH, Huiskes R, Grootenboer HJ. Articular contact in a three-dimensional model of the knee. J Biomech. 1991;24: 1019–1031.

33. Li G, Lopez O, Rubash H. Variability of a Three-Dimensional Finite Element Model Constructed Using Magnetic Resonance Images of a Knee for Joint Contact Stress Analysis. J Biomech Eng. 2001;123: 341–346.

34. Adouni M, Shirazi-Adl A. Partitioning of Knee Joint Internal Forces in Gait Is Dictated By the Knee Adduction Angle and Not By the Knee Adduction Moment. J Biomech. Elsevier; 2014;47: 1696–703.

35. Lu TW, O'Connor JJ. Bone position estimation from skin marker co-ordinates using global optimisation with joint constraints. J Biomech. 1999;32: 129–134.

36. Thelen DG, Won Choi K, Schmitz AM. Co-simulation of neuromuscular dynamics and knee mechanics during human walking. J Biomech Eng. 2014;136: 21033.

37. Peterfy CG, Guermazi a., Zaim S, Tirman PFJ, Miaux Y, White D, et al. Whole-organ magnetic resonance imaging score (WORMS) of the knee in osteoarthritis. Osteoarthr Cartil. 2004;12: 177–190.

38. D'Lima DD, Steklov N, Patil S, Colwell CW. The Mark Coventry award: In vivo knee forces during recreation and exercise after knee arthroplasty. Clin Orthop Relat Res. 2008;466: 2605–2611.

39. Kutzner I, Heinlein B, Graichen F, Bender a., Rohlmann a., Halder a., et al. Loading of the knee joint during activities of daily living measured in vivo in five subjects. J Biomech. Elsevier; 2010;43: 2164–2173.

40. Escamilla R. Knee biomechanics of the dynamic squat exercise. Med Sci Sports Exerc. 2001; 127–141.

41. Lynn S, Noffal G. Lower Extremity Biomechanics During a Regular and Counterbalanced Squat. J Strength Cond Res. 2012;26: 2417–2425.

42. Chinkulprasert C, Vachalathiti R, Powers CM. Patellofemoral joint forces and stress during forward step-up, lateral step-up, and forward step-down exercises. J Orthop Sports Phys Ther. 2011;41: 241–248.

43. Schipplein OD, Andriacchi TP. Interaction between active and passive knee stabilizers during level walking. J Orthop Res. 1991;9: 113–119.

44. Kutzner I, Heinlein B, Dymke J, Bender A, Halder AM, Bergmann G. The effect of valgus braces on medial compartment load of the knee joint - in vivo load measurements in three subjects. J Biomech. 2011;44: 1354–1360.

45. Yamaguchi S, Gamada K, Sasho T, Kato H, Sonoda M, Banks S a. In vivo kinematics of anterior cruciate ligament deficient knees during pivot and squat activities. Clin Biomech. Elsevier Ltd; 2009;24: 71–6.

46. Qi W, Hosseini A, Tsai T-Y, Li J-S, Rubash HE, Li G. In vivo kinematics of the knee during weight bearing high flexion. J Biomech. Elsevier; 2013;46: 1576–82.

47. D'Lima DD, Steklov N, Fregly BJ, Banks S a., Colwell CW. In vivo contact stresses during activities of daily living after knee arthroplasty. J Orthop Res. 2008;26: 1549–1555.

48. Woo SLY, Chan SS, Yamaji T. Biomechanics of knee ligament healing, repair and reconstruction. J Biomech. 1997;30: 431–439.

49. Van Ginckel A, Verdonk P, Victor J, Witvrouw E. Cartilage status in relation to return to sports after anterior cruciate ligament reconstruction. Am J Sport Med. 2013;41: 550–559.

50. D'Lima DD, Fregly BJ, Patil S, Steklov N, Colwell CW. Knee joint forces: prediction, measurement, and significance. Proc Inst Mech Eng H. 2012;226: 95–102.

Supplementary material

Studied exercises

Five repetitions of the following exercises were measured. For each exercise, the load-bearing phase was analyzed.

- **Gait:** walking at self-selected speed across the motion lab (8m). A trial was successful, when each foot strike was on a separate force plate. Only the stance phase was analyzed and was defined as the period during which the vertical component of the ground reaction force exceeded 20N.
- **Stair ascending (AscSt):** ascending a standard four step staircase (step height = 0.16m and tread length = 0.31m) at self-selected speed. Only the stance phase was analyzed and was defined as the period during which the vertical component of the ground reaction force exceeded 20N.
- **Stair descending (DesSt):** descending a standard four step staircase (step height = 0.16m and tread length = 0.31m) at self-selected speed. Only the stance phase was analyzed and was defined as the period during which the vertical component of the ground reaction force exceeded 20N.
- **Stand up (StUp)** rising from a chair without using the arms to full standing position. A backless and armless chair was used and chair height was standardized to the height of the lateral femoral knee marker. Both feet and the chair were placed on a different force plate. Stand up was analyzed from the instantaneous minimum in the vertical ground reaction force under the feet, till the vertical ground reaction force started to fluctuate around bodyweight. Starting from the instant of maximum peak vertical ground reaction force above body weight, thereafter the ground reaction force decreases below body weight until it again increased. The subsequent maximum was defined as the end of stand up.
- **Sit Down (SitD):** sitting on a chair from full standing without using the arms. Sit down was analyzed from the first 1,5% decrease in ground reaction force under the feet till the instantaneous minimum in ground reaction force after maximum ground reaction force.
- **Squat (Sq):** squat down from upright standing to 90° self-perceived knee flexion and rise back. Participants started in upright standing, with arms fixed in the loin and both feet on a separate force plate. The squat was analyzed from first 1,5% decrease in vertical ground reaction force till stabilizing in a zone around 1,5% of the ground reaction force.
- **Forward lunge (FLunge):** from upright standing with arms in scapular plane, stepping forward onto a separate force plate, lowering the body till the trailing knee touches the ground and returning to starting position. Step length was standardized to 80% of the leg length. Forward lunge was analyzed when the stepping leg had contact with the force plate determined as the period when the vertical ground reaction force exceeded 20N.
- **Sideward lung (SLunge):** from upright standing with arms in scapular plane, stepping sideward onto a separate force plate, lowering the body till approximately 90° knee flexion in the stepping leg and returning to start position. Step length was standardized to 80% of the leg length. Sideward lunge was analyzed when the stepping leg had contact with the force plate determined as the period when the vertical ground reaction force exceeded 20N.
- **Single leg hop (SLH):** performing a single leg hop with the arms fixed in the loin. Single leg

hop was analyzed during two phases i.e. the push-off phase (SLH_{po}) and weight-acceptance phased (SLH_{wa}). SLH_{po} ranged from the minimal vertical position of the sacrum marker till release of the force plate, determined as the vertical ground reaction force below 20N. SLH_{wa} ranged from ground contact (vertical ground reaction force exceeds 20N) till minimum in vertical position of the sacrum marker.

Division of cartilage in different zones

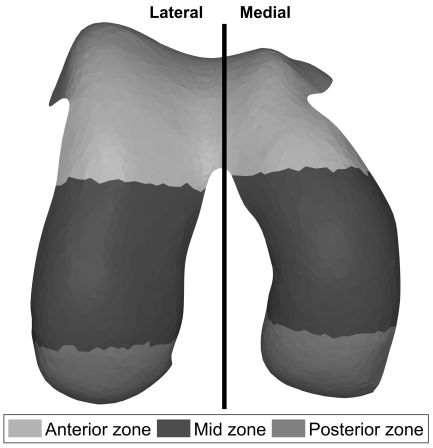

Figure 3.9: **Supplementary figure 1.**
Division of the femoral cartilage in three zones, based on the method proposed by Peterfy et al., 2004. The anterior zone was defined as the zone before the anterior end of the intercondylar notch. The mid zone was defined as the area between the anterior end of the intercondylar notch and 60% of the distance to the most posterior end of the femoral condyle. And the posterior zone was defined as the area behind the line at 60% of the distance to the most posterior end of the condyle. For the analysis of the patellofemoral contact pressure, the zones of the medial and lateral condyle were combined.

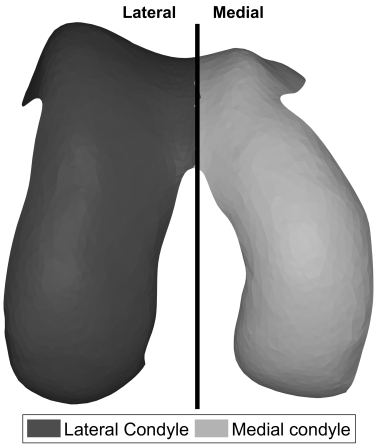

Figure 3.10: **Supplementary figure 2.**
Division of the femoral cartilage in a medial and lateral compartment.

Average trunk angles

Table 3.1: Average trunk angles

	Average			Minimum			Maximum			Range of Motion		
	Trunk flexion	Trunk bending	Trunk rotation	Trunk flexion	Trunk bending	Trunk rotation	Trunk flexion	Trunk bending	Trunk rotation	Trunk flexion	Trunk bending	Trunk rotation
StUp	-25.03°± 11.3	-0.01°± 0.5	0.45°± 0.2	-41.11°± 8.3	-2.03°± 2.3	-1.37°± 3	-7.71°± 5.2	2.11°± 2.5	2.36°± 2.7	33.4°± 6.3	4.14°± 2.2	3.73°± 1.2
SitD	-25.03°± 11.3	-0.01°± 0.5	0.45°± 0.2	-41.11°± 8.3	-2.03°± 2.3	-1.37°± 3	-7.71°± 5.2	2.11°± 2.5	2.36°± 2.7	33.4°± 6.3	4.14°± 2.2	3.73°± 1.2
Sq	-21.44°± 9.2	0.18°± 0.2	-0.05°± 0.4	-35.29°± 9.7	-1.83°± 1.6	-2.8°± 4	-6.07°± 5.3	2.84°± 3.7	3.53°± 3.8	29.22°± 8.8	4.67°± 2.8	6.33°± 3.1
Gait	-10.23°± 0.7	1.6°± 3.3	1.35°± 6.8	-12.49°± 6	-6.34°± 2.7	-9.53°± 2.9	-8.32°± 6.1	6.96°± 2.2	10.04°± 4.9	4.17°± 1.5	13.29°± 1.8	19.56°± 5.4
AscSt	-13.55°± 1	-0.22°± 6.2	0.29°± 1.5	-15.91°± 6.2	-9.13°± 2.9	-3.26°± 3.3	-11.16°± 6.3	8.63°± 3.1	2.78°± 2.3	4.75°± 1.3	17.76°± 4.6	6.05°± 2.2
DesSt	-9.82°± 1.5	0.21°± 3.3	1.41°± 1.7	-12.51°± 6.3	-5.67°± 2.7	-3.26°± 3	-6.42°± 6.1	5.7°± 2.2	4.56°± 2.3	6.09°± 1.7	11.37°± 3.3	7.82°± 3
FLunge	-11.54°± 1.5	6.78°± 2.3	2.83°± 1.4	-14.96°± 5.9	-0.74°± 2.4	-2.63°± 7.7	-6.03°± 4.8	10.02°± 4.5	5.22°± 7.8	8.94°± 3	10.75°± 4.4	7.84°± 3.4
SLunge	-14.87°± 2.9	-0.8°± 1.5	2.53°± 2.3	-19.5°± 8.1	-5.95°± 3.7	-3.15°± 3.8	-7.39°± 5.5	3.29°± 7	7.07°± 4.4	12.12°± 5	9.25°± 5.4	10.22°± 4.2
SLHpo	-21.98°± 4.3	3.74°± 8.2	4.27°± 2.1	-28.25°± 10.8	-11.83°± 5.6	-3.3°± 6.6	-13.47°± 5.8	12.77°± 7	10.02°± 6.8	14.78°± 8.7	24.61°± 9.1	13.32°± 6.3
SLHwa	-17.43°± 2.4	-0.04°± 3.8	-0.65°± 0.5	-20.94°± 10.2	-6.3°± 3	-3.53°± 5.3	-13.18°± 7.4	4.8°± 5.2	1.97°± 7.7	7.76°± 5.8	11.1°± 4.2	5.49°± 4.9

Supplementary table 1: Average, minimum, maximum and range of motion of the trunk angles (± standard deviation) during each exercise. Trunk flexion: negative value indicates flexion, positive extension. Trunk bending: negative value indicates contralateral bending, positive ipsilateral bending. Trunk rotation: negative value indicates ipsilateral rotation, positive contralateral rotation.

Animation of the exercises

Movies of a representative subject are provided with the according pressure patterns and the contact force.

Un-normalized zonal pressure results

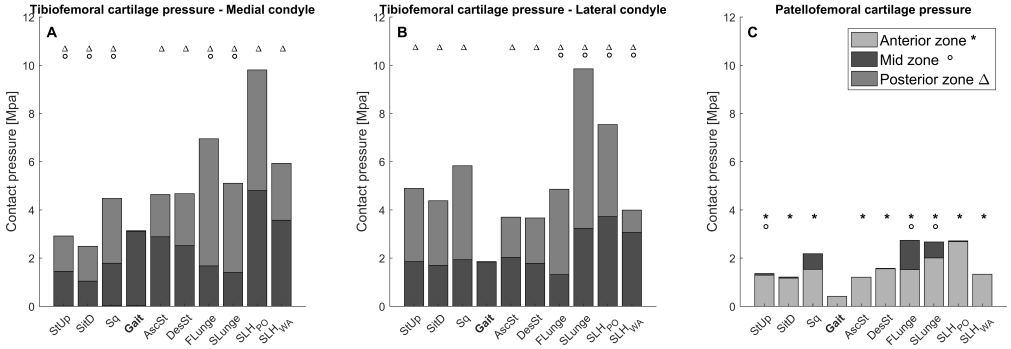

Figure 3.11: **Supplementary figure 3.** The average maximum tibiofemoral pressure on the anterior (light gray), mid (dark gray) and posterior (gray) zone of the medial condyle (A) and lateral condyle (B). The average maximum patellofemoral pressure on the anterior (green), mid (purple) and posterior (red) zone of the femur. $\star\star$, $\circ$ and Δ indicates a significant difference in anterior, mid or posterior zone pressure, respectively compared to gait (α_{bc}=0.0056).

Chapter 4

Knee cartilage thickness, T1ρ and T2 relaxation time are related to articular cartilage loading in healthy adults

Sam Van Rossom, Colin R Smith, Lianne Zevenbergen, Darryl G Thelen, Benedicte Vanwanseele, Dieter Van Assche, Ilse Jonkers

Published in *PLoS One*(2017),12 (1)

Abstract

Cartilage is responsive to the loading imposed during cyclic routine activities. However, the local relation between cartilage in terms of thickness distribution and biochemical composition and the local contact pressure during walking has not been established. The objective of this study was to evaluate the relation between cartilage thickness, proteoglycan and collagen concentration in the knee joint and knee loading in terms of contact forces and pressure during walking.

3D gait analysis and MRI (3D-FSE, $T1\rho$ relaxation time and T2 relaxation time sequence) of fifteen healthy subjects were acquired. Experimental gait data was processed using musculoskeletal modeling to calculate the contact forces, impulses and pressure distribution in the tibiofemoral joint. Correlates to local cartilage thickness and mean $T1\rho$ and T2 relaxation times of the weight-bearing area of the femoral condyles were examined.

Local thickness was significantly correlated with local pressure: medial thickness was correlated with medial condyle contact pressure and contact force, and lateral condyle thickness was correlated with lateral condyle contact pressure and contact force during stance. Furthermore, average $T1\rho$ and T2 relaxation time correlated significantly with the peak contact forces and impulses. Increased $T1\rho$ relaxation time correlated with increased shear loading, decreased $T1\rho$ and T2 relaxation time correlated with increased compressive forces and pressures.

Thicker cartilage was correlated with higher condylar loading during walking, suggesting that cartilage thickness is increased in those areas experiencing higher loading during a cyclic activity such as gait. Furthermore, the proteoglycan and collagen concentration and orientation derived from $T1\rho$ and T2 relaxation measures were related to loading.

Keywords: Cartilage thickness · Gait · $T1\rho$ · T2 · Contact force · Motion analysis · Knee

Introduction

Healthy cartilage is essential for optimal joint function as it distributes loading and reduces friction between articulating bones. Mechanical factors are known to influence cartilage homeostasis, and are therefore essential for the maintenance of cartilage health[1–3]. In order to better understand the role of loading on the pathomechanics of degenerative cartilage diseases, such as osteoarthritis (OA), it is important to understand the influence of mechanical factors on the thickness and composition of cartilage.

Cartilage thickness has been used as an in-vivo measure of cartilage health. Previous research found that cartilage adapts to chronic loading patterns occurring during walking[4]. Increased cartilage volume was found with increased physical activity level in healthy children and with increased muscle cross-sectional area in healthy adults[5,6]. A positive correlation between knee external adduction moment (KAM) and medial cartilage thickness or medial to lateral thickness ratio in a cohort of healthy adults was reported[7–9]. Knee and shoulder cartilage thinning was observed in paraplegic patients due to unloading[10,11]. This shows that cartilage is sensitive to mechanical stimuli during routine daily life activities. Additionally, it was suggested that cyclic and repetitive loading patterns, during walking in particular, dominate the biologic and structural response of cartilage[8]. Indeed, knee flexion angle at heel strike was correlated with the thickness distribution of the medial femur condyle and the thickest region of cartilage was found to coincide with the contact region at heel strike[8,12]. Therefore, they hypothesized that cartilage was thicker in the load-bearing regions of the knee as a long term adaptation to the high compressive forces at heel strike[4,12,13].

In the past, external joint moments were used to estimate knee loading and to analyze the relationship with cartilage thickness. However, as external moments represent the combined effects of muscle, ligament and cartilage contact forces, they do not explicitly characterize the internal loads acting on the cartilage. While these forces cannot be measured in-vivo, novel musculoskeletal modeling techniques allow estimation of muscle and ligament forces and consequently knee contact forces and even local contact pressure[14,15]. As a result, a more detailed description of joint loading can now be provided to explore the correlation with local cartilage structural properties.

Structural changes in cartilage are often preceded by changes in biochemical composition[16–18]. Initial cartilage deterioration induces loss of proteoglycans and increases in water content in combination with disorganization and loss of the collagen matrix[19]. Advancements in magnetic resonance (MR) imaging and more specific $T1\rho$ and T2 mapping have been used to identify these early changes in matrix-composition. Increased $T1\rho$ relaxation time, as observed in OA patients, is related to proteoglycan loss, whereas increased T2 relaxation time is related to collagen deterioration and disorganization[20–24]. These relaxation times can therefore be used to evaluate cartilage condition and biologic response to loading. Indirect estimates of loading were previously used to evaluate the relation with cartilage composition. No differences in $T1\rho$ or T2 relaxation times between healthy active and sedentary adults were found[22]. Six weeks of unloading resulted in significantly increased $T1\rho$ and T2 relaxation times, suggesting that changes in the biochemical composition result from unloading. However $T1\rho$ and T2 values were restored to baseline after 4 weeks of weight-bearing[25]. A decrease in T2 relaxation time was found after a standardized training period [26,27]. $T1\rho$ relaxation times were increased after running a marathon[28]. This showed that loading could possibly modify cartilage composition. A higher ratio of the quadriceps medial to lateral cross-sectional area was found to relate to higher frontal plane loading during walking and higher $T1\rho$ and T2 relaxation times for the whole joint complex, however the relation between frontal plane loading and $T1\rho$ and T2 relaxation

times was not directly tested[29]. Thus, there is no confirmed association between cartilage composition and increased frontal plane loading. Acute compressive loading resulted in a significant decreased $T1\rho$ and T2 relaxation time of the medial condyle in healthy adults[30]. Furthermore, $T1\rho$ and T2 relaxation times were found to be lower in healthy persons subjected to higher sagittal plane moments during a drop jump, suggesting a protective response of cartilage to loading[31]. However healthy subjects with higher KAM, and thus increased frontal plane loading during the drop jump presented elevated $T1\rho$ values in the medial compartment compared to the lateral compartment[31]. These in-vivo findings suggest that joint loads exceeding the physiological weight-bearing capacity of cartilage might induce cartilage degeneration[32]. In support of these in-vivo findings, in-vitro studies also demonstrated that mechanical loading can promote either synthesis or breakdown of the cartilage components depending on loading regimes[33,34]. Furthermore, animal experiments showed that the cartilage composition and mechanical properties adapt to mechanical stimulation[35]. Although indirect evidence exists that cartilage thickness and biochemical composition relate to loading, none of these studies related structural and biochemical outcome parameters to local cartilage loading in a whole joint complex during functional activities.

This exploratory study relates local femoral cartilage thickness and biochemical composition to cartilage tissue loading during walking. MR imaging was used to measure cartilage thickness, proteoglycan and collagen content, while a multibody musculoskeletal model was used to estimate cartilage contact pressures. Higher cartilage loading is expected to relate to increased thickness and to lower $T1\rho$ and T2 relaxation times, indicative for a higher proteoglycan and collagen concentration and orientation.

Materials and methods

Subjects

Fifteen healthy subjects, with no history of knee injuries were recruited to participate in the current study Table 4.1. Experimental motion analysis data and MR-images of all participants were acquired on the same day (mean time between motion analysis and MR-acquisition = 2h). An overview of the overall study design is provided in figure 4.1. All procedures were approved by the university hospital Leuven ethics committee (s56093) and informed written consent was obtained from all participants.

Motion analysis

Data collection

A 10-camera Vicon system (Vicon, Oxford Metrics 100Hz) was used to capture three-dimensional marker positions during gait. Synchronously, ground reaction forces were captured using two force plates embedded in the walkway (AMTI, Watertown, USA, 1000Hz). Retro-reflective markers were placed according to an extended Plug-in-Gait marker set (S1 Fig)[36]. After a static calibration trial, participants were instructed to walk barefoot at their habitual walking speed (mean walking speed = 1.39 $\pm$ 0.12 m/s, range 1.19 – 1.59m/s) across the motion lab (8m). Three trials with valid force plate contact were captured and retained for further processing. Ground reaction forces were filtered using a second order Butterworth low pass filter, with cut-off level at 30Hz and marker positions were filtered using a smoothing spline with cut-off at 6Hz before entering the musculoskeletal modeling workflow.

Table 4.1: Patient characteristics

Demographics	
Gender	8 Male/7 Female
Weight	70.49 ± 7.24 kg
Height	1.77 ± 0.06 m
Age	30.73 ± 5.84 years
Dominant leg	13 Right /2 Left
Walking speed	1.39 ± 0.12 m/s
First peak GRF	765.07 ± 85.93 N
Second peak GRF	791.55 ± 86.01 N
Alignment*	183.87 ± 2.18°
Leg difference	0.0068 ± 0.0044 m

∗Alignment of the anatomical axis was determined on lying MRI, values $> 180°$ indicate valgus.

Musculoskeletal modeling

Muscle and knee contact forces were estimated using a scaled 3D musculoskeletal model that has been presented previously[37]. A customized knee joint allowing 6 degrees of freedom (DoF) tibiofemoral and patellofemoral joint kinematics was implemented in a generic lower extremity model[38]. The model included 44 musculotendon actuators spanning the right hip, knee and ankle. Additionally, 14 bundles of non-linear springs represented the major knee ligaments and capsule. Cartilage contact pressure was calculated using a non-linear elastic foundation formulation that calculates the local contact pressure based on the penetration depth between overlapping cartilage surface meshes[39]. Uniform cartilage thickness distribution was assumed in both joints, with a combined thickness of 4mm and 7mm in the tibiofemoral and patellofemoral joint respectively. An elastic modulus of 10MPa and a Poisson's ratio of 0.45 was defined for the cartilage[40,41]. The lower extremity model was implemented in SIMM with the Dynamics Pipeline (Musculographics Inc., Santa Rosa, CA) and SD/Fast (Parametric Technology Corp., Needham, MA) used to generate the multibody equations of motion[42].

After scaling the generic model to the subjects' anthropometry, joint angles were calculated using inverse kinematics[43]. Next, the muscle activations and secondary knee kinematics (11 DoF), required to reproduce the measured primary hip, knee and ankle accelerations were computed using the concurrent optimization of muscle activations and kinematics (COMAK) algorithm[39]. Only the knee flexion angle was prescribed during the optimization, while secondary tibiofemoral and all patellofemoral DoF evolved as a function of muscle, ligament and contact forces[37,39,44].

For each trial, the timing of the two peaks of the resultant tibiofemoral contact force during the stance phase was determined and the coinciding mean and maximal contact pressures, contact areas, as well as the components of the contact forces expressed in the femur reference frame were analyzed. Furthermore, the impulse of the contact forces and the average contact pressure over the whole stance phase was calculated. These load describing parameters were not normalized to bodyweight nor dimensions, as this represents a more physiological estimate of tissue level loading. All variables were analyzed for the medial, lateral and combined femoral condyle(s) for each trial and then averaged over the three trials.

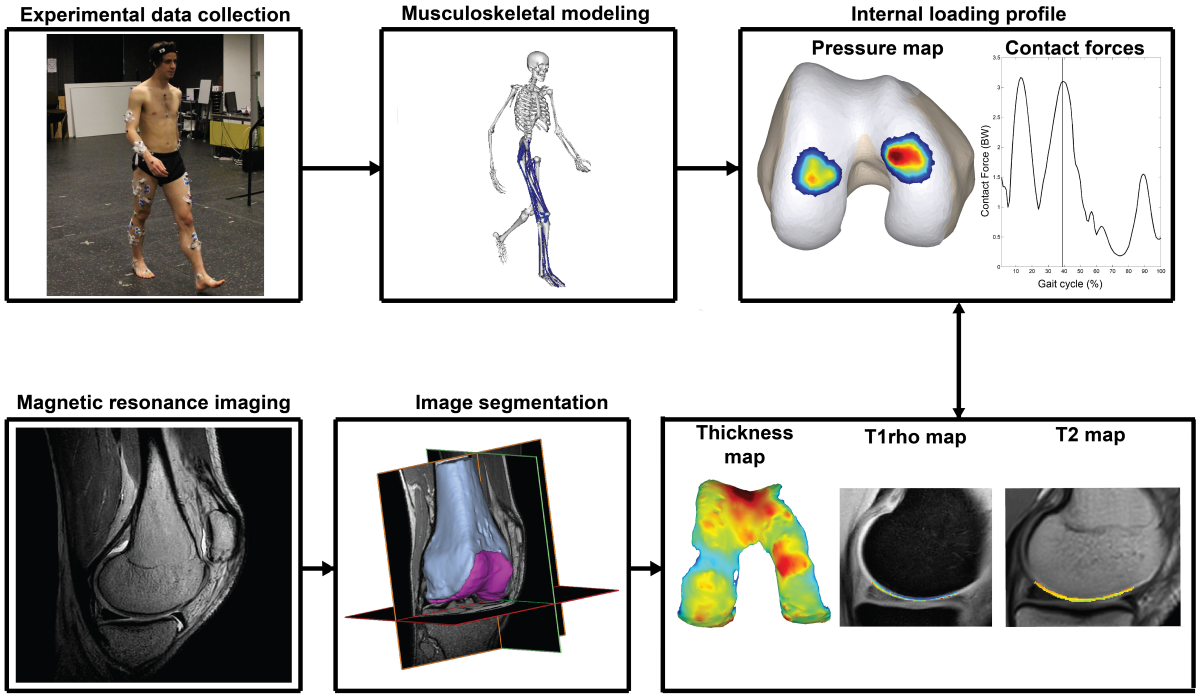

Figure 4.1: **Schematic overview of the workflow.**
Experimental gait data was collected and processed using musculoskeletal modeling in order to calculate the cartilage contact force and pressure distribution. High resolution MR-images were captured and segmented to calculate thickness maps and to outline the cartilage on the $T1\rho$ and T2 maps. Loading parameters were correlated with the peak and mean thickness, mean $T1\rho$ relaxation time and mean T2 relaxation time to explore the relation between localized loading and cartilage thickness and composition.

Medical imaging

Imaging of the dominant leg was performed on a 3T Ingenia scanner, with a standard transmit and receive knee coil (Philips Healthcare, Best, The Netherlands). After one hour standardized rest in order to eliminate the influence of previous loading, participants were positioned in supine position with the knee in neutral internal rotation and full extension. During the scans the knee was fixated to minimize movement. The following scanning sequences were acquired: 1) a high resolution 3D-fast spin echo acquisition (3D-FSE), 2) $T1\rho$ relaxation time sequence and 3) T2 relaxation time sequence. MRI sequence parameters are listed in Table 4.2.

The femoral cartilage and distal part of the femur were manually segmented by the same author (SVR) from the 3D high-resolution images (Mimics Innovation Suite, Materialise, Leuven, Belgium). 3D triangulated surfaces of the distal femur (subchondral bone) and the femoral cartilage were created. Next, a cartilage thickness distribution map was generated by computing the minimum distance between the subchondral bone surface and the cartilage surface for every vertex of the cartilage surface in the surface normal direction[45]. The average and peak cartilage thickness was calculated for the weight-bearing area of the medial and the lateral condyle. The weight-bearing area was defined as the area between the anterior end of the intercondylar notch and 60% of the distance to the most posterior end of the femoral condyles[46,47]. The peak thickness of the weight-bearing zone was defined as the mean of the top 10% of all thickness values in the weight-bearing zone, whereas the mean thickness was calculated using all thickness values of the weight-bearing region[45]. Next, the subject-specific thickness maps were anisotropically registered to the generic cartilage

Table 4.2: Overview of the MRI sequence parameters.

	3D-FSE	$T1\rho$	T2
TR (ms) / TE (ms)	1800/120	5.9587/3.082	4000/11-22-33-44-55-66-77-88
Field of view (cm)	16	16	16
Matrix	268 x 268	292 x 256	160 x 160
Slice thickness (mm)	1	4	4
Echo train length	85	64	12
Bandwidth (kHz)	562	522	367
Number of excitations	2	1	1
Number of slices	320	20	20
Acquisition time (min)	5.94	17.20	5.24
Time of recovery (ms)	/	2000	/
Time of spinlock (ms)	/	0/10/20/40/60	/
Frequency of spinlock (Hz)	/	500	/

mesh used in the musculoskeletal model (S1 Text). The 3D volumetric meshes were registered on the $T1\rho$ and T2 images to outline the cartilage regions of interest. Relaxation time maps for the $T1\rho$ and T2 sequences were generated using a pixel-by-pixel based evaluation of the mono-exponential Levenberg-Marquardt fitting algorithm[48]:

$$M(TSL) \propto e^{-\frac{TSL}{T1\rho}}$$

$$M(TE) \propto e^{-\frac{TE}{T2}}$$

Voxels with a $T1\rho$ relaxation time >130ms or T2 relaxation time >100ms were excluded to avoid artifacts due to partial volume effects with synovial fluid[49]. An average $T1\rho$ and T2 relaxation time was calculated for the weight-bearing part of the medial and lateral femur condyle separately and for both condyles together. $T1\rho$ values of one single subject were excluded from the analysis due to image artifacts, resulting in higher relaxation times.

Statistical analysis

Differences between the medial and lateral condyle load describing parameters, mean and peak thickness, $T1\rho$ and T2 relaxation time were tested by a Wilcoxon paired-samples test. The average and peak thickness of the weight bearing zone of the medial and lateral condyle were correlated to the different loading variables using a one-tailed Spearman rank correlation coefficient. Furthermore, the correlation between thickness and the local pressure was calculated for every individual mesh face in contact, resulting in a correlation map indicative of the relation between local thickness and loading in the respective contact regions. The relation between cartilage composition and loading was analyzed by correlating the average relaxation times of the weight-bearing zone of the total knee and of the medial and lateral condyle to their respective loading variables, using a two-tailed Spearman rank correlation coefficient. Significance level was set at $p = 0.05$ for all conducted statistical tests in MATLAB (MATLAB 2012b, The Math Works, Inc., Natick, Massachusetts, USA).

Table 4.3: Average and standard deviations of all loading variables.

	Total knee Average ± Deviation	Medial condyle Average ± Deviation	Lateral condyle Average ± Deviation	P-value
Mean Pressure [MPa]				
First peak	5.97 ± 0.74	6.01 ± 0.57	5.8 ± 1.32	0.3028
Second peak	5.35 ± 0.5	6.12 ± 0.72	4.21 ± 0.54	0.0001*
Maximal Pressure [MPa]				
First peak	13.93 ± 2.08	12.75 ± 1.54	12.49 ± 2.91	0.4887
Second peak	12.26 ± 1.25	12.17± 1.39	8.67 ± 1.29	0.0001*
Average Pressure during Stance [MPa]	3.648 ± 0.275	3.981 ± 0.424	3.211 ± 0.283	0.0002*
First peak contact force [N]				
Anterior-Posterior	483.95 ± 201.99	344.39 ± 128.64	139.56 ± 86.26	0.0001*
Compression	2062.35 ± 308.01	1230.65 ± 201.57	831.7 ± 247.3	0.0012*
Medial-lateral	10.81 ± 46.98	-248.92 ± 31.03	259.72 ± 60.49	0.6387
Resultant	2125.59 ± 328.56	1308.46 ± 204.86	885.28 ± 259.87	0.0006*
Second peak contact force [N]				
Anterior-Posterior	11.19 ± 167.09	-18.47 ± 120.51	29.66 ± 50.19	0.0084*
Compression	2012.64 ± 290.35	1355.55 ± 216.19	657.09 ± 132.02	0.0001*
Medial-lateral	-94.52 ± 28.35	-315.87 ± 64.06	221.35 ± 56.21	0.0001*
Resultant	2023.62 ± 279.35	1399.47 ± 213.91	697.54 ± 138.47	0.0001*
Impulse [N*s]				
Anterior-Posterior	86.28 ± 54.8	51.48 ± 31.79	34.81 ± 24.3	0.0004*
Compression	863.74 ± 108.26	536.69 ± 96.99	327.04 ± 52.92	0.0001*
Medial-lateral	-22.1 ± 7.57	-125.63 ± 18.39	103.53 ± 16.52	0.0001*
Resultant	875.7 ± 104.07	559.92 ± 94.88	347.24 ± 54.28	0.0001*

$*$ indicates a significant difference between medial and lateral loading ($p < 0.05$)

Results

The average and standard deviations of all loading variables are summarized in table 4.3. Contact areas on the medial condyle were on average 251 ± 25mm^2 and 279 ± 36mm^2 during the first and second peak, respectively. Contact areas on the lateral condyle were on average 177 ± 14mm^2 and 215 ± 40mm^2 for the first and second peak, respectively. Medial resultant contact forces were 1308 ± 205N and 1399 ± 214N for the first and second peak, respectively and were significantly higher than the lateral resultant contact forces, which were 885 ± 260N and 698 ± 138N for the first and second peak, respectively (Table 4.3). Mean and maximal pressures on the medial condyle at the first peak were not significantly higher than the pressures on the lateral condyle (6.01 - 12.75MPa and 5.80 - 12.49MPa for the medial and lateral mean and peak pressures, respectively) (Table 4.3). In contrast, mean and maximal pressures on the medial condyle at the second peak were significantly higher than the pressures on the lateral condyle (6.12 - 12.17MPa and 4.21 - 8.67MPa for the medial and lateral mean and peak pressures, respectively). Mean thickness of the medial and lateral condyle was on average 2.70 ± 0.38mm and 2.44 ± 0.28mm, respectively. Average peak thickness was 3.77 ± 0.57mm and 3.46 ± 0.38mm for the medial and lateral condyle, respectively. The weight-bearing part of the medial condyle was significantly thicker compared to the lateral condyle (P = 0.0034 and P = 0.03 for the mean and peak thickness, respectively). Medial and lateral $T1\rho$ relaxation times were on average 41.59 ± 5.49ms and 46.23 ± 7.18ms, respectively. $T1\rho$ relaxation time of the medial condyle was significantly lower compared to the lateral condyle (P = 0.004). Medial and lateral average T2 relaxation times were 59.42 ± 7.18ms and 57.41 ± 10.30ms, respectively.

Mean and peak thickness of the lateral and medial condyle correlated significantly with the load de-

Table 4.4: Significant correlations between cartilage thickness and the loading parameters. Spearman correlation coefficient and p-value are given.

	Medial thickness		Lateral thickness	
	Mean	Peak	Mean	Peak
Total knee				
First peak contact force				
Anterior-posterior	0.48 (0.036)	n.s	0.55 (0.019)	0.55 (0.019)
Compression	0.45 (0.047)	n.s	n.s	n.s
Second peak contact force				
Compression	0.62 (0.008)	0.57 (0.014)	0.57 (0.015)	n.s
Resultant	0.62 (0.008)	0.57 (0.014)	0.57 (0.015)	n.s
Average pressure during stance	0.78 (0.001)	0.73 (0.001)	0.55 (0.019)	n.s
Medial Condyle				
Second peak contact forc				
Compression	0.55 (0,018)	0.60 (0.010)	n.a.	n.a.
Resultant	0. 54 (0,020)	0.56 (0.017)	n.a.	n.a.
Average pressure during stance	0.58 (0,014)	0.71 (0.002)	n.a.	n.a.
Lateral Condyle				
Impulse				
Anterior-posterior	n.a.	n.a.	n.s	0.50 (0.030)
Compression	n.a.	n.a.	0.46 (0.043)	0.50 (0.029)
Medial-lateral	n.a.	n.a.	0.53 (0.024)	n.s
Resultant	n.a.	n.a.	0.46 (0.043)	0.50 (0.029)
Average pressure during stance	n.a.	n.a.	0.57 (0.015)	0.71 (0.002)
First peak mean pressure	n.a.	n.a.	n.s	0.49 (0.032)
First peak max pressure	n.a.	n.a.	n.s	0.50 (0.031)

n.s.: not significant, n.a.: not applicable

scribing parameters (Table 4.4). Mean and peak thickness of both the medial and lateral condyle correlated significantly with the compressive and resultant contact force of the total knee. Likewise, the mean and peak thickness of the medial condyle correlated significantly with the compressive and resultant contact force on the medial condyle at second peak. However, these correlations were not confirmed for the lateral condyle. Nevertheless, the mean and peak lateral thickness correlated significantly with the lateral condyle impulses. In line with the correlations found for the contact forces, the mean and peak cartilage thickness of both condyles as well as the medial and lateral condyle thickness correlated significantly with the average pressure on the total knee as well as on the medial and lateral condyle, respectively. Scatterplots of the significant correlations are provided in supplementary material (S2, S3, S4 and S5 Figs).

The correlation map (Fig 4.2) showed that the area where local cartilage thickness correlated with local pressure was larger for the lateral condyle. For the medial condyle, 5.13% of the contact area at the first peak (12.87 mm^2) and 20.67% of the contact area at the second peak (57.75 mm^2) had a thickness that was significantly correlated with its local pressure (mean R = 0.49 ± 0.05, range: 0.44 – 0.58 and mean R = 0.53 ± 0.07, range: 0.44 – 0.79 at the first and second peak, respectively). For the lateral condyle, 30.56% of the contact area at the first peak (54.06 mm^2) and 17.86% of the contact area at the second peak (38.48 mm^2)

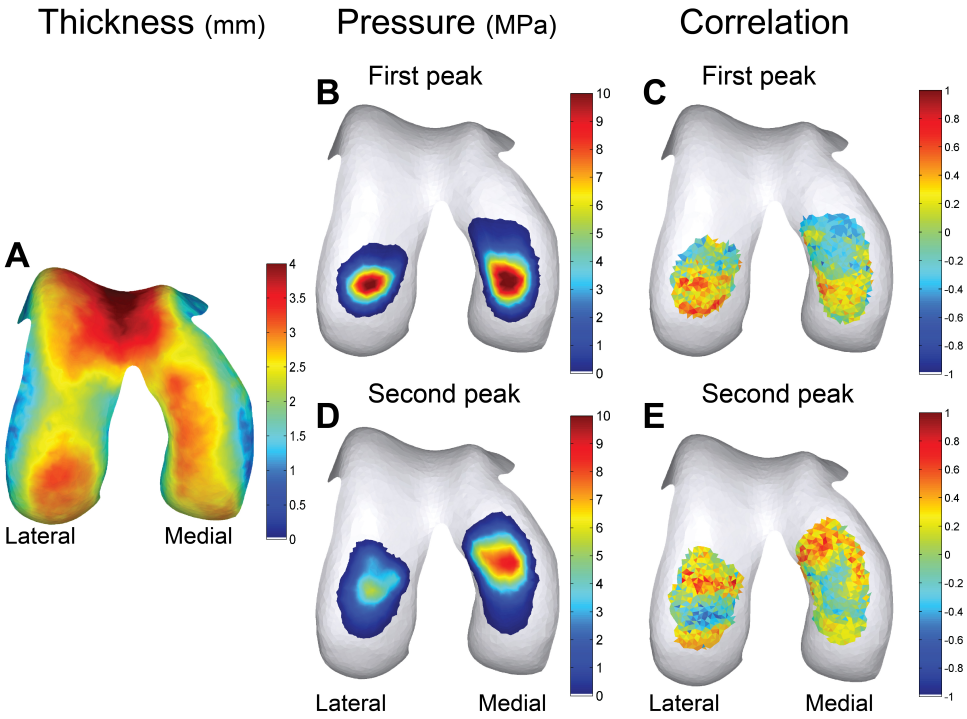

Figure 4.2: **Local correlations between cartilage pressure and thickness.** (A) Average thickness distribution of all subjects, (B) Average pressure map of the first peak, (D) Average pressure map of the second peak. (C & E) Correlation map of the correlations between the mesh face specific thickness and pressure. (C) Shows the correlations at the first peak, (E) shows the correlations at the second peak.

had a thickness that was significantly correlated with its local pressure (mean R = 0.55 ± 0.07, range: 0.45 – 0.71 and mean R = 0.57 ± 0.1, range: 0.45 – 0.83 at the first and second peak, respectively).

Significant correlations between the average $T1\rho$ relaxation times and load describing parameters were found (Table 4.5). The average whole joint $T1\rho$ relaxation time was significantly correlated with the total knee impulses and contact forces at second peak. The average whole joint T2 relaxation time was significantly correlated with the second peak total knee compressive contact force (R = -0.53, P = 0.047), second peak total knee resultant contact force (R = -0.53, P = 0.047) and average total pressure during stance (R = -0.59, P = 0.020). Furthermore, the relation between total knee loading and average whole joint $T1\rho$ relaxation time was confirmed at compartmental level: the average medial $T1\rho$ relaxation time was significantly correlated with the medial contact force at second peak and with the medial condyle impulse, whereas the average lateral $T1\rho$ relaxation time was significantly correlated with the total knee and lateral condyle contact forces at second peak. A full overview of the correlations is presented in S1, S2 and S3 Tables.

Discussion

The present study examined if femoral cartilage thickness and biochemical composition, measured by magnetic resonance imaging correlated with knee loading during walking, as calculated using musculoskeletal modeling. The results indicate that thicker cartilage on both the medial and lateral condyle was related to higher loading in the medial and lateral compartment, with higher $T1\rho$ relaxation time being related to increased shear loading and lower $T1\rho$ and T2 relaxation time being related to increased compression. This

Table 4.5: Significant correlations between average $T1\rho$ relaxation time and the loading parameters. Spearman correlation coefficient and p-value are given.

	Total knee $T1\rho$	**Medial condyle** $T1\rho$	**Lateral condyle** $T1\rho$
Total knee			
First peak contact force			
Anterior -posterior	n.s.	0.56 (0.042)	n.s.
Second peak contact force			
Anterior -posterior	0.66 (0.013)	n.s.	0.68 (0.010)
Compression	-0.55 (0.043)	n.s.	-0.59 (0.030)
Resultant	-0.55 (0.043)	n.s.	-0.59 (0.030)
Impulse			
Anterior -posterior	0.56 (0.042)	n.s.	0.71 (0.006)
Compression	-0.56 (0.042)	n.s.	n.s.
Resultant	-0.54 (0.048)	n.s.	n.s.
Medial condyle			
Second peak contact force			
Medial-lateral	n.a.	0.62 (0.021)	n.a.
Impulse			
Anterior -posterior	n.a.	0.69 (0.008)	n.a.
Medial-lateral	n.a.	0.75 (0.003)	n.a.
Lateral condyle			
Second peak contact force			
Anterior -posterior	n.a.	n.a.	0.70 (0.007)
Medial-lateral	n.a.	n.a.	-0.66 (0.012)

n.s.: not significant, n.a.: not applicable

paper is, to the best of our knowledge, the first to relate local cartilage thickness and $T1\rho$ and T2 relaxation times to the local mechanical loading at the articular surface.

In agreement with previous research, this study found a significant correlation between mean and peak thickness of the weight-bearing region of both condyles and overall cartilage loading (S2 and S3 Figs)[7–9]. Due to the specific methodology used i.e. a musculoskeletal model allowing the separate calculation of lateral and medial contact forces and pressures, local condyle thickness was found to related to local condyle loading (S2 and S3 Figs). These findings suggest that the thickness of cartilage may be adapted to the cyclic loads experienced during ambulation. Medial condyle thickness distribution was mostly related to the second peak loading, whereas lateral condyle thickness was mostly related to the first peak loading. The fact that lateral condyle loading was highest at the first peak compared to the second peak can possibly explain this finding[51,52]. Local lateral condyle thickness distribution was more correlated to its local pressure, possibly because the lateral contact area was smaller compared to the medial contact area[8,12]. This resulted in a more isolated effect of loading in one region, whereas the effect of loading was more distributed on the medial condyle. Previous research demonstrated a relation between KAM and medial condyle thickness, whereas we are first to describe the relation between cartilage thickness and cartilage loading of both condyles[7–9]. More specific, an additional relation between lateral condyle loading and lateral condyle thickness was found. This can be explained by the use of a more detailed estimate of internal joint loading, provided by muscu-

loskeletal modeling, which takes muscle and ligament forces into account to determine joint loading, instead of using external estimates of joint loading as KAM. Indeed, KAM is an estimate of the ratio of loading between the medial and lateral condyles and does not accurately capture the magnitude of lateral compartment cartilage loading[53,54]. As a consequence, only a relation between an estimation of medial loading and medial thickness was previously found and confirmed by our findings.

Besides the relation with cartilage thickness, biochemical composition estimated by $T1\rho$ and T2 relaxation times was also related to cartilage contact forces and pressures during gait. In the past, indirect estimates of loading were related to cartilage $T1\rho$ and T2 relaxation times[29–31]. Results suggested that changes in biochemical composition occur secondary to loading, as reflected in the increased $T1\rho$ relaxation time after unloading or running a marathon[25,28]. Furthermore lower $T1\rho$ and T2 relaxation times were found in healthy persons subjected to higher sagittal plane moments during a drop jump[31]. Since a drop jump is performed less frequently compared to walking, one could expect a stronger relation between biochemical composition and loads during a more habitual cyclic activity such as walking. The present results further reinforce these insights and indicate that $T1\rho$ and T2 relaxation time can be related to loading. Surprisingly, direction of the force seems to be an important determinant of cartilage composition: Higher $T1\rho$ relaxation times were related to anterior-posterior shear loading (S4 and S5 Figs), whereas lower $T1\rho$ relaxation times were related to medial-lateral contact forces (S4 and S5 Figs). In contrast, both lower $T1\rho$ and T2 relaxation times were related to higher compressive forces and pressures (S4 and S5 Figs). $T1\rho$ relaxation time is related to cartilage proteoglycan concentration and T2 relaxation time is related to cartilage collagen concentration and orientation[20–24]. This suggests that in the presence of higher compressive forces, upregulation of the proteoglycan and collagen synthesis in the extracellular matrix may occur as a chronic response to loading due to a higher mechanical stimulation of the chondrocytes[33,34]. This finding is comparable to the decreased T2 relaxation times found after a standardized training period, suggesting adaptations of the extracellular matrix due to the imposed mechanical loading[26,27]. Similarly higher shear forces are known to accelerate cartilage deterioration and can explain the lower proteoglycan concentration, reflected as higher $T1\rho$ relaxation time[33,34]. Next to loading magnitude and direction, loading time is an important factor explaining the inter-subject differences in $T1\rho$ relaxation time: As a result, correlations between $T1\rho$ relaxation time and impulses of the contact force and were sometimes stronger compared to the correlation with the peak and average contact forces. Using higher resolution $T1\rho$ and T2 images, future research can possibly reveal more regional relations between loading and relaxation times and differentiate between the different cartilage layers.

The results of the present study indicate that cartilage is indeed responsive to mechanical stimuli during gait. However, it should be noted that the correlations between cartilage structural or biochemical parameters and loading variables are rather low. This implies that a large portion of the variability in thickness, proteoglycan concentration or collagen concentration and organization is determined by other factors such as genetics, age and geometric characteristics of the joint[6,55]. By considering other frequent activities of daily living (e.g. rising from a chair and stair ascending) of which some may impose higher knee loading, a more exhaustive relation between cartilage thickness distribution and composition and local pressure distribution may be found. As these motions load other regions of the condyles than gait and thus may provide an additional local stimulus for cartilage remodeling.

Nonetheless, this study contributes to the current understanding of how cartilage thickness and composition is related to joint loading during walking, the results should be interpreted with respect to its limitations.

First, the current analysis used a generic knee model. In future work, the effect of subject-specific detail on cartilage pressure should be explored by including subject-specific cartilage geometries in the knee model. This way the effect of subject-specific detail on cartilage pressure, now lost by using a uniform scaled generic geometry, could be better accounted for. However, currently this methodological adaptation is not yet feasible. Secondly, registration of the subject-specific MRI-based mesh to the generic mesh of the musculoskeletal model will have reduced spatial resolution that might have weakened the calculated correlations between the local thickness and pressure. Third, not all relations between cartilage thickness and biochemical composition and cartilage loading reached significance, but most of their relations support the observed findings. However, due to the large amount of calculated correlations in this exploratory study, one should be careful not over interpreting these results as some may be the results of chance and may not reflect causality.

In conclusion, we found that in a cohort of healthy adults thicker cartilage is associated with higher cartilage loading during walking on a compartmental level. Proteoglycan concentration, estimated using $T1\rho$ mapping, was correlated with loading with increased proteoglycan concentration being related to higher compressive forces but decreased proteoglycan concentration being related to higher shear forces. Finally, collagen content and organization, estimated using T2 mapping, was correlated with loading, with increased collagen concentration and organization being related to higher pressures and compressive forces.

References

1. Andriacchi TP, Favre J. The Nature of In Vivo Mechanical Signals That Influence Cartilage Health and Progression to Knee Osteoarthritis. Curr Rheumatol Rep. 2014;16: 463–470.
2. Carter DR, Beaupré GS, Wong M, Smith RL, Andriacchi TP, Schurman DJ. The Mechanobiology of Articular Cartilage Development and Degeneration. Clin Orthop Relat Res. 2004;427: S69–S77.
3. Chen C, Tambe DT, Deng L, Yang L. Biomechanical properties and mechanobiology of the articular chondrocyte. Am J Physiol Cell Physiol. 2013;305: C1202-8.
4. Chaudhari AMW, Briant PL, Bevill SL, Koo S, Andriacchi TP. Knee kinematics, cartilage morphology, and osteoarthritis after ACL injury. Med Sci Sports Exerc. 2008;40: 215–22.
5. Jones G, Ding C, Glisson M, Hynes K, Ma D, Cicuttini F. Knee articular cartilage development in children: A longitudinal study of the effect of sex, growth, body composition, and physical activity. Pediatr Res. 2003;54: 230–236.
6. Hudelmaier M, Glaser C, Englmeier K-H, Reiser M, Putz R, Eckstein F. Correlation of knee-joint cartilage morphology with muscle cross-sectional areas vs. anthropometric variables. Anat Rec Part A. 2003;270: 175–184.
7. Andriacchi TP, Mündermann A, Smith RL, Alexander EJ, Dyrby CO, Koo S. A framework for the in vivo pathomechanics of osteoarthritis at the knee. Ann Biomed Eng. 2004;32: 447–457.
8. Koo S, Andriacchi TP. A comparison of the influence of global functional loads vs. local contact anatomy on articular cartilage thickness at the knee. J Biomech. 2007;40: 2961–2966.
9. Blazek K, Favre J, Asay J, Erhart-Hledik J, Andriacchi T. Age and obesity alter the relationship between femoral articular cartilage thickness and ambulatory loads in individuals without osteoarthritis. J Orthop Res. 2014;32: 394–402.
10. Vanwanseele B, Eckstein F, Knecht H, Spaepen A, Stüssis E. Longitudinal Analysis of Cartilage Atrophy in the Knees of Patients with Spinal Cord Injury. Arthritis Rheum. 2003;48: 3377–3381.
11. Vanwanseele B, Eckstein F, Hadwighorst H, Knecht H, Spaepen A, Stüssi E. In Vivo Precision of Quantitative Shoulder Cartilage Measurements, and Changes after Spinal Cord Injury. Magn Reson Med. 2004;51: 1026–1030.
12. Koo S, Rylander JH, Andriacchi TP. Knee joint kinematics during walking influences the spatial cartilage thickness distribution in the knee. J Biomech. Elsevier; 2011;44: 1405–1409.
13. Li G, Park SE, DeFrate LE, Schutzer ME, Ji L, Gill TJ, et al. The cartilage thickness distribution in the tibiofemoral joint and its correlation with cartilage-to-cartilage contact. Clin Biomech. 2005;20: 736–744.
14. Fregly BJ. Design of Optimal Treatments for Neuromusculoskeletal Disorders using Patient-Specific Multibody Dynamic Models. Int J Comput Vis Biomech. 2009;2: 145–155.
15. Winby CR, Lloyd DG, Besier TF, Kirk TB. Muscle and external load contribution to knee joint contact loads during normal gait. J Biomech. Elsevier; 2009;42: 2294–300.
16. Burstein D, Bashir A, Gray ML. MRI techniques in early stages of cartilage disease. Invest Radiol. 2000;35: 622–38.
17. Freemont AJ, Hoyland JA. Morphology, mechanisms and pathology of musculoskeletal ageing. J Pathol. 2007;211: 252–259.
18. Goto H, Fujii M, Iwama Y, Aoyama N, Ohno Y, Sugimura K. Magnetic resonance imaging (MRI) of articular cartilage of the knee using ultrashort echo time (uTE) sequences with spiral acquisition. J Med Imaging Radiat Oncol. 2012;56: 318–23.
19. Lohmander LS. Articular cartilage and osteoarthrosis. The role of molecular markers to monitor breakdown, repair and disease. J Anat. 1994;184: 477–492.
20. Keenan KE, Besier TF, Pauly JM, Han E, Rosenberg J, Smith RL, et al. Prediction of glycosaminoglycan content in human cartilage by age, $T1\rho$ and T2 MRI. Osteoarthr Cartil. Elsevier Ltd; 2011;19: 171–9.
21. Li X, Cheng J, Lin K, Saadat E, Bolbos RI, Jobke B, et al. Quantitative MRI using $T1\rho$ and T2 in human osteoarthritic cartilage specimens: Correlation with biochemical measurements and histology. Magn Reson Imaging. Elsevier Inc.; 2011;29: 324–334.
22. Stahl R, Luke A, Li X, Carballido-Gamio J, Ma CB, Majumdar S, et al. T1rho, T2 and focal knee cartilage abnormalities in physically active and sedentary healthy subjects versus early OA patients–a 3.0-Tesla MRI study. Eur Radiol. 2009;19: 132–43.
23. Wang L, Chang G, Xu J, Vieira RLR, Krasnokutsky S, Abramson S, et al. T1rho MRI of menisci and cartilage in patients with osteoarthritis at 3T. Eur J Radiol. Elsevier Ireland Ltd; 2012;81: 2329–36.

24. Matzat SJ, van Tiel J, Gold GE, Oei EHG. Quantitative MRI techniques of cartilage composition. Quant Imaging Med Surg. 2013;3: 162–74.

25. Souza RB, Baum T, Wu S, Feeley BT, Kadel N, Li X, et al. Effects of unloading on knee articular cartilage T1rho and T2 magnetic resonance imaging relaxation times: a case series. J Orthop Sports Phys Ther. 2012;42: 511–20.

26. Koli J, Multanen J, Kujala UM, Häkkinen A, Nieminen MT, Kautiainen H, et al. Effects of Exercise on Patellar Cartilage in Women with Mild Knee Osteoarthritis. Med Sci Sports Exerc. 2015;47: 1767–1774.

27. Munukka M, Waller B, Rantalainen T, Häkkinen A, Nieminen MT, Lammentausta E, et al. Efficacy of progressive aquatic resistance training for tibiofemoral cartilage in postmenopausal women with mild knee osteoarthritis: A randomised controlled trial. Osteoarthr Cartil. 2016;24: 1708–1717.

28. Luke AC, Stehling C, Stahl R, Li X, Kay T, Takamoto S, et al. High-field magnetic resonance imaging assessment of articular cartilage before and after marathon running: does long-distance running lead to cartilage damage? Am J Sports Med. 2010;38: 2273–80.

29. Kumar D, Subburaj K, Lin W, Karampinos DC, McCulloch CE, Li X, et al. Quadriceps and hamstrings morphology is related to walking mechanics and knee cartilage MRI relaxation times in young adults. J Orthop Sports Phys Ther. 2013;43: 881–90.

30. Souza RB, Stehling C, Wyman BT, Hellio Le Graverand M-P, Li X, Link TM, et al. The effects of acute loading on T1rho and T2 relaxation times of tibiofemoral articular cartilage. Osteoarthr Cartil. 2010;18: 1557–63.

31. Souza RB, Fang C, Luke A, Wu S, Li X, Majumdar S. Relationship between knee kinetics during jumping tasks and knee articular cartilage MRI T1rho and T2 relaxation times. Clin Biomech. Elsevier Ltd; 2012;27: 403–8.

32. Felson D, Lawrence R, Dieppe P, Hirsch R, Helmick C, Jordan J, et al. Osteoarthritis: New Insights. Part 1: The Disease and Its Risk Factors. Ann Intern Med. 2000;133: 637–639.

33. Ackermann B, Steinmeyer J. Collagen biosynthesis of mechanically loaded articular cartilage explants. Osteoarthr Cartil. 2005;13: 906–914.

34. Bleuel J, Zaucke F, Brüggemann G-P, Niehoff A. Effects of Cyclic Tensile Strain on Chondrocyte Metabolism: A Systematic Review. PLoS One. 2015;10:

35. Vanwanseele B, Lucchinetti E, Stüssi E. The effects of immobilization on the characteristics of articular cartilage: Current concepts and future directions. Osteoarthr Cartil. 2002;10: 408–419.

36. Davis RB, Ounpuu S, Tyburski D, Gage JR. A gait analysis data collection and reduction technique. Hum Mov Sci. 1991;10: 575–587.

37. Lenhart RL, Kaiser J, Smith CR, Thelen DG. Prediction and Validation of Load-Dependent Behavior of the Tibiofemoral and Patellofemoral Joints During Movement. Ann Biomed Eng. 2015;43: 2675–2685.

38. Arnold EM, Ward SR, Lieber RL, Delp SL. A model of the lower limb for analysis of human movement. Ann Biomed Eng. 2010;38: 269–79.

39. Smith RC, Choi KW, Negrut D, Thelen DG. Efficient Computation of Cartilage Contact Pressures within Dynamic Simulations of Movement. Comput Methods Biomech Biomed Eng Imaging Vis. 2016

40. Blankevoort L, Kuiper JH, Huiskes R, Grootenboer HJ. Articular contact in a three-dimensional model of the knee. J Biomech. 1991;24: 1019–1031.

41. Li G, Lopez O, Rubash H. Variability of a Three-Dimensional Finite Element Model Constructed Using Magnetic Resonance Images of a Knee for Joint Contact Stress Analysis. J Biomech Eng. 2001;123: 341–346.

42. Delp, Scott L; Loan JP. A computational framework for simulation and analysis of human movement. Comput Sci Eng. 2000; 46–55.

43. Smith CR, Vignos MF, Lenhart RL, Kaiser J, Thelen DG. The Influence of Component Alignment and Ligament Properties on Tibiofemoral Contact Forces in Total Knee Replacement. J Biomech Eng. 2016;138: 1–10.

44. Lu TW, O'Connor JJ. Bone position estimation from skin marker co-ordinates using global optimisation with joint constraints. J Biomech. 1999;32: 129–134.

45. Thelen DG, Won Choi K, Schmitz AM. Co-simulation of neuromuscular dynamics and knee mechanics during human walking. J Biomech Eng. 2014;136: 21033.

46. Draper CE, Besier TF, Gold GE, Fredericson M, Fiene A, Beaupre GS, et al. Is cartilage thickness different in young subjects with and without patellofemoral pain? Osteoarthr Cartil. 2006;14: 931–937.

47. Eckstein F, Hudelmaier M, Wirth W, Kiefer B, Jackson R, Yu J, et al. Double echo steady state magnetic resonance imaging of knee articular cartilage at 3 Tesla: a pilot study for the Osteoarthritis Initiative. Ann Rheum Dis. 2006;65: 433–441.

48. Erhart-Hledik JC, Favre J, Andriacchi TP. New insight in the relationship between regional patterns of knee cartilage thickness, osteoarthritis disease severity, and gait mechanics. J Biomech. Elsevier; 2015;48: 3868–3875.

49. Li X, Benjamin Ma C, Link TM, Castillo D-D, Blumenkrantz G, Lozano J, et al. In vivo T1rho and T2 mapping of articular cartilage in osteoarthritis of the knee using 3 T MRI. Osteoarthr Cartil. 2007;15: 789–97.

50. Souza RB, Kumar D, Calixto N, Singh J, Schooler J, Subburaj K, et al. Response of knee cartilage T1rho and T2 relaxation times to in vivo mechanical loading in individuals with and without knee osteoarthritis. Osteoarthr Cartil. 2014;22.

51. D'Lima DD, Steklov N, Fregly BJ, Banks S a., Colwell CW. In vivo contact stresses during activities of daily living after knee arthroplasty. J Orthop Res. 2008;26: 1549–1555.

52. Fregly BJ, Besier TF, Lloyd DG, Delp SL, Banks S a, Pandy MG, et al. Grand challenge competition to predict in vivo knee loads. J Orthop Res. 2012;30: 503–13.

53. Hurwitz DE, Ryals AB, Case JP, Block JA, Andriacchi TP. The knee adduction moment during gait in subjects with knee osteoarthritis is more closely correlated with static alignment than radiographic disease severity, toe out angle and pain. J Orthop Res. 2002;20: 101–107.

54. Meireles S, De Groote F, Reeves ND, Verschueren S, Maganaris C, Luyten F, et al. Knee contact forces are not altered in early knee osteoarthritis. Gait Posture. Elsevier B.V.; 2016;45: 115–120.

55. Moyer R, Wirth W, Duryea J, Eckstein F. Anatomical alignment, but not goniometry, predicts femorotibial cartilage loss as well as mechanical alignment: Data from the Osteoarthritis Initiative. Osteoarthr Cartil. Elsevier Ltd; 2016;24: 254–261.

Supplementary material

S1 Text

Registration of subject-specific cartilage mesh on the generic mesh

The subject-specific thickness maps were anisotropically registered to the generic cartilage mesh used in the musculoskeletal model. Therefore, the generic mesh was scaled non-uniformly to better match the size of the subject-specific mesh. Next, both meshes were positioned onto each other using an iterative closest point algorithm. Subsequently, for all faces of the subject-specific mesh the intersection point of a line through the face center in face normal direction and the generic mesh was determined. Last, the subject-specific thickness of the face was assigned to the intersected face of the generic mesh.

S1 Fig

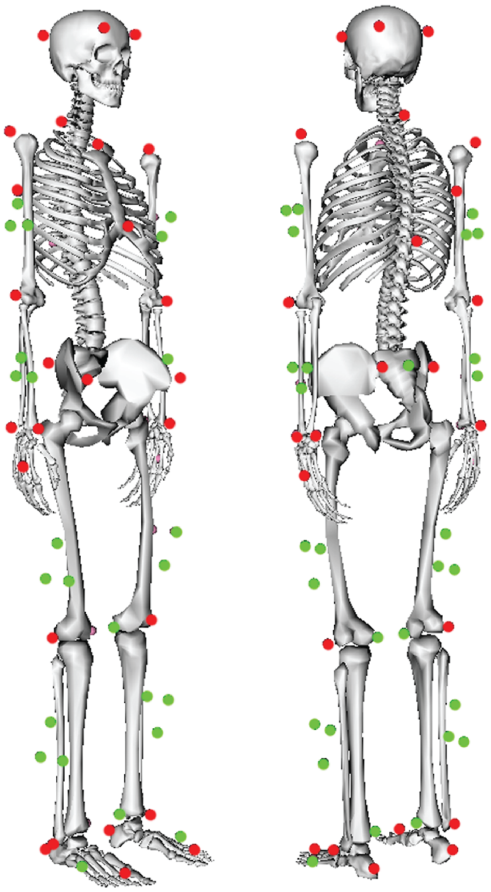

Figure 4.3: **Extended Plug-in-Gait markerset**
The full-body extended Plug-in-Gait marker set used during the motion capture. Additional to the original full-body Plug-in-Gait marker set, this marker set is comprised of three-marker clusters on the upper and lower arms and legs and anatomical markers on the sacrum, medial femur epicondyles and the medial malleoli, resulting in a total of 65 markers. Markers in dark gray are the original Plug-in-Gait markers. Light gray markers are the additionally placed markers.

S2 Fig

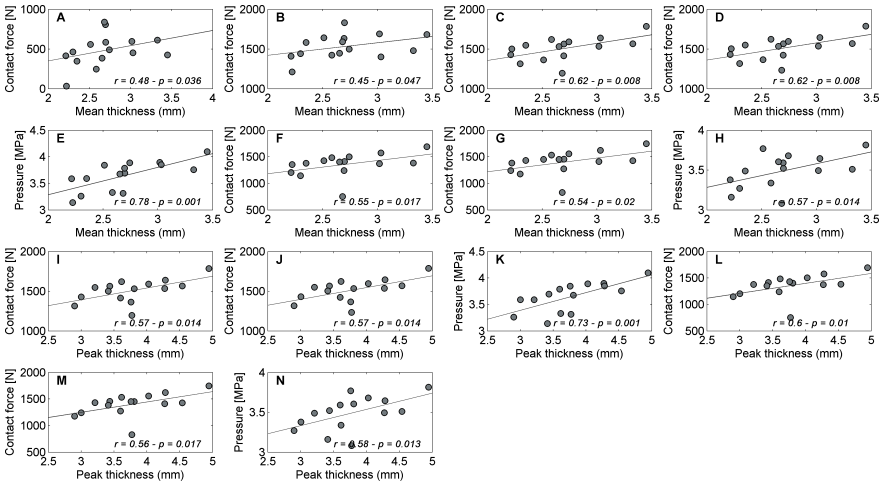

Figure 4.4: **Correlations between medial thickness and loading**
Scatterplots of the significant correlations between mean medial thickness and (A) first peak total knee anterior-posterior contact force, (B) first peak total knee compressional contact force, (C) second peak total knee compressional contact force, (D) second peak total knee resultant contact force, (E) average total pressure during stance, (F) second peak medial compressional contact force, (G) second peak medial resultant contact force and (H) average medial pressure during stance. Between peak medial thickness and (I) second peak total knee compressional contact force, (J) second peak total knee resultant contact force, (K) average total knee pressure during stance, (L) second peak medial compressional contact force, (M) second peak medial resultant contact force and (N) average medial pressure during stance.

S3 Fig

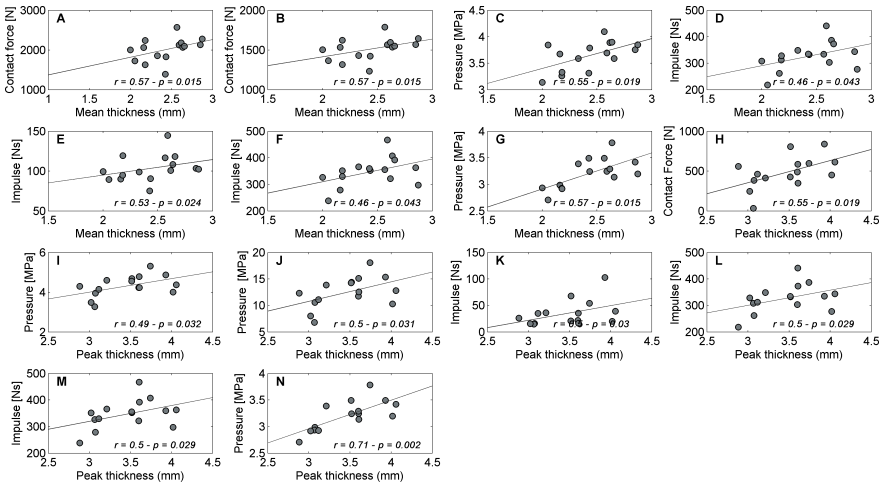

Figure 4.5: **Correlations between lateral thickness and loading**
Scatterplots of the significant correlations between mean lateral thickness and (A) second peak total knee compressional contact force, (B) second peak total knee resultant contact force, (C) average total knee pressure during stance, (D) Lateral compressional impulse, (E) lateral medial-lateral impulse, (F) lateral resultant impulse and (G) average later pressure during stance. Between peak lateral thickness and (H) first peak total knee anterior-posterior contact force, (I) first peak lateral mean pressure, (J) fist peak lateral maximum pressure, (K) lateral anterior-posterior impulse, (L) lateral compressional impulse, (M) lateral resultant impulse and (N) average lateral pressure during stance.

S4 Fig

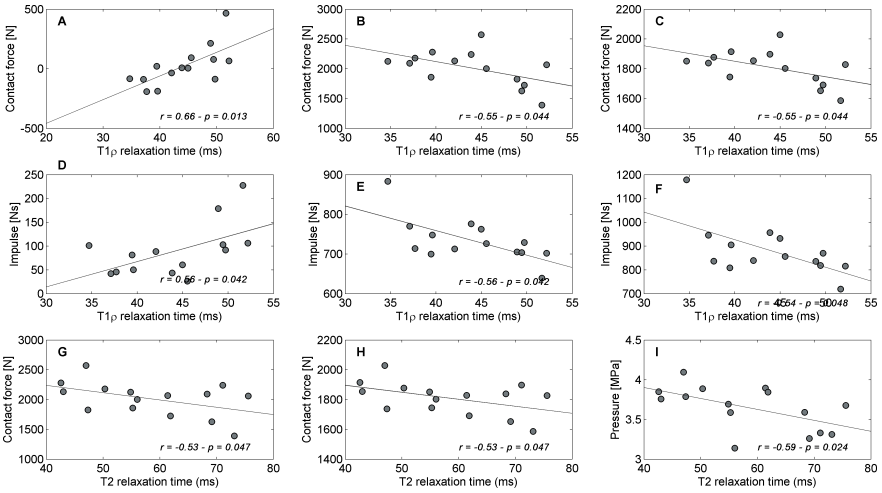

Figure 4.6: **Correlations between whole joint $T1\rho$ and T2 relaxation time and loading variables** Scatterplots of the significant correlations between the average total $T1\rho$ relaxation time and (A) second peak total knee anterior-posterior contact force, (B) second peak total knee compressional contact force, (C) second peak total knee resultant contact force, (D) total anterior-posterior impulse, (E) total compressional impulse and (F) total resultant impulse. Between the average total T2 relaxation time and (G) second peak total knee compressional contact force, (H) second peak total knee resultant contact force, (I) average total knee pressure during stance.

S5 Fig

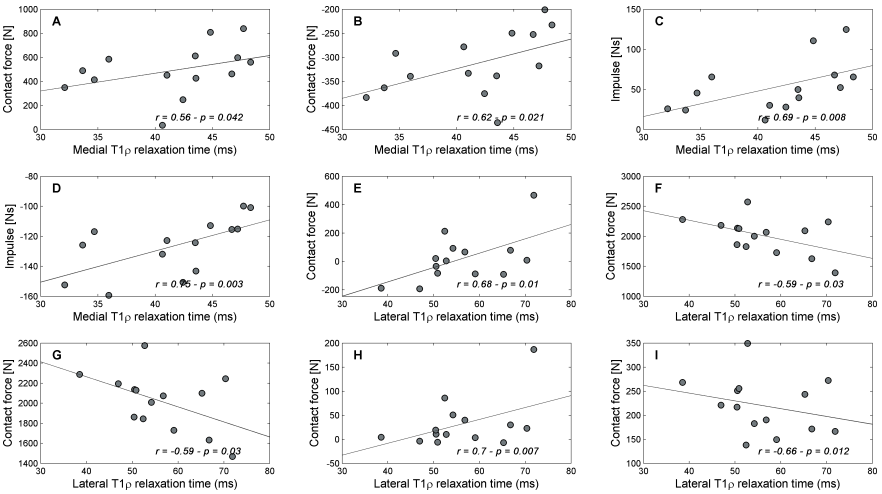

Figure 4.7: **Correlations between medial and lateral condyle $T1\rho$ relaxation time and loading variables** Scatterplots of the significant correlations between the average medial $T1\rho$ relaxation time and (A) first peak total knee anterior-posterior contact force, (B) second peak medial knee medial-lateral contact force, (C) medial anterior-posterior impulse and (D) medial medial-lateral impulse. Between the average lateral $T1\rho$ relaxation time and (E) second peak total knee anterior-posterior contact force, (F) second peak total knee compressional contact force, (G) second peak total knee resultant contact force, (H) second peak lateral anterior-posterior contact force and (I) second peak lateral medial-lateral contact force.

S Tables

supplementary tables can be retrieved in the online version of the paper.
Included tables:

- All calculated correlations for the total knee
- All calculated correlations for the medial condyle
- All calculated correlations for the lateral condyle
- Cartilage parameters for each subject

Chapter 5

Topographical variation of human femoral articular cartilage thickness, T1ρ and T2 relaxation time is related to local loading during walking

Sam Van Rossom, Mariska Wesseling, Dieter Van Assche, Ilse Jonkers

Submitted to *Cartilage*

Abstract

Early detection of degenerative changes in the cartilage matrix composition is essential for evaluating early interventions that slow down OA initiation. $T1\rho$ and T2 relaxation times were found to be effective for detecting early changes in proteoglycan and collagen content in-vivo. To use these MRI methods, it is important to document the topographical variation in cartilage thickness, and $T1\rho$ and T2 relaxation times in a healthy population. As OA is partially mechanically driven, the relation between these MR based parameters and localized mechanical loading during walking was further investigated. MR-images were acquired in 14 healthy adults and cartilage thickness and $T1\rho$ and T2 relaxation times were determined. Experimental gait data was collected and processed using musculoskeletal modeling to identify weight-bearing zones and estimate the contact force impulse during gait. Variation of the cartilage properties (i.e. thickness, $T1\rho$ and T2) over the femoral cartilage was analyzed and compared between the weight-bearing and non-weight-bearing zone of the medial and lateral condyle as well as the trochlea. Medial condyle cartilage thickness was correlated to the contact force impulse ($r = 0.78$, $p = 0.0026$). Lower $T1\rho$, indicating increased proteoglycan content, was found in the medial weight-bearing zone. T2 was higher in all weight-bearing zones compared to the non-weight-bearing zones, indicating lower collagen content. The current results suggest that medial condyle cartilage is adapted as a long-term protective response to the localized loading during a frequently performed task and that the weight-bearing zone of the medial condyle has superior weight-bearing capacities compared to the non-weight-bearing zones.

Keywords: Cartilage loading · Thickness · $T1\rho$ relaxation time · T2 relaxation time · Gait

Introduction

Osteoarthritis (OA) is one of the most prevalent chronic joint disorders affecting millions of people worldwide. It is a chronic degenerative disease with a multifactorial cause, which mostly affects the knee joint[1,2]. Currently, no effective therapeutic interventions exist that overcome or delay the progression of OA[3]. Early detection of degenerative changes in the cartilage is needed, as this would allow earlier intervention at a point where cartilage degeneration is minimal and where OA progression can be significantly delayed.

Frontal plane radiographs are used to diagnose OA, more specific with presence of osteophytes, subchondral bone sclerosis, cysts and joint space narrowing reflecting cartilage loss, resulting in a Kellgren-Lawrence-score ≥ 2[4–6]. However, to allow early intervention, methods that detect changes in the cartilage composition before irreversible, morphological changes occur are required. Classification of early OA is currently based on clinical scoring (i.e. presence of pain), standard radiographs (i.e. Kellgren-Lawrence-score < 2) and anatomical MRI scoring, evaluating cartilage and/or meniscal degeneration and presence of bone marrow lesions, however so far these evaluations do not account for changes in cartilage composition[6]. Indeed, recently, quantitative magnetic resonance imaging (MRI) methods were developed that reflect the biochemical composition of the articular cartilage extracellular matrix[7–11]. $T1\rho$ relaxation time can be used to assess proteoglycan content, whereas T2 relaxation time can be used as a measure of collagen content and orientation[12,13]. Increased $T1\rho$ relaxation time has been associated with a decreased proteoglycan concentration, which is one of the early degenerative changes in the cartilage extracellular matrix[10,14]. Increased T2 relaxation time has been related to increased collagen anisotropy and collagen loss[8,15]. Consequently, these sequences can be used for monitoring biochemical changes in extracellular matrix composition of the cartilage and therefore allow for an early detection of degenerative changes accompanied with OA before the onset of structural cartilage degeneration.

Insights gained from cadaveric and ex-vivo studies, documented regional differences in cartilage structure and extracellular matrix composition[16–18]. Cartilage homeostasis is at least partly regulated by mechanical loading and consequently local variations in loading could possibly explain the observed variation in extracellular matrix structure and composition[19,20]. Biochemical analysis of cartilage explants showed that the weight-bearing regions of the cartilage had increased sulphated glycosaminoglycan (GAG) concentration compared to the non-weight-bearing region[21]. Furthermore, GAG/collagen ratio was shown to be lower in the non-weight-bearing region compared to the weight-bearing region[18]. Topographical variation in proteoglycan synthesis was observed in adult ovine cartilage, whereas this topographical variation was not observed in neonatal ovine cartilage. This suggests that the topographical variation in proteoglycan concentration is caused by the topographical variation in weight-bearing stress after birth as the neonatal cartilage was not exposed previously to the weight-bearing stress[17].

As MRI relaxation times reflect the interaction between water and the surrounding matrix macromolecules, this topographical variability in matrix composition will be reflected in the cartilage relaxation times[12]. Previously, $T1\rho$ relaxation time values were observed to be lower in the weight-bearing regions of the lateral and medial femoral condyles, suggesting increased proteoglycan content in these regions and therefore increased weight-bearing capacity of the cartilage[22,23]. In contrast, T2 relaxation times were found to be heterogeneously distributed over the medial and lateral condyle and did not differ between weight-bearing and non-weight-bearing regions or was higher in the regions not covered by the meniscus[24–26]. Additionally, thickness, $T1\rho$ and T2 relaxation times of the femoral cartilage were found to be related to the contact

forces acting on the cartilage during walking[27]. However, the above-mentioned studies were based on a rather theoretical determination of the weight-bearing zone, restricting it to the position of the meniscus. Musculoskeletal modelling on the other hand has the potential to estimate the local cartilage pressures during locomotion, which allows for a more accurate description of the weight-bearing zones and local cartilage loading.

Therefore, to successfully investigate early changes in matrix composition using quantitative MRI methods, it is important to understand the topographical variation in cartilage structure, $T1\rho$ and T2 relaxation times in a healthy population. Therefore, the purpose of this study was to analyze the topographical variation of the cartilage thickness, $T1\rho$ and T2 relaxation times of the healthy femoral condyles and relate this to localized loading during walking, calculated using musculoskeletal modelling.

Methods

Subjects

Fourteen healthy volunteers (mean age: 30.64 ± 6.04years, mean weight: 71.24 ± 6.89kg and mean height: 178 ± 6.52cm) were recruited for participation in the current study. Participants were included when they were asymptomatic and had no history of knee injury or surgery. The study was approved by the local ethics committee and written informed consent was obtained from all participants.

Medical imaging

Imaging of the dominant leg was performed on a 3T Ingenia scanner after one hour standardized rest (Philips Healthcare, Best, The Netherlands). Participants were positioned in supine position with the knee in full extension and neutral rotation. The following scanning sequences were acquired: 1) A high-resolution 3D-fast spin echo (3D-FSE) acquisition used for soft tissue segmentation (Repetition time (TR)/ Echo time (TE) = 1800/120ms, field of view = 16cm, matrix = 268 x 268, slice thickness = 1mm, echo train length = 85, bandwidth = 562 kHz, number of excitations (NEX) = 2, number of slices = 320, acquisition time = 5.94min). 2) $T1\rho$ relaxation time sequence (TR/TE = 5.9587/3.082ms, time of recovery = 2000ms, field of view = 16cm, matrix = 292 x 256, slice thickness = 4mm, echo train length = 64, bandwidth = 522 kHz, time of spinlock (SLT) =0/10/20/40/60ms, frequency of spinlock = 500Hz, number of slices = 20, total acquisition time = 17.20min). 3) T2 relaxation time sequence (TR = 4000ms, TE = 11/22/33/44/55/66/77/88ms, field of view = 16cm, matrix = 160 x 160, slice thickness = 4mm, echo train length = 12, bandwidth = 367 kHz, number of slices = 20, acquisition time = 5.24min).

Image processing and cartilage segmentation

The same operator semi-automatically segmented the femoral cartilage and femur bone from the high-resolution images (3D-FSE) and 3D triangulated surfaces were created (Mimics Innovation Suite, Materialise, Leuven, Belgium). The segmented subject-specific cartilage surfaces were transformed onto the generic cartilage surface that is used in the musculoskeletal model using an advanced non-rigid deformation procedure (Mimics Innovation Suite, Materialise, Leuven, Belgium). Subsequently, cartilage thickness was calculated based on the minimal distance between the subchondral bone surface and the morphed cartilage surface for each vertex of the cartilage surface individually[28]. Relaxation time maps were generated by a pixel-by-pixel

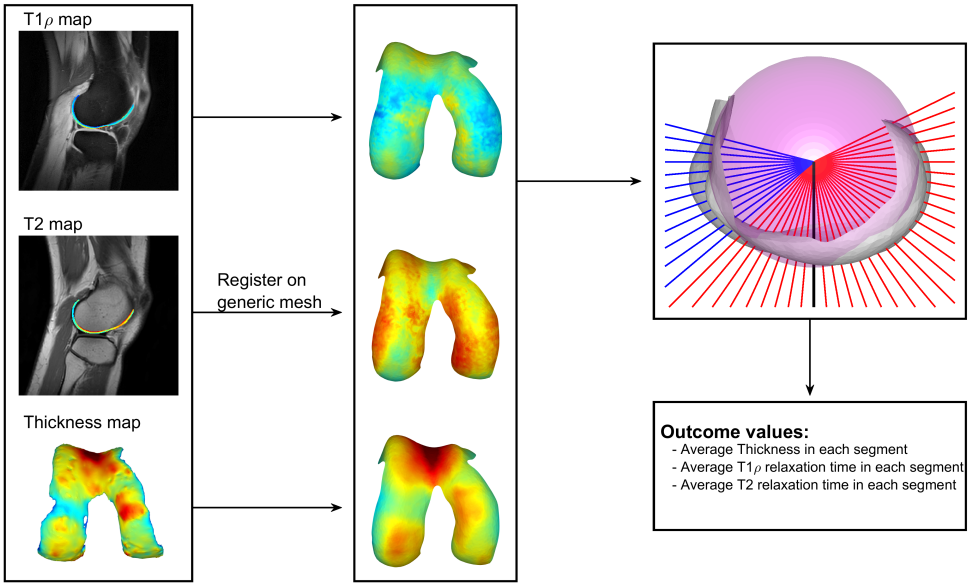

Figure 5.1: **Methodological overview.**
First, subject-specific, thickness, $T1\rho$ and T2 relaxation time maps were registered on the generic mesh. Subsequently, the generic mesh was divided in angular segments with increments of 5° clockwise and counterclockwise from the vertical line (black line). Last, average thickness, $T1\rho$ and T2 relaxation time was determined in each segment separately. Furthermore, the analyses were conducted for the tibiofemoral (red lines) and trochlear cartilage (blue lines) separately.

based evaluation of the mono-exponential Levenberg-Marquardt fitting algorithm[29]:

$$M(TSL) \propto e^{-\frac{TSL}{T1\rho}}$$
$$M(TE) \propto e^{-\frac{TE}{T2}}$$

The morphed cartilage surfaces were rigidly registered to the relaxation time maps and relaxation time values were assigned to the corresponding surface vertices (Figure 5.1).

The location-dependent profile of the thickness, $T1\rho$ and T2 relaxation time was evaluated over the cartilage surface over angular segments of 5°. To do so, a sphere was fitted onto the medial and lateral cartilage condyle vertices separately using a least-squares fitting algorithm. Next, the generic mesh was positioned in neutral postion and from the vertical line (angle 0°) the cartilage was divided in angular segments with 5° increments clockwise and counter-clockwise (i.e. negative angles are more towards posterior; Figure 5.1). The cartilage was further subdivided in tibiofemoral and trochlear cartilage. The intercondylar notch was used to differentiate between the trochlear and tibiofemoral cartilage (Figure 5.1).

Subsequently, the average $T1\rho$ and T2 relaxation time and average thickness was calculated in each angular segment (Figure 5.1). Relaxation times between 1 and 100ms were used to avoid outliers caused by a bad fit (0ms) or by synovial fluid and chemical shift artifact (>100ms)[26]. Additionally, the homogeneity was quantified by calculating the ratio of variability (expressed as the standard deviation) and the average thickness or relaxation times in a particular zone.

Motion analysis

Experimental motion data was collected on the same day as the medical imaging. A 10-camera Vicon system (Vicon Oford Metrics, 100Hz) was used to capture three-dimensional marker positions while participants were walking at self-selected speed across the motion lab. Simultaneously, ground reaction forces were measured using force plates embedded in the ground. Markers were placed according to an extended full-body Plug-in-Gait markerset[27,30]. Three trials with valid force plate contact were captured and retained for further processing.

Muscle and knee contact forces were calculated using a generic musculoskeletal model that was scaled to the subjects' anthropometry[31]. A validated customized knee joint that allows six degrees of freedom (DoF) tibiofemoral and patellofemoral joint kinematics was implemented in the generic lower extremity model[31,32]. Lower limb muscles were represented by 44 musculotendon actuators and the major knee ligaments as well as the posterior capsule were represented by 14 bundles of non-linear springs. An elastic foundation contact model was used to calculate the cartilage contact pressure[32,33]. Uniform cartilage thickness distribution was assumed in both joints, with a combined thickness of 4mm and 7mm in the tibiofemoral and patellofemoral joint, respectively[28,34,35]. Cartilage elastic modulus was set at 10MPa and Poisson's ratio at 0.45[36–38]. The lower extremity model was implemented in SIMM with the Dynamics Pipeline (Musculographics Inc., Santa Rosa, CA) and SD/Fast (Parametric Technology Corp., Needham, MA) used to generate the multibody equations of motion. This model was found to be accurate in predicting contact forces measured using instrumented implants with a root-mean-square (RMS) error below 0.33BW[39].

After scaling the generic model to the subject anthropometry, joint angles were calculated using inverse kinematics. Next, muscle forces required to generate the measured joint kinematics were calculated using the concurrent optimization of muscle forces and kinematics algorithm that solves for the secondary kinematics (11 DoF), while minimizing the weighted sum of squared muscle activations and contact energy[40]. This algorithm allows the kinematics in the secondary tibiofemoral and patellofemoral DoF to evolve as function of muscle, ligament and contact forces, since only the primary DoF (i.e. hip flexion, hip adduction, hip rotation, knee flexion and ankle flexion) were prescribed to reproduce the measured values during the optimization[32,33,40]. Lastly, the impulse on each mesh element was calculated by integrating the resultant contact force on each element over time. The impulse on each angular segment was calculated by summing the impulses on each mesh face in each angular segment.

Statistics

The weight-bearing zone was determined as the zone on which impulse was estimated during the stance phase. The local relation over the different angular segments between the relaxation times or thickness values and impulses in the weight-bearing zone was evaluated using a Spearman Rank correlation coefficient. Differences in $T1\rho$ and T2 relaxation times and thickness between weight-bearing and non-weight-bearing areas were analyzed using a Wilcoxon signed rank test. Alpha level was set at 0.05 and all statistical tests were performed in MATLAB (MATLAB 2016b, The Math Works, Inc., Natick, Massachusetts, USA).

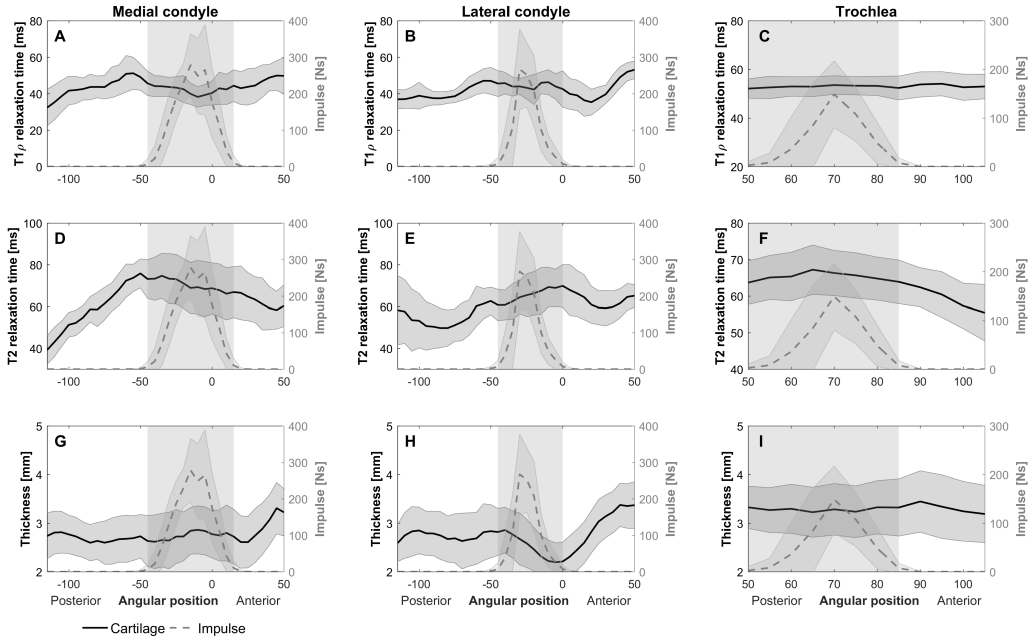

Figure 5.2: **Angular distribution.**
Angle-dependent analysis of the $T1\rho$ relaxation time (upper row), T2 relaxation time (middle row) and thickness (lower row) over the medial condyle (A, D and G), lateral condyle (B, E and H) and trochlea (C, F and I) in black. Additionally, the angular distribution of the impulse during walking is shown in a gray, dashed line. The weight-bearing area is indicated by the gray zone.

Results

In the current cohort of healthy participants, the weight-bearing zone on the medial condyle during gait was identified between $-45°$ posterior and $15°$ anterior, whereas the weight-bearing zone on the lateral condyle was observed between $-45°$ posterior and $0°$ anterior (Figure 5.2).

Thickness

The cartilage thickness of the weight-bearing zone of the lateral condyle was found to be significantly lower than the thickness of the non-weight-bearing zone (Figure 5.3 C). The thickness of the weight-bearing zone of the medial condyle was significantly correlated to the contact force impulse on the medial weight-bearing zone (R = 0.78, p = 0.0026).

$T1\rho$ relaxation time

Topographical variation in $T1\rho$ relaxation times over the different angles is presented in figure 5.2. The $T1\rho$ relaxation time of the weight-bearing zone of the medial condyle was found to be significantly lower than the $T1\rho$ relaxation time of the non-weight-bearing zone (Figure 5.3A). The $T1\rho$ relaxation time in the medial weight-bearing zone was negatively correlated to the impulse on the medial weight-bearing zone (R = -0.71, p = 0.008). In contrast, the $T1\rho$ relaxation time of the weight-bearing zone of the trochlea was positively correlated to the impulse on the weight-bearing zone on the trochlea (R = 0.98, p = 0.0004).

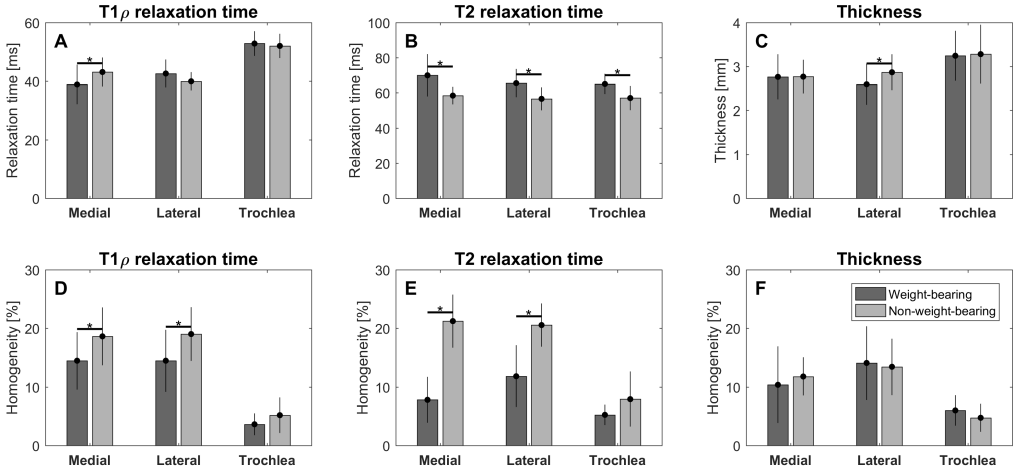

Figure 5.3: **Comparison weight-bearing vs non-weight-bearing.**
Differences in $T1\rho$ relaxation time (A), T2 relaxation time (B) and thickness (C) between the weight-bearing (dark gray) and non-weight-bearing (light gray) zones. Differences in homogeneity in $T1\rho$ relaxation time (D), T2 relaxation time (E) and thickness (F) between the weight-bearing (dark gray) and non-weight-bearing (light gray) zones. A lower value indicates a more homogeneous distribution whereas a higher value indicates a more heterogeneous distribution. * indicates a significant difference between weight-bearing and non-weight-bearing (alpha <0.05).

The $T1\rho$ relaxation time was found to be distributed significantly more homogeneous in the weight-bearing zones of both condyles than the non-weight-bearing zones. Whereas no difference in homogeneity was observed for the trochlea (Figure 5.3D).

T2 relaxation time

Topographical variation in T2 relaxation time over the different angles is presented in figure 5.2. The T2 relaxation time of the weight-bearing zones of both condyles was found to be significantly higher than the T2 relaxation time of the non-weight-bearing zones (Figure 5.3B). Furthermore, the T2 relaxation time of the weight-bearing zone of the trochlea was significantly higher than the T2 relaxation time of the non-weight-bearing zone of the trochlea (Figure 5.3B). No significant correlation between T2 relaxation time and impulse on the weight-bearing zones was observed for the medial and lateral condyle. The T2 relaxation time of the weight-bearing zone of the trochlea was positively correlated with the impulse on the weight-bearing zone of the trochlea ($R = 0.79$, $p = 0.028$).

The T2 relaxation time was found to be distributed significantly more homogeneous in the weight-bearing zones of both condyles than the non-weight-bearing zones. Whereas no difference in homogeneity was observed for the trochlea (Figure 5.3E).

Discussion

The present study evaluated the topographical variation in MRI-based measures of matrix composition and morphology of femoral cartilage of healthy adults. Cartilage thickness was used to assess cartilage morphology. $T1\rho$ mapping was used to indirectly investigate proteoglycan content and T2 mapping was used to indirectly assess collagen content and orientation. Furthermore, the relation between localized loading and

these cartilage-describing parameters was evaluated. Cartilage $T1\rho$ and T2 relaxation time and thickness were found to vary over the medial and lateral condyles, whereas less variation was observed in the trochlear cartilage. Furthermore, these parameters differ in the weight-bearing zones compared to the non-weight-bearing zones.

In agreement with previous research, this study observed a location dependent variation in cartilage thickness[41,42]. Although, no differences in cartilage thickness between the weight-bearing and non-weight-bearing zones were observed, a strong correlation between localized loading on the medial condyle and the medial condyle cartilage thickness was observed. This suggests that localized loading contributes to the variation in cartilage thickness, with locations exposed to increased loading having thicker cartilage. Previously, the anterior-posterior thickness distribution was found to relate to the knee flexion extension angle at heel strike[42–44]. As the authors assumed this time instant to coincide with high compressive forces, they hypothesized that the thicker cartilage was a long term protective response to high loading[42–44]. In support of this hypothesis, the current study confirmed that the weight-bearing region as a whole is adapted to the cumulative loading perceived during stance, (as reflected in the impulse of the contact force). Whereas previously, it was only found to be related to the knee position at heel strike. In agreement with other studies, no relation between cartilage thickness of the lateral condyle and lateral condyle loading was observed. The absence of this relation was previously attributed to different contact mechanics compared to the medial condyle[42,43,45].

In the current study, the $T1\rho$ relaxation time of the weight-bearing zone on the medial condyle was found to be lower than the non-weight-bearing zone, whereas no difference was observed between the weight-bearing and non-weight-bearing zone on the lateral condyle. This is in line with previous studies that observed lower $T1\rho$ relaxation times in the weight-bearing zones[22,46]. On the other hand, in line with the present results no difference in $T1\rho$ relaxation time between weight-bearing and non-weight-bearing zones of the lateral condyle was previously observed[47]. Cartilage matrix composition was previously suggested to be affected by localized loading. Since the medial condyle receives a higher fraction of the loading during walking, this may suggest that the proteoglycan content of the lateral condyle cartilage is less adapted to mechanical loading during walking. Consequently, variation in $T1\rho$ relaxation time of the lateral condyle cartilage is more affected by other factors such as genetics, age or mechanical loading during other movements that load the lateral condyle more.

As $T1\rho$ relaxation time is related to proteoglycan content, our results suggest that the cartilage in the weight-bearing zone of the medial condyle contains more proteoglycans. This finding agrees with previous work that observed higher GAG content in the contacting zones of the femoral condyles compared to the non-contacting zones[21,48]. In line, $T1\rho$ relaxation time was found to be related to the aggregate modulus of cartilage, with higher relaxation times being related to lower aggregate modulus[23]. This indicates that the cartilage in the weight-bearing zone of the medial condyle has superior biomechanical properties and therefore, better able to withstand the high compressive forces experienced during locomotion. The fact that no differences in $T1\rho$ relaxation times of the lateral condyle and trochlear cartilage were observed can possibly be attributed to the fact that the lateral condyle and trochlea are less involved in weight-bearing loading during gait. Indeed, the estimated impulse on the trochlear cartilage was lower compared to the tibiofemoral impulses. Furthermore, the trochlear cartilage may be more exposed to shear stresses by the gliding movement of the patella during the flexion-extension cycle.

The current results regarding the T2 relaxation times suggest that the collagen concentration and orientation is lower in the weight-bearing zones compared to the non-weight-bearing zones. Similar to previous studies, T2 relaxation time was found to be higher in the weight-bearing zones of both the medial and the lateral condyle as well as the trochlea[24,25,49]. However, in the present study the collagen in the weight-bearing regions is distributed more homogeneously. Assuming that a homogeneous collagen orientation is the primal contributor to the cartilage resistance against shear forces and not collagen content, the current results suggest that the cartilage in the weight-bearing region has superior mechanical properties. On the other hand, a less dense collagen network with higher or equal concentration of proteoglycans would suggest an increased capacity of the extracellular matrix to sustain compressive loads experienced during walking, as this would increase the capacity to deform under compression.

When interpreting the results of the current study one should consider the use of a generic cartilage mesh to project cartilage thickness and relaxation times. This way, the effect of subject specific detail in cartilage structure and constitution may have been lost, consequently weakening the observed relation between loading and MRI-based parameters. Furthermore, the generic mesh assumes a uniformly distributed cartilage thickness in the calculation of contact pressures. As a consequence, regional variation in loading is imposed through the motion characteristics (i.e. kinematics) rather than the local variation in cartilage shape.

In conclusion, we observed a topographical variation in cartilage thickness and matrix components estimated using quantitative MRI (i.e. $T1\rho$ and T2 mapping). The topographical variation in the medial condyle cartilage thickness was found to be related to localized cartilage loading and could therefore be interpreted as a long-term protective response of the cartilage to loading. This indicates that zones, experiencing higher local loading during walking have thicker cartilage. Lastly, superior weight-bearing capacities, more specific increased proteoglycan and decreased collagen content in the weight-bearing region of the medial condyle were observed compared to the non-weight-bearing region of the medial condyle.

References

1. Felson DT, Lawrence RC, Dieppe PA, Hirsch R, Helmick CG, Jordan JM, et al. Osteoarthritis: New insights - Part 1: The disease and its risk factors. Annals of Internal Medicine. 2000. pp. 635–646.
2. Lories RJ, Luyten FP. The bone–cartilage unit in osteoarthritis. Nat Rev Rheumatol. Nature Publishing Group; 2011;7: 43–49.
3. McAlindon TE, Bannuru RR, Sullivan MC, Arden NK, Berenbaum F, Bierma-Zeinstra SM, et al. OARSI guidelines for the non-surgical management of knee osteoarthritis. Osteoarthr Cartil. Elsevier Ltd; 2014;22: 363–388.
4. Risberg MA, Holm I, Tjomsland O, Ljunggren E, Ekeland A. Prospective study of changes in impairments and disabilities after anterior cruciate ligament reconstruction. J Orthop Sport Phys Ther. 1999;29: 400–412.
5. Kellgren JH, Lawrence JS. Radiological Assessment of Osteo-Arthrosis. Ann Rheum Dis. 1957;16: 494–502.
6. Luyten FP, Denti M, Filardo G, Kon E, Engebretsen L. Definition and classification of early osteoarthritis of the knee. Knee Surgery, Sport Traumatol Arthrosc. 2012;20: 401–406.
7. Li X, Cheng J, Lin K, Saadat E, Bolbos RI, Jobke B, et al. Quantitative MRI using T1ρ and T2 in human osteoarthritic cartilage specimens: Correlation with biochemical measurements and histology. Magn Reson Imaging. Elsevier Inc.; 2011;29: 324–334.
8. Stahl R, Luke A, Li X, Carballido-Gamio J, Ma CB, Majumdar S, et al. T1rho, T2 and focal knee cartilage abnormalities in physically active and sedentary healthy subjects versus early OA patients–a 3.0-Tesla MRI study. Eur Radiol. 2009;19: 132–43.
9. Keenan KE, Besier TF, Pauly JM, Han E, Rosenberg J, Smith RL, et al. Prediction of glycosaminoglycan content in human cartilage by age, T1ρ and T2 MRI. Osteoarthr Cartil. Elsevier Ltd; 2011;19: 171–9.
10. Wheaton AJ, Dodge GR, Elliott DM, Nicoll SB, Reddy R. Quantification of cartilage biomechanical and biochemical properties via T1rho magnetic resonance imaging. Magn Reson Med. 2005;54: 1087–93.
11. Mosher TJ, Walker E a, Petscavage-Thomas J, Guermazi a. Osteoarthritis year 2013 in review: imaging. Osteoarthritis Cartilage. 2013;21: 1425–35.
12. Crema MD, Frank W, Marra MD, Burstein D, Gold GE, Eckstein MF, et al. Articular Cartilage in the Knee: Current MR Imaging Techniques and Applications in Clinical. Radiographics. 2011;31: 37–61.
13. Xia Y, Moody JB, Burton-Wurster N, Lust G. Quantitative in situ correlation between microscopic MRI and polarized light microscopy studies of articular cartilage. Osteoarthr Cartil. 2001;9: 393–406.
14. Akella SVS, Regatte RR, Gougoutas AJ, Borthakur A, Shapiro EM, Kneeland JB, et al. Proteoglycan-Induced Changes in T 1ρ-Relaxation of Articular Cartilage at 4T. 2001;423: 419–423.
15. Matzat SJ, van Tiel J, Gold GE, Oei EHG. Quantitative MRI techniques of cartilage composition. Quant Imaging Med Surg. 2013;3: 162–74.
16. Shepherd DE, Seedhom BB. Thickness of human articular cartilage in joints of the lower limb. Ann Rheum Dis. 1999;58: 27–34.
17. Little CB, Ghosh P. Variation in proteoglycan metabolism by articular chondrocytes in different joint regions is determined by post-natal mechanical loading. Osteoarthr Cartil. 1997;5: 49–62.
18. Stenhamre H, Slynarski K, Petrén C, Tallheden T, Lindahl A. Topographic variation in redifferentiation capacity of chondrocytes in the adult human knee joint. Osteoarthr Cartil. 2008;16: 1356–1362.
19. Andriacchi TP, Favre J. The Nature of In Vivo Mechanical Signals That Influence Cartilage Health and Progression to Knee Osteoarthritis. Curr Rheumatol Rep. 2014;16: 463–470.
20. Carter DR, Beaupré GS, Wong M, Smith RL, Andriacchi TP, Schurman DJ. The Mechanobiology of Articular Cartilage Development and Degeneration. Clin Orthop Relat Res. 2004;427: S69–S77.
21. Rogers BA, Murphy CL, Cannon SR, Briggs TWR. Topographical variation in glycosaminoglycan content in human articular cartilage. J Bone Jt Surg [Br]. 2006;88: 1670–4.
22. Nozaki T, Kaneko Y, Yu HJ, Kaneshiro K, Schwarzkopf R, Hara T, et al. T1rho mapping of entire femoral cartilage using depth- and angle-dependent analysis. Eur Radiol. European Radiology; 2016;26: 1952–1962.
23. Hatcher CC, Collins AT, Kim SY, Michel LC, Mostertz WC, Ziemian SN, et al. Relationship between T1rho magnetic resonance imaging, synovial fluid biomarkers, and the biochemical and biomechanical properties of cartilage. J Biomech. Elsevier Ltd; 2017;55: 18–26.

24. Surowiec RK, Lucas EP, Fitzcharles EK, Petre BM, Dornan GJ, Giphart JE, et al. T2 values of articular cartilage in clinically relevant subregions of the asymptomatic knee. Knee Surgery, Sport Traumatol Arthrosc. 2014;22: 1404–1414.

25. Shiomi T, Nishii T, Nakata K, Tamura S, Tanaka H, Yamazaki Y, et al. Three-dimensional topographical variation of femoral cartilage T2 in healthy volunteer knees. Skeletal Radiol. 2013;42: 363–370.

26. Kaneko Y, Nozaki T, Yu H, Chang A, Kaneshiro K, Schwarzkopf R, et al. Normal T2 map profile of the entire femoral cartilage using an angle/layer-dependent approach. J Magn Reson Imaging. 2015;42: 1507–1516.

27. Van Rossom S, Smith CR, Zevenbergen L, Thelen DG, Vanwanseele B, Van Assche D, et al. Knee Cartilage Thickness, T1ρ and T2 Relaxation Time Are Related to Articular Cartilage Loading in Healthy Adults. PLoS One. 2017;12: e0170002.

28. Draper CE, Besier TF, Gold GE, Fredericson M, Fiene A, Beaupre GS, et al. Is cartilage thickness different in young subjects with and without patellofemoral pain? Osteoarthr Cartil. 2006;14: 931–937.

29. Li X, Benjamin Ma C, Link TM, Castillo D-D, Blumenkrantz G, Lozano J, et al. In vivo T1rho and T2 mapping of articular cartilage in osteoarthritis of the knee using 3 T MRI. Osteoarthr Cartil. 2007;15: 789–97.

30. Davis RB, Ounpuu S, Tyburski D, Gage JR. A gait analysis data collection and reduction technique. Hum Mov Sci. 1991;10: 575–587.

31. Arnold EM, Ward SR, Lieber RL, Delp SL. A model of the lower limb for analysis of human movement. Ann Biomed Eng. 2010;38: 269–79.

32. Lenhart RL, Kaiser J, Smith CR, Thelen DG. Prediction and Validation of Load-Dependent Behavior of the Tibiofemoral and Patellofemoral Joints During Movement. Ann Biomed Eng. 2015;43: 2675–2685.

33. Smith RC, Choi KW, Negrut D, Thelen DG. Efficient Computation of Cartilage Contact Pressures within Dynamic Simulations of Movement. Comput Methods Biomech Biomed Eng Imaging Vis. 2016;

34. Hudelmaier M, Glaser C, Englmeier K-H, Reiser M, Putz R, Eckstein F. Correlation of knee-joint cartilage morphology with muscle cross-sectional areas vs. anthropometric variables. Anat Rec Part A. 2003;270: 175–184.

35. Eckstein F, Reiser M, Englmeier KH, Putz R. In vivo morphometry and functional analysis of human articular cartilage with quantitative magnetic resonance imaging–from image to data, from data to theory. Anat Embryol (Berl). 2001;203: 147–73.

36. Blankevoort L, Kuiper JH, Huiskes R, Grootenboer HJ. Articular contact in a three-dimensional model of the knee. J Biomech. 1991;24: 1019–1031.

37. Li G, Lopez O, Rubash H. Variability of a Three-Dimensional Finite Element Model Constructed Using Magnetic Resonance Images of a Knee for Joint Contact Stress Analysis. J Biomech Eng. 2001;123: 341–346.

38. Adouni M, Shirazi-Adl A. Partitioning of Knee Joint Internal Forces in Gait Is Dictated By the Knee Adduction Angle and Not By the Knee Adduction Moment. J Biomech. Elsevier; 2014;47: 1696–703.

39. Smith CR, Vignos MF, Lenhart RL, Kaiser J, Thelen DG. The Influence of Component Alignment and Ligament Properties on Tibiofemoral Contact Forces in Total Knee Replacement. J Biomech Eng. 2016;138: 1–10.

40. Thelen DG, Won Choi K, Schmitz AM. Co-simulation of neuromuscular dynamics and knee mechanics during human walking. J Biomech Eng. 2014;136: 21033.

41. Eckstein F, Winzheimer M, Hohe J, Englmeier KH, Reiser M. Interindividual variability and correlation among morphological parameters of knee joint cartilage plates: Analysis with three-dimensional MR imaging. Osteoarthr Cartil. 2001;9: 101–111.

42. Koo S, Rylander JH, Andriacchi TP. Knee joint kinematics during walking influences the spatial cartilage thickness distribution in the knee. J Biomech. Elsevier; 2011;44: 1405–1409.

43. Scanlan SF, Favre J, Andriacchi TP. The relationship between peak knee extension at heel-strike of walking and the location of thickest femoral cartilage in ACL reconstructed and healthy contralateral knees. J Biomech. Elsevier; 2013;46: 849–854.

44. Li G, Park SE, DeFrate LE, Schutzer ME, Ji L, Gill TJ, et al. The cartilage thickness distribution in the tibiofemoral joint and its correlation with cartilage-to-cartilage contact. Clin Biomech. 2005;20: 736–744.

45. Koo S, Andriacchi TP. A comparison of the influence of global functional loads vs. local contact anatomy on articular cartilage thickness at the knee. J Biomech. 2007;40: 2961–2966.

46. Bolbos RI, Link TM, Benjamin Ma C, Majumdar S, Li X. T1ρ relaxation time of the meniscus and its relationship with T1ρ of adjacent cartilage in knees with acute ACL injuries at 3 T. Osteoarthr Cartil. Elsevier Ltd; 2009;17: 12–18.

47. Goto H, Iwama Y, Fujii M, Aoyama N, Kubo S, Kuroda R, et al. A preliminary study of the T1rho values of normal knee cartilage using 3T-MRI. Eur J Radiol. Elsevier Ireland Ltd; 2012;81: e796-803.

48. Mayerhoefer ME, Welsch GH, Mamisch TC, Kainberger F, Weber M, Nemec S, et al. The in vivo effects of unloading and compression on T1-Gd (dGEMRIC) relaxation times in healthy articular knee cartilage at 3.0 Tesla. Eur Radiol. 2010;20: 443–449.

49. Hannila I, Susanna Räinä S, Tervonen O, Ojala R, Nieminen MT. Topographical variation of T2 relaxation time in the young adult knee cartilage at 1.5 T. Osteoarthr Cartil. 2009;17: 1570–1575.

Chapter 6

The influence of knee joint geometry and alignment on the tibiofemoral load distribution: a computational study

Sam Van Rossom, Mariska Wesseling, Colin R Smith, Darryl G Thelen, Benedicte Vanwanseele, Dieter Van Assche, Ilse Jonkers

Submitted to *Journal of Orthopaedic Research*

Abstract

Deviations in knee joint geometry and alignment were previously related to an increased risk for knee OA. These were hypothesized to influence the load distribution over the articular cartilage. Therefore, this study evaluated the effect of altered knee joint geometry and alignment in the coronal and transverse plane on the medial-lateral load distribution and ligament strain using a musculoskeletal modelling approach.

Joint kinematics during gait were measured in fifteen healthy adults. Using different musculoskeletal models with altered geometry of the tibia plateau or knee joint malalignment in the coronal and transverse plane, the resulting muscle, ligament and contact forces were calculated. Next, the distribution of the load over the medial and lateral condyle was analyzed and compared to the reference loading distribution, with neutral geometry and alignment, using repeated-measures ANOVA and individual t-tests, with a bonferroni-corrected alpha level.

Coronal plane malalignment significantly affected the load distribution. Small changes in coronal tibial slope had less pronounced effects on the load distribution, but increased ligament strains. Transverse plane joint geometry changes or malalignment only minimally affected the load distribution.

Coronal plane knee malalignment affected knee loading, with increased varus alignment resulting in increased medial loading. This confirms a causal relation between coronal malalignment and increased medial compartment loading and suggests a potential role of aberrant coronal plane alignment on OA initiation. Altered coronal tibial slope induced increased ligament strains, potentially contributing to a cascade of knee laxity and subsequently more extreme knee malalignment.

Keywords: Contact forces · Malalignment · Tibial slope · Ligament strain · Osteoarthritis

Introduction

Multiple factors contribute to the initiation of knee osteoarthritis (OA) and ultimately articular cartilage breakdown[1]. Knee joint geometry as well as joint alignment were previously identified as risk factors for knee OA development by affecting the knee loading distribution[2–4]. In a neutrally aligned joint, the medial condyle is predominantly loaded during walking[5]. Risk factors for knee OA (e.g. alignment and knee laxity) are hypothesized to affect the knee load distribution, therefore increasing the stress on the different knee joint structures, more specifically the ligaments, menisci, articular cartilage and subchondral bone[6]. Cartilage loss is at least partly regulated by mechanical loading. It is suggested that cartilage loss occurs more in regions that are subjected to high loading [7,8]. Joint geometry and malalignment will in turn induce regional differences in loading.

Altered coronal plane joint geometry, more specifically increased elevation of the lateral tibial plateau and an increased coronal tibial slope were previously related to an increased risk for knee OA initiation[9,10]. In the transverse plane, increased internal tibial torsion is hypothesized to increase compressive and shear loading on the medial condyle and has been related to knee OA[11–14]. These deviations in joint geometry indeed affect joint congruity and therefore have the potential to influence knee loading distribution[7]. OA patients with internal tibial torsion were found to walk with an increased knee adduction moment (KAM), suggesting increased loading and compression of the medial condyle as a potential contributor to knee OA[15]. Apart from its role in altering the knee load distribution and therefore increased risk for knee OA initiation, joint geometry may also induce malalignment of the knee joint in a later stage of the OA process itself[10].

Deviations in joint alignment, especially varus and valgus malalignment, were previously related to an increased risk for bone marrow lesions and cartilage loss in the medial and lateral condyle, respectively[16–18]. Using KAM as an indirect measure of medial condyle loading, the degree of varus alignment was found to be directly proportional to KAM [19–22]. This suggests that varus malalignment increases loading on the medial condyle and could therefore contribute to OA initiation and progression[3,23–27].

Besides their effect on the knee joint loading, altered joint geometry and alignment may influence the stability provided by the ligaments. Given the relation between knee instability and OA, ligamentous laxity was previously suggested to contribute to the initiation and progression of knee OA [28–31]. Ligamentous laxity and the consequent knee instability could cause a shift in contact locations towards infrequently loaded regions. As in these regions the cartilage is less suited for loading, degenerative changes in the cartilage could be induced[32,33]. However, the potential role of altered joint geometry and malalignment in aberrant ligament lengthening behavior and therefore knee instability is currently unexplored.

Despite their clinical significance, the effect of alterations in joint geometry and alignment on knee cartilage loading distribution and ligament strains cannot be investigated in-vivo. In-vitro, it was found that, after correcting for valgus malalignment, lateral condyle pressure was decreased with a concomitant increase in medial contact pressure[34]. Additionally, under static loading, varus alignment resulted in increased medial condyle pressure[35,36]. To corroborate these in-vitro findings, musculoskeletal modelling can be used to assess and quantify the isolated effect of alignment or geometry on the contact force distribution over the articular cartilage. Since other influencing factors, such as ligament properties, height, weight can be kept constant[37]. This approach has already been used to study the effect of implant alignment on loading distribution, suggesting that coronal plane joint alignment after total knee replacement had a substantial

influence on the medial-lateral contact force distribution[38–41]. In contrast, no effect of transverse plane alignment of the tibia component on the contact force distribution was observed[39]. However, given the clearly different geometry of the implant and the native knee joint, these insights cannot be directly translated to the effect of altered joint geometry and malalignment on altered knee joint loading in the native joint.

Therefore, the purpose of this study was to investigate the effect of alterations in knee joint geometry and malalignment in the coronal and transverse plane on cartilage loading distribution as well as the ligament strains using a musculoskeletal modelling approach. This analysis has a role in identifying the isolated contribution of each of these geometrical factors previously related to an increased OA initiation risk and progression, to alterations in cartilage loading.

Methods

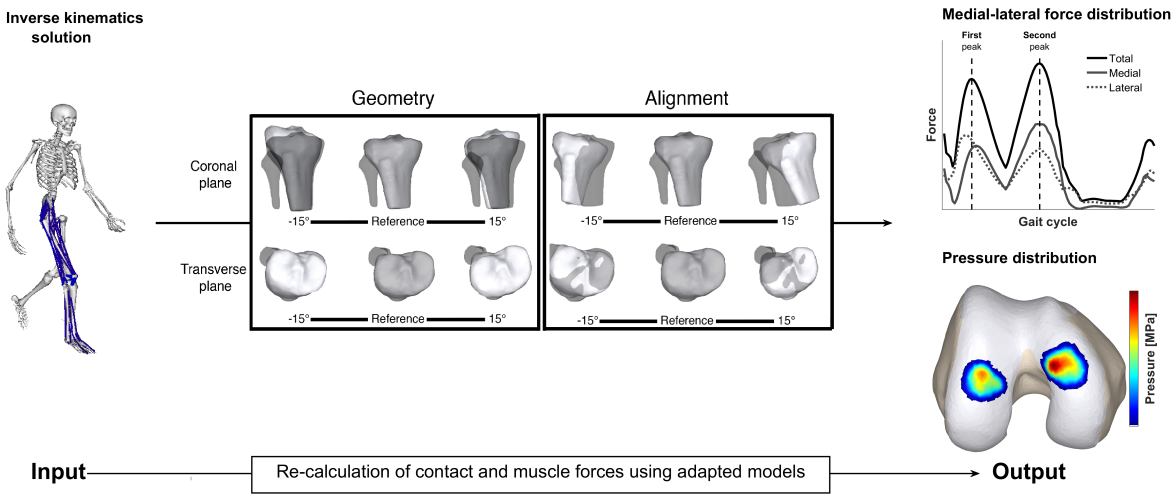

Figure 6.1: **Overview of the methodology.**
A scaled musculoskeletal model was used to calculate the kinematics during walking. Next, the muscle forces and contact forces were calculated with models in which the alignment of the knee or the position of the tibia plateau, to simulate a deviating joint geometry was systematically changed from 1° to 15° from its reference position in the coronal and transverse plane in steps of 2°. Subsequently, the effect on the contact force and pressure distribution was analyzed and compared with the reference loading pattern obtained with the original model.

Experimental procedure

Barefoot walking at self-selected speed (1.39 ± 0.12 m/s) was measured in fifteen healthy adults (8 males, 7 females, mean age = 30.73 ± 5.84 years, mean weight = 70.49 ± 7.24 and mean height = 177.47 ± 6.61). A ten-camera Vicon system was used to capture three-dimensional marker trajectories (100Hz, Vicon, Oxford Metrics, Oxford, UK). Markers were positioned according to an extended full-body Plug-in-Gait marker set (Supplementary material S1). Simultaneously, ground reaction forces were measured, using two ground-embedded force plates (1000Hz, AMTI, Watertown, USA). Three trials per subject were retained for further

processing. The university hospital ethics committee approved all procedures (s56093) and written informed consent was obtained.

Musculoskeletal modeling

A customized knee joint with 6 degrees of freedom (DoF) in the patellofemoral and tibiofemoral joint was implemented in a generic lower extremity model[42,43]. Each leg of the musculoskeletal model contains 44 musculotendon actuators and 14 bundles of non-linear springs, representing the major knee ligaments and posterior capsule. Cartilage contact pressure was calculated based on the penetration depth of the overlapping cartilage surface meshes, using a non-linear elastic foundation formulation[44]. The cartilage was assumed to be uniformly distributed with a combined thickness of 4 and 7mm for the tibiofemoral and patellofemoral joint, respectively[45–47]. The elastic modulus of the cartilage was defined as 10 MPa and Poisson's ratio as 0.45[48–50]. This model was implemented in SIMM with the Dynamics Pipeline (Musculographics Inc., Santa Rosa, CA) and SD/Fast (Parametric Technology Corp., Needham, MA) was used to generate the multibody equations of motion.

To generate the reference simulations, the generic model was scaled based on the marker locations in a static calibration trial and the subject's mass. Next, an inverse kinematics procedure was used to calculate the joint kinematics based on the measured 3D marker trajectories[51]. Subsequently, the muscle activations required to reproduce the measured primary hip, knee and ankle accelerations were estimated using the concurrent optimization of muscle activations and kinematics algorithm, in which the weighted sum of squared muscle activations and contact energy were minimized[44]. The secondary tibiofemoral and all patellofemoral DoF evolved as a function of muscle, ligament and contact forces, since only the knee flexion angle was prescribed during the optimization[43,44,52].

To generate the simulations with varied joint alignment and geometry, the scaled musculoskeletal model was modified as described in Figure 6.1. The effect of variation in joint geometry was investigated by altering the orientation of the tibia plateau in the coronal and transverse plane, while keeping the knee alignment unchanged. This mimicked a more elevated medial or lateral tibia plateau, representative of altered coronal tibial slope (coronal plane) or mimicked a tibia with a higher or lower degree of tibial torsion (transverse plane). The effect of malalignments in the coronal and transverse plane was investigated by altering the relative orientation of the tibia relative to the femur in the coronal and transverse plane. This resulted in a more varus or valgus aligned knee (coronal plane) or a more internally or externally rotated knee (transverse plane). For both joint geometry and alignment in the coronal and transverse plane, each parameter was systematically varied from $\pm 1^\circ$ to $\pm 15^\circ$ from its neutral position in steps of 2°[3,37]. This resulted in a dataset containing 3 simulations for each type of modification for each subject. In total, 3060 simulations were generated: 51 simulations for 15 subjects for each type of modification).

After these modifications to the musculoskeletal models, simulations with the reference input kinematics and ground reaction forces (GRF) were generated using the similar modelling workflow as described above (figure 6.1). When simulating malalignment, the location of the foot with respect to the measured GRF application point is changed. To ensure that for these simulations the application of the ground reaction force to the foot was identical to the reference simulation, the center of pressure (of the ground reaction force) was expressed in the local reference frame of the foot. We assumed that compensations in the trunk kinematics would account for any dynamic inconsistency[53].

Data analysis

The timing of the two peaks in the resultant tibiofemoral contact force was identified and the coinciding knee adduction moment (KAM), contact force magnitude and mean pressure was analyzed. All variables, except KAM were analyzed for the medial and lateral condyle separately. KAM was scaled to body mass, contact forces were scaled to bodyweight (BW) and contact pressures were scaled to bodyweight and knee dimensions (BW*A^2). Furthermore, peak ligament strains were determined for the anterior and posterior cruciate ligament (ACL and PCL), as well as the medial and lateral collateral ligament (MCL and LCL). Ligament strain was calculated by:

$$\epsilon = \frac{l - l_0}{l_0}$$

with l_0 being the ligament length in the reference position and l being the ligament length. A repeated-measures ANOVA was used to check for significant differences in contact force, contact pressure and ligament strain between the different geometries or alignments separately. When a significant effect for geometry or alignment was found, all imposed geometries or alignments were individually compared to the reference simulation using a paired t-test. Significance level was set at $\alpha = 0.05$ and a Bonferroni correction was applied to correct for the multiple testing ($\alpha_{BC} = 0.003125$). All statistical tests were conducted in MATLAB (MATLAB 2016b, The Math Works, Inc., Natick, Massachusetts, USA).

Results

Knee geometry

Coronal plane

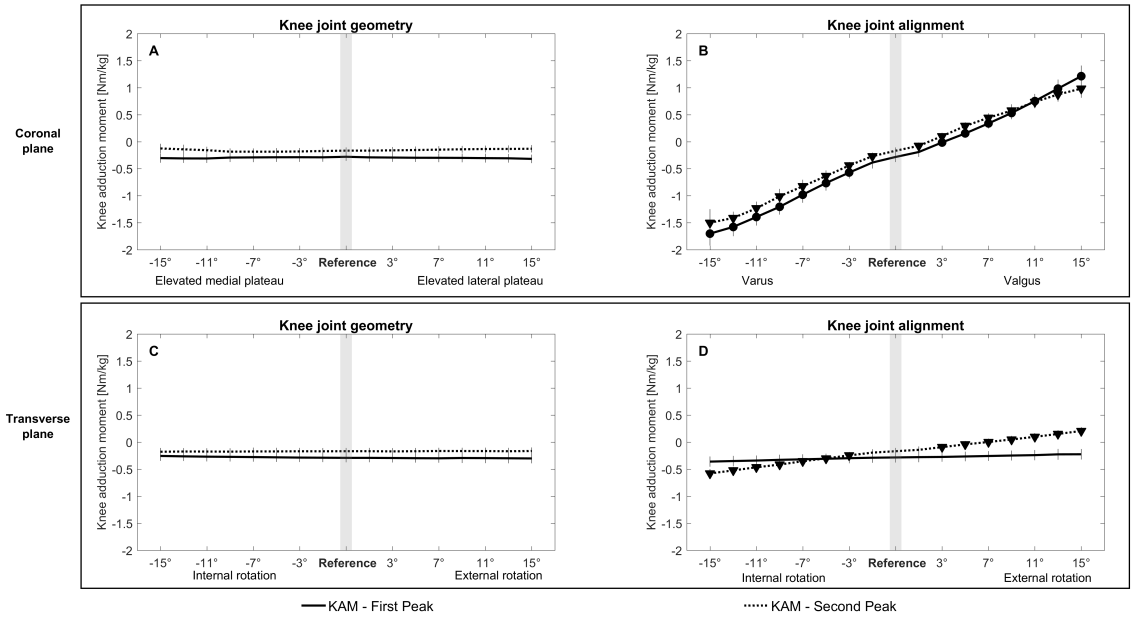

Figure 6.2: **Effect on the external knee adduction moment**
The effect of an altered joint geometry in A) the coronal plane, C) the transverse plane and an altered joint alignment in B) the coronal plane and D) the transverse plane on the external knee adduction moment at the first peak (FP, solid line) and at the second peak (SP, dashed line). A significant difference compared to the reference simulation (gray bar) is indicated by a solid dot (first peak) and a solid triangle (second peak). (α_{BC}=0.0031)

KAM was not significantly affected by the coronal plane geometry of the tibia plateau (Figure 6.2A, Table 6.1). However, medial-lateral force distribution was significantly altered when the medial or lateral tibial plateau was elevated more than 5° and 7°, respectively (Figure 6.3A, Table 6.1). First and second peak medial contact force were significantly increased when the medial plateau was elevated beyond 7°. The first and second peak lateral contact force were significantly decreased when the medial plateau was elevated beyond 11° and 5°. In contrast, first and second peak lateral contact force were significantly increased when the lateral plateau was elevated beyond 9° and 7°, respectively. Second peak medial contact force was significantly decreased when the lateral plateau was elevated beyond 13° (Figure 6.3A). Medial mean pressure was significantly increased when the medial plateau was elevated beyond 9° and 11° at the first and second peak, respectively, whereas lateral mean pressure at the second peak was significantly decreased when the medial plateau was elevated beyond 7° (Figure 6.4A). Lateral mean pressure was significantly increased when the lateral plateau was elevated beyond 15° and 9° at the first and second peak, respectively (Figure 6.4A, Table 6.1). Results for the effect on the total knee contact force are reported in supplementary material (S2).

ACL peak strain was significantly increased when the lateral plateau was elevated beyond 13°, whereas PCL peak strain was significantly increased when the medial plateau was elevated beyond 15° (Figure 6.5A, Table 6.1). MCL and LCL peak strain were significantly affected when the medial or the lateral tibial

plateau was elevated beyond 3°: An elevated medial plateau resulted in increased MCL peak strain, but decreased LCL peak strain, whereas an elevated lateral plateau resulted in a decreased MCL peak strain and increased LCL peak strain (Figure 6.5A).

Contact area location was not altered when the coronal plane orientation of the tibial plateau was changed (supplementary figure 6.10).

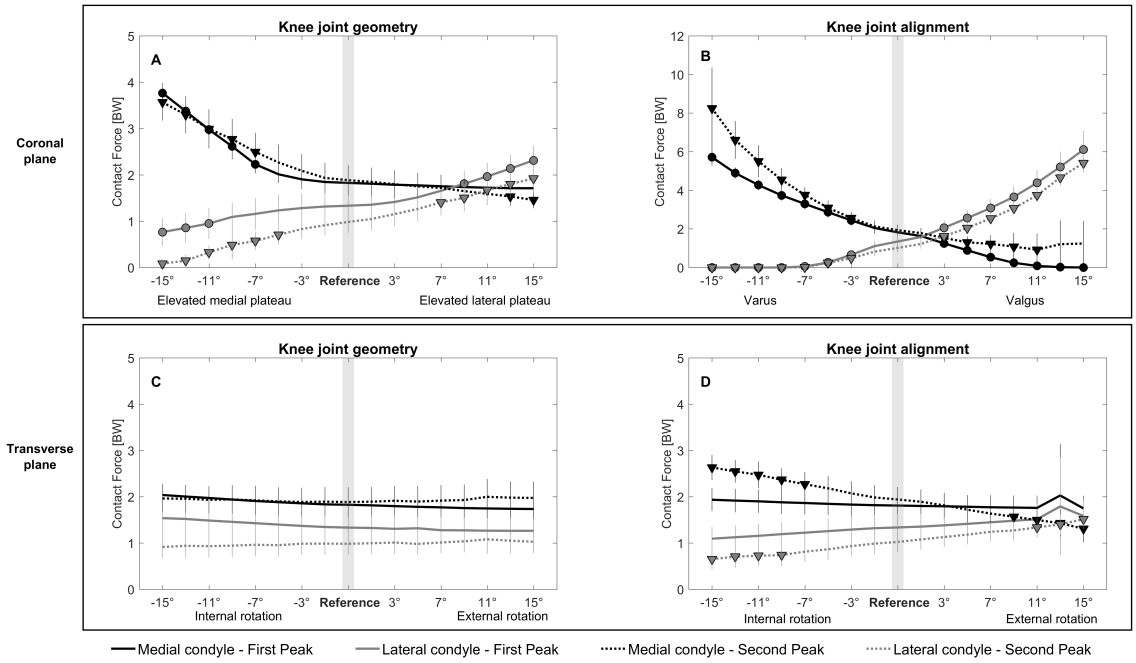

Figure 6.3: **Effect on the contact force distribution**
The effect of an altered joint geometry in A) the coronal plane, C) the transverse plane and an altered joint alignment in B) the coronal plane and D) the transverse plane on the knee contact force distribution at the first peak (FP, solid line) and at the second peak (SP, dashed line). The black line shows the effect on the medial condyle contact force, and the gray line shows the effect on the lateral condyle contact force. A significant difference compared to the reference simulation (gray bar) is indicated by a solid dot (first peak) and a solid triangle (second peak). (α_{BC}=0.0031)

Table 6.1: Altered geometry and malalignment conditions in the coronal plane resulting in significantly altered loading conditions.

		Extreme	Significant from	Reference value	Significant from	Extreme
Coronal plane - geometry		**Elevated medial plateau**				**Elevated lateral plateau**
Knee adduction moment (Nm/kg)	*First Peak*	-	-	-0.28 ± 0.08	-	-
	Second Peak	-	-	-0.17 ± 0.06	-	-
Medial contact force (BW)	*First Peak*	3.76 ± 0.22	2.23 ± 0.2 (7°)	1.83 ± 0.23	-	-
	Second Peak	3.57 ± 0.39	2.5 ± 0.41 (7°)	1.89 ± 0.32	1.53 ± 0.2 (13°)	1.46 ± 0.18
Lateral contact force (BW)	*First Peak*	0.76 ± 0.31	0.95 ± 0.33 (11°)	1.33 ± 0.31	1.81 ± 0.28 (9°)	2.31 ± 0.32
	Second Peak	0.08 ± 0.1	0.7 ± 0.2 (5°)	0.98 ± 0.23	1.4 ± 0.28 (7°)	1.92 ± 0.3
Medial contact pressure ($BW * A^2$)	*First Peak*	0.013 ± 0.002	0.01 ± 0.001 (9°)	0.008 ± 0.001	-	-
	Second Peak	0.012 ± 0.002	0.01 ± 0.001 (11°)	0.008 ± 0.001	-	-
Lateral contact pressure($BW * A^2$)	*First Peak*	-	-	0.008 ± 0.002	0.011 ± 0.002 (15°)	0.011 ± 0.002
	Second Peak	0.001 ± 0.001	0.004 ± 0.001 (7°)	0.006 ± 0.001	0.007 ± 0.001 (9°)	0.008 ± 0.001
ACL strain (%)	*Peak strain*	-	-	5.7 ± 1.51	7.82 ± 1.28 (13°)	8.49 ± 1.33
PCL strain (%)	*Peak strain*	0.64 ± 1.24	0.64 ± 1.24 (15°)	-2.41 ± 2.49	-	-
MCL strain (%)	*Peak strain*	18.55 ± 1.1	5.46 ± 0.69 (3°)	2.43 ± 1.18	-0.19 ± 1.52 (3°)	-5.26 ± 2.09
LCL strain (%)	*Peak strain*	3.06 ± 2	1.79 ± 1.16 (3°)	4.92 ± 0.96	7.8 ± 0.79 (3°)	19.72 ± 0.66

		Extreme	Significant from	Reference value	Significant from	Extreme
Coronal plane - alignment		**Varus**				**Valgus**
Knee adduction moment (Nm/kg)	*First Peak*	-1.7 ± 0.22	-0.57 ± 0.11 (3°)	-0.28 ± 0.08	-0.01 ± 0.08 (3°)	1.21 ± 0.2
	Second Peak	-1.5 ± 0.25	-0.27 ± 0.07 (1°)	-0.17 ± 0.06	-0.08 ± 0.06 (1°)	0.98 ± 0.17
Medial contact force (BW)	*First Peak*	5.71 ± 0.44	2.44 ± 0.27 (3°)	1.83 ± 0.23	1.25 ± 0.23 (3°)	0 ± 0
	Second Peak	8.24 ± 2.11	2.57 ± 0.3 (3°)	1.89 ± 0.32	1.53 ± 0.29 (3°)	-
Lateral contact force (BW)	*First Peak*	0 ± 0	0.66 ± 0.27 (3°)	1.33 ± 0.31	2.06 ± 0.37 (3°)	6.1 ± 0.97
	Second Peak	0 ± 0	0.48 ± 0.17 (3°)	0.98 ± 0.23	1.62 ± 0.23 (3°)	5.41 ± 0.49
Medial contact pressure ($BW * A^2$)	*First Peak*	0.016 ± 0.002	0.01 ± 0.001 (3°)	0.008 ± 0.001	0.007 ± 0.001 (3°)	0 ± 0
	Second Peak	0.023 ± 0.005	0.01 ± 0.001 (3°)	0.008 ± 0.001	0.007 ± 0.001 (3°)	-
Lateral contact pressure ($BW * A^2$)	*First Peak*	0 ± 0	0.006 ± 0.002 (3°)	0.008 ± 0.002	0.013 ± 0.003 (5°)	0.022 ± 0.003
	Second Peak	0 ± 0	0.004 ± 0.001 (3°)	0.006 ± 0.001	0.008 ± 0.001 (3°)	0.019 ± 0.004
ACL strain (%)	*Peak strain*	18.75 ± 2.17	8.61 ± 1.28 (9°)	5.7 ± 1.51	8.64 ± 1.94 (5°)	22.33 ± 3.73
PCL strain (%)	*Peak strain*	10.97 ± 1.52	-4.19 ± 1.11 (3°)	-2.41 ± 2.49	1.7 ± 1.57 (7°)	5.29 ± 0.56
MCL strain (%)	*Peak strain*	22.56 ± 1.99	3.78 ± 1.13 (1°)	2.43 ± 1.18	0.66 ± 1.27 (3°)	12.04 ± 2.06
LCL strain (%)	*Peak strain*	25.87 ± 3.33	8.59 ± 2.21 (5°)	4.92 ± 0.96	9.12 ± 1.45 (3°)	22.04 ± 2.35

Transverse plane

KAM and contact force distribution were not significantly affected by the transverse plane geometry of the tibia plateau (Figure 6.2C and 6.3C, Table 6.2). Medial mean pressure at the second peak was only significantly increased when the tibial plateau was rotated internally for 15°, whereas medial mean pressure on the first peak was significantly increased when the tibial plateau was rotated externally for 15° (Figure 6.4C, Table 6.2). Results for the effect on the total knee contact force and pressure are reported in supplementary material (S2).

ACL peak strain was significantly increased when the tibial plateau was internally rotated beyond 11°, but was significantly decreased beyond 13° external rotation. PCL peak strain was significantly increased when the plateau was externally rotated beyond 13° (Figure 6.5C, Table 6.2). MCL peak strain was significantly increased when the tibial plateau was internally rotated beyond 9°, whereas LCL peak strain was not significantly affected (Figure 6.5C).

Contact location on the medial tibia plateau was located more anteriorly when the tibial plateau was internally rotated, whereas contact location on the medial tibia plateau moved more posterior when the tibial plateau was externally rotated. The opposite pattern was observed on the lateral tibial plateau (supplementary figure 6.11).

Knee alignment

Coronal plane

KAM was significantly altered beyond 3° and 1° varus and valgus alignment at first and second peak, respectively. KAM significantly increased with increased varus alignment, whereas decreased KAM was observed with increased valgus alignment (Figure 6.2B, Table 6.1).

Medial-lateral force and pressure distribution were significantly altered beyond 3° varus and valgus alignment: medial contact force and pressure significantly increased with increased varus alignment, while the lateral contact force and pressure decreased (Figure 6.3B and 6.4B, Table 6.1). Lateral contact force and pressure significantly increased with increased valgus alignment, while medial contact force and pressure decreased (Figure 6.3B and 6.4B). Results for the effect on the total knee contact force are reported in supplementary material (S2).

ACL peak strain was significantly increased beyond 9° varus and 5° valgus. PCL peak strain was significantly increased beyond 7° varus and valgus, however at 3° varus PCL peak strain was significantly decreased (Figure 6.5B, Table 6.1). MCL peak strain was significantly increased beyond 1° varus and 7° valgus. However, at 3° valgus MCL peak strain was significantly decreased compared to the reference simulation. LCL peak strain was significantly increased beyond 5° varus and 3° valgus (Figure 6.5B).

Contact area location was not altered when the coronal plane alignment was changed (supplementary figure 6.12).

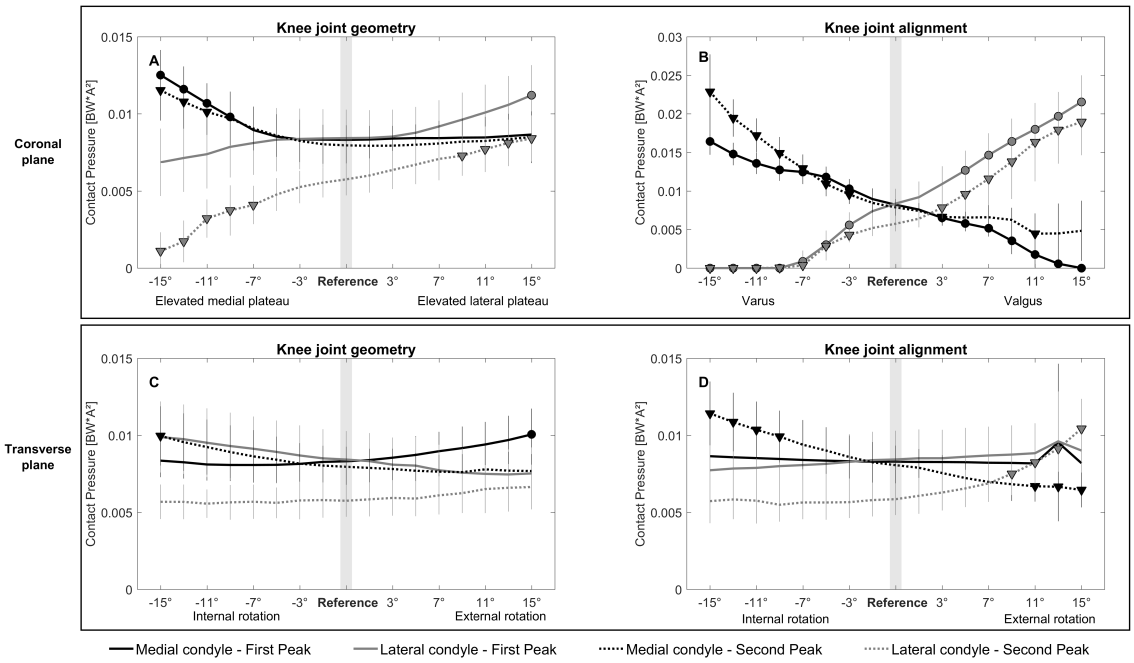

Figure 6.4: **Effect on the contact pressure distribution**
The effect of an altered joint geometry in A) the coronal plane, C) the transverse plane and an altered joint alignment in B) the coronal plane and D) the transverse plane on the knee contact pressure distribution at the first peak (FP, solid line) and at the second peak (SP, dashed line). The black line shows the effect on the medial condyle contact pressure, and the gray line shows the effect on the lateral condyle contact pressure. A significant difference compared to the reference simulation (gray bar) is indicated by a solid dot (first peak) and a solid triangle (second peak). (α_{BC}=0.0031)

Transverse plane

Altering knee alignment in the transverse plane only significantly affected KAM and the load distribution during the second peak: KAM was increased when the knee was internally rotated beyond 3°, whereas KAM was decreased when the knee was externally rotated beyond 3° (Figure 6.2D, Table 6.2).

Medial contact force was increased when the knee was internally rotated beyond 7° internal rotation, while lateral contact force was decreased when the knee was internally rotated beyond 9° (Figure 6.3D, Table 6.2). Lateral contact force was increased when the knee was externally rotated beyond 11°, but medial contact force was decreased when the knee was externally rotated beyond 9° (Figure 6.3D). Medial mean pressure was increased when the knee was internally rotated beyond 9° internal rotation. Lateral mean pressure was increased when the knee was externally rotated beyond 9°, but medial mean pressure was decreased when the knee was externally rotated beyond 11° (Figure 6.4D, Table 6.2). Results for the effect on the total knee contact force are reported in supplementary material (S2).

ACL peak strain was significantly increased when the knee was internally rotated beyond 11° and was only significantly decreased at 13° external rotation. PCL peak strain was significantly increased when the knee was externally rotated beyond 13° (Figure 6.5D, Table 6.2). MCL peak strain was significantly increased when the knee was internally rotated beyond 9°, whereas LCL peak strain was not significantly affected (Figure 6.5D).

Contact location on the medial tibia plateau was located more anteriorly when the knee was internally rotated, whereas contact location on the medial tibia plateau moved more posterior when the knee was externally rotated. The opposite pattern was observed on the lateral tibial plateau (supplementary figure 6.13).

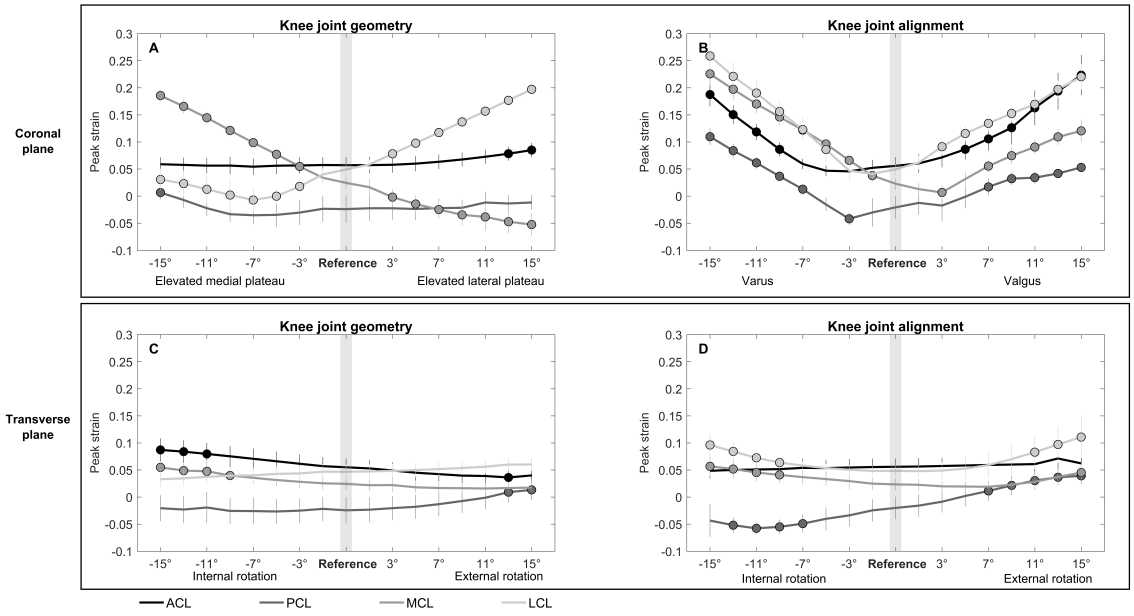

Figure 6.5: **Effect on the ligament strains**
The effect of an altered joint geometry in A) the coronal plane, C) the transverse plane and an altered joint alignment in B) the coronal plane and D) the transverse plane on the peak ligament strain. A significant difference compared to the reference simulation (gray bar) is indicated by a solid dot. (α_{BC}=0.0031)

Table 6.2: Altered geometry and malalignment conditions in the transverse plane resulting in significantly altered loading conditions.

		Extreme	Significant from	Reference value	Significant from	Extreme
Transverse plane - geometry		**Internal rotation**				**External rotation**
Knee adduction moment (Nm/kg)	*First Peak*	-	-	-0.29 ± 0.08	-	-
	Second Peak	-	-	-0.17 ± 0.06	-	-
Medial contact force (BW)	*First Peak*	-	-	1.83 ± 0.23	-	-
	Second Peak	-	-	1.89 ± 0.32	-	-
Lateral contact force (BW)	*First Peak*	-	-	1.33 ± 0.31	-	-
	Second Peak	-	-	0.98 ± 0.23	-	-
Medial contact pressure ($BW * A^2$)	*First Peak*	-	-	0.008 ± 0.001	0.01 ± 0.002 (15°)	0.01 ± 0.002
	Second Peak	0.01 ± 0.002	0.01 ± 0.002 (15°)	0.008 ± 0.001	-	-
Lateral contact pressure ($BW * A^2$)	*First Peak*	-	-	0.008 ± 0.002	-	-
	Second Peak	-	-	0.006 ± 0.001	-	-
ACL strain (%)	*Peak strain*	8.7 ± 2.13	7.97 ± 2.02 (11°)	5.49 ± 1.61	3.62 ± 1.34 (13°)	-
PCL strain (%)	*Peak strain*	-	-	-2.45 ± 2.44	0.89 ± 1.91 (13°)	1.33 ± 1.9
MCL strain (%)	*Peak strain*	5.47 ± 1.16	3.98 ± 1.2 (9°)	2.44 ± 1.18	-	-
LCL strain (%)	*Peak strain*	-	-	4.67 ± 1.33	-	-

		Extreme	Significant from	Reference value	Significant from	Extreme
Transverse plane - alignment		**Internal rotation**				**External rotation**
Knee adduction moment (Nm/kg)	*First Peak*	-	-	-0.28 ± 0.09	-	-
	Second Peak	-0.58 ± 0.08	-0.24 ± 0.06 (3°)	-0.17 ± 0.06	-0.09 ± 0.06 (3°)	0.21 ± 0.07
Medial contact force (BW)	*First Peak*	-	-	1.81 ± 0.26	-	-
	Second Peak	2.63 ± 0.27	2.27 ± 0.27 (7°)	1.94 ± 0.27	1.57 ± 0.28 (9°)	1.31 ± 0.29
Lateral contact force (BW)	*First Peak*	-	-	1.34 ± 0.3	-	-
	Second Peak	0.65 ± 0.22	0.74 ± 0.24 (9°)	1.02 ± 0.21	1.34 ± 0.22 (11°)	1.51 ± 0.21
Medial contact pressure ($BW * A^2$)	*First Peak*	-	-	0.008 ± 0.001	-	-
	Second Peak	0.011 ± 0.002	0.01 ± 0.002 (9°)	0.008 ± 0.001	0.007 ± 0.001 (11°)	0.006 ± 0.001
Lateral contact pressure ($BW * A^2$)	*First Peak*	-	-	0.008 ± 0.002	-	-
	Second Peak	-	-	0.006 ± 0.001	0.008 ± 0.001 (9°)	0.01 ± 0.002
ACL strain (%)	*Peak strain*	-	-	5.59 ± 1.56	-	-
PCL strain (%)	*Peak strain*	-	-4.91 ± 1.62 (7°)	-2.01 ± 2.08	1.12 ± 1.79 (7°)	3.92 ± 1.53
MCL strain (%)	*Peak strain*	5.67 ± 1.83	4.09 ± 1.5 (9°)	2.34 ± 1.13	4.52 ± 1.59 (15°)	4.52 ± 1.59
LCL strain (%)	*Peak strain*	9.61 ± 2.02	6.37 ± 0.89 (9°)	4.82 ± 1.03	8.29 ± 3.11 (11°)	11.08 ± 3.88

Discussion

The present study indicates that the medial-lateral tibiofemoral load distribution and ligament strains during walking are sensitive to both the joint geometry and alignment in the coronal plane, representative for coronal tibial slope and knee varus-valgus malalignment, whereas it is less sensitive to changes in joint geometry and alignment in the transverse plane. Since OA initiation and progression have previously been attributed to excessive mechanical loading induced by joint malalignment and geometry, these results may contribute to a better understanding of the relation between deviating knee geometry or alignment and altered knee loading and ultimately onset and progression of degenerative cartilage diseases.

Relatively small alterations in knee alignment significantly affect the knee loading distribution. In neutral alignment, more loading is taken up by the medial condyle[5]. Coronal plane knee malalignment significantly affected the medial-lateral force distribution beyond 3° additional varus or valgus compared to the reference position. Additional varus resulted in increased medial condyle loading, while additional valgus resulted in increased lateral condyle loading, with a simultaneous load reduction on the opposite condyle. As a measure of medial condyle loading, KAM was previously found to be directly proportional to the degree of coronal plane malalignment[19]. In support of this, our results showed a clear dependence of coronal plane knee alignment on the load distribution in terms of knee contact forces as well as KAM. This indicates that coronal plane malalignment could impose excessive stress on the articular cartilage and subchondral bone and could therefore potentially contribute to knee OA disease initiation and progression[6]. Additionally, altering coronal plane alignment resulted in increased ligament strains of all four ligaments. This suggests that increased malalignment causes increased movement in the knee that needs to be stabilized by all ligaments, causing the increased strains. Previously, knee instability was observed in patients with established knee OA[29]. As the ligaments are experiencing more strains during walking in presence of coronal plane knee malalignment, this would suggest that the chronic excessive stretching of the ligaments could contribute to additional knee instability, which could accelerate the degenerative changes in the cartilage.

Altered coronal plane joint geometry, indicative of altered coronal tibial slope, also significantly affected the medial-lateral force distribution, although to a lesser extent than the knee joint alignment. A more elevated medial tibia plateau resulted in increased medial loading and decreased lateral loading, whereas the opposite was observed with a more elevated lateral tibia plateau. The medial-lateral pressure distribution was affected in a similar way as the medial-lateral force distribution, although the pressure distribution was only significantly affected from more severe changes in coronal tibial slope. This can be explained by the fact that next to the contact force distribution the contact area was significantly increased and consequently diminishing the influence of the alterations in coronal tibial slope on the pressure distribution (Contact area changes are reported in supplementary material S3). Remarkably, in the simulations of an altered joint geometry, KAM was not significantly changed, whereas the medial-lateral force distribution was significantly changed. This shows the benefit of calculating the contact force distribution instead of solely relying on KAM as an estimate of medial condyle loading. Therefore, medial contact force could be a more sensitive biomarker for early detection of OA, instead of using KAM. This would allow an earlier detection of OA and consequently interventions to delay OA progression could be taken earlier. Indeed, an increased risk for accelerated knee OA was already found among patients with malalignment and an increased coronal tibial slope, whereas this relation was not present in patients with a neutrally aligned knee[9]. This observation is in line with our result that the loading distribution was not significantly affected when tibial slope was altered in the range of tibial slopes previously observed in the patients with neutral knee alignment. This suggests

that in knees with neutral alignment, small deviations in the coronal tibia angle may be tolerated or that the effect on the cartilage loading alone is not sufficient to contribute to degenerative changes in the cartilage.

Ligament behavior is strongly affected by the presence of altered coronal tibial slope, therefore imposing chronic stress and long-lasting stretch on the knee ligaments during daily life activities as walking. Peak strains of the collateral ligaments were significantly affected by small changes in the coronal tibia angle, which is representative for an altered joint geometry. A more elevated medial tibial plateau resulted in significantly increased MCL peak strains, whereas a more elevated lateral tibial plateau resulted in significantly increased LCL peak strains. As a consequence, this could potentially introduce coronal plane knee laxity and potentially resulting in increased knee instability, which were previously identified as risk factor for knee OA initiation and progression[29,54]. Hence, coronal plane knee laxity likely adds to a vicious circle, with articular cartilage degeneration contributing to joint malalignment and subsequently altered joint loading and increasing articular cartilage breakdown[29,30]. This would imply that subtle alterations in joint geometry could introduce joint malalignment later in life, which in turn would introduce altered loading and accelerate OA progression.

The effects of alterations in joint geometry and alignment in the transverse plane on the loading distribution were less pronounced compared to the alterations in the coronal plane. No effect on the force distribution was observed when solely the rotational alignment of the tibial plateau was altered. When the transverse plane alignment was altered, the force distribution was only significantly affected during terminal stance. From 7° internal rotation and onwards, medial condyle loading was increased accompanied by decreased lateral loading. Besides a small effect on the loading distribution, altered knee geometry and alignment in the transverse plane also increased the peak strains of the MCL and LCL. As in the coronal plane, this likely contributes to transverse plane laxity, which causes knee instability. Similarly to an altered transverse plane knee alignment, knee instability in the transverse plane was previously observed after ACL-injury. This is reflected in altered knee kinematics and can be interpreted as a change in transverse plane alignment[55–57]. Altered contact regions were previously observed after ACL-injury[58]. Since these cartilage regions are less adapted to the loading, degenerative changes in the cartilage could occur and might partially contribute to the increased incidence of OA after ACL-injury[32,59,60]. This suggests that transverse plane alignment might contribute to OA initiation by affecting knee stability (by its effect on the ligaments) and therefore contact locations and not by significantly affecting the loading magnitude on the condyles.

The current results provide additional insight in the isolated effect of an altered joint geometry or joint malalignment on the distribution of loading over the articular cartilage, however the current results should be evaluated with respect to some limitations. Firstly, the approach used in the current study to simulate the effect of different knee alignments, did not include any patient specific compensations in the hip, knee or ankle kinematics to reduce knee loading. Therefore, our results are representative for a situation without compensatory gait mechanisms and possibly overestimate the effect of altered knee alignment on the loading distribution. Secondly, the effect of alterations in knee alignment on joint loading might be overestimated as the orientation of the ground reaction force was not changed along with the change in center of pressure location with respect to the foot. However, our assumption that trunk movement would account for any dynamic inconsistency introduced by repositioning the tibia seems feasible, as increased trunk movement was previously observed in OA patients with malalignment[19]. Thirdly, the fact that the rather strict Bonferroni-correction was used to correct for multiple testing could have resulted in an underestimation of significant differences.

The present study illustrated a clear dependence of coronal plane joint alignment on the medial-lateral force distribution. Increased varus alignment, starting from 3° varus, was related to increased medial loading, providing further insight in the relation between varus malalignment and medial knee OA. In addition, small changes in coronal plane tibial geometries resulted directly in increased ligament strains. These findings suggest a possible influence of coronal tibial slope on ligament laxity on the long term, which could contribute to joint malalignment and consequently altered joint loading. An altered joint geometry or alignment in the coronal plane had a more pronounced effect on knee joint loading compared to alterations in the transverse plane. This may imply that deviations in the coronal plane are more important contributors to knee OA disease initiation and progression, compared to deviations in the transverse plane.

References

1. Hunter DJ, Felson DT. Osteoarthritis. BMJ. 2006;332: 639–42.
2. Baker-LePain JC, Lane NE. Role of bone architecture and anatomy in osteoarthritis. Bone. Elsevier Inc.; 2012;51: 197–203.
3. Brouwer GM, Van Tol AW, Bergink AP, Belo JN, Bernsen RMD, Reijman M, et al. Association between valgus and varus alignment and the development and progression of radiographic osteoarthritis of the knee. Arthritis Rheum. 2007;56: 1204–1211.
4. Hunter D, Nevitt M, Lynch J, Kraus VB, Katz JN, Collins JE, et al. Longitudinal validation of periarticular bone area and 3D shape as biomarkers for knee OA progression? Data from the FNIH OA Biomarkers Consortium. Ann Rheum Dis. 2015; annrheumdis-2015-207602.
5. Schipplein OD, Andriacchi TP. Interaction between active and passive knee stabilizers during level walking. J Orthop Res. 1991;9: 113–119.
6. Andriacchi TP, Favre J. The Nature of In Vivo Mechanical Signals That Influence Cartilage Health and Progression to Knee Osteoarthritis. Curr Rheumatol Rep. 2014;16: 463–470.
7. Neogi T, Bowes MA, Niu J, De Souza KM, Vincent GR, Goggins J, et al. Magnetic resonance imaging-based three-dimensional bone shape of the knee predicts onset of knee osteoarthritis: Data from the osteoarthritis initiative. Arthritis Rheum. 2013;65: 2048–2058.
8. Williams TG, Vincent G, Bowes M, Cootes T, Balamoody S, Hutchinson C, et al. Automatic segmentation of bones and inter-image anatomical correspondence by volumetric statistical modelling of knee MRI. 2010 7th IEEE Int Symp Biomed Imaging From Nano to Macro, ISBI 2010 - Proc. 2010; 432–435.
9. Driban JB, Stout AC, Duryea J, Lo GH, Harvey WF, Price LL, et al. Coronal tibial slope is associated with accelerated knee osteoarthritis: data from the Osteoarthritis Initiative. BMC Musculoskelet Disord. BMC Musculoskeletal Disorders; 2016;17: 1–8.
10. Haverkamp DJ, Schiphof D, Bierma-Zeinstra SM, Weinans H, Waarsing JH. Variation in joint shape of osteoarthritic knees. Arthritis Rheum. 2011;63: 3401–3407.
11. Duparc F, Thomine JM, Simonet J, Biga N. Femoral and tibial bone torsions associated with medial femoro-tibial osteoarthritis. Index of cumulative torsions. Orthop Traumatol Surg Res. Elsevier Masson SAS; 2014;100: 69–74.
12. Eckhoff DG. Effect of limb malrotation on malalignment and osteoarthritis. Orthop Clin North Am. 1994;25: 405–415.
13. Eckhoff DG, Johnston RJ, Stamm ER, Kilcoyne RF, Wiedel JD. Version of the osteoarthritic knee. J Arthroplasty. 1994;9: 73–79.
14. Turner MS. The association between tibial torsion and knee joint pathology. Clin Orthop Relat Res. 1994; 47–51.
15. Krackow KA, Mandeville DS, Rachala SR, Bayers-Thering M, Osternig LR. Torsion deformity and joint loading for medial knee osteoarthritis. Gait Posture. Elsevier B.V.; 2011;33: 625–629.
16. Moisio K, Chang A, Eckstein F, Chmiel JS, Wirth W, Almagor O, et al. Varus-valgus alignment reduced risk of subsequent cartilage loss in the less loaded compartment. Arthritis Rheum. 2011;63: 1002–1009.
17. Hayashi D, Englund M, Roemer FW, Niu J, Sharma L, Felson DT, et al. Knee malalignment is associated with an increased risk for incident and enlarging bone marrow lesions in the more loaded compartments: The MOST study. Osteoarthr Cartil. Elsevier Ltd; 2012;20: 1227–1233.
18. Moyer R, Wirth W, Duryea J, Eckstein F. Anatomical alignment, but not goniometry, predicts femorotibial cartilage loss as well as mechanical alignment: Data from the Osteoarthritis Initiative. Osteoarthr Cartil. Elsevier Ltd; 2016;24: 254–261.
19. Turcot K, Armand S, Lübbeke A, Fritschy D, Hoffmeyer P, Suvà D. Does knee alignment influence gait in patients with severe knee osteoarthritis? Clin Biomech. Elsevier Ltd; 2013;28: 34–39.
20. van Egmond N, Stolwijk N, van Heerwaarden R, van Kampen A, Keijsers NLW. Gait analysis before and after corrective osteotomy in patients with knee osteoarthritis and a valgus deformity. Knee Surgery, Sport Traumatol Arthrosc. Springer Berlin Heidelberg; 2016; 1–10.
21. Weidenhielm L, Svensson OK, Broström LÅ, Rudberg U. Change in adduction moment about the knee after high tibial osteotomy and prosthetic replacement in osteoarthrosis of the knee. Clin Biomech. 1992;7: 91–96.

22. Hurwitz DE, Ryals AB, Case JP, Block JA, Andriacchi TP. The knee adduction moment during gait in subjects with knee osteoarthritis is more closely correlated with static alignment than radiographic disease severity, toe out angle and pain. J Orthop Res. 2002;20: 101–107.

23. Sharma L, Song J, Felson DT, Cahue S, Shamiyeh E, Dunlop DD. The role of knee alignment in disease progression and functional decline in knee osteoarthritis. JAMA. 2001;286: 188–195.

24. Cicuttini F, Wluka A, Hankin J, Wang Y. Longitudinal study of the relationship between knee angle and tibiofemoral cartilage volume in subjects with knee osteoarthritis. Rheumatology. 2004;43: 321–324.

25. Huizinga MR, Gorter J, Demmer A, Bierma-Zeinstra SMA, Brouwer RW. Progression of medial compartmental osteoarthritis 2–8 years after lateral closing-wedge high tibial osteotomy. Knee Surgery, Sport Traumatol Arthrosc. Springer Berlin Heidelberg; 2016;

26. Tanamas S, Hanna FS, Cicuttini FM, Wluka AE, Berry P, Urquhart DM. Does knee malalignment increase the risk of development and progression of knee osteoarthritis? A systematic review. Arthritis Care Res. 2009;61: 459–467.

27. Miyazaki T, Wada M, Kawahara H, Sato M, Baba H, Shimada S. Dynamic load at baseline can predict radiographic disease progression in medial compartment knee osteoarthritis. Ann Rheum Dis. 2002;61: 617–622.

28. Felson DT, Lawrence RC, Dieppe PA, Hirsch R, Helmick CG, Jordan JM, et al. Osteoarthritis: New insights - Part 1: The disease and its risk factors. Annals of Internal Medicine. 2000. pp. 635–646.

29. Lewek MD, Rudolph KS, Snyder-Mackler L. Control of frontal plane knee laxity during gait in patients with medial compartment knee osteoarthritis. Osteoarthr Cartil. 2004;12: 745–751.

30. Lewek MD, Ramsey DK, Snyder-mackler L, Rudolph KS. Knee Stabilization in Patients With Medial Compartment Knee Osteoarthritis. Arthritis Rheum. 2005;52: 2845–2853.

31. Sharma L, Lou C, Felson DT, Dunlop DD, Kirwan-Mellis G, Hayes KW, et al. Laxity in healthy and osteoarthritic knees. Arthritis Rheum. 1999;42: 861–870.

32. Chaudhari AMW, Briant PL, Bevill SL, Koo S, Andriacchi TP. Knee kinematics, cartilage morphology, and osteoarthritis after ACL injury. Med Sci Sports Exerc. 2008;40: 215–22.

33. Andriacchi TP, Mündermann A, Smith RL, Alexander EJ, Dyrby CO, Koo S. A framework for the in vivo pathomechanics of osteoarthritis at the knee. Ann Biomed Eng. 2004;32: 447–457.

34. Quirno M, Campbell KA, Singh B, Hasan S, Jazrawi L, Kummer F, et al. Distal femoral varus osteotomy for unloading valgus knee malalignment: a biomechanical analysis. Knee Surgery, Sport Traumatol Arthrosc. Springer Berlin Heidelberg; 2015;

35. Agneskirchner JD, Hurschler C, Wrann CD, Lobenhoffer P. The Effects of Valgus Medial Opening Wedge High Tibial Osteotomy on Articular Cartilage Pressure of the Knee: A Biomechanical Study. Arthrosc - J Arthrosc Relat Surg. 2007;23: 852–861.

36. Riegger-Krugh C, Gerhart TN, Powers WR, Hayes WC. Tibiofemoral Contact Pressures in Degenerative Joint Disease. Clin Orthop Relat Res. 1998;348: 233–245.

37. Thompson JA, Hast MW, Granger JF, Piazza SJ, Siston RA. Biomechanical effects of total knee arthroplasty component malrotation: A computational simulation. J Orthop Res. 2011;29: 969–975.

38. Heller MO, Taylor WR, Perka C, Duda GN. The influence of alignment on the musculo-skeletal loading conditions at the knee. Langenbeck's Arch Surg. 2003;388: 291–297.

39. Chen Z, Wang L, Liu Y, He J, Lian Q, Li D, et al. Effect of component mal-rotation on knee loading in total knee arthroplasty using multi-body dynamics modeling under a simulated walking gait. J Orthop Res. 2015;33: 1287–1296.

40. Lerner ZF, DeMers MS, Delp SL, Browning RC. How tibiofemoral alignment and contact locations affect predictions of medial and lateral tibiofemoral contact forces. J Biomech. Elsevier; 2015;48: 644–650.

41. Smith CR, Vignos MF, Lenhart RL, Kaiser J, Thelen DG. The Influence of Component Alignment and Ligament Properties on Tibiofemoral Contact Forces in Total Knee Replacement. J Biomech Eng. 2016;138: 1–10.

42. Arnold EM, Ward SR, Lieber RL, Delp SL. A model of the lower limb for analysis of human movement. Ann Biomed Eng. 2010;38: 269–79.

43. Lenhart RL, Kaiser J, Smith CR, Thelen DG. Prediction and Validation of Load-Dependent Behavior of the Tibiofemoral and Patellofemoral Joints During Movement. Ann Biomed Eng. 2015;43: 2675–2685.

44. Smith RC, Choi KW, Negrut D, Thelen DG. Efficient Computation of Cartilage Contact Pressures within Dynamic Simulations of Movement. Comput Methods Biomech Biomed Eng Imaging Vis. 2016;

45. Hudelmaier M, Glaser C, Englmeier K-H, Reiser M, Putz R, Eckstein F. Correlation of knee-joint cartilage morphology with muscle cross-sectional areas vs. anthropometric variables. Anat Rec Part A. 2003;270: 175–184.

46. Eckstein F, Reiser M, Englmeier KH, Putz R. In vivo morphometry and functional analysis of human articular cartilage with quantitative magnetic resonance imaging–from image to data, from data to theory. Anat Embryol (Berl). 2001;203: 147–73.

47. Draper CE, Besier TF, Gold GE, Fredericson M, Fiene A, Beaupre GS, et al. Is cartilage thickness different in young subjects with and without patellofemoral pain? Osteoarthr Cartil. 2006;14: 931–937.

48. Blankevoort L, Kuiper JH, Huiskes R, Grootenboer HJ. Articular contact in a three-dimensional model of the knee. J Biomech. 1991;24: 1019–1031.

49. Li G, Lopez O, Rubash H. Variability of a Three-Dimensional Finite Element Model Constructed Using Magnetic Resonance Images of a Knee for Joint Contact Stress Analysis. J Biomech Eng. 2001;123: 341–346.

50. Adouni M, Shirazi-Adl A. Partitioning of Knee Joint Internal Forces in Gait Is Dictated By the Knee Adduction Angle and Not By the Knee Adduction Moment. J Biomech. Elsevier; 2014;47: 1696–703.

51. Lu TW, O'Connor JJ. Bone position estimation from skin marker co-ordinates using global optimisation with joint constraints. J Biomech. 1999;32: 129–134.

52. Thelen DG, Won Choi K, Schmitz AM. Co-simulation of neuromuscular dynamics and knee mechanics during human walking. J Biomech Eng. 2014;136: 21033.

53. Wesseling M, De Groote F, Meyer C, Corten K, Simon JP, Desloovere K, et al. Gait alterations to effectively reduce hip contact forces. J Orthop Res. 2015;33: 1094–1102.

54. Bytyqi D, Shabani B, Lustig S, Cheze L, Gjurgjeala NK, Neyret P. Gait knee kinematic alterations in medial osteoarthritis: three dimensional assessment. Int Orthop. 2014;38: 1191–1198.

55. Yamaguchi S, Gamada K, Sasho T, Kato H, Sonoda M, Banks S a. In vivo kinematics of anterior cruciate ligament deficient knees during pivot and squat activities. Clin Biomech (Bristol, Avon). Elsevier Ltd; 2009;24: 71–6.

56. Georgoulis AD, Papadonikolakis A, Papageorgiou CD, Mitsou A, Stergiou N. Three-dimensional tibiofemoral kinematics of the anterior cruciate ligament-deficient and reconstructed knee during walking. Am J Sports Med. 2003;31: 75–9.

57. Andriacchi TP, Dyrby CO. Interactions between kinematics and loading during walking for the normal and ACL deficient knee. J Biomech. 2005;38: 293–8.

58. Van De Velde SK, Bingham JT, Hosseini A, Kozanek M, DeFrate LE, Gill TJ, et al. Increased tibiofemoral cartilage contact deformation in patients with anterior cruciate ligament deficiency. Arthritis Rheum. 2009;60: 3693–3702.

59. Lohmander LS, Ostenberg a, Englund M, Roos H. High prevalence of knee osteoarthritis, pain, and functional limitations in female soccer players twelve years after anterior cruciate ligament injury. Arthritis Rheum. 2004;50: 3145–52.

60. von Porat a, Roos EM, Roos H. High prevalence of osteoarthritis 14 years after an anterior cruciate ligament tear in male soccer players: a study of radiographic and patient relevant outcomes. Ann Rheum Dis. 2004;63: 269–273.

Supplementary material

Extended Plug-in-Gait markerset

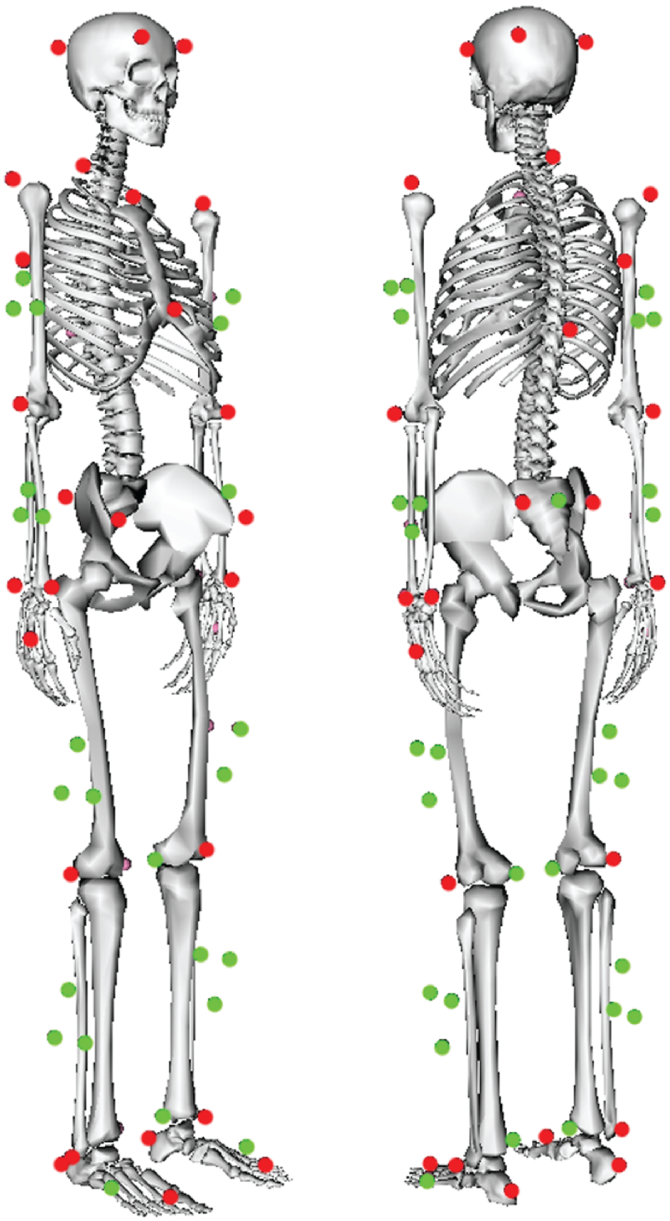

Figure 6.6: **Extended Plug-in-Gait markerset**
The full-body extended Plug-in-Gait marker set used during the motion capture. Additional to the original full-body Plug-in-Gait marker set, this marker set is comprised of three-marker clusters on the upper and lower arms and legs and anatomical markers on the sacrum, medial femur epicondyles and the medial malleoli, resulting in a total of 65 markers. Markers in dark gray are the original Plug-in-Gait markers. light gray markers are the additionally placed markers.

Effect on the total knee contact force

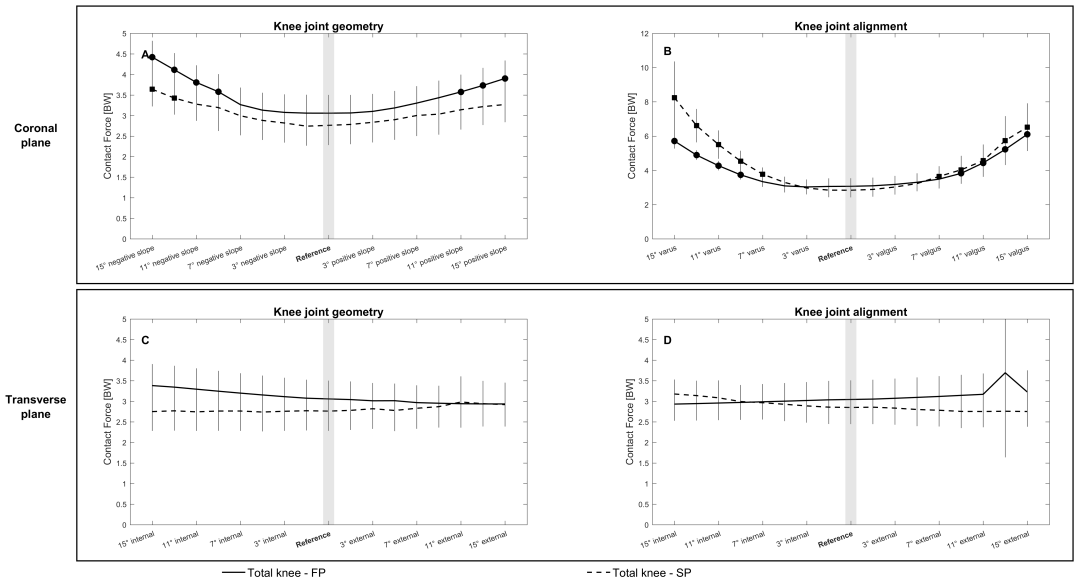

Figure 6.7: The effect of an altered joint geometry in A) the coronal plane, C) the transverse plane and an altered joint alignment in B) the coronal plane and D) the transverse plane on the total knee contact force at the first peak (solid line) and at the second peak (dashed line). A significant difference compared to the reference simulation (gray bar) is indicated by a solid dot (first peak) and a solid square (second peak).(α_{BC}=0.0031)

Effect on the total knee contact pressure

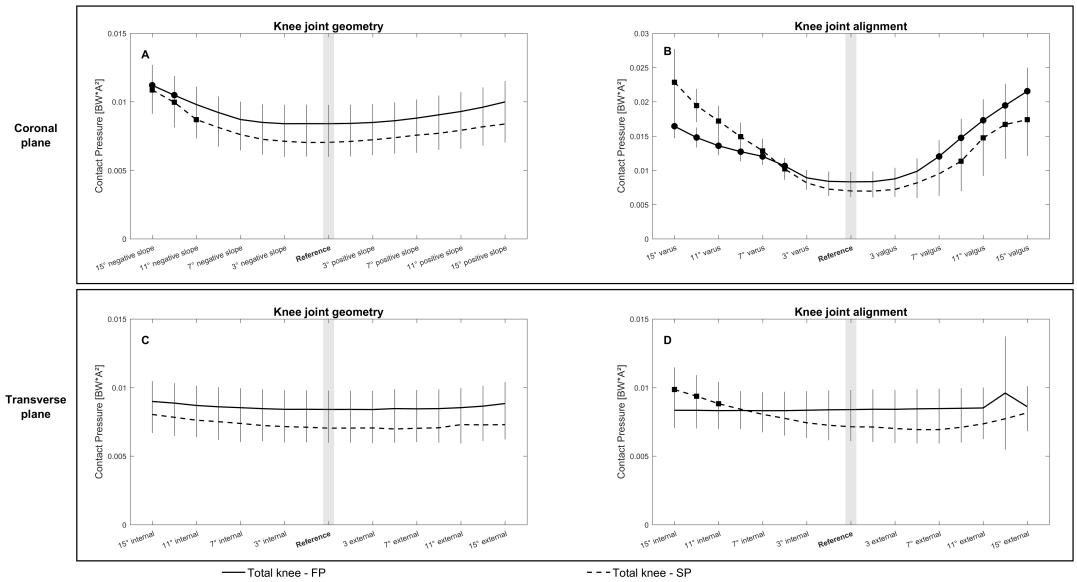

Figure 6.8: The effect of an altered joint geometry in A) the coronal plane, C) the transverse plane and an altered joint alignment in B) the coronal plane and D) the transverse plane on the total knee contact pressure at the first peak (solid line) and at the second peak (dashed line). A significant difference compared to the reference simulation (gray bar) is indicated by a solid dot (first peak) and a solid square (second peak).(α_{BC}=0.0031)

Effect on the contact area

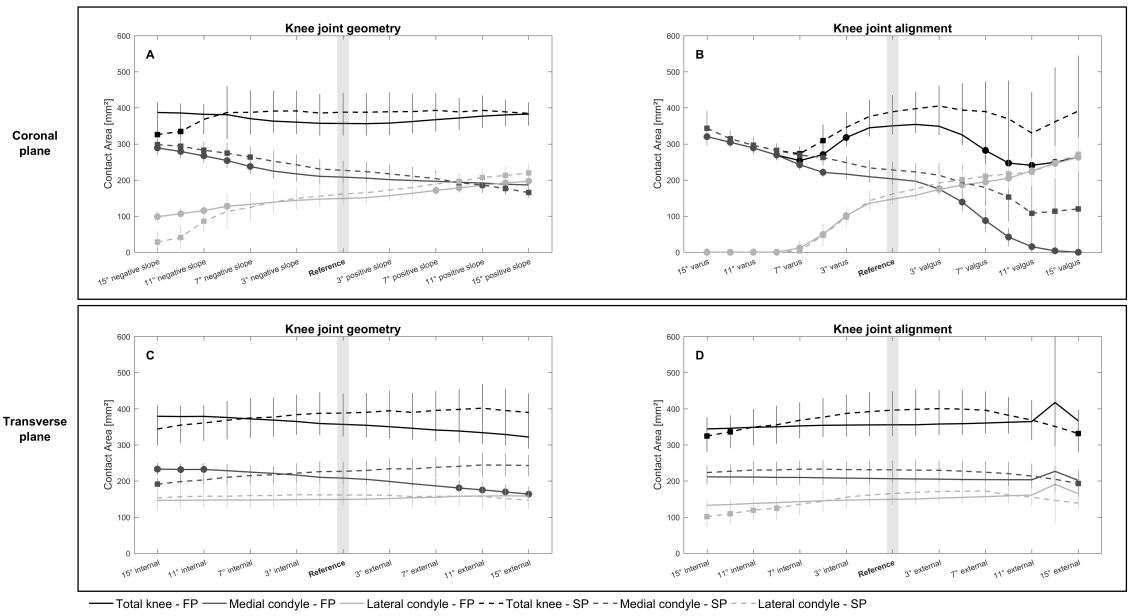

Figure 6.9: The effect of an altered joint geometry in A) the coronal plane, C) the transverse plane and an altered joint alignment in B) the coronal plane and D) the transverse plane on the contact area at the first peak (solid line) and at the second peak (dashed line). The black line shows the effect on the total knee contact area, the dark gray line shows the effect on the medial condyle contact area, and the light gray line shows the effect on the lateral condyle contact area. A significant difference compared to the reference simulation (gray bar) is indicated by a solid dot (first peak) and a solid square (second peak).(α_{BC}=0.0031)

Effect on the contact location

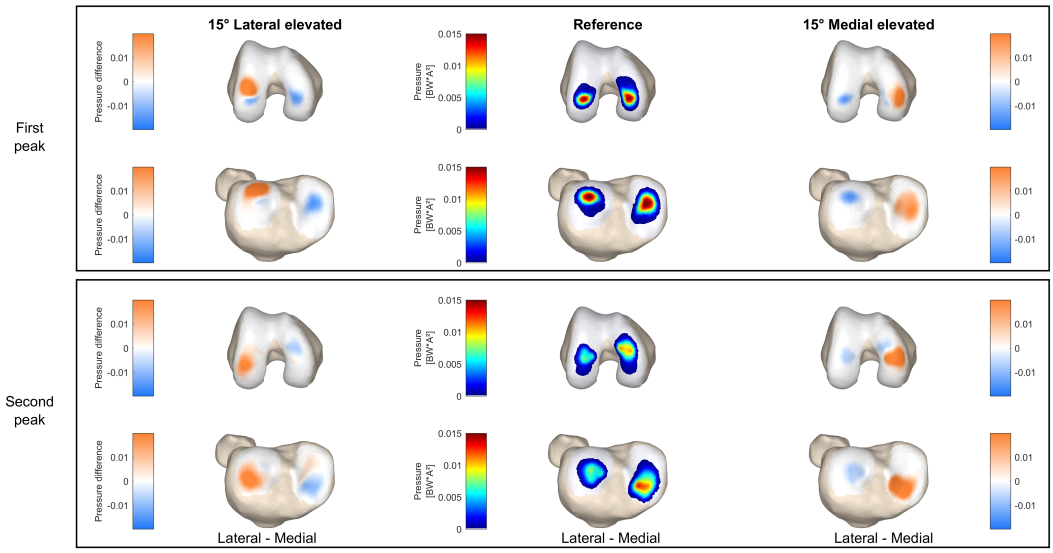

Figure 6.10: **The effect of an altered joint geometry in the coronal plane on the contact location.** The reference pressure pattern at first and second peak are shown, as well as the difference pattern with the extreme variations: 15°elevated medial and lateral tibial plateau. Orange indicates more loading with respect to the reference simulation, blue indicates less loading with respect to the reference simulation.

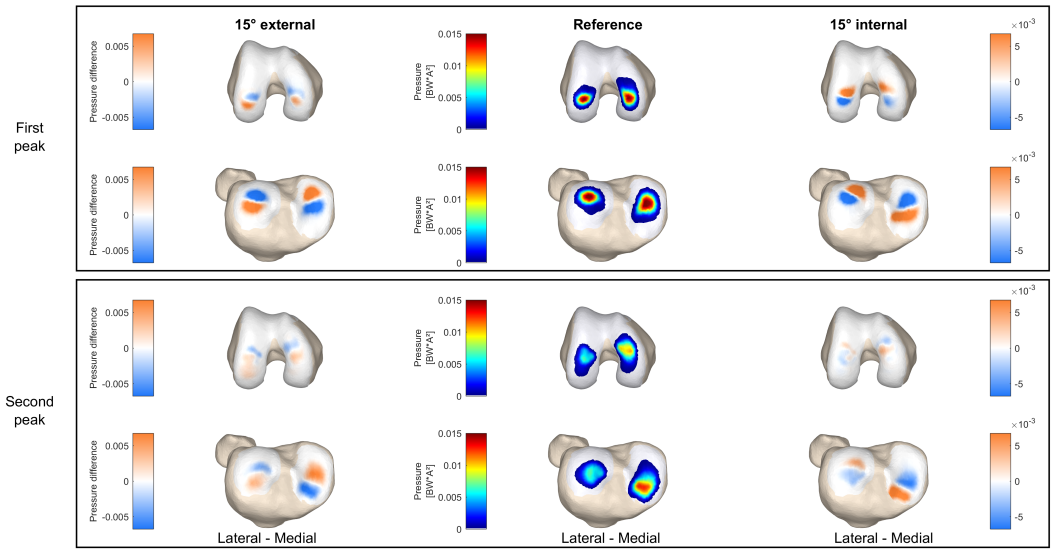

Figure 6.11: **The effect of an altered joint geometry in the transverse plane on the contact location.** The reference pressure pattern at first and second peak are shown, as well as the difference pattern with the extreme variations: 15°externally and internally rotated tibia plateau. Orange indicates more loading with respect to the reference simulation, blue indicates less loading with respect to the reference simulation.

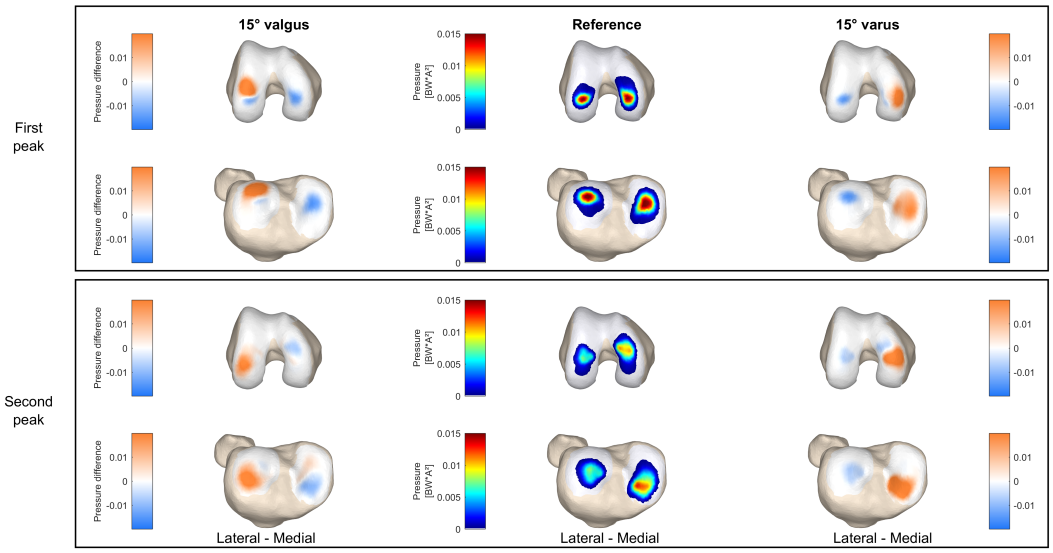

Figure 6.12: **The effect of an altered joint alignment in the coronal plane on the contact location.** The reference pressure pattern at first and second peak are shown, as well as the difference pattern with the extreme variations: 15°varus and valgus. Orange indicates more loading with respect to the reference simulation, blue indicates less loading with respect to the reference simulation.

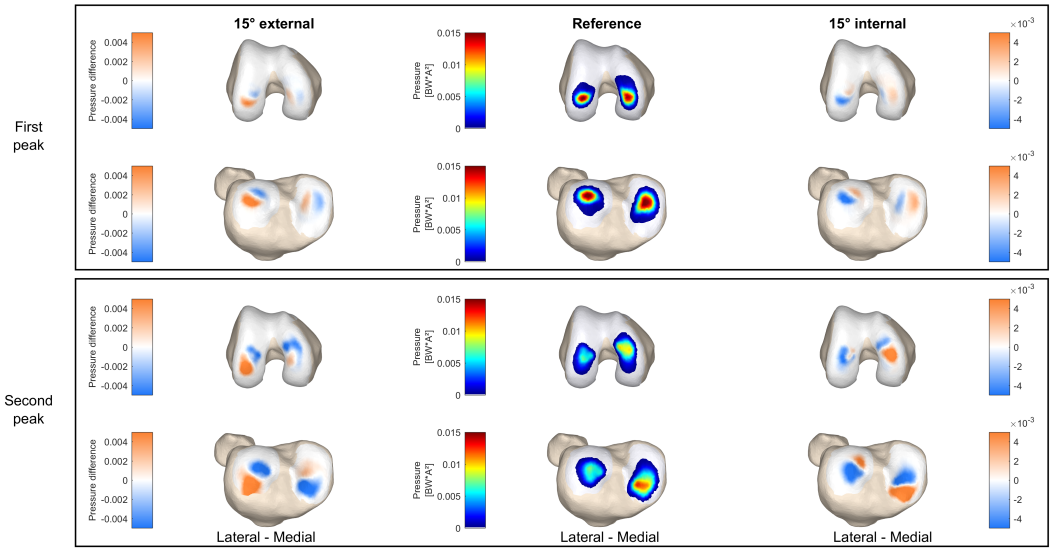

Figure 6.13: **The effect of an altered joint alignment in the transverse plane on the contact location.** The reference pressure pattern at first and second peak are shown, as well as the difference pattern with the extreme variations: 15°externally and internally rotated tibia. Orange indicates more loading with respect to the reference simulation, blue indicates less loading with respect to the reference simulation.

Chapter 7

Medial and lateral tibiofemoral articular cartilage defects do not alter compartmental loading during walking

Sam Van Rossom, Nidal Khatib, Cathy Holt, Dieter Van Assche, Ilse Jonkers

Submitted to *Osteoarthritis and Cartilage*

Abstract

Objective: Healthy cartilage is essential for optimal joint function. Although, articular cartilage defects are highly prevalent in the active population and hamper joint function, the effect of articular cartilage defects on knee loading is not yet documented. Therefore, the present study compared knee contact forces and pressures between patients with tibiofemoral cartilage defects and healthy controls. Potentially this provides additional insights in movement adaptations and the role of altered loading in the progression from defect towards OA.

Design: Experimental gait data collected in 15 patients with isolated cartilage defects (8 medial involvement, 7 lateral-involvement) and 19 healthy asymptomatic controls was processed using a musculoskeletal model to calculate contact forces and pressures. Differences between two patient groups and controls were evaluated using Kruskal-Wallis tests and individually compared using Mann-Whitney-U tests ($\alpha < 0.05$).

Results: The patients with lateral involvement walked significantly slower compared to the healthy controls. No adaptations in the movement pattern that resulted in decreased loading on the injured condyle were observed. Additionally the location of loading was not significantly affected.

Conclusions: The current results suggest that isolated cartilage defects do not induce significant changes in the knee joint loading pattern. Consequently, the involved condyle will capture a similar amount of force that should be distributed over the remaining cartilage surrounding the cartilage defect. This may cause local degenerative changes in the cartilage and in combination with inflammatory responses, might play a key role in the progression from articular cartilage defect to a more severe OA phenotype.

Keywords: Contact forces · Cartilage defect · Gait · Contact pressure · Osteoarthritis

Introduction

Healthy knee hyaline cartilage is essential for optimally distributing loading over the subchondral bone, for reducing friction between the articulating bones and inherent to its physiology optimizing longevity of joint function. However, articular cartilage defects following knee injury are highly prevalent in the active population, with approximately 36% of all athletes presenting full-thickness chondral defects[1]. Often articular cartilage defects are accompanied by knee pain, swelling and loss of function, ultimately restricting the quality of life of the patients[2–4]. Due to the limited repair capacity of articular cartilage, the prognosis of full recovery is rather limited[5]. As an articular cartilage defect may hamper joint homeostasis in the long term, the risk for osteoarthritis (OA) development is increased[5]. Indeed, large cohort studies indicated that the majority of isolated cartilage defects in the knee joint (age >40years) progress to OA within 2 years when left untreated, and 30% of this population require a total knee replacement within 10 years[6–8]. Therefore, surgical interventions that aim to restore the articular cartilage surface were developed, however their long-term outcome is still under debate and studies indicate that the major amount of surgical interventions should even be discouraged[3,9,10]. Therefore, conservative approaches aiming to slow down the progression from defect to OA (e.g. strength training to increase knee stability) are highly relevant[3]. These interventions focus on regaining joint homeostasis, knee stability and restoring normal load distribution, since aberrant mechanical load distribution is thought to contribute to the development of OA[3,11].

In knee OA and after ACL-rupture, gait adaptations to reduce pain and discomfort were documented[2–4,12]. However, the role of adaptive movement strategies have only been scarcely studied in patients with isolated cartilage defects in the knee. Gait adaptations following surgical intervention to restore isolated cartilage defects (more specific: MACI) were reported and suggested protective gait adaptations even up to 12-months following treatment[13,14]. On the other hand, one recent study in untreated patients with articular cartilage defects reported no differences in knee reaction forces compared to healthy controls after controlling for gait speed and quadriceps strength before any surgical intervention[15]. However, in this study, individual compartmental loading was not reported and the contribution of the muscle and ligament forces on the knee loading was neglected. Patient-specific gait analysis in combination with a complex musculoskeletal model of the knee allows the analysis of knee joint loading in terms of compartmental contact forces and might be a more sensitive measure to investigate changes in the knee loading distribution.

Therefore, the present study investigates if movement adaptations in patients with an isolated articular cartilage defect on the femur condyles affects the loading distribution in the knee. Our hypothesis was that patients with tibiofemoral articular cartilage defects would alter their gait pattern to unload the involved compartment. This may help in identifying the potential role of movement adaptations in shifting weight-bearing loading away from the involved compartment and the role of conservative approaches in restoring normal loading.

Methods

Participants

Fifteen patients with an isolated full-thickness articular cartilage defect ($> 1cm^2$ and ICRS-grade $\geq$3)) on the femoral condyle or tibia plateau were included in the current study. Patients were subdivided in

two groups according to defect location (i.e. medial (n = 8) and lateral condyle (n = 7). Additional inclusion-criteria were BMI <35kg/m^2 and age between 18 and 50 years. Patients were excluded when degeneration of the joint, joint space narrowing (>50%), uncorrected ligament instability, uncorrected axial malalignment (> 5°), uncorrected patellar maltracking or instability, patellofemoral lesion, meniscal defect, tumor, infection, autoimmune inflammatory arthropathy were present or if they had surgical intervention within 6 months prior to the study recruitment. To compare patients' data, nineteen healthy asymptomatic adults with no history of knee-injury were included. All procedures were approved by the university hospital Leuven ethics committee and by the Cardiff & Vale University Health Board ethics committee. Informed written consent was obtained from all participants prior to the measurements.

Motion analysis

During a standard motion analysis, three dimensional marker trajectories were recorded along with ground reaction forces using 6-axis force plates embedded in the ground. Participants were measured in Leuven (Movements & posture Analysis Laboratory Leuven, KU Leuven) and in Cardiff (Arthritis Research UK Biomechanics and Bioengineering Centre, Cardiff University). At center 1, marker trajectories were recorded using a 10-camera VICON system (Vicon, Oxford Metrics, UK, 100Hz). Ground reaction forces were recorded using three force plates embedded in the ground (AMTI, Watertown, USA, 1000Hz). In total, 65 reflective markers were placed according to a full-body Plug-in-Gait marker-set, extended with additional anatomical markers on the sacrum, medial femur epicondyles and the medial malleoli and three marker clusters on the upper and lower arms and legs[16]. At center 2, marker trajectories were recorded using a 9-camera Qualisys system (Qualisys, Qualisys Medical AB, Sweden, 120Hz). Ground reaction forces were recorded using four force plates embedded in the ground (Bertec, Columbus, USA, 1080Hz). In total, 54 reflective markers were placed according to a full-body Helen-Hayes marker-set, extended with addition markers on the thigh, shank and foot[17]. After a standing calibration trial, all participants were instructed to walk at self-selected speed across the motion lab until at least three trials with valid force plate contact were captured. Before pooling data of the two different centers, consistency in kinematic and contact force data of control subjects between centers was statistically verified.

Tibiofemoral contact forces and pressures were calculated using a scaled 3D musculoskeletal model, that was previously presented[18]. An extended knee model, that allows 6 degrees of freedom (DoF) patellofemoral and 6 DoF tibiofemoral movement was implemented in a generic full-body model[19]. Each leg included 44 musculotendon actuators spanning the hip, knee and ankle and 14 bundles of non-linear springs that represent the major knee ligaments and posterior capsule. A non-linear elastic foundation formulation was used to calculate the cartilage contact pressures, based on the penetration depth of the overlapping surface meshes of the contact model[20]. The cartilage was modelled with a uniformly distributed thickness of 4mm tibiofemoral and 7mm patellofemoral[21–23]. The elastic modulus and poisons ratio were assumed as 10MPa and 0.45, respectively[24–26]. This model was implemented in SIMM with the Dynamics Pipeline (Musculographics Inc., Santa Rosa, CA) and SD/Fast (Parametric Technology Corp., Needham, MA) to generate the multibody equations of motion.

At first, the generic model was scaled to the subjects' anthropometry. Next, the measured marker trajectories were recalculated to the joint kinematics (pelvic translations and rotations, hip flexion, hip adduction, hip rotation, knee flexion and ankle flexion) using inverse kinematics[27]. Subsequently, the muscle forces and secondary knee kinematics (11 DoF, i.e. all except knee flexion) required to generate the measured primary

hip, knee and ankle accelerations were estimated using the concurrent optimization of muscle activations and kinematics algorithm. In the optimization the weighted sum of squared muscle activations and contact energy were minimized[20]. As only the knee flexion angle was used in the optimization, joint kinematics in the secondary knee DoF evolved as a function of muscle, ligament and contact forces[18,20,28]. This model was previously found to be sensitive for predicting contact forces measured with instrumented implants with a root-mean-square (RMS) error below 0.33BW[29].

Patient reported outcome measures

The Knee Osteoarthritis Outcome Score (KOOS) was completed by all patients and control subjects on the day of analysis, prior to being assessed in the experimental motion analysis[30]. Subscores included in the analysis were pain, symptoms, activities of daily living and quality of life.

Statistics

For each trial, the stance phase was identified as the period in which the ground reaction force exceeded 20N. Next, the magnitude and timing of the first and second peak (FP and SP) of the resultant tibiofemoral contact force was determined during the first and second half of the stance phase, respectively as well as the minimum force during single leg support (MS). Furthermore, the concomitant average and maximum pressure over the contact surface was analyzed. Each variable was determined for the total knee as well as for the medial and lateral condyle separately and were averaged over three trials. Additionally, the joint angles in the trunk, hip, knee and ankle at FP, SP and MS as well as their respective range of motion (RoM) and the joint moments in the hip, knee and ankle at FP, SP and MS were analyzed. Furthermore, the point of application of the total knee, medial and lateral contact force expressed in the local reference frame of the femur at FP, SP and MS were analyzed. Joint moments were scaled to body mass, contact forces were scaled to bodyweight (BW) and contact pressures were scaled to bodyweight and knee dimensions ($BW * A^2$). Between group differences were examined using a Kruskall-wallis test. When significant ($p < 0.05$) differences were found, pairwise comparisons using Mann-Whitney U-tests with Bonferroni-corrected alpha levels to correct for multiple group comparisons, were performed to determine if the patient groups were significantly different from the control group (α_{BC}=0.025). All test were conducted in MATLAB (MATLAB 2016b, The Math Works, Inc., Natick, Massachusetts, USA). Finally, the difference in pressure distribution at FP, SP and MS between patients and healthy controls was determined and visually inspected (figure 7.2).

Results

Patient characteristics

Both patient groups scored significantly worse self-reported subjective outcomes than the controls. Patients with lateral compartment involvement were significantly heavier, had a higher BMI and walked slower compared to the healthy control group. A more detailed overview of group characteristics can be found in table 7.1.

Table 7.1: Subject characteristics

	Controls	Medial involvement	C. vs Med.	Lateral involvement	C. vs Lat.
Sample size	19	8		7	
Gender (M/F)	10/9	6/2		6/1	
Mass (kg)	71.1 ± 7.85	74.33 ± 5.36	0.3	88.8 ± 16.67	0.011*
Height (cm)	175.95 ± 7.33	174.94 ± 4.16	0.852	174.59 ± 6.12	0.602
BMI (kg/m^2)	22.95 ± 2.03	24.29 ± 1.68	0.075	29.07 ± 4.82	0.001*
Age (Years)	29.95 ± 5.9	34.63 ± 8.62	0.192	36.86 ± 12.23	0.213
Stance time (s)	0.65 ± 0.04	0.65 ± 0.05	0.69	0.69 ± 0.05	0.133
Gait speed (m/s)	1.36 ± 0.15	1.33 ± 0.21	0.894	1.18 ± 0.12	0.021*
KOOS					
Quality of life	96.4 ± 4.63	52.5 ± 32.59	< 0.001*	64.57 ± 20.57	0.002*
Activies of daily life	99.24 ± 1.79	71.94 ± 21.64	<0.001*	73.71 ± 23.15	<0.001*
Symptoms	98.98 ± 2.27	56.02 ± 29.23	< 0.001*	61.14 ± 26.61	< 0.001*
Pain	97.94 ± 4.26	57.54 ± 30.19	< 0.001*	67.57 ± 21.24	< 0.001*

Joint kinematics and kinetics

Joint kinematics during walking were not significantly different between the healthy controls and patients presenting medial compartment involvement. Patients with lateral compartment involvement presented a reduced hip adduction range of motion (9.83°± 1.94 vs 12.21°± 1.84 in the control group, p = 0.013), increased plantarflexion at the first peak (-8.25°± 3.35 vs -1.74°± 5.86 in the control group) and increased proximal tibia translation at the second peak (1,1 ± 0.1mm vs 0.9 ± 0.33 mm in the control group, p = 0.004). Patients with medial compartment involvement presented an increased knee adduction moment at midstance (-0.19 ± 0.07kg vs -0.11 ± 0.04kg in the control group, p = 0.018). The remainder of the joint moments were not significantly different between groups (figure 7.1). Figures of the joint angles and moments are provided in supplementary material figure 7.3 and figure 7.4.

Knee loading

Knee joint loading variables were not significantly different between patients with medial involvement and healthy controls (figure 7.1). In patients with lateral compartment involvement, peak medial condyle contact force during loading response was significantly lower compared to the healthy control group (1.54 ± 0.18 vs 1.84 ± 0.23 in the control group, p = 0.008). The remainder of the knee joint loading variables were not significantly different between patients with lateral involvement and healthy controls (table 7.2).

Loading location

Point of application of the total knee, medial and lateral contact forces were found not to be significantly different between groups (supplementary material, figure 7.5). Additionally, the contact pressure distribution on the femur cartilage did not show a clear difference compared to the contact pressure distribution observed in healthy controls (figure 7.2).

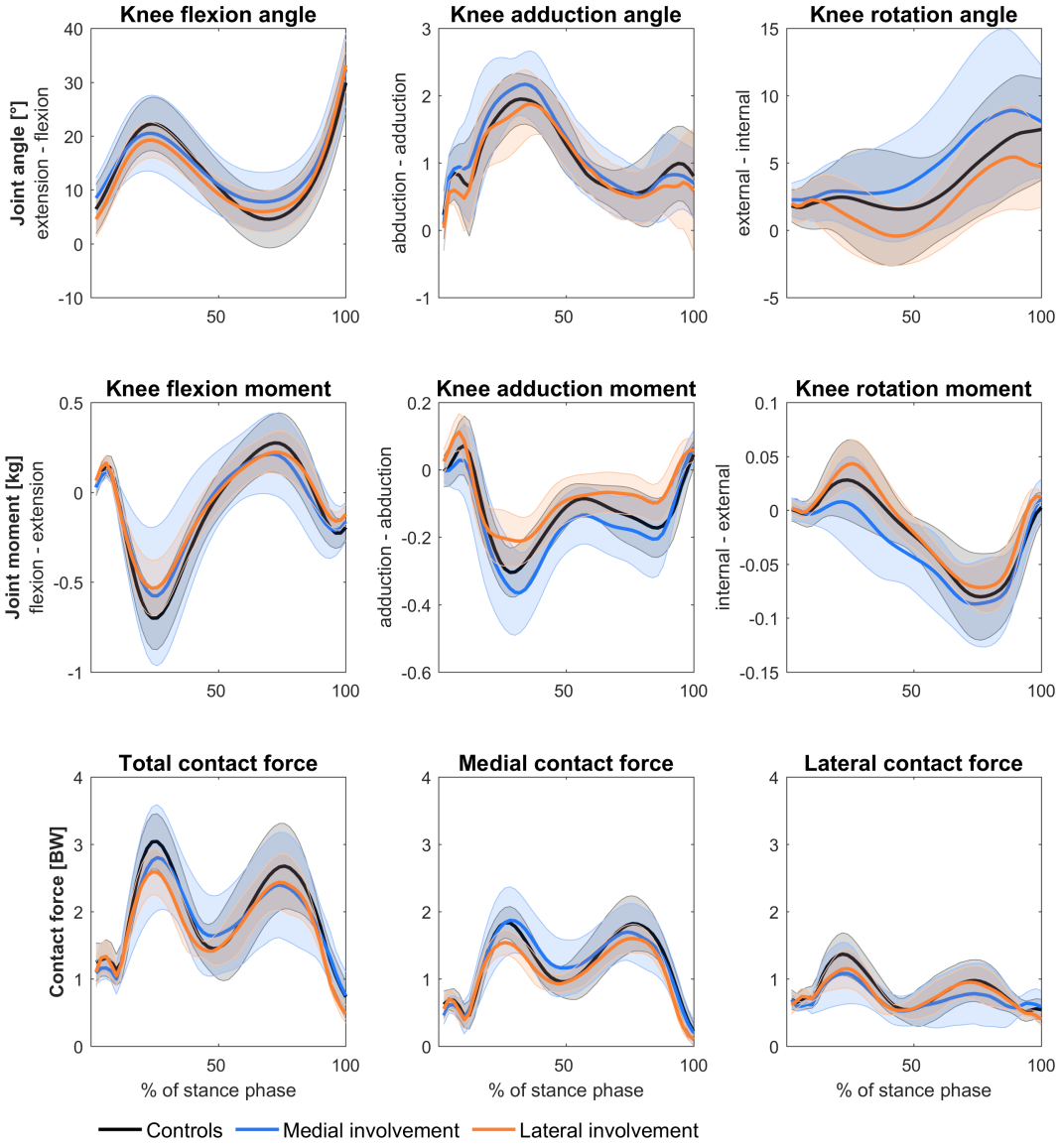

Figure 7.1: **Average curves of the knee kinematics, kinetics and contact forces.**
Average patterns of the knee joint angles, knee moments and knee contact force. Gray area represents the healhy controls, blue the patients with medial compartment involvement and orange the patients with lateral compartment involvement.

Discussion

The current study evaluated cartilage loading during walking at self-selected speeds in patients suffering from isolated articular cartilage defects in an otherwise healthy joint and compared the loading to a cohort of healthy controls with no joint symptoms. Cartilage loading was evaluated in terms of contact forces and pressures using musculoskeletal modeling and using patient-specific gait patterns. This allowed to evaluate if patient-specific gait adaptations, in response to articular cartilage defects alter the compartmental loading magnitude and location. This can further enhance our understanding in the role of aberrant mechanical loading on the long term increased incidence of OA in patients with an articular cartilage defect.

Table 7.2: Loading values for each group

First peak	Controls	Medial-involvement	Main effect	C vs Med	Lateral-involvement	C vs Lat
Total knee	Average ± Standard deviation	Average ± Standard deviation	p-value	p-value	Average ± Standard deviation	p-value
Contact force $[BW]$	3.09 ± 0.39	2.97 ± 0.7	0.063	-	2.62 ± 0.33	-
Mean pressure $[BW * A^2]$	0.009 ± 0.001	0.008 ± 0.002	0.172	-	0.007 ± 0.002	-
Max pressure $[BW * A^2]$	0.02 ± 0.004	0.019 ± 0.003	0.183	-	0.017 ± 0.004	-
Medial Condyle						
Contact force $[BW]$	1.84 ± 0.23	1.92 ± 0.49	0.039*	0.614	1.54 ± 0.18	0.008*
Mean pressure $[BW * A^2]$	0.009 ± 0.001	0.009 ± 0.002	0.085	-	0.007 ± 0.002	-
Max pressure $[BW * A^2]$	0.018 ± 0.003	0.018 ± 0.003	0.165	-	0.015 ± 0.004	-
Lateral Condyle						
Contact force $[BW]$	1.35 ± 0.29	1.15 ± 0.33	0.229	-	1.16 ± 0.29	-
Mean pressure $[BW * A^2]$	0.009 ± 0.002	0.008 ± 0.002	0.18	-	0.007 ± 0.002	-
Max pressure $[BW * A^2]$	0.018 ± 0.004	0.016 ± 0.005	0.229	-	0.015 ± 0.004	-
Midstance						
Total knee						
Contact force $[BW]$	1.2 ± 0.37	1.45 ± 0.67	0.454	-	1.25 ± 0.31	-
Mean pressure $[BW * A^2]$	0.005 ± 0.001	0.005 ± 0.001	0.131	-	0.004 ± 0.001	-
Max pressure $[BW * A^2]$	0.01 ± 0.002	0.012 ± 0.002	0.051	-	0.009 ± 0.002	-
Medial Condyle						
Contact force $[BW]$	0.82 ± 0.22	1.09 ± 0.46	0.061	-	0.84 ± 0.18	-
Mean pressure $[BW * A^2]$	0.005 ± 0.001	0.006 ± 0.001	0.038*	0.067	0.005 ± 0.001	0.248
Max pressure $[BW * A^2]$	0.01 ± 0.002	0.012 ± 0.002	0.025*	0.094	0.009 ± 0.002	0.133
Lateral Condyle						
Contact force $[BW]$	0.42 ± 0.19	0.4 ± 0.28	0.416	-	0.44 ± 0.19	-
Mean pressure $[BW * A^2]$	0.004 ± 0.001	0.004 ± 0.001	0.813	-	0.004 ± 0.001	-
Max pressure $[BW * A^2]$	0.008 ± 0.002	0.008 ± 0.002	0.709	-	0.008 ± 0.002	-
Second peak						
Total knee						
Contact force $[BW]$	2.77 ± 0.65	2.52 ± 0.81	0.317	-	2.48 ± 0.41	-
Mean pressure $[BW * A^2]$	0.007 ± 0.001	0.007 ± 0.001	0.079	-	0.006 ± 0.001	-
Max pressure $[BW * A^2]$	0.016 ± 0.003	0.017 ± 0.003	0.061	-	0.014 ± 0.002	-
Medial Condyle						
Contact force $[BW]$	1.87 ± 0.39	1.77 ± 0.44	0.16	-	1.61 ± 0.22	-
Mean pressure $[BW * A^2]$	0.008 ± 0.001	0.008 ± 0.001	0.037*	0.3	0.007 ± 0.001	0.064
Max pressure $[BW * A^2]$	0.016 ± 0.003	0.017 ± 0.003	0.064	-	0.014 ± 0.002	-
Lateral Condyle						
Contact force $[BW]$	1.02 ± 0.34	0.84 ± 0.48	0.562	-	0.98 ± 0.25	-
Mean pressure $[BW * A^2]$	0.006 ± 0.001	0.006 ± 0.002	0.598	-	0.005 ± 0	-
Max pressure $[BW * A^2]$	0.012 ± 0.002	0.012 ± 0.003	0.487	-	0.011 ± 0.001	-

In line with previous observations, both cartilage defect patient groups in the present study reported significantly worse subjective pain, symptoms, performance of daily living activities and quality of life[2–4]. Gait adaptations, related to a pain avoidance strategy were previously reported in OA-patients[31,32]. It was therefore expected that during walking similar adaptive strategies could be identified in patients with articular cartilage defects to reduce loading on the involved knee compartment[33]. In contrast, very limited gait adaptations in the movement pattern were observed when compared to asymptomatic controls. This suggests that isolated cartilage defects do not induce major changes in the gait pattern itself. Characteristically of OA patients, the knee adduction moment at midstance was increased in patients with medial involvement[34–36]. However, this increase in knee adduction moment did not result in significantly increased medial compartment contact forces and therefore may not play a key role in further cartilage degeneration. Therefore, it is likely that the previously reported kinematic and kinetic changes after cartilage reparative surgeries, such as MACI-surgery are merely a consequence of the open knee surgery and the post-operative period without weight-bearing and with rehabilitation and may be indicative of an incomplete restoration of normal joint function 12 months after surgery [13,14,37].

Walking speed of the patient group with lateral compartment involvement, was significantly slower com-

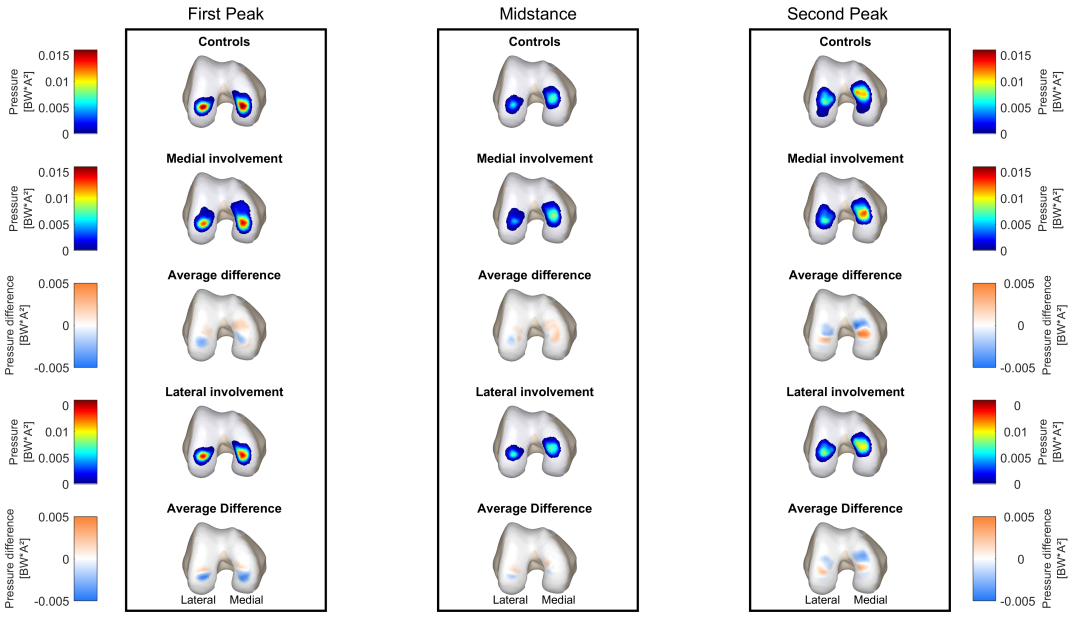

Figure 7.2: **Contact pressure distribution**
Average contact pressure patterns at first peak, midstance and second peak for the healthy control group and the patients with medial and lateral compartment involvement. Furthermore, the average difference between the pressure pattern in patients and the healthy control pressure pattern is shown. Orange indicates more loading in the patient on that specific location, blue indicates decreased loading compared to the controls.

pared to the healthy asymptomatic controls. In previous literature, patients with articular cartilage defects and after cartilage repair were found to decrease their self-selected walking speed to avoid pain and symptoms, presumably to reduce loading in the knee induced by the momentum of gait, as increased walking speed was previously found to result in increased joint loading[13–15]. During gait at self-selected speed, contact forces were indeed not different from the contact forces in healthy asymptomatic controls and modified movement patterns to unload the injured condyle could not be confirmed. Recently, no differences in joint reaction forces were observed between patients with articular cartilage defects and asymptomatic controls after controlling for walking speed and could further confirm the present findings[15].

Therefore, we need to conclude that in the studied patient cohort with medial and lateral compartment involvement no significant differences in magnitude and loading location were found in the involved nor the uninvolved compartment. As loading magnitude was not different, a comparable force magnitude needs to be distributed over the remaining cartilage surrounding the articular cartilage defect. This is of concern as in-vitro studies previously observed increased pressure at the defect rim posing additional stress on the remaining healthy cartilage[38,39]. Furthermore, isolated cartilage lesions do not affect the loading location in the joint since neither the contact pressure distribution, nor the point of application of the contact forces was significantly changed between groups. In ACL-deficient knees altered contact locations were previously observed and were hypothesized to result in excessive loading of cartilage that is not adapted to the normal loading experienced during walking[40,41]. This local increase in loading may disrupt cartilage homeostasis and consequently initiate degenerative changes.

Interestingly, in this population with isolated cartilage defects loading magnitude and location were not

altered at the time of evaluation (between 6 and 36 months post event). Nevertheless, part of these patients will progress towards (early) OA[6–8]. Altered loading is accepted to contribute to OA progression, since in patients with established OA altered joint moments and contact forces are often suggested to contribute to further degeneration of the cartilage[36]. In contrast, in early OA patients knee moments and total knee loading were not significantly different[36]. Recently, it was shown that also in early OA patients small differences in joint kinematics resulted in altered medial-lateral load distribution and contact location[42]. Since the loading magnitude and location are not significantly altered in this population with isolated cartilage defects in an otherwise healthy joint included in this study, it may be important to investigate further and identify additional factors that may induce the altered loading magnitude and location that will induce the altered loading conditions associated with early OA. Regarding this, the role of altered transverse plane kinematics and kinetics in the presence of ligamentous laxity have previously been suggested as major contributing factors[42,43].

The results of the current study indicate that localized degenerative changes in the cartilage following isolated cartilage defects are not induced by altered compartmental loading or by altered contact locations. Since no gait modifications that unload the involved compartment were identified, it is more likely that strain-induced local degenerative changes at the defect rim contribute to the progression from articular cartilage defect to a more severe OA phenotype. In support of this, a decrease in proteoglycans in the cartilage of the lesion rim and an increased amount of osteophytes were found 20 weeks after experimentally creating a femoral cartilage defect in rabbits[44]. Additionally to this, local degenerative changes in the cartilage surrounding the defect and cartilage degeneration will be further accelerated by the presence of inflammatory cytokines, proteases and deregulation of growth factors that will trigger catabolic responses of the chondrocytes and the surrounding musculoskeletal tissue[45,46].

Some limitations need to be considered when interpreting the results of the current study. First, sample size of the patient cohort was limited. Given the heterogeneity of the patient group, in terms of sample characteristics, exact chondral defect locations and duration of defect presence, our results need to be confirmed by a larger sample. Secondly, despite careful selection it is possible that, less-severe comorbidity might have been present, which may affect the variability of our findings. In terms of the methodology, the model that was used in the current study comprises a generic knee model, with a uniformly distributed cartilage thickness. Consequently, the effect of a cartilage defect on the calculated contact pressure distribution is neglected. Therefore, the observed deviations are mostly determined by deviations in joint kinematics and external forces. Lastly, the optimization algorithm used in the current study (i.e. concurrent optimization of muscle forces and kinematics) did not account for subject-specific muscle contractions. This effect is however considered to be minimal as co-contraction of the lower-limb muscles was not altered in patients with an articular cartilage defect[47–50].

Conclusions

Contrary to our expectations, patients with articular cartilage defects did not adapt their movement pattern to unload the injured femoral condyle during walking at self-selected speed. This indicates that the remaining healthy cartilage surrounding the defect should capture and distribute the knee loading. This may cause local degenerative changes in the cartilage, which in combination with inflammatory responses might play a key role in the progression from an articular cartilage defect to a more severe OA phenotype.

References

1. Flanigan DC, Harris JD, Trinh TQ, Siston RA, Brophy RH. Prevalence of chondral defects in Athletes' Knees: A systematic review. Med Sci Sports Exerc. 2010;42: 1795–1801.
2. Heir S, Nerhus TK, Røtterud JH, Løken S, Ekeland A, Engebretsen L, et al. Focal cartilage defects in the knee impair quality of life as much as severe osteoarthritis: a comparison of knee injury and osteoarthritis outcome score in 4 patient categories scheduled for knee surgery. Am J Sports Med. 2010;38: 231–7.
3. Wondrasch B, Arøen A, Røtterud JH, Høysveen T, Bølstad K, Risberg MA. The feasibility of a 3-month active rehabilitation program for patients with knee full-thickness articular cartilage lesions: the Oslo Cartilage Active Rehabilitation and Education Study. J Orthop Sports Phys Ther. 2013;43: 310–24.
4. Engelhart L, Nelson L, Lewis S, Mordin M, Demuro-Mercon C, Uddin S, et al. Validation of the Knee Injury and Osteoarthritis Outcome Score subscales for patients with articular cartilage lesions of the knee. Am J Sports Med. 2012;40: 2264–72.
5. Tetteh ES, Bajaj S, Ghodadra NS. Basic Science and Surgical Treatment Options for Articular Cartilage Injuries of the Knee. J Orthop Sports Phys Ther. 2012;42: 243–253.
6. Davies-Tuck ML, Wluka AE, Wang Y, Teichtahl AJ, Jones G, Ding C, et al. The natural history of cartilage defects in people with knee osteoarthritis. Osteoarthr Cartil. 2008;16: 337–342.
7. Spahn G, Hofmann G. Focal cartilage defects within the medial knee compartment. predictors for osteoarthritis progression. Z Orthop Unfall. 2014;152: 480–488.
8. Wang Y, Ding C, Wluka AE, Davis S, Ebeling PR, Jones G, et al. Factors affecting progression of knee cartilage defects in normal subjects over 2 years. Rheumatology. 2006;45: 79–84.
9. Mithoefer K, Hambly K, Della Villa S, Silvers H, Mandelbaum BR. Return to sports participation after articular cartilage repair in the knee: scientific evidence. Am J Sports Med. 2009;37 Suppl 1: 167S–76S.
10. Devitt BM, Bell SW, Webster KE, Feller JA, Whitehead TS. Surgical treatments of cartilage defects of the knee: Systematic review of randomised controlled trials. Knee. Elsevier B.V.; 2017;
11. Andriacchi TP, Favre J. The Nature of In Vivo Mechanical Signals That Influence Cartilage Health and Progression to Knee Osteoarthritis. Curr Rheumatol Rep. 2014;16: 463–470.
12. Løken S, Ludvigsen TC, Høysveen T, Holm I, Engebretsen L, Reinholt FP. Autologous chondrocyte implantation to repair knee cartilage injury: ultrastructural evaluation at 2 years and long-term follow-up including muscle strength measurements. Knee Surg Sports Traumatol Arthrosc. 2009;17: 1278–88.
13. Ebert JR, Robertson WB, Lloyd DG, Zheng MH, Wood DJ, Ackland T. Traditional vs accelerated approaches to postoperative rehabilitation following matrix-induced autologous chondrocyte implantation (MACI): comparison of clinical, biomechanical and radiographic outcomes. Osteoarthritis Cartilage. 2008;16: 1131–40.
14. Ebert JR, Lloyd DG, Ackland T, Wood DJ. Knee biomechanics during walking gait following matrix-induced autologous chondrocyte implantation. Clin Biomech (Bristol, Avon). Elsevier Ltd; 2010;25: 1011–7.
15. Thoma LM, McNally MP, Chaudhari AM, Best TM, Flanigan DC, Siston RA, et al. Differential knee joint loading patterns during gait for individuals with tibiofemoral and patellofemoral articular cartilage defects in the knee. Osteoarthr Cartil. Elsevier Ltd; 2017; 1–9.
16. Davis RB, Ounpuu S, Tyburski D, Gage JR. A gait analysis data collection and reduction technique. Hum Mov Sci. 1991;10: 575–587.
17. Kadaba MP, Ramakrishnan HK, Wootten ME. Measurement of lower extremity kinematics during level walking. J Orthop Res. 1990;8: 383–92.
18. Lenhart RL, Kaiser J, Smith CR, Thelen DG. Prediction and Validation of Load-Dependent Behavior of the Tibiofemoral and Patellofemoral Joints During Movement. Ann Biomed Eng. 2015;43: 2675–2685.
19. Arnold EM, Ward SR, Lieber RL, Delp SL. A model of the lower limb for analysis of human movement. Ann Biomed Eng. 2010;38: 269–79.
20. Smith RC, Choi KW, Negrut D, Thelen DG. Efficient Computation of Cartilage Contact Pressures within Dynamic Simulations of Movement. Comput Methods Biomech Biomed Eng Imaging Vis. 2016;
21. Hudelmaier M, Glaser C, Englmeier K-H, Reiser M, Putz R, Eckstein F. Correlation of knee-joint cartilage morphology with muscle cross-sectional areas vs. anthropometric variables. Anat Rec Part A. 2003;270: 175–184.

22. Eckstein F, Reiser M, Englmeier KH, Putz R. In vivo morphometry and functional analysis of human articular cartilage with quantitative magnetic resonance imaging–from image to data, from data to theory. Anat Embryol (Berl). 2001;203: 147–73.

23. Draper CE, Besier TF, Gold GE, Fredericson M, Fiene A, Beaupre GS, et al. Is cartilage thickness different in young subjects with and without patellofemoral pain? Osteoarthr Cartil. 2006;14: 931–937.

24. Blankevoort L, Kuiper JH, Huiskes R, Grootenboer HJ. Articular contact in a three-dimensional model of the knee. J Biomech. 1991;24: 1019–1031.

25. Li G, Lopez O, Rubash H. Variability of a Three-Dimensional Finite Element Model Constructed Using Magnetic Resonance Images of a Knee for Joint Contact Stress Analysis. J Biomech Eng. 2001;123: 341–346.

26. Adouni M, Shirazi-Adl A. Partitioning of Knee Joint Internal Forces in Gait Is Dictated By the Knee Adduction Angle and Not By the Knee Adduction Moment. J Biomech. Elsevier; 2014;47: 1696–703.

27. Lu TW, O'Connor JJ. Bone position estimation from skin marker co-ordinates using global optimisation with joint constraints. J Biomech. 1999;32: 129–134.

28. Thelen DG, Won Choi K, Schmitz AM. Co-simulation of neuromuscular dynamics and knee mechanics during human walking. J Biomech Eng. 2014;136: 21033.

29. Smith CR, Vignos MF, Lenhart RL, Kaiser J, Thelen DG. The Influence of Component Alignment and Ligament Properties on Tibiofemoral Contact Forces in Total Knee Replacement. J Biomech Eng. 2016;138: 1–10.

30. Roos EM, Roos HP, Lohmander LS, Ekdahl C, Beynnon BD. Knee Injury and Osteoarthritis Outcome Score (KOOS)–development of a self-administered outcome measure. J Orthop Sports Phys Ther. 1998;28: 88–96.

31. Turcot K, Armand S, Fritschy D, Hoffmeyer P, Suvà D. Sit-to-stand alterations in advanced knee osteoarthritis. Gait Posture. 2012;36: 68–72.

32. Turcot K, Armand S, Lübbeke A, Fritschy D, Hoffmeyer P, Suvà D. Does knee alignment influence gait in patients with severe knee osteoarthritis? Clin Biomech. Elsevier Ltd; 2013;28: 34–39.

33. Løken S, Heir S, Holme I, Engebretsen L, Arøen A. 6-year follow-up of 84 patients with cartilage defects in the knee. Knee scores improved but recovery was incomplete. Acta Orthop. 2010;81: 611–618.

34. Landry SC, McKean KA, Hubley-Kozey CL, Stanish WD, Deluzio KJ. Knee biomechanics of moderate OA patients measured during gait at a self-selected and fast walking speed. J Biomech. 2007;40: 1754–1761.

35. Zeni JA, Higginson JS. Differences in gait parameters between healthy subjects and persons with moderate and severe knee osteoarthritis: A result of altered walking speed? Clin Biomech. Elsevier Ltd; 2009;24: 372–378.

36. Meireles S, De Groote F, Reeves ND, Verschueren S, Maganaris C, Luyten F, et al. Knee contact forces are not altered in early knee osteoarthritis. Gait Posture. Elsevier B.V.; 2016;45: 115–120.

37. Van Assche D, Staes F, Van Caspel D, Vanlauwe J, Bellemans J, Saris DB, et al. Autologous chondrocyte implantation versus microfracture for knee cartilage injury: a prospective randomized trial, with 2-year follow-up. Knee Surg Sports Traumatol Arthrosc. 2010;18: 486–95.

38. Raimondi MT, Pietrabissa R. Contact pressures at grafted cartilage lesions in the knee. Knee Surgery, Sport Traumatol Arthrosc. 2005;13: 444–450.

39. Kock NB, Smolders JMH, Van Susante JLC, Buma P, Van Kampen A, Verdonschot N. A cadaveric analysis of contact stress restoration after osteochondral transplantation of a cylindrical cartilage defect. Knee Surgery, Sport Traumatol Arthrosc. 2008;16: 461–468.

40. Chaudhari AMW, Briant PL, Bevill SL, Koo S, Andriacchi TP. Knee kinematics, cartilage morphology, and osteoarthritis after ACL injury. Med Sci Sports Exerc. 2008;40: 215–22.

41. Van De Velde SK, Bingham JT, Hosseini A, Kozanek M, DeFrate LE, Gill TJ, et al. Increased tibiofemoral cartilage contact deformation in patients with anterior cruciate ligament deficiency. Arthritis Rheum. 2009;60: 3693–3702.

42. Meireles S, Wesseling M, Smith CR, Thelen DG, Verschueren S, Jonkers I. Medial knee loading is increased in subjects with early OA compared to healthy controls during gait but not step-up-and-over task. Plos One (Under Rev.

43. Andriacchi TP, Mündermann A, Smith RL, Alexander EJ, Dyrby CO, Koo S. A framework for the in vivo pathomechanics of osteoarthritis at the knee. Ann Biomed Eng. 2004;32: 447–457.

44. Lefkoe TP, Trafton PG, Ehrlich MG, Walsh WR, Dennehy DT, Barrach HJ, et al. An experimental model of femoral condylar defect leading to osteoarthrosis. J Orthop Trauma. 1993;7: 458–67.

45. Schulze-Tanzil G. Activation and dedifferentiation of chondrocytes: Implications in cartilage injury and repair. Ann Anat. Elsevier; 2009;191: 325–338.

46. Hedbom E, Häuselmann HJ. Cellular and Molecular Life Sciences Molecular aspects of pathogenesis in osteoarthritis: the role of inflammation. 2002;59: 45–53.

47. Heiden TL, Lloyd DG, Ackland TR. Knee joint kinematics, kinetics and muscle co-contraction in knee osteoarthritis patient gait. Clin Biomech (Bristol, Avon). Elsevier Ltd; 2009;24: 833–41.

48. Hubley-Kozey CL, Hill NA, Rutherford DJ, Dunbar MJ, Stanish WD. Co-activation differences in lower limb muscles between asymptomatic controls and those with varying degrees of knee osteoarthritis during walking. Clin Biomech. Elsevier Ltd; 2009;24: 407–414.

49. Coats-Thomas MS, Miranda DL, Badger GJ, Fleming BC. Effects of ACL reconstruction surgery on muscle activity of the lower limb during a jump-cut maneuver in males and females. J Orthop Res. 2013;31: 1890–6.

50. Thoma LM, McNally MP, Chaudhari AM, Flanigan DC, Best TM, Siston RA, et al. Muscle co-contraction during gait in individuals with articular cartilage defects in the knee. Gait Posture. 2016;48: 68–73.

Supplementary material

Joint angles between groups

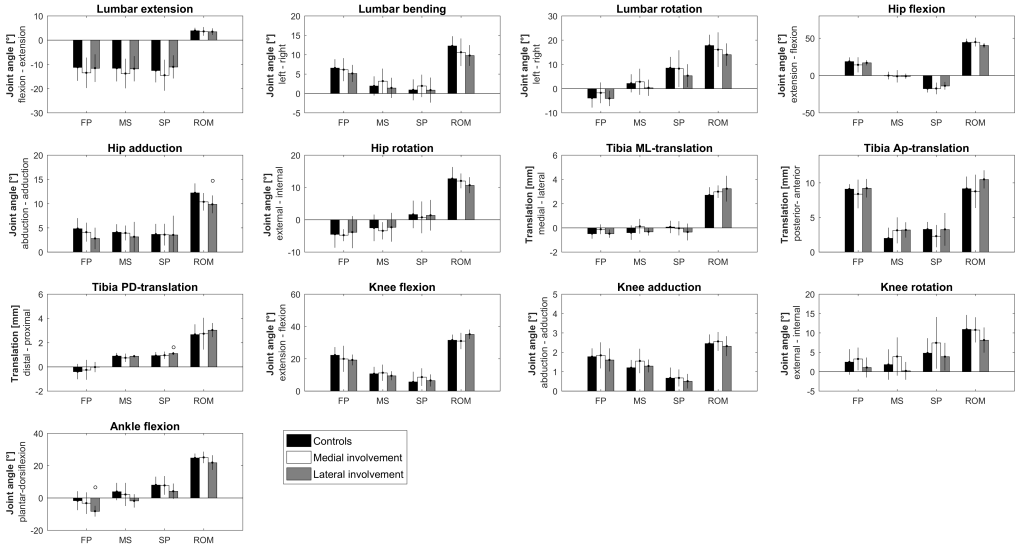

Figure 7.3: **Joint angles between groups.**
Joint angles at first peak (FP), midstance (MS) and second peak (SP) as well as their range of motion are shown. * indicates a significant difference between the patients with medial compartment involvement and the control group, ∘ indicates a significant difference between the patients with lateral compartment involvement and the control group.

Joint moments between groups

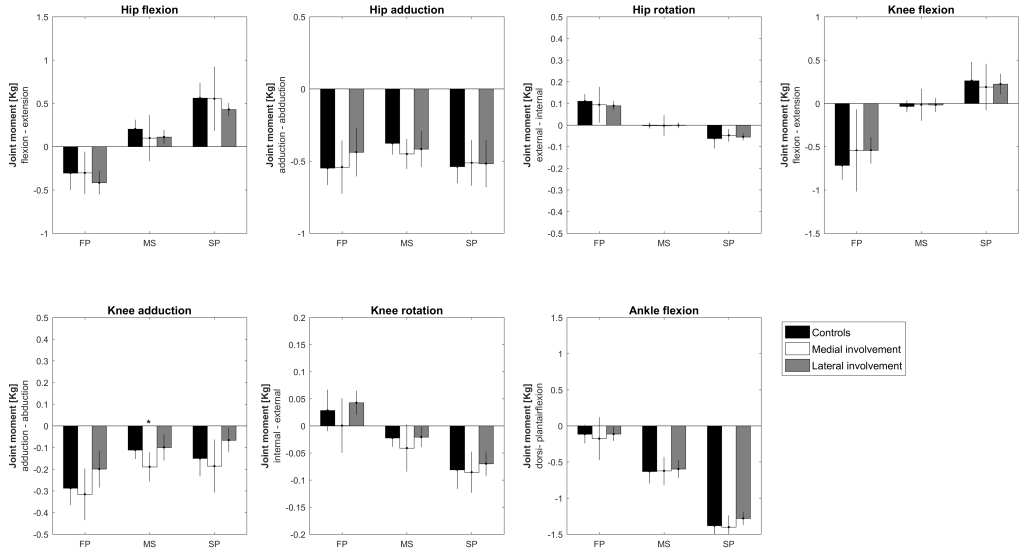

Figure 7.4: **Joint moments between groups.**
Joint moments at first peak (FP), midstance (MS) and second peak (SP) are shown. * indicates a significant difference between the patients with medial compartment involvement and the control group, ∘ indicates a significant difference between the patients with lateral compartment involvement and the control group.

Location of the point of application of the contact forces between groups

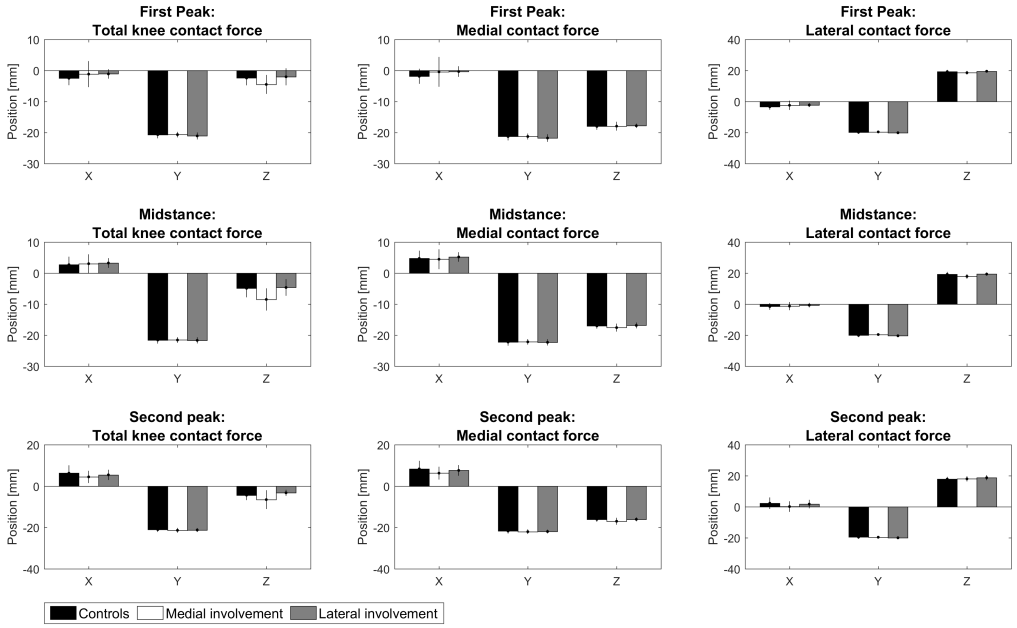

Figure 7.5: **Point of application of the contact forces.**
Point of application of the total knee, medial and lateral contact force expressed in the femur reference frame at FP, SP and MS are shown. * indicates a significant difference between the patients with medial compartment involvement and the control group, ○ indicates a significant difference between the patients with lateral compartment involvement and the control group.

Chapter 8

General discussion

The aim of this PhD was to evaluate the relation between movement, knee loading and cartilage structural and matrix properties and how this relation is affected under the influence of OA predisposing factors. These insights will on the long term contribute to a better understanding of the role of mechanical signals in joint cartilage homeostasis, cartilage degeneration or repair and aid in optimally tuning rehabilitation protocols following knee injury.

This overarching goal was studied in three main objectives that were further elaborated in five different studies. Firstly, cartilage loading in the different knee joint compartments was evaluated during different functional activities (Study I). Secondly, the relation between cartilage loading, structural (i.e. thickness) and matrix properties (i.e. proteoglycan and collagen content estimated using quantitative MRI) was investigated in a cohort of healthy adults (Study II and III). Thirdly, the effect of previously identified risk factors for knee OA, on cartilage loading was studied, since these factors were previously hypothesized to affect the relation between knee joint movement and loading (Study IV and V).

In the discussion, we will first formulate specific conclusions based on these individual study results. Next, a general discussion presenting integrative insights will be stated. Lastly, limitations of this work will be discussed and suggestions for further research will be formulated.

Specific conclusions

Objective I: Evaluation of knee loading during different clinically relevant tasks and its relevance for rehabilitation after knee injury

During rehabilitation, one of the challenges is to protect the knee from excessive forces, while providing sufficient stimuli to regain muscle strength and restore normal function. However, the inclusion and staging of exercises in rehabilitation protocols after knee injury is currently expert-based as a thorough description of knee contact forces during different exercises is lacking[1–3]. Therefore, in study I we quantified muscle forces, joint contact forces and shear forces in the different knee joint compartments during frequently performed activities in daily life and rehabilitation.

Hypothesis study I: Quantification of knee joint loading can support a grading in exercise intensity and allow for the design of more evidence-based rehabilitation programs.

In this study, experimental motion data was collected in fifteen healthy adults during nine standardized activities used in daily life (more specific: gait, stair ascent and descent, stand up, sit down) and rehabilitation (more specific: squat, forward and sideward lunge and single leg hop). Musculoskeletal modelling was used to calculate muscle as well as contact and shear forces in the different knee joint compartments, specifically the medial and lateral condyle and the patellofemoral compartment. Average and maximum contact and shear forces in the different compartments as well as muscle forces were compared between exercises and compartments using repeated-measures ANOVAs. Compartmental forces were individually compared for each exercise and exercises were further compared against gait using dependent t-tests. Loading during gait was considered as reference loading, as during rehabilitation weight-bearing walking is an important milestone for progression towards more demanding exercises[3,4].

Restoration of muscle strength is one of the key elements for successful rehabilitation[3,5,6]. Therefore, the inclusion of appropriate exercises that facilitate the knee musculature is mandatory. Knee extensor muscle force production was significantly higher in all studied exercises when compared to gait. This indicates that all exercises could potentially train quadriceps muscles and could therefore be included in a comprehensive rehabilitation protocol that aims to optimize knee joint stability in patients with insufficient quadriceps muscle recruitment. On the other hand, none of the exercises trained the knee flexor musculature and consequently rehabilitation protocols should be supplemented with dedicated exercises that focus in particular on knee flexor strengthening.

Although extensor muscle force production was significantly higher compared to gait in all exercises, squat, sit down and stand up resulted in the lowest tibiofemoral contact forces. Consequently, these exercises can be used to train the knee extensor musculature early in rehabilitation without exposing the tibiofemoral joint to high contact forces. All other therapeutic exercises (i.e. lunges, single leg hopping) resulted in significantly higher contact forces compared to gait. Furthermore, all studied exercises imposed higher patellofemoral contact forces than gait.

Apart from differences in contact force magnitude, a redistribution of the contact forces over the condyles was observed. During walking, the medial condyle receives the majority of loading[7–9]. This was also observed during stair ascent and descent, forward lunges and single leg hopping. However, during stand up, sit down, squat and sideward lunges, the lateral condyle loading exceeded medial condyle loading. Based on these results, differential loading of a specific compartment can be achieved by careful exercise selection. The magnitude of compartmental contact forces was directly related to the compartmental shear forces and therefore appropriate selection of exercises will also modulate the shear forces in the specific compartment. Lastly, in exercises with more knee flexion, the contact forces were more distributed towards the posterior region of the femoral condyles. Therefore, it is important to adapt the range of motion of knee flexion during the exercises, in patients presenting cartilage damage in the posterior part of the femoral condyles.

In conclusion, we found that advanced biomechanical analyses can provide useful insights for the design of more progressive rehabilitation programs. Loading and shear forces in a specific knee compartment can be gradually incorporated through thoughtful selection of exercises. Consequently, muscle strengthening exercise inclusion can be better staged and may result in less knee joint reactivity. For instance, a squat could be included early in rehabilitation as it provides an increased training stimulus for the knee extensor muscles, without imposing high contact forces in the tibiofemoral compartment. However, long-term follow-up studies in patients are required to confirm the effectiveness of these progressive rehabilitation programs.

Objective II: Investigate cartilage structure and matrix-composition using MRI and its relation to knee joint loading in healthy adults

Mechanical factors support the regulation of cartilage homeostasis and therefore chronic loading patterns could dominate the biologic and structural response of the cartilage[10–12]. Additionally, cartilage thickness and matrix composition were found to vary over the femoral condyle[13–16]. As in-vitro studies showed that the biosynthetic activity of the chondrocytes is either promoted or inhibited by mechanical loading, it was hypothesized that cartilage structure and matrix composition are adapted as a protective response to the imposed persistent cyclic loading, more specific as present during walking[10–12,17–25]. Using medical imaging and novel musculoskeletal modelling methods we further corroborated these findings in-vivo in two different studies: study II investigated the relation between loading and cartilage properties of the central zone of the medial and lateral femur condyle in a healthy population. Study III investigated the local relation between loading and cartilage properties in the weight-bearing and non-weight-bearing zones of the medial and lateral condyle, as well as the patellofemoral compartment.

In study II, knee loading during walking was related to cartilage thickness, $T1\rho$ and T2 relaxation time in the central region of the medial and lateral condyle. This provides insight in how cartilage thickness and relaxation times, indicative for matrix components are adapted to loading during walking in a healthy population.

Hypothesis study II: Higher cartilage loading in the central zone of the medial and lateral condyle is expected to relate to increased thickness and to lower $T1\rho$ and T2 relaxation times, indicative of a higher proteoglycan and collagen concentration and orientation.

In this study, MRI was used to determine average and peak thickness as well as average $T1\rho$ and T2 relaxation time of the cartilage in the central zone of the medial and lateral condyle of fifteen healthy adults. The central zone was determined as the area between the anterior end of the femoral notch and 60% of the distance to the most posterior end of the femoral condyles[26,27]. Musculoskeletal modelling was used to determine loading of the medial and lateral compartment during walking, in terms of contact forces and pressures. The relation between cartilage structural and compositional properties was related to compartmental loading using spearman rank correlation coefficients.

In agreement with previous studies that used an estimate of knee loading, we found significant correlations between cartilage thickness in the central zone of the condyles and total and compartmental knee loading across subjects[11,28,29]. Our findings suggest that persons who experience higher loads during walking have thicker cartilage as a protective adaptation to the cyclic loads. More in detail, medial condyle cartilage thickness was mostly related to second peak loading, whereas lateral condyle cartilage thickness was mostly related to first peak loading. Furthermore, cartilage thickness of the lateral condyle was correlated more to its zonal loading, as reflected in the higher correlations between lateral condyle loading and lateral condyle cartilage thickness compared to the correlations found for the medial condyle. This can be explained by the smaller lateral contact area compared to the medial contact area resulting in more localized loading on the lateral condyle, but more distributed loading on the medial condyle. This will induce more localized

changes in cartilage thickness of the former than the latter[11,30].

Besides cartilage thickness, proteoglycan and collagen content, estimated by $T1\rho$ and T2 relaxation time mapping respectively, were found to relate to cartilage loading during walking. Remarkably, concentration of the matrix constituents was also related to loading direction. In agreement with our hypothesis, increased proteoglycan concentration (indicated by a decreased $T1\rho$ relaxation time) was related to higher compressive forces. In contrast, decreased proteoglycan concentration (indicated by an increased $T1\rho$ relaxation time) was correlated with higher shear forces. Lastly, increased collagen content and organization (indicated by decreased T2 relaxation time) was related to higher pressures and compressive forces.

In conclusion, we found that in a cohort of healthy adults higher compressive loading during walking is correlated with increased thickness, proteoglycan and collagen concentration. This suggests that the increased thickness, proteoglycan and collagen content of the cartilage in the central zone of the femur is an adaptive response to the compressive loading during walking.

In study III, we investigated the local variation in cartilage thickness, $T1\rho$ and T2 relaxation times over the femoral condyle in healthy adults and compared cartilage thickness and relaxation times between weight-bearing and non-weight-bearing zones.

Hypothesis study III: Local variation in loading during walking relates to increased thickness and lower $T1\rho$ and T2 relaxation times, indicative of higher proteoglycan and collagen concentration and therefore increased weight-bearing capacities compared to the non-weight-bearing zone.

In this study, we used magnetic resonance imaging to visualize knee joint cartilage and estimated cartilage thickness, proteoglycan and collagen content of fourteen healthy adults. Distribution of cartilage thickness and relaxation times over the articular cartilage surface was investigated using an angle-dependent approach[31–33]. Additionally, experimental gait data were collected and a musculoskeletal model was used to calculate contact force impulse on the cartilage surface and to define the weight-bearing and non-weight-bearing zones during walking. Subsequently, the average thickness and $T1\rho$ and T2 relaxation times in the weight-bearing zones were compared to the non-weight-bearing zones.

No differences in cartilage thickness between weight-bearing and non-weight-bearing zones were observed. For the weight-bearing zone of the medial condyle, a strong positive correlation between localized loading and cartilage thickness was observed, suggesting that the location of thickest cartilage on the articular surface coincides with the location of highest loading during stance. Although previous studies observed that the location of thickest cartilage on the medial condyle coincides with the contact location at heel strike, we are the first to confirm that the weight-bearing zone as a whole is adapted to the cumulative loading (estimated by the contact force impulse) perceived during the stance phase of the gait cycle[30,34,35].

In agreement with our hypothesis, lower $T1\rho$ relaxation time, indicative of increased proteoglycan content was observed in the weight-bearing zone of the medial condyle compared to the non-weight-bearing zone. In contrast to our hypothesis, collagen content, as reflected in the T2 relaxation time in the weight-bearing

zone of the medial condyle, was lower compared to the non-weight-bearing zone. These results suggest that, the weight-bearing zone of the medial condyle has a less dense collagen network with a higher concentration of proteoglycans. This would imply an increased capacity of the extracellular matrix to sustain compressive loads as this would increase its capacity to deform under compression. Consequently, our results indicate that the cartilage in the weight-bearing zone of the medial condyle has superior biochemical properties in terms of proteoglycan content and is therefore better suited to withstand the high compressive forces experienced during walking.

On the other hand, no differences in $T1\rho$ relaxation time in the weight-bearing zone and the non-weight-bearing zone of the lateral condyle or trochlea were observed. During walking most loading is captured by the medial condyle, therefore the proteoglycan content of the lateral condyle and trochlea may be less adapted to mechanical loading experienced during walking. Consequently, variation in cartilage proteoglycan content in these zones may be more affected by other factors such as genetics, age or mechanical loading during movements that load these zones more.

In conclusion, we found local differences in cartilage thickness and matrix composition over the femoral articular cartilage surface that can be related to its local loading during walking and was especially prevalent on the medial condyle. Furthermore, the weight-bearing zone of the medial condyle was found to have superior weight-bearing capacities compared to the non-weight-bearing zone, suggesting a local protective adaptation of the cartilage to loading.

Objective III: Analyze the effect of osteoarthritis predisposing factors on the knee load distribution

Subject- and joint-related risk factors that contribute to knee OA initiation and progression by initiating degenerative pathways were previously identified[36–46]. Therefore, the effect of specific joint-related OA risk factors, i.e. tibiofemoral joint geometry and alignment as well as the presence of an isolated articular cartilage defect on knee joint loading were investigated in study IV and V.

In study IV, the isolated effect of altered coronal and transverse plane knee joint geometry and alignment on the cartilage load distribution and on the ligament elongation was investigated using musculoskeletal modelling. This approach allows to study the isolated effect of altered joint geometry and alignment. Joint geometry and alignment was systematically changed in a range that is observed in a normal population[47,48]. This is not possible in a patient population where only the combined effect of multiple factors (e.g. movement adaptations, malalignment, muscle weakness, pain) on joint loading can be evaluated.

Hypothesis study IV: Altered tibiofemoral geometry and alignment will result in increased compartmental loading, indicative of increased OA initiation risk.

In this sensitivity study, the alignment and geometry of the tibiofemoral joint was systematically changed between $\pm 15°$ in steps of $2°$ from its reference position in the coronal and transverse plane. Experimental motion data collected in 15 healthy adults and was then processed using the musculoskeletal model that incorporated the different alignment and geometry changes. Subsequently, load distribution at peak loading as well as the peak ligament strains were analyzed and compared to the reference simulation.

The medial-lateral tibiofemoral load distribution and ligament strains during walking were sensitive to changes in both joint geometry and alignment in the coronal plane, representative for coronal tibial slope and knee varus-valgus alignment respectively, but were less sensitive to changes in joint geometry and alignment in the transverse plane.

Already small alterations in knee alignment (from $3°$ onwards) significantly affected the knee loading distribution. Varus increased loading on the medial condyle, while valgus increased loading on the lateral condyle. Simultaneously, a load reduction on the opposite condyle was observed. These findings confirm the role of varus malalignment in medial compartment overloading, a factor previously associated with increased risk of medial knee OA initiation and progression.

Altered coronal plane joint geometry, indicative of altered coronal tibial slope, significantly affected the medial-lateral force distribution, although to a lesser extent than the knee joint alignment in the coronal plane (from $7°$ onwards). A more elevated medial tibia plateau resulted in increased medial condyle loading and decreased lateral condyle loading, whereas the opposite was observed with a more elevated lateral tibia plateau. This suggests that small changes in coronal tibial angle are more forgiving in neutrally aligned knees presenting a smaller effect on cartilage load distribution and therefore a smaller potential risk of cartilage degeneration.

In addition, altered coronal tibial slope strongly affected peak strains in the collateral ligaments. A more elevated medial tibial plateau significantly increased peak strains in the medial collateral ligament, whereas a more elevated lateral tibial plateau resulted in significantly increased peak strains in the lateral collateral ligament. On the long term, coronal plane knee laxity and instability, a previously identified risk factor for knee OA could be introduced due to adaptive creep of the ligaments and consequent prolonged stretching[44,49]. Hence, coronal plane knee laxity likely adds to a vicious circle, initiated by knee instability and consequent knee malalignment inducing altered joint loading and this might increase articular cartilage breakdown[44,45]. These findings imply that subtle alterations in joint geometry (i.e. coronal tibial angle) have the potential to introduce joint malalignment later in life, which in turn could introduce altered loading and therefore accelerate OA progression.

Alterations in joint geometry and alignment in the transverse plane had a less pronounced effect on the load distribution compared to the effect of alterations in the coronal plane. When altering the rotational alignment of the tibial plateau, no effect on the force distribution was observed. Altered transverse plane alignment, only significantly affected the force distribution during terminal stance.

In conclusion, this simulation-based study investigated the isolated effect of variations in coronal and transverse plane joint geometry and alignment on the medial-lateral load distribution during walking. This study provides additional insights on the isolated role of variations in joint geometry and alignment on knee load distribution, which might affect OA disease progression by increasing local cartilage loading.

In study V, the effect of an isolated articular cartilage defect on knee joint loading was evaluated. This study therefore provides additional insights in the role of isolated articular cartilage defects in an otherwise healthy knee joint in OA development, since isolated articular cartilage defects were previously identified as predisposing factors for knee OA.

Hypothesis study V: patients with isolated articular cartilage defects in an otherwise healthy knee joint will present kinematic adaptations, inducing a loading avoidance strategy that decreases the loading on the injured site.

In this study, experimental motion data was recorded in fifteen patients with isolated cartilage defects and compared to data of nineteen asymptomatic healthy controls. Patients were further categorized based on defect location in a group of patients with medial- vs lateral-involvement. Contact forces and pressures in the tibiofemoral joint were calculated using a musculoskeletal model. To evaluate altered loading magnitude in the involved and non-involved compartment, peak total knee, medial and lateral contact forces and pressures during the first and second part of the stance phase were compared for the involved and non-involved compartment of the patients with the controls. Additionally, to evaluate if an articular cartilage defect resulted in altered contact locations in the involved and non-involved compartment, the contact pressure distribution at the instance of peak loading was analyzed as well as the center of pressure location.

Although both patients groups reported significantly worse subjective outcome, no changes in the kine-

matic and kinetic behavior during gait were observed, this despite the expected changes in the movement pattern. Similarly, decreased walking speed was previously found as a successful strategy to avoid pain and symptoms, however the self-selected walking speed was only decreased in patients with a cartilage defect in the lateral condyle[50–52].

Following on these observations but in contrast to our hypothesis, unloading of the involved condyle was not confirmed in the current patient cohort. This is in line with a recent study that failed to identify differences in joint reaction forces when controlling for walking speed and quadriceps strength[52]. Following an isolated cartilage defect in an otherwise healthy knee joint, the compartmental forces were unaltered, therefore distributing a similar force magnitude over the cartilage surrounding the defect. In addition, the contact pressure distribution was not significantly altered. Consequently, the stress on the cartilage surrounding the defect will be increased and this may initiate degenerative changes contributing to the progression from defect to OA[53–57]. Indeed, a decrease in proteoglycan content in the cartilage of the lesion rim and an increased amount of osteophytes was found 20 weeks after experimentally creating a femoral cartilage defect[58]. Our findings indicate that following a localized cartilage defect, the localized degenerative changes in the cartilage due to the locally increased loading have a role in the initiation of OA. This in contrast to the altered compartmental loading or contact locations. that were confirmed in this work in case of malalignment or previously observed after ACL-rupture and in early OA patients, respectively[28,59–61].

In conclusion, an isolated full-thickness cartilage defect does not result in distinctive adaptations of joint kinematics and therefore joint loading. Therefore, isolated cartilage defects might contribute to OA progression by imposing increased stress on the cartilage surrounding the defect and therefore initiating local degenerative changes. This increased stress on the defect rim in combination with cytokines and growth factors will trigger catabolic responses of the chondrocytes, protective responses of the surrounding tissue and will induce accelerated cartilage degeneration that may explain the progression to OA[62].

General conclusions

Musculoskeletal modelling provides a more sensitive estimate of the compartmental load distribution in the knee compared to external joint moments and can therefore contribute to an enhanced insight in the role of cartilage loading during movement in maintaining joint cartilage homeostasis

In a clinical setting, external joint moments are widely used to estimate joint loading. However, external moments combine the effect of the reaction forces due to the ground reaction force and the joint kinematics, but neglect the effect of muscle and ligament forces on the knee contact forces. Therefore, they do not explicitly characterize the internal loads acting on the cartilage. The knee adduction moment is widely used to estimate medial condyle loading[63,64]. A strong correlation between the knee adduction moment and medial condyle contact force measured in a single instrumented implant was observed[65]. However, its accuracy is still highly debated as some studies observed that besides the knee adduction moment also other kinematic (i.e. knee adduction angle) and kinetic (i.e. knee flexion moment) variables contribute to the knee contact force[66–68]. Therefore, a decrease in knee adduction moment does no guarantee decreased medial condyle loading and may not be a valid estimate during movements other than gait[68,69].

Indeed, in this work, changes in frontal plane knee joint moments were not necessarily accompanied by changes in medial and lateral contact forces. For instance in study IV, no changes in the knee adduction moment were observed when alterations in joint geometry were simulated, while significant changes in medial condyle loading were observed. On the other hand, in study V differences in the knee adduction moment were present, whereas no differences in knee contact forces were found between patients with articular cartilage defects and healthy controls. These findings indicate that not only changes in external forces and joint angles (as reflected in the frontal plane knee moment) need to be considered, but that coinciding alterations in muscle and ligament forces will affect the medial-lateral load distribution. When solely relying on external moments, these alterations in muscle and ligament forces are neglected. This is especially relevant to take into account when the goal is to evaluate joint loading in a patient population in which muscle co-contraction and ligament laxity are present as these would affect the calculated contact forces[44,70–74].

Additionally, the ability of the musculoskeletal modelling workflow to separately calculate medial and lateral compartmental loading, allowed to relate lateral condyle loading to lateral condyle cartilage thickness. Using the knee adduction moment, only a relation between the knee adduction moment and medial condyle cartilage thickness was found, which is in agreement with the fact that the knee adduction moment is only an estimate of the medial condyle loading and the medial-to-lateral load distribution.

This shows the added benefit of calculating medial and lateral knee contact forces as a more sensitive description of loading at the joint level, instead of solely relying on the knee adduction moment as an estimate of medial condyle loading. Therefore, medial condyle contact forces may be a more sensitive biomarker for early detection of OA. Early detection of knee OA is uttermost important, as it would allow interventions that protect the joint integrity and delay OA progression to be taken before structural damage is present. This is important as it was hypothesized that the effect of interventions that try to delay OA progression may be confounded by a (too) late inclusion of patients when structural deterioration is already advanced[75].

Currently, gait modification strategies aiming to decrease the knee adduction moment are used in rehabilitation in order to avoid pain and slow down the progression of OA, by diminishing medial condyle loading[76–78]. These strategies and rehabilitation guidelines rely exclusively on the knee adduction moment. However, our findings suggest that the medial condyle contact force could be a more appropriate target in rehabilitation instead of the knee adduction moment, especially in the early stages of the disease. Current developments of real time implementations of muscle optimization techniques as part of virtual reality training suits will undoubtedly allow providing feedback in terms of joint contact forces.

Cartilage structure and composition are locally adapted to mechanical loading imposed during walking

As the chondrocytes are mechanosensitive, loading during daily life has the potential to affect cartilage homeostasis. In this, chronic loading patterns were hypothesized to dominate the biologic and structural response of the cartilage, e.g. by thickening and increasing proteoglycan and collagen content [10–12]. Indeed, in-vitro studies observed that mechanical loading can either promote or inhibit the biosynthetic activity of the chondrocytes and is necessary for the maintenance of a stable articular cartilage phenotype[17–25,79,80]. Furthermore, loading was found to influence cartilage extracellular matrix distribution, as reflected in a region-dependent distribution of cartilage extracellular matrix composition over the femur condyles[16,81–83]. By combining magnetic resonance imaging and musculoskeletal modeling, this study is the first to confirm mechano-adaptive responses of the cartilage to loading during walking in a whole joint complex in vivo.

Firstly, we observed a significant relation between total and zonal knee loading during walking and the zonal cartilage thickness. Furthermore, a strong significant correlation between the location of loading in the weight-bearing zones during walking and the local thickness distribution of the medial condyle was found. Both findings extend previous work that related medial condyle cartilage thickness to the knee adduction moment or to the knee flexion angle at heel strike[11,29,30,34,35]. Extending these previous studies that only used a proxy for local knee joint loading, our findings indicate that the cartilage thickness of the whole weight-bearing region of the medial condyle is adapted to the cumulative loading during walking, therefore confirming a protective local cartilage response in the whole knee joint to the high cyclic loads through life (figure 8.1).

Secondly, the matrix composition of the cartilage in the knee joint complex could be related to loading magnitude and loading type during walking. More specifically, we observed increased loading magnitude, in particular increased compressive loading, to be related to increased proteoglycan content in the central zone of the condyles and the weight-bearing zone of the medial condyle. These findings suggest that the extracellular matrix of the weight-bearing zone of the medial condyle is adapted to loading during walking by increasing the proteoglycan content, resulting in superior weight-bearing capacities to withstand the high compressive loads during walking[84–86].

In contrast to the medial condyle, no differences in cartilage thickness and $T1\rho$ relaxation time were found in the weight-bearing zone compared to the non-weight-bearing zone of the lateral condyle and trochlea. In addition, the local loading in the lateral compartment was not correlated to the region-specific thickness distribution. The fact that the lateral condyle and the trochlea are less involved in weight-bearing during walking and that therefore the cartilage in these compartments is less adapted to loading during walking may be a potential explanation[8]. However, we observed a significant correlation between lateral

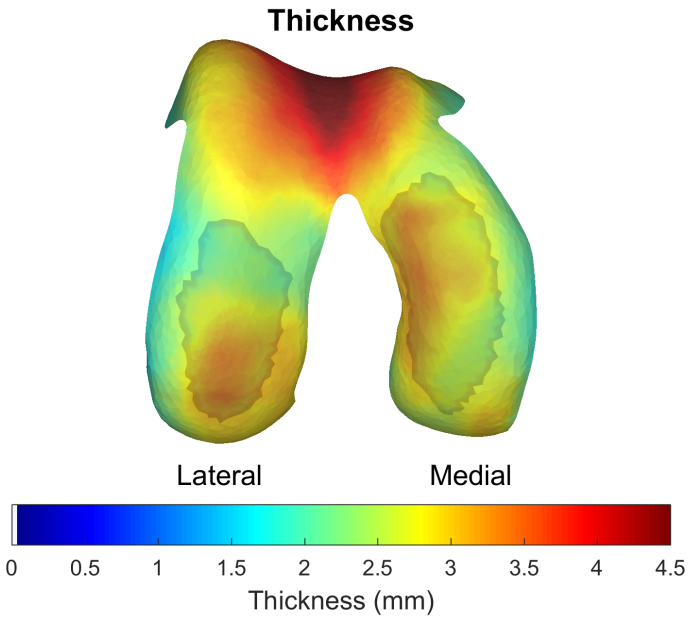

Figure 8.1: **Average thickness distribution.**
The whole weight-bearing zone during the stance phase is indicated by the gray area, showing a good agreement between zones of thicker cartilage and zones of loading.

condyle loading and the thickness of the central part of the lateral condyle when comparing between subjects. This might indicate that the local adaptation of the cartilage less involved in weight-bearing during walking is regulated by other factors such as bone geometry, growth factors, genetics or loading during other motions.

In conclusion, long-term cartilage adaptations related to loading imposed during a chronic cyclic activity of daily life were confirmed in the knee complex in vivo and were especially prevalent in the medial condyle cartilage. In this, we were able to show that the weight-bearing zone of the medial condyle is thicker and contains a higher amount of proteoglycans, indicating that this zone is better able to deform and therefore cushion the compressive loading imposed during walking to the subchondral bone.

Deviations in knee geometry and alignment as well as articular cartilage defects have the potential to contribute to OA initiation and progression by affecting knee joint load distribution and ligament state

OA is a multifactorial disease that ultimately ends in irreversible structural and functional failure of the joint[87]. Subject- and joint-related risk factors for OA development were previously identified[36–46]. It is likely that these joint-related risk factors cause aberrant mechanical loading and therefore contribute to OA initiation and progression, by triggering catabolic pathways that are more likely to be activated in people that are genetically predisposed to OA[88,89]. Previously knee malalignment and an articular cartilage defect were identified as risk factors for OA initiation as these could potentially affect the cartilage load distribution[36–43,90,91]. This work shows that coronal plane malalignment but not an isolated articular cartilage defect could affect knee load distribution, therefore both factors have a distinct role in OA initiation.

Coronal plane alignment and especially varus alignment increased medial condyle loading, which might pose additional stress on the different knee structures, more specific the ligaments, cartilage, meniscus and

subchondral bone. Varus and valgus malalignment were previously related to an increased risk for bone marrow lesions and cartilage loss in the medial and lateral condyle, respectively[92–96]. Our studies support that minimal changes in varus and valgus malalignment can cause altered loading in the medial and lateral condyle, respectively. However, so far only an association between varus malalignment and increased knee adduction moment used as a proxy estimate of medial condyle loading was reported[97–100]. This can now be further confirmed by our findings, as a clear effect of malalignment on the knee load distribution was observed, even when the knee adduction moment was not altered.

An articular cartilage defect was found to have no distinct effect on the cartilage load distribution at the level of gait kinematics and kinetics compared to control subjects. Furthermore, no changes in cartilage loading on the involved compartment were reported. This finding is in contrast to the gait adaptations previously reported following MACI-surgery. The absence of clear compensatory mechanisms in our cohort suggests that isolated articular cartilage defects do not induce alterations in gait kinematics and that these may be merely the consequence of adaptations following the open knee surgery.

It is however important to emphasize that in the presence of an articular cartilage defect the same magnitude of loading is applied to the injured cartilage, whereas the area of healthy cartilage that can distribute the loading over the subchondral bone is decreased due to the absence of part of the articular cartilage surface. Therefore, locally higher stress on the defect rim can be present, spreading into the healthy cartilage surrounding the defect, instead of equally distributing the load over the contact surface[53,54]. This is likely to be further aggravated in the presence of other OA predisposing factors such as joint geometry and malalignment. Therefore, careful evaluation of the joint geometry and alignment at the time of diagnosis is crucial in identifying patients at risk for the development of early OA and should be taken into account when determining their treatment. Interestingly, loading magnitude and location were not altered in presence of isolated cartilage defects. Nevertheless, part of these patients will progress towards (early) OA[55–57]. In patients with established OA, altered knee joint moments and contact forces were confirmed and these are suggested to contribute to further degeneration of the cartilage[66]. In contrast, in early OA patients, knee moments and total knee loading were not significantly different[66]. It is only recently that our research group was able to show that in these patients small differences in transverse plane joint kinematics during walking cause altered medial-lateral load distribution and contact locations[60]. In contrast to this work, loading magnitude and location were not significantly altered in patients with isolated cartilage defects, suggesting that additional factors other than the presence of a cartilage defect will induce the altered loading conditions observed in early OA. Altered transverse plane kinematics and kinetics due to the presence of ligamentous laxity have previously been suggested to play a key role in the altered contact locations[28,60]. Likewise, changes in the transverse plane knee geometry and alignment induced similar changes in contact locations. Both these findings support the hypothesis that with ligamentous laxity and altered joint geometry, transverse plane malalignment can be induced affecting transverse plane joint position that consequently alters contact locations in the joint. Consequently, localized tissue effects rather than gross altered compartmental loading have a potential role in the initiation of OA following a localized cartilage defect[28,59]. This being further catalyzed by the presence of growth factors and cytokines that will trigger catabolic responses of the chondrocytes and a reactive response of the surrounding tissue.

In conclusion, both alignment and an articular cartilage defect have a role in altered articular cartilage loading, therefore affecting cartilage homeostasis and initiating degenerative pathways that ultimately lead to OA initiation.

Restoration of a normal loading pattern during walking should be a specific goal during rehabilitation of knee conditions

In agreement with previous in-vitro and in-vivo studies, we found that cartilage is locally adapted to chronic loading patterns induced by repetitive activities such as walking. This indicates that factors that affect the physiological load distribution during walking may disrupt normal cartilage homeostasis by activating catabolic pathways, therefore ultimately leading to OA initiation[10,37,90,91].

Compensatory movement adaptations in the walking pattern were previously identified in several knee injuries (e.g. ACL-rupture, OA) to avoid pain and discomfort[97,101–103]. Therefore, a physiotherapist should be aware of movement strategies that patients adopt as these can cause cyclic overloading and/or a shift in contact location to cartilage zones with less weight-bearing capacity[61]. This cyclic overloading of cartilage, that is less adapted to this loading, might initiate local degenerative changes in the cartilage and may ultimately contribute to OA initiation[10,28]. Likewise, during a rehabilitation session the physiotherapist should be aware of adaptive movement strategies that shift the load distribution in the joint. Consequently, minimization of adaptive movement strategies and therefore restoration of normal joint loading are key factors in rehabilitation following knee injury or in the presence of knee OA.

In addition to restoring normal joint loading, the insights in the current work may help a physiotherapist to adapt the rehabilitation exercises to avoid loading a specific compartment. For instance, deep knee flexion (such as during forward lunges) should be avoided when cartilage damage is present on the posterior part of the condyles. Alternatively, by adapting trunk, knee or foot position a physiotherapist may adapt the alignment of the knee joint center with respect to the ground reaction force vector and consequently the external joint moments as well as the knee joint loading will be affected[104–106].

Additionally, the strong correlation between local cartilage thickness and constitution with local loading in the weight-bearing zone of the tibiofemoral condyle during walking suggests that the tibiofemoral joint is ideally tuned to bear loading associated with walking. However, during different rehabilitation exercises, knee loading magnitude and contact location were found to be highly variable and different from walking. This suggests that during rehabilitation exercises, cartilage regions might be loaded that are less predisposed to bear this loading. Therefore, a gradual progression and correct instructions, as well as careful evaluation of the joint reactivity is required during rehabilitation. This is important as joint reactivity was previously found to induce arthrogenic muscle inhibition[107,108]. Consequently, rehabilitation might be slowed down, as arthrogenic muscle inhibition induces muscle weakness and prevents strengthening of the muscles[107,109–111]. Therefore, including appropriate strengthening exercises that result in less knee joint reactivity will result in a more efficient progression.

Whereas physical therapy will focus on restoring active knee stability to control normal joint loading and movement, the role of orthopedic bracing and surgical interventions in the treatment following isolated cartilage defects may need to be reconsidered. Orthopedic knee braces could be used to reduce compartmental joint loading. Therefore, valgus braces were previously used to reduce medial condyle loading, as a valgus brace creates an additional external abduction moment to reduce loading on the medial condyle[9,112]. Based on our results, bracing could be considered in patients with early medial knee OA and persons with varus malalignment in order to slow down the progression of OA, by diminishing medial condyle loading. However, according to the present results the use of valgus braces in patients with an articular cartilage

defect is less relevant as no differences in joint loading were observed. Nevertheless, a valgus brace could be used to diminish medial compartment loading and therefore joint reactivity and the local degenerative changes around the lesion.

Based on the results obtained on loading following isolated cartilage defects and in the presence of joint malalignment, the use of surgical interventions to restore physiological joint loading should be considered. For this, high-tibial osteotomies (HTO) are often used to treat unicompartmental OA in patients with knee malalignment by restoring neutral alignment and ultimately physiological joint loading[113–116]. Furthermore, the current results support the guideline for neutral axis restoration when varus or valgus malalignment ($> 3°$ deviation from neutral) is present, in order to compensate for the increased compartmental loading when treating isolated cartilage defects. As such, the success-rate of a surgical treatment of an articular cartilage defect can be increased[116–118]. However, one should be careful not to over-correct the axis alignment, as a small deviation from a neutral knee alignment already resulted in significantly increased compartmental loading. This can explain the increased incidence of lateral knee OA previously observed after over-correcting varus malalignment with HTO[119].

To better understand the effect of altered loading on OA initiation multi-center trials in patients with isolated cartilage defects in an otherwise healthy joint that report three-dimensional motion capture as outcome parameters, are indispensable

Data collection of patients with isolated cartilage defects in an otherwise healthy knee joint was performed in Leuven and Cardiff. Multicenter studies are useful, as patient recruitment may be complicated when strict in- and exclusion criteria need to be applied (e.g. absence of concomitant injury) and when large comprehensive datasets (e.g. medical imaging in combination with motion capture) are collected. The data of this study are to the best of our knowledge the only that can be used as reference for power calculation to determine the data sample needed to evaluate the role of isolated cartilage defects on knee joint loading. Indeed, based on the observed variances describing medial compartment loading in the present cohort, future studies would require >100 participants in each group to observe significant differences in contact forces of the medial compartment between patients with an articular cartilage defect and healthy controls (statistical power of 0,80). Given the limited variation in lateral compartment loading in the current cohort, no firm conclusions on the required sample size could be drawn. Therefore, multicenter studies will be the only way to obtain biomechanical data in a relevant patient cohort.

In this work, integrated three-dimensional motion capture data from two centers that used different marker placement protocols was pooled to increase sample size. The use of different marker-protocols is considered a risk as previous studies indicated that although sagittal plane motions were comparable, out-of-sagittal plane motions (i.e. ab-adduction and internal-external rotation) were less comparable between the different marker-protocols[120]. This indicates that motion data obtained using different marker-protocols and different kinematic models could not be directly compared to each other and differences between studies should be interpreted with respect to inherent kinematic model assumptions, such as joint center locations[121]. In this work, data obtained using an extended Plug-in-Gait[122] protocol in Leuven and extended Helen-Hayes[123] protocol in Cardiff was processed using the same musculoskeletal modelling workflow. Comparing the joint kinematics obtained in healthy adults, we only observed a small difference in knee rotation and hip flexion angle during the first part of the stance phase and in the ankle angle between the two centers (figure 8.2).

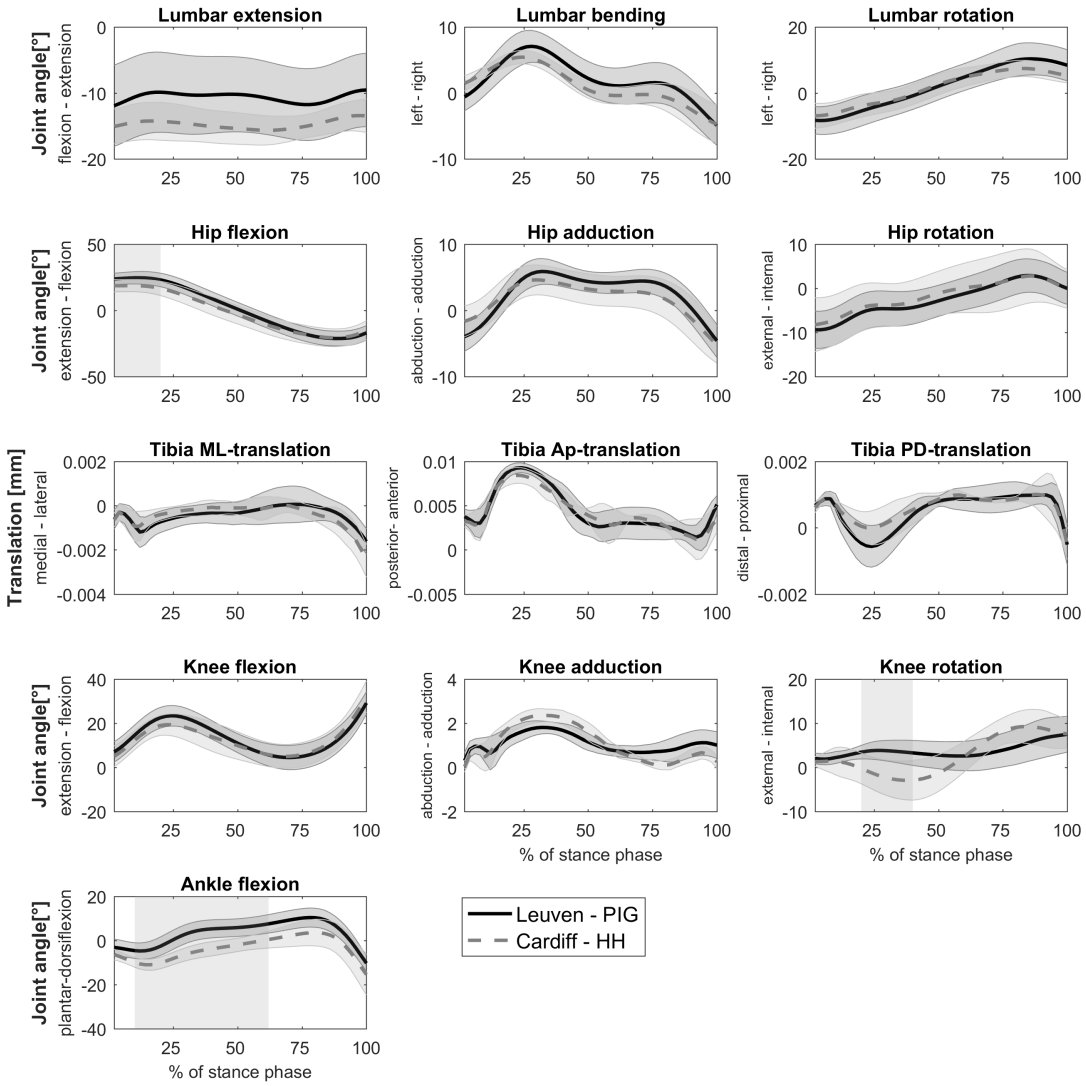

Figure 8.2: Comparison between kinematics assessed in healthy controls at Leuven (black) and at Cardiff (gray dotted line). Gray zone indicates the phases of the stance phase in which a significant difference between Leuven and Cardiff was found using 1D-SPM-analysis[124].

More importantly, these kinematic differences did not result in significant differences in joint contact forces or pressures (figure 8.3). This indicates that in future studies data collected in different clinical centers can be pooled after checking the consistency in healthy control subjects. This can be useful to increase statistical power of the study and therefore also the generalizability of the obtained results. This might be especially relevant in studies that investigate pathologies that are not highly prevalent in the general population or when strict exclusion criteria need to be applied (e.g. the absence of additional degenerative changes in the knee joint and the absence of concomitant injuries).

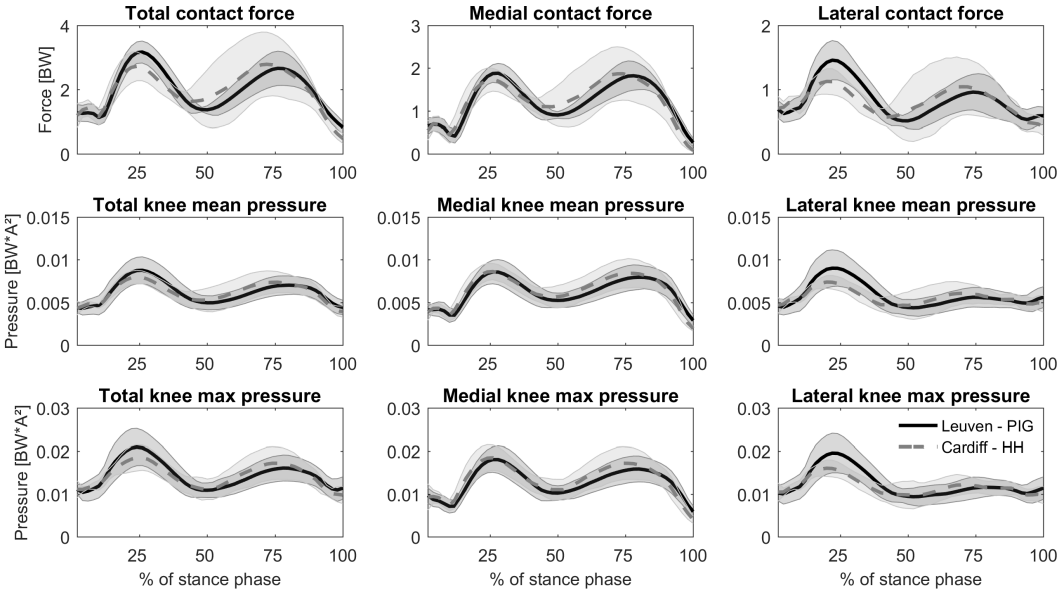

Figure 8.3: Comparison between contact forces and pressures calculated from the motion data assessed in healthy controls at Leuven (black) and at Cardiff (gray dotted line). Gray zone indicates the phases of the stance phase in which a significant difference between Leuven and Cardiff was found using 1D-SPM-analysis[124].

The combined insights from musculoskeletal modelling studies and clinical patient studies have a unique potential to provide further insights in the role of mechanical loading in multifactorial diseases such as OA

Clinical studies investigating patient-adaptations to pain and discomfort following a specific injury or disease (e.g. ACL-rupture and OA) have been useful in the past. Likewise, the effect of a specific surgery can be investigated by comparing measurements in relevant patient cohorts before and after the intervention. However, the effect of one single parameter cannot be investigated in this type of studies as the result of a measurement can be confounded by multiple factors. For instance joint laxity, pain, muscle inhibition and weakness can all interact and affect joint loading. Consequently, a cause-effect relationship cannot be established based on experimental data obtained in patients alone[125]. In contrast, musculoskeletal modelling studies can be used in addition to assess the effect of one single parameter, while other factors can be kept constant[47,125]. Furthermore, they give access to in-vivo muscle and contact forces that cannot be measured non-invasively, but that are useful parameters when investigating the role of mechanical loading to disease etiology and progression or to better understand the treatment responses.

However, it is without any doubt that a more integrative approach, combining both types of studies, would be preferable as both will contribute specific insights and their combination would result in a more comprehensive understanding of movement and pathology.

Limitations

This PhD contributes to a better understanding of the role of knee loading to cartilage tissue adaptation and factors affecting the cartilage load distribution. However, the findings of this PhD should be interpreted with respect to some limitations.

Limitations related to the experimental protocol

First, MR-images were acquired at different time points during the day. Previous studies measuring cartilage thickness and relaxation times immediately before and after a specific exercise (e.g. squatting, running), found an immediate effect of preceding loading on cartilage thickness and relaxation times[126,127]. Additionally it was found that more intense exercises (e.g. running) have a larger effect on cartilage tissue deformation[126]. Furthermore, changes in cartilage thickness but not cartilage volume were observed throughout the day[128]. Consequently, movement history preceding the MRI-acquisition might affect thickness values and relaxation times. Therefore in the current work, all participants had one hour standardized supine rest before the actual acquisition of the MR-images[129,130].

Secondly, the number of subjects in the different studies is limited. Therefore, generalizability to larger populations should be done with caution. Furthermore, the studied population in studies I – IV is limited to healthy control subjects. Therefore, results cannot be generalized to a pathologic population such as OA. Since the OA disease process affects cartilage/bone constitution and physiology, the relation between loading and cartilage adaptations may be substantially different compared to healthy joint conditions.

Thirdly, these studies neglected the state of the meniscus and subchondral bone, although OA is a disease of the whole joint and not only a disease of the cartilage[131]. Therefore, an interplay between different factors including cartilage state and tissue reactivity as well as meniscus and subchondral bone state, can contribute to the onset and progression of OA. Therefore, the effect of meniscus and subchondral bone state on cartilage loading and matrix composition is not included in the current analysis.

Fourthly, this work considered the role of cartilage loading as factor affecting cartilage composition evaluated using MRI, and its consequent role in OA initiation. Although self-reported function was considered in the patient cohort following acute cartilage lesion, pain was not scored. This is of concern as it was previously found that patient's coping response to pain and discomfort is an important determinant of surgery outcome[132]. Therefore, the psychological, environmental or social influences are excluded which might explain part of the variation observed in the biomechanical factors and more general the variable risk of OA initiation following an isolated cartilage lesion

Limitations related to the musculoskeletal model

Direct non-invasive measurement of joint loading in-vivo in healthy adults is currently not possible. Therefore, musculoskeletal modelling is used to provide this information. However, the musculoskeletal modelling workflow that uses a scaled generic musculoskeletal model inherently holds some assumptions that might affect the calculated knee contact forces.

Firstly, this model incorporates generic bone geometries, which is known to affect the calculated contact

forces[133,134]. More importantly, this model uses a generic cartilage geometry with a uniformly distributed cartilage thickness and cartilage properties. However, the assumption of uniform thickness may not be valid as a location dependent variation in thickness was observed in study II and III. Furthermore, cartilage mechanical properties (i.e. elastic modulus) were found to be related to the cartilage relaxation times[84–86]. We observed local variation in relaxation times over the articular cartilage surface, which is in contrast to our assumption that the whole cartilage layer has uniform elastic properties. This assumption might especially affect the results of study V, as the articular cartilage defect was not modelled. Therefore, the estimated contact pressures and forces mainly reflect the effect of the kinematic and kinetic behavior of the subjects.

Secondly, the generic model comprises generic muscle and ligament parameters. However, these parameters might not be representative for pathologic subjects as in patients muscle weakness and joint laxity is often present[44,135–137]. Contact forces are calculated based on the muscle, ligament and joint reaction forces and therefore they might be underestimated when muscle weakness is present, as in this case more muscles should be recruited to balance the external moment. Additionally, subject-specific variation in muscle and ligament moment arms is not included. Especially in the presence of excessive knee laxity, moment arm lengths might be affected which could result in less accurately determined muscle and ligament forces, which will ultimately invalidate the calculated contact forces.

Thirdly, the model lacks a direct implementation of the menisci and this might affect the contact pressure distribution. One of the functions of the menisci is to distribute the contact force over the underlying cartilage. By enlarging the contact area this results in decreased peak pressures compared to a situation without menisci[138]. However, the total knee contact force will not be altered, as this is calculated based on the pressure and the contact area.

Fourthly, muscle activations were estimated using an optimization routine (i.e. concurrent optimization of muscle forces and kinematics), instead of using measured subject-specific muscle activations. In the optimization, the weighted sum of squared muscle activations and contact energy was minimized[139]. However, this optimization criterion may not be as valid in a patient population as in a healthy population. For instance, in patients with knee OA co-contraction of the lower leg muscles was observed, presumably to increase knee stability[70,72,73]. As muscle activations are minimized in the optimization, the estimated muscle forces might not fully capture the effect of muscle co-contraction. Co-contraction would increase the knee contact forces, resulting in an underestimation of the knee contact forces. However, in patients with an articular cartilage defect no alterations in co-contraction were previously described, therefore limiting the potential confounding effect on the results[140]. However, the absence of muscle co-contraction in our cohort of patients with isolated cartilage defects should be further confirmed.

Fifthly, no direct validation of the calculated contact forces with measured contact forces was possible. A complete validation of the model would consist of a kinematic and a dynamic validation. In terms of the kinematic validation, the correctness of the estimated secondary knee kinematics based on the optimization formulation (i.e. concurrent optimization of muscle forces and kinematics) should be verified. Indeed, as in the optimization only the knee flexion angle was prescribed, the kinematics in the secondary degrees of freedom of the knee (i.e. varus/valgus, internal/external rotation and tibial translations) evolved as a function of contact forces, muscle forces and ligament forces. Therefore, the estimated tibiofemoral and patellofemoral kinematics using this model and optimization method were previously found to be consistent with the kinematics measured using dynamic MRI, therefore confirming its kinematic validity[141]. However, it was not

possible to re-evaluate the validity of the secondary knee kinematics during the movements used in the current study using dynamic MRI. In terms of the dynamic validation, this would require a direct comparison between calculated contact forces and contact forces measured with instrumented implants during the different tasks studied in this work. The model used in this PhD was previously used to calculate contact forces with instrumented implant data provided through the *Grand Challenge competition to predict in vivo knee loads*[142]. This dataset is used as benchmark data that enables researchers to validate estimates of knee contact forces with in-vivo measured contact forces. The current model estimated the contact forces based on the *Grand Challenge* dataset, with an average root mean square error below 0.40BW, indicating a good correspondence between the measured and calculated contact forces and therefore confirming its dynamic validity for gait[143]. As, in-vivo contact forces cannot be measured non-invasively, no direct validation of the model for use in the intact knee joint is currently feasible.

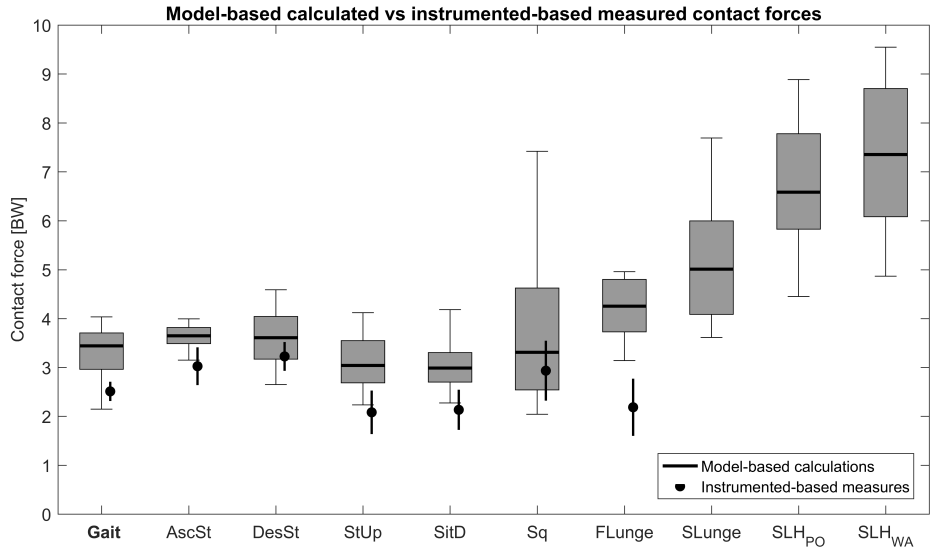

Figure 8.4: Measured contact forces (black dot) vs calculated contact forces (gray area). AscSt: stair ascent, DesSt: stair descent, StUp: stand up, SitD: sit down, Sq: squat, Flunge: Forward lunge, SLunge: Sideward lunge, SLHpo: single leg hop push-off, SLHwa: single leg hop weight-acceptance. Measured contact forces are obtained from different studies using instrumented implants[7,142,144–155].

Comparing calculated contact forces based on our data, a good agreement in contact force for the movements for which instrumented implant data was available can be confirmed (figure 8.4). For all motions, the calculated contact forces were consistently higher compared to the measured contact forces. This can possibly be attributed to the fact that the measured contact forces were assessed in older persons who had a total knee replacement, whereas we calculated the contact force in a young healthy population. Consequently, the movement dynamics are likely to be altered, causing a reduction in total knee contact force. Forward lunge had the largest discrepancy between measured and calculated contact force[144,145]. This can partially be explained by the fact that in the instrumented-based dataset this motion was executed rather static and subjects with a total knee replacement were allowed to rest their hands on a handlebar during the lunge execution, whereas during our measurements lunge was a dynamic movement. Consequently the effect of dynamic muscle activity on the contact forces during a forward lunge was diminished in the instrumented-based dataset[145]. Additionally, step length is likely to be different however, this was not reported in the other studies.

Future work

Investigate the relation between knee loading and cartilage properties in patient populations

The relation between cartilage loading and cartilage thickness and $T1\rho$ and T2 relaxation times was conducted in healthy adults. Aging and obesity were found to decrease the relationship between the knee adduction moment and cartilage thickness[29]. Furthermore, patients with OA were found to have a relative decrease in medial condyle cartilage thickness with a higher knee adduction moment[28,156,157]. This decrease in thickness in osteoarthritic cartilage suggests that the cellular response is not adequate to adapt to the repetitive loads causing further cartilage degeneration[158]. However, the relation between internal cartilage loading and cartilage properties (i.e. thickness and $T1\rho$ and T2 relaxation times) is not yet investigated in OA-patients. Insights in this relationship will further contribute to a better understanding of the role of cartilage loading in degenerative cartilage diseases, as in this population multiple factors are possibly affecting joint loading (e.g. altered kinematics, malalignment, joint laxity) and multiple factors will affect cartilage constitution and pathophysiology therefore altering the relation between cartilage loading and cartilage load bearing capacity.

Increase subject-specific detail in the knee model

The magnitude and profile of the calculated contact-forces are still different compared to the ones measured using instrumented implants[7,142,159,160]. Altered movement dynamics can partially explain the discrepancy between measured and calculated contact forces. However, for the calculation of contact forces in an intact knee joint one could assume that increasing subject-specific detail in the musculoskeletal model might further increase the accuracy of the calculated muscle and contact forces. Subject-specific detail can be increased at different levels:

Inclusion of subject-specific knee geometries was previously found to increase the accuracy of calculated knee contact forces[133]. Furthermore, the inclusion of subject-specific knee alignment was found to be a crucial factor to obtain an accurate medial-lateral load distribution[143]. Similarly, including subject-specific bone geometries and muscle attachment points was previously observed to increase the accuracy of the hip contact force calculation[134]. However to do this, subject-specific musculoskeletal models need to be created based on medical imaging data (i.e. MRI, CT), imposing a substantial financial burden.

Incorporation of a subject-specific contact model in the knee would allow to account for individual cartilage geometry and thickness when calculating the contact forces and the pressure distribution. Furthermore, this way the direct effect of an articular cartilage defect could be investigated and provide additional insights in the progression from defect to OA.

Adapting the mechanical properties of the cartilage layer in the contact model based on the estimates of cartilage matrix composition would allow to account for degenerative changes in the cartilage and individual differences in matrix composition. Previously $T1\rho$ and T2 relaxation times were found to be related to the biomechanical properties of the cartilage (i.e. Young's modulus, aggregate modulus and dynamic modulus), therefore it should be possible to locally adapt the elastic modulus and Poisson's Ratio of the cartilage[84–86].

Inclusion of subject-specific muscle and ligament-properties would allow to account for the effect of ligament laxity and muscle weakness on the calculated contact pressure distribution and knee kinematics. For this, additional tests (e.g. strength measurements and laxity test) are needed, as well as optimization algorithms to estimate the muscle and ligament parameters, as these cannot be directly measured non-invasively.

Investigate the effect of patellofemoral lesion on the movement and joint loading pattern

In the current project, only patients with an isolated tibiofemoral cartilage defect were included. Patellofemoral cartilage defects are after medial femur condyle defects the second most common and in the current analysis they are overlooked[161,162]. This is of concern as OA in the patellofemoral joint was found to be a precursor of tibiofemoral OA[163]. To increase the understanding of patellofemoral loading in presence of a patellofemoral cartilage lesion, inclusion of these patients is required. This is especially relevant as the patellofemoral compartment was found to be exposed to high shear forces and consequently patellofemoral cartilage degeneration might be initiated earlier. Furthermore, the effect of patellofemoral cartilage defects on the loading of the tibiofemoral compartment is currently not documented, as a patellofemoral cartilage defect might affect the knee flexion angle, to avoid force from the quadriceps muscle and patella tendon compressing the patella on the femur during walking, this will consequently affect the contact location in the tibiofemoral joint.

Inclusion of additional rehabilitation exercises

To increase the understanding of loading imposed during rehabilitation exercises, the current analysis could be extended to more exercises or variations used in rehabilitation. Currently, only closed kinetic chain exercises were included in this project, but open kinetic chain exercises should be included as well. Currently, open kinetic chain exercises are less favored in rehabilitation as they are hypothesized to impose more shear loading on the knee, however cartilage loading during these exercises is not yet evaluated[164,165]. Furthermore, joint loading during other techniques and exercise modalities (e.g. gait modification strategies, partial weight-bearing, bracing, alterG treadmill walking, pivoting) should be evaluated to gain additional insight in their role in altered compartmental or joint loading. Therefore, rehabilitation specialists would benefit from additional analysis of loading, including shear and compressive forces, during a wide variety of exercises currently used in activities of daily living as in rehabilitation.

Additionally, it is known that a physiotherapist can guide specific motion during rehabilitation exercises. To do so, the trunk, knee or foot position can be adapted by the physiotherapist, consequently the alignment of the knee joint center with respect to the ground reaction force vector is changed which will affect the external joint moments and consequently the knee joint loading[104–106]. Therefore, magnitude and location of joint loading during different execution modalities should be evaluated as well.

Furthermore, the effect of aberrant loading on other joints and the potential effect of rehabilitation there on should be investigated, as comorbidity is often found in other joints of OA patients on the long-term. Indeed, 72% of the persons treated with total knee replacement for knee OA were found to develop OA in the contralateral hip[166], indicating that altered joint loading in the other joints of the lower-limbs can cause degenerative changes in the cartilage remotely from the primary involved joint.

References

1. Assche D Van, Caspel D Van, Staes F, Saris DB, Bellemans J, Vanlauwe J, et al. Implementing one standardized rehabilitation protocol following autologous chondrocyte implantation or microfracture in the knee results in comparable physical therapy management. Physiother Theory Pract. 2011;27: 125–36.
2. Edwards PK, Ackland T, Ebert JR. Clinical Rehabilitation Guidelines for Matrix-induced Autologous Chondrocyte Implantation (MACI) on the Tibiofemoral Joint. J Orthop Sports Phys Ther. 2013;44: 102–119.
3. Hambly K, Bobic V, Wondrasch B, Van Assche D, Marlovits S. Autologous chondrocyte implantation postoperative care and rehabilitation: science and practice. Am J Sports Med. 2006;34: 1020–38.
4. Mithoefer K, Hambly K, Logerstedt D, Ricci M, Silvers H, Della Villa S. Current concepts for rehabilitation and return to sport after knee articular cartilage repair in the athlete. J Orthop Sports Phys Ther. 2012;42: 254–73.
5. Begalle RL, Distefano LJ, Blackburn T, Padua D a. Quadriceps and hamstrings coactivation during common therapeutic exercises. J Athl Train. 2012;47: 396–405.
6. Hirschmüller A, Baur H, Braun S, Kreuz PC, Südkamp NP, Niemeyer P. Rehabilitation after autologous chondrocyte implantation for isolated cartilage defects of the knee. Am J Sports Med. 2011;39: 2686–96.
7. D'Lima DD, Steklov N, Patil S, Colwell CW. The Mark Coventry award: In vivo knee forces during recreation and exercise after knee arthroplasty. Clin Orthop Relat Res. 2008;466: 2605–2611.
8. Schipplein OD, Andriacchi TP. Interaction between active and passive knee stabilizers during level walking. J Orthop Res. 1991;9: 113–119.
9. Kutzner I, Heinlein B, Dymke J, Bender A, Halder AM, Bergmann G. The effect of valgus braces on medial compartment load of the knee joint - in vivo load measurements in three subjects. J Biomech. 2011;44: 1354–1360.
10. Andriacchi TP, Favre J. The Nature of In Vivo Mechanical Signals That Influence Cartilage Health and Progression to Knee Osteoarthritis. Curr Rheumatol Rep. 2014;16: 463–470.
11. Koo S, Andriacchi TP. A comparison of the influence of global functional loads vs. local contact anatomy on articular cartilage thickness at the knee. J Biomech. 2007;40: 2961–2966.
12. Chen C, Tambe DT, Deng L, Yang L. Biomechanical properties and mechanobiology of the articular chondrocyte. Am J Physiol Cell Physiol. 2013;305: C1202-8.
13. Rogers BA, Murphy CL, Cannon SR, Briggs TWR. Topographical variation in glycosaminoglycan content in human articular cartilage. J Bone Jt Surg [Br]. 2006;88: 1670–4.
14. Mayerhoefer ME, Welsch GH, Mamisch TC, Kainberger F, Weber M, Nemec S, et al. The in vivo effects of unloading and compression on T1-Gd (dGEMRIC) relaxation times in healthy articular knee cartilage at 3.0 Tesla. Eur Radiol. 2010;20: 443–449.
15. Bevill SL, Briant PL, Levenston ME, Andriacchi TP. Central and peripheral region tibial plateau chondrocytes respond differently to in vitro dynamic compression. Osteoarthr Cartil. Elsevier Ltd; 2009;17: 980–987.
16. Little CB, Ghosh P. Variation in proteoglycan metabolism by articular chondrocytes in different joint regions is determined by post-natal mechanical loading. Osteoarthr Cartil. 1997;5: 49–62.
17. Ackermann B, Steinmeyer J. Collagen biosynthesis of mechanically loaded articular cartilage explants. Osteoarthr Cartil. 2005;13: 906–914.
18. Bleuel J, Zaucke F, Brüggemann G-P, Niehoff A. Effects of Cyclic Tensile Strain on Chondrocyte Metabolism: A Systematic Review. PLoS One. 2015;10: e0119816.
19. Thibault M, Poole AR, Buschmann MD. Cyclic compression of cartilagdbone explants in vitro leads to physical weakening , mechanical breakdown of collagen and release of matrix fragments. J Orthop Res. 2002;20: 1265–1273.
20. Chen C, Bhargava M, Lin PM, Torzilli PA. Time , stress , and location dependent chondrocyte death and collagen damage in cyclically loaded articular cartilage. 2003;21: 888–898.
21. Chen C, Lust NBG, Bank RA, Iekoppele JM. Compositional and Metabolic Changes in Damaged Cartilage are Peak-Stress, Stress-Rate, and Loading-Duration Dependent. J Orthop Res. 1999;17: 870–879.
22. Quinn TM, Maung AA, Grodzinsky AJ. Physical and Biological Regulation of Proteoglycan Turnover around Chondrocytes in Cartilage Explants: Implications for Tissue Degradation and Repair. Ann New York Acad Sci. 1999;878: 420–441.

23. Steinmeyer J, Knue S, Raiss RX, Pelzer I. Effects of intermittently applied cyclic loading on proteoglycan metabolism and swelling behaviour of articular cartilage explants. Osteoarthr Cartil. 1999;7: 155–164.

24. Wolf A, Raiss RX, Steinmeyer J. Fibronectin metabolism of cartilage explants in response to the frequency of intermittent loading. 2003;21: 1081–1089.

25. Sauerland K, Raiss RX, Steinmeyer J. Proteoglycan metabolism and viability of articular cartilage explants as modulated by the frequency of intermittent loading. Osteoarthr Cartil. 2003;11: 343–350.

26. Eckstein F, Hudelmaier M, Wirth W, Kiefer B, Jackson R, Yu J, et al. Double echo steady state magnetic resonance imaging of knee articular cartilage at 3 Tesla: a pilot study for the Osteoarthritis Initiative. Ann Rheum Dis. 2006;65: 433–441.

27. Erhart-Hledik JC, Favre J, Andriacchi TP. New insight in the relationship between regional patterns of knee cartilage thickness, osteoarthritis disease severity, and gait mechanics. J Biomech. Elsevier; 2015;48: 3868–3875.

28. Andriacchi TP, Mündermann A, Smith RL, Alexander EJ, Dyrby CO, Koo S. A framework for the in vivo pathomechanics of osteoarthritis at the knee. Ann Biomed Eng. 2004;32: 447–457.

29. Blazek K, Favre J, Asay J, Erhart-Hledik J, Andriacchi T. Age and obesity alter the relationship between femoral articular cartilage thickness and ambulatory loads in individuals without osteoarthritis. J Orthop Res. 2014;32: 394–402.

30. Koo S, Rylander JH, Andriacchi TP. Knee joint kinematics during walking influences the spatial cartilage thickness distribution in the knee. J Biomech. Elsevier; 2011;44: 1405–1409.

31. Nozaki T, Kaneko Y, Yu HJ, Kaneshiro K, Schwarzkopf R, Hara T, et al. T1rho mapping of entire femoral cartilage using depth- and angle-dependent analysis. Eur Radiol. European Radiology; 2016;26: 1952–1962.

32. Kaneko Y, Nozaki T, Yu H, Chang A, Kaneshiro K, Schwarzkopf R, et al. Normal T2 map profile of the entire femoral cartilage using an angle/layer-dependent approach. J Magn Reson Imaging. 2015;42: 1507–1516.

33. Surowiec RK, Lucas EP, Fitzcharles EK, Petre BM, Dornan GJ, Giphart JE, et al. T2 values of articular cartilage in clinically relevant subregions of the asymptomatic knee. Knee Surgery, Sport Traumatol Arthrosc. 2014;22: 1404–1414.

34. Scanlan SF, Favre J, Andriacchi TP. The relationship between peak knee extension at heel-strike of walking and the location of thickest femoral cartilage in ACL reconstructed and healthy contralateral knees. J Biomech. Elsevier; 2013;46: 849–854.

35. Li G, Park SE, DeFrate LE, Schutzer ME, Ji L, Gill TJ, et al. The cartilage thickness distribution in the tibiofemoral joint and its correlation with cartilage-to-cartilage contact. Clin Biomech. 2005;20: 736–744.

36. Palazzo C, Nguyen C, Lefevre-Colau MM, Rannou F, Poiraudeau S. Risk factors and burden of osteoarthritis. Ann Phys Rehabil Med. 2016;59: 134–138.

37. Andriacchi TP, Favre J, Erhart-Hledik JC, Chu CR. A Systems View of Risk Factors for Knee Osteoarthritis Reveals Insights into the Pathogenesis of the Disease. Ann Biomed Eng. 2015;43: 376–387.

38. Brouwer GM, Van Tol AW, Bergink AP, Belo JN, Bernsen RMD, Reijman M, et al. Association between valgus and varus alignment and the development and progression of radiographic osteoarthritis of the knee. Arthritis Rheum. 2007;56: 1204–1211.

39. Johnson VL, Hunter DJ. The epidemiology of osteoarthritis. Best Pract Res Clin Rheumatol. Elsevier Ltd; 2014;28: 5–15.

40. Allen KD, Golightly YM. Epidemiology of osteoarthritis: state of the evidence. Rheumatol, Curr Opin. 2015;27: 276–283.

41. Baker-LePain JC, Lane NE. Role of bone architecture and anatomy in osteoarthritis. Bone. Elsevier Inc.; 2012;51: 197–203.

42. Hunter D, Nevitt M, Lynch J, Kraus VB, Katz JN, Collins JE, et al. Longitudinal validation of periarticular bone area and 3D shape as biomarkers for knee OA progression? Data from the FNIH OA Biomarkers Consortium. Ann Rheum Dis. 2015; annrheumdis-2015-207602.

43. Felson D, Lawrence R, Dieppe P, Hirsch R, Helmick C, Jordan J, et al. Osteoarthritis: New Insights. Part 1: The Disease and Its Risk Factors. Ann Intern Med. 2000;133: 637–639.

44. Lewek MD, Rudolph KS, Snyder-Mackler L. Control of frontal plane knee laxity during gait in patients with medial compartment knee osteoarthritis. Osteoarthr Cartil. 2004;12: 745–751.

45. Lewek MD, Ramsey DK, Snyder-mackler L, Rudolph KS. Knee Stabilization in Patients With Medial Compartment Knee Osteoarthritis. Arthritis Rheum. 2005;52: 2845–2853.

46. Sharma L, Lou C, Felson DT, Dunlop DD, Kirwan-Mellis G, Hayes KW, et al. Laxity in healthy and osteoarthritic knees. Arthritis Rheum. 1999;42: 861–870.

47. Thompson JA, Hast MW, Granger JF, Piazza SJ, Siston RA. Biomechanical effects of total knee arthroplasty component malrotation: A computational simulation. J Orthop Res. 2011;29: 969–975.

48. Bellemans J, Colyn W, Vandenneucker H, Victor J. The chitranjan ranawat award: Is Neutral Mechanical Alignment Normal for All Patients? Clin Orthop Relat Res. 2012;470: 45–53.

49. Bytyqi D, Shabani B, Lustig S, Cheze L, Gjurgjeala NK, Neyret P. Gait knee kinematic alterations in medial osteoarthritis: three dimensional assessment. Int Orthop. 2014;38: 1191–1198.

50. Ebert JR, Lloyd DG, Ackland T, Wood DJ. Knee biomechanics during walking gait following matrix-induced autologous chondrocyte implantation. Clin Biomech (Bristol, Avon). Elsevier Ltd; 2010;25: 1011–7.

51. Ebert JR, Robertson WB, Lloyd DG, Zheng MH, Wood DJ, Ackland T. Traditional vs accelerated approaches to post-operative rehabilitation following matrix-induced autologous chondrocyte implantation (MACI): comparison of clinical, biomechanical and radiographic outcomes. Osteoarthritis Cartilage. 2008;16: 1131–40.

52. Thoma LM, McNally MP, Chaudhari AM, Best TM, Flanigan DC, Siston RA, et al. Differential knee joint loading patterns during gait for individuals with tibiofemoral and patellofemoral articular cartilage defects in the knee. Osteoarthr Cartil. Elsevier Ltd; 2017; 1–9.

53. Raimondi MT, Pietrabissa R. Contact pressures at grafted cartilage lesions in the knee. Knee Surgery, Sport Traumatol Arthrosc. 2005;13: 444–450.

54. Kock NB, Smolders JMH, Van Susante JLC, Buma P, Van Kampen A, Verdonschot N. A cadaveric analysis of contact stress restoration after osteochondral transplantation of a cylindrical cartilage defect. Knee Surgery, Sport Traumatol Arthrosc. 2008;16: 461–468.

55. Davies-Tuck ML, Wluka AE, Wang Y, Teichtahl AJ, Jones G, Ding C, et al. The natural history of cartilage defects in people with knee osteoarthritis. Osteoarthr Cartil. 2008;16: 337–342.

56. Spahn G, Hofmann G. Focal cartilage defects within the medial knee compartment. predictors for osteoarthritis progression. Z Orthop Unfall. 2014;152: 480–488.

57. Wang Y, Ding C, Wluka AE, Davis S, Ebeling PR, Jones G, et al. Factors affecting progression of knee cartilage defects in normal subjects over 2 years. Rheumatology. 2006;45: 79–84.

58. Lefkoe TP, Trafton PG, Ehrlich MG, Walsh WR, Dennehy DT, Barrach HJ, et al. An experimental model of femoral condylar defect leading to osteoarthrosis. J Orthop Trauma. 1993;7: 458–67.

59. Sutter EG, Widmyer MR, Utturkar GM, Spritzer CE, Garrett WE, DeFrate LE. In Vivo Measurement of Localized Tibiofemoral Cartilage Strains in Response to Dynamic Activity. Am J Sports Med. 2015;43: 370–376.

60. Meireles S, Wesseling M, Smith CR, Thelen DG, Verschueren S, Jonkers I. Medial knee loading is increased in subjects with early OA compared to healthy controls during gait but not step-up-and-over task. Plos One (Under Rev.)

61. Van De Velde SK, Bingham JT, Hosseini A, Kozanek M, DeFrate LE, Gill TJ, et al. Increased tibiofemoral cartilage contact deformation in patients with anterior cruciate ligament deficiency. Arthritis Rheum. 2009;60: 3693–3702.

62. Schulze-Tanzil G. Activation and dedifferentiation of chondrocytes: Implications in cartilage injury and repair. Ann Anat. Elsevier; 2009;191: 325–338.

63. Chang a H, Moisio KC, Chmiel JS, Eckstein F, Guermazi A, Prasad P V, et al. External knee adduction and flexion moments during gait and medial tibiofemoral disease progression in knee osteoarthritis. Osteoarthritis Cartilage. Elsevier Ltd; 2015;23: 1099–1106.

64. Baliunas AJ, Hurwitz DE, Ryals AB, Karrar A, Case JP, Block JA, et al. Increased knee joint loads during walking are present in subjects with knee osteoarthritis. Osteoarthr Cartil. 2002;10: 573–579.

65. Zhao D, Banks SA, Mitchell KH, D'Lima DD, Colwell CW, Fregly BJ. Correlation between knee adduction torque and medial contact force for a variety of gait patterns. J Orthop Res. 2007; 789–797.

66. Meireles S, De Groote F, Reeves ND, Verschueren S, Maganaris C, Luyten F, et al. Knee contact forces are not altered in early knee osteoarthritis. Gait Posture. Elsevier B.V.; 2016;45: 115–120.

67. Adouni M, Shirazi-Adl A. Partitioning of Knee Joint Internal Forces in Gait Is Dictated By the Knee Adduction Angle and Not By the Knee Adduction Moment. J Biomech. Elsevier; 2014;47: 1696–703.

68. Walter JP, D'Lima DD, Colwell CW, Fregly BJ. Decreased knee adduction moment does not guarantee decreased medial contact force during gait. J Orthop Res. 2010;28: 1348–1354.

69. Meyer AJ, D'Lima DD, Besier TF, Lloyd DG, Colwell CW, Fregly BJ. Are external knee load and EMG measures accurate indicators of internal knee contact forces during gait? J Orthop Res. 2013;31: 921–929.

70. Heiden TL, Lloyd DG, Ackland TR. Knee joint kinematics, kinetics and muscle co-contraction in knee osteoarthritis patient gait. Clin Biomech (Bristol, Avon). Elsevier Ltd; 2009;24: 833–41.

71. Coats-Thomas MS, Miranda DL, Badger GJ, Fleming BC. Effects of ACL reconstruction surgery on muscle activity of the lower limb during a jump-cut maneuver in males and females. J Orthop Res. 2013;31: 1890–6.

72. Hubley-Kozey CL, Hill NA, Rutherford DJ, Dunbar MJ, Stanish WD. Co-activation differences in lower limb muscles between asymptomatic controls and those with varying degrees of knee osteoarthritis during walking. Clin Biomech. Elsevier Ltd; 2009;24: 407–414.

73. Hubley-Kozey C, Deluzio K, Dunbar M. Muscle co-activation patterns during walking in those with severe knee osteoarthritis. Clin Biomech. 2008;23: 71–80.

74. Sturnieks DL, Besier TF, Lloyd DG. Muscle activations to stabilize the knee following arthroscopic partial meniscectomy. Clin Biomech. Elsevier Ltd; 2011;26: 292–297.

75. Luyten FP, Denti M, Filardo G, Kon E, Engebretsen L. Definition and classification of early osteoarthritis of the knee. Knee Surgery, Sport Traumatol Arthrosc. 2012;20: 401–406.

76. Fregly BJ, D'Lima DD, Colwell CW. Effective gait patterns for offloading the medial compartment of the knee. J Orthop Res. 2009;27: 1016–1021.

77. Fregly BJ, Reinbolt J a, Rooney KL, Mitchell KH, Chmielewski TL. Design of patient-specific gait modifications for knee osteoarthritis rehabilitation. IEEE Trans Biomed Eng. 2007;54: 1687–95.

78. Gerbrands TA, Pisters MF, Vanwanseele B. Individual selection of gait retraining strategies is essential to optimally reduce medial knee load during gait. Clin Biomech. Elsevier Ltd; 2014;29: 828–834.

79. Haugh MG, Ph D, Meyer EG, Ph D, Thorpe SD. Temporal and Spatial Changes in Cartilage-Matrix-Specific Gene Expression in Mesenchymal Stem Cells in Response to Dynamic Compression. TISSUE Eng Part A. 2011;17: 23–25.

80. Bian L, Zhai DY, Zhang EC, Mauck RL, Burdick JA. Matrix Synthesis and Distribution and Suppresses. TISSUE Eng Part A. 2012;18.

81. Stenhamre H, Slynarski K, Petrén C, Tallheden T, Lindahl A. Topographic variation in redifferentiation capacity of chondrocytes in the adult human knee joint. Osteoarthr Cartil. 2008;16: 1356–1362.

82. Shepherd DE, Seedhom BB. Thickness of human articular cartilage in joints of the lower limb. Ann Rheum Dis. 1999;58: 27–34.

83. Wu P, Delassus E, Patra D, Liao W, Sandell LJ. Effects of Serum and Compressive Loading on the Cartilage Matrix Synthesis and Spatiotemporal Deposition Around Chondrocytes in 3D Culture. TISSUE Eng Part A. 2013;19: 13–15.

84. Hatcher CC, Collins AT, Kim SY, Michel LC, Mostertz WC, Ziemian SN, et al. Relationship between T1rho magnetic resonance imaging, synovial fluid biomarkers, and the biochemical and biomechanical properties of cartilage. J Biomech. Elsevier Ltd; 2017;55: 18–26.

85. Nissi MJ, Rieppo J, Töyräs J, Laasanen MS, Kiviranta I, Nieminen MT, et al. Estimation of mechanical properties of articular cartilage with MRI - dGEMRIC, T2 and T1 imaging in different species with variable stages of maturation. Osteoarthr Cartil. 2007;15: 1141–1148.

86. Lammentausta E, Kiviranta P, Nissi MJ, Laasanen MS, Kirivanta I, Nieminen MT, et al. T2 relaxation time and delayed gadolinium-enhanced MRI of cartilage (dGEMRIC) of human patellar cartilage at 1.5 T and 9.4 T: Relationships with tissue mechanical properties. J Orthop Res. 2006;24: 366–74.

87. Nuki G. Osteoarthritis: a problem of joint failure. Z Rheumatol. 1999;58(3): 142–7.

88. Peach CA, Carr AJ, Loughlin J. Recent advances in the genetic investigation of osteoarthritis. Trends Mol Med. 2005;11: 186–

89. Warner S, Valdes A. The Genetics of Osteoarthritis: A Review. J Funct Morphol Kinesiol. 2016;1: 140–153.

90. Tetsworth K, Paley D. Malalignment and degenerative arthropathy. Orthop Clin North Am. 1994;25: 367–377.

91. Andriacchi TP, Mündermann A. The role of ambulatory mechanics in the initiation and progression of knee osteoarthritis. Curr Opin Rheumatol. 2006;18: 514–518.

92. Neogi T, Bowes MA, Niu J, De Souza KM, Vincent GR, Goggins J, et al. Magnetic resonance imaging-based three-dimensional bone shape of the knee predicts onset of knee osteoarthritis: Data from the osteoarthritis initiative. Arthritis Rheum. 2013;65: 2048–2058.

93. Williams TG, Vincent G, Bowes M, Cootes T, Balamoody S, Hutchinson C, et al. Automatic segmentation of bones and inter-image anatomical correspondence by volumetric statistical modelling of knee MRI. 2010 7th IEEE Int Symp Biomed Imaging From Nano to Macro, ISBI 2010 - Proc. 2010; 432–435.

94. Moisio K, Chang A, Eckstein F, Chmiel JS, Wirth W, Almagor O, et al. Varus-valgus alignment reduced risk of subsequent cartilage loss in the less loaded compartment. Arthritis Rheum. 2011;63: 1002–1009.

95. Hayashi D, Englund M, Roemer FW, Niu J, Sharma L, Felson DT, et al. Knee malalignment is associated with an increased risk for incident and enlarging bone marrow lesions in the more loaded compartments: The MOST study. Osteoarthr Cartil. Elsevier Ltd; 2012;20: 1227–1233.

96. Moyer R, Wirth W, Duryea J, Eckstein F. Anatomical alignment, but not goniometry, predicts femorotibial cartilage loss as well as mechanical alignment: Data from the Osteoarthritis Initiative. Osteoarthr Cartil. Elsevier Ltd; 2016;24: 254–261.

97. Turcot K, Armand S, Lübbeke A, Fritschy D, Hoffmeyer P, Suvà D. Does knee alignment influence gait in patients with severe knee osteoarthritis? Clin Biomech. Elsevier Ltd; 2013;28: 34–39.

98. Weidenhielm L, Svensson OK, Broström LÅ, Rudberg U. Change in adduction moment about the knee after high tibial osteotomy and prosthetic replacement in osteoarthrosis of the knee. Clin Biomech. 1992;7: 91–96.

99. Hurwitz DE, Ryals AB, Case JP, Block JA, Andriacchi TP. The knee adduction moment during gait in subjects with knee osteoarthritis is more closely correlated with static alignment than radiographic disease severity, toe out angle and pain. J Orthop Res. 2002;20: 101–107.

100. Georgoulis AD, Papadonikolakis A, Papageorgiou CD, Mitsou A, Stergiou N. Three-dimensional tibiofemoral kinematics of the anterior cruciate ligament-deficient and reconstructed knee during walking. Am J Sports Med. 2003;31: 75–9.

101. Kumar D, Kothari A, Souza RB, Wu S, Benjamin Ma C, Li X. Frontal plane knee mechanics and medial cartilage MR relaxation times in individuals with ACL reconstruction: A pilot study. Knee. Elsevier B.V.; 2014;21: 881–885.

102. Levinger P, Menz HB, Morrow AD, Feller J a, Bartlett JR, Bergman NR. Lower limb biomechanics in individuals with knee osteoarthritis before and after total knee arthroplasty surgery. J Arthroplasty. 2013;28: 994–999.

103. Teng H-L, Powers CM. Sagittal Plane Trunk Posture Influences Patellofemoral Joint Stress During Running. J Orthop Sport Phys Ther. 2014;44: 785–792.

104. Farrokhi S, Pollard CD, Souza RB, Chen Y-J, Reischl S, Powers CM. Trunk position influences the kinematics, kinetics, and muscle activity of the lead lower extremity during the forward lunge exercise. J Orthop Sports Phys Ther. 2008;38: 403–9.

105. Escamilla RF, Macleod TD, Wilk KE, Paulos L, Andrews JR. ACL strain and tensile forces for weight bearing and non—weight-bearing exercises after ACL reconstruction: A guide to exercise selection. J Orthop Sport Phys Ther. 2012;42: 208–220.

106. Callaghan MJ, Parkes MJ, Hutchinson CE, Felson DT. Factors associated with arthrogenous muscle inhibition in patellofemoral osteoarthritis. Osteoarthr Cartil. Elsevier Ltd; 2014;22: 742–746.

107. Hassan BS, Doherty SA, Mockett S, Doherty M. Effect of pain reduction on postural sway, proprioception, and quadriceps strength in subjects with knee osteoarthritis. Ann Rheum Dis. 2002;61: 422–428.

108. Rice DA, Mcnair PJ. Quadriceps Arthrogenic Muscle Inhibition: Neural Mechanisms and Treatment Perspectives. Semin Arthritis Rheum. Elsevier Inc.; 2010;40: 250–266.

109. Hopkins j T, Ingersoll CD. Arthrogenic Muscle inhibition: A Limiting Factor in Joint Rehabilitation. J Sport Rehabil. 2000;9: 135–159.

110. Palmieri RM, Weltman A, Edwards JE, Tom JA, Saliba EN, Mistry DJ, et al. Pre-synaptic modulation of quadriceps arthrogenic muscle inhibition. Knee Surgery, Sport Traumatol Arthrosc. 2005;13: 370–376.

111. Moyer RF, Birmingham TB, Bryant DM, Giffin JR, Marriott KA, Leitch KM. Biomechanical effects of valgus knee bracing: A systematic review and meta-analysis. Osteoarthr Cartil. 2015;23: 178–188.

112. Leutloff D, Tobian F, Perka C. High tibial osteotomy for valgus and varus deformities of the knee. Int Orthop. 2001;25: 93–96.

113. Lee DC, Byun SJ. High tibial osteotomy. Knee Surg Relat Res. 2012;24: 61–69.

114. Heller MO, Taylor WR, Perka C, Duda GN. The influence of alignment on the musculo-skeletal loading conditions at the knee. Langenbeck's Arch Surg. 2003;388: 291–297.

115. Amis AA. Biomechanics of high tibial osteotomy. Knee Surgery, Sport Traumatol Arthrosc. 2013;21: 197–205.

116. Alford JW, Cole BJ. Cartilage Restoration, Part 1: Basic Science, Historical Perspective, Patient Evaluation, and Treatment Options. Am J Sports Med. 2005;33: 295–306.

117. Alford JW. Cartilage Restoration, Part 2: Techniques, Outcomes, and Future Directions. Am J Sports Med. 2005;33: 443–460.

118. Hernigou P, Medevielle D, Debeyre J, Goutallier D. Proximal tibial osteotomy for osteoarthritis with varus deformity. A ten to thirteen-year follow-up study. J Bone Joint Surg Am. 1987;69: 332–54.

119. Ferrari A, Benedetti MG, Pavan E, Frigo C, Bettinelli D, Rabuffetti M, et al. Quantitative comparison of five current protocols in gait analysis. Gait Posture. 2008;28: 207–16.

120. Kainz H, Modenese L, Lloyd DG, Maine S, Walsh HPJ, Carty CP. Joint kinematic calculation based on clinical direct kinematic versus inverse kinematic gait models. J Biomech. Elsevier; 2016;49: 1658–1669.

121. Davis RB, Ounpuu S, Tyburski D, Gage JR. A gait analysis data collection and reduction technique. Hum Mov Sci. 1991;10: 575–587.

122. Kadaba MP, Ramakrishnan HK, Wootten ME. Measurement of lower extremity kinematics during level walking. J Orthop Res. 1990;8: 383–92.

123. Pataky TC. Generalized n -dimensional biomechanical field analysis using statistical parametric mapping. J Biomech. Elsevier; 2010;43: 1976–1982.

124. Delp SL, Anderson FC, Arnold AS, Loan P, Habib A, John CT, et al. OpenSim: open-source software to create and analyze dynamic simulations of movement. IEEE Trans Biomed Eng. 2007;54: 1940–50.

125. Eckstein F, Lemberger B, Gratzke C, Hudelmaier M, Glaser C, Englmeier K-H, et al. In vivo cartilage deformation after different types of activity and its dependence on physical training status. Ann Rheum Dis. 2005;64: 291–5.

126. Mosher TJ, Liu Y, Torok CM. Functional cartilage MRI T2 mapping: evaluating the effect of age and training on knee cartilage response to running. Osteoarthr Cartil. Elsevier Ltd; 2010;18: 358–364.

127. Waterton JC, Solloway S, Foster JE, Keen MC, Gandy S, Middleton BJ, et al. Diurnal variation in the femoral articular cartilage of the knee in young adult humans. Magn Reson Med. 2000;43: 126–132.

128. Eshed I, Trattnig S, Sharon M, Arbel R, Nierenberg G, Konen E, et al. Assessment of cartilage repair after chondrocyte transplantation with a fibrin-hyaluronan matrix–correlation of morphological MRI, biochemical T2 mapping and clinical outcome. Eur J Radiol. Elsevier Ireland Ltd; 2012;81: 1216–23.

129. Van Ginckel A, Verdonk P, Victor J, Witvrouw E. Cartilage status in relation to return to sports after anterior cruciate ligament reconstruction. Am J Sport Med. 2013;41: 550–559.

130. Roos EM, Arden NK. Strategies for the prevention of knee osteoarthritis. Nat Rev Rheumatol. Nature Publishing Group; 2016;12: 92–101.

131. Baert IAC, Lluch E, Mulder T, Nijs J, Noten S, Meeus M. Does pre-surgical central modulation of pain influence outcome after total knee replacement? A systematic review. Osteoarthr Cartil. Elsevier Ltd; 2016;24: 213–223.

132. Gerus P, Sartori M, Besier TF, Fregly BJ, Delp SL, Banks S a, et al. Subject-specific knee joint geometry improves predictions of medial tibiofemoral contact forces. J Biomech. Elsevier; 2013;46: 2778–86.

133. Wesseling M, De Groote F, Bosmans L, Bartels W, Meyer C, Desloovere K, et al. Subject-specific geometrical detail rather than cost function formulation affects hip loading calculation. Comput Methods Biomech Biomed Engin. Taylor & Francis; 2016;19: 1475–1488.

134. Van Assche D, Van Caspel D, Vanlauwe J, Bellemans J, Saris DB, Luyten FP, et al. Physical activity levels after characterized chondrocyte implantation versus microfracture in the knee and the relationship to objective functional outcome with 2-year follow-up. Am J Sports Med. 2009;37 Suppl 1: 42S–49S.

135. Løken S, Ludvigsen TC, Høysveen T, Holm I, Engebretsen L, Reinholt FP. Autologous chondrocyte implantation to repair knee cartilage injury: ultrastructural evaluation at 2 years and long-term follow-up including muscle strength measurements. Knee Surg Sports Traumatol Arthrosc. 2009;17: 1278–88.

136. Ebert JR, Lloyd DG, Wood DJ, Ackland TR. Isokinetic knee extensor strength deficit following matrix-induced autologous chondrocyte implantation. Clin Biomech (Bristol, Avon). 2012;27: 588–94.

137. Wang H, Chen T, Gee AO, Hutchinson ID, Stoner K, Warren RF, et al. Altered regional loading patterns on articular cartilage following meniscectomy are not fully restored by autograft meniscal transplantation. Osteoarthr Cartil. Elsevier Ltd; 2015;23: 462–468.

138. Lenhart RL, Smith CR, Vignos MF, Kaiser J, Heiderscheit BC, Thelen DG. Influence of Step Rate and Quadriceps Load Distribution on Patellofemoral Cartilage Contact Pressures during Running. J Biomech. Elsevier; 2015;48: 2871–2878.

139. Thoma LM, McNally MP, Chaudhari AM, Flanigan DC, Best TM, Siston RA, et al. Muscle co-contraction during gait in individuals with articular cartilage defects in the knee. Gait Posture. 2016;48: 68–73.

140. Lenhart RL, Kaiser J, Smith CR, Thelen DG. Prediction and Validation of Load-Dependent Behavior of the Tibiofemoral and Patellofemoral Joints During Movement. Ann Biomed Eng. 2015;43: 2675–2685.

141. Fregly BJ, Besier TF, Lloyd DG, Delp SL, Banks S a, Pandy MG, et al. Grand challenge competition to predict in vivo knee loads. J Orthop Res. 2012;30: 503–13.

142. Smith CR, Vignos MF, Lenhart RL, Kaiser J, Thelen DG. The Influence of Component Alignment and Ligament Properties on Tibiofemoral Contact Forces in Total Knee Replacement. J Biomech Eng. 2016;138: 1–10.

143. Varadarajan KM, Moynihan AL, D'Lima D, Colwell CW, Li G. In vivo contact kinematics and contact forces of the knee after total knee arthroplasty during dynamic weight-bearing activities. J Biomech. 2008;41: 2159–2168.

144. D'Lima DD, Steklov N, Fregly BJ, Banks S a., Colwell CW. In vivo contact stresses during activities of daily living after knee arthroplasty. J Orthop Res. 2008;26: 1549–1555.

145. D'Lima DD, Patil S, Steklov N, Slamin JE, Colwell CW. Tibial forces measured in vivo after total knee arthroplasty. J Arthroplasty. 2006;21: 255–262.

146. D'Lima DD, Fregly BJ, Patil S, Steklov N, Colwell CW. Knee joint forces: prediction, measurement, and significance. Proc Inst Mech Eng H. 2012;226: 95–102.

147. Taylor SJG, Walker PS, Perry JS, Cannon SR, Woledge R. The forces in the distal femur and the knee during walking and other activities measured by telemetry. J Arthroplasty. 1998;13: 428–435.

148. Taylor SJG, Walker PS. Forces and moments telemetered from two distal femoral replacements during various activities. J Biomech. 2001;34: 839–848.

149. Zhao D, Banks SA, Lima DDD, Jr CWC, Fregly BJ. In Vivo Medial and Lateral Tibial Loads during Dynamic and High Flexion Activities. J Orthop Res. 2007; 593–602.

150. Kutzner I, Heinlein B, Graichen F, Bender a., Rohlmann a., Halder a., et al. Loading of the knee joint during activities of daily living measured in vivo in five subjects. J Biomech. Elsevier; 2010;43: 2164–2173.

151. Heinlein B, Kutzner I, Graichen F, Bender A, Rohlmann A, Halder AM, et al. ESB clinical biomechanics award 2008: Complete data of total knee replacement loading for level walking and stair climbing measured in vivo with a follow-up of 6-10 months. Clin Biomech. Elsevier Ltd; 2009;24: 315–326.

152. Bergmann G, Bender A, Dymke J, Duda G, Damm P. Standardized loads acting in hip implants. PLoS One. 2016;11.

153. Stylianou AP, Guess TM, Kia M. Multibody Muscle Driven Model of an Instrumented Prosthetic Knee During Squat and Toe Rise Motions. J Biomech Eng. 2013;135: 41008.

154. Mündermann A, Dyrby CO, D'Lima DD, Colwell CW, Andriacchi TP. In vivo knee loading characteristics during activities of daily living as measured by an instrumented total knee replacement. J Orthop Res. 2008;26: 1167–1172.

155. Andriacchi TP, Koo S, Scanlan SF. Gait Mechanics Influence Healthy Cartilage Morphology and Osteoarthritis of the Knee. J Bone Jt Surg. 2009;91: 95–101.

156. Favre J, Scanlan SF, Erhart-Hledik JC, Blazek K, Andriacchi TP. Patterns of femoral cartilage thickness are different in asymptomatic and osteoarthritic knees and can be used to detect disease-related differences between samples. J Biomech Eng. 2013;135: 101002–10.

157. Fujisawa T, Hattori T, Takahashi K, Kuboki T, Yamashita A, Takigawa M. Cyclic Mechanical Stress Induces Extracellular Matrix Degradation in Cultured Chondrocytes via Gene Expression of Matrix Metalloproteinases and Interleukin-11. J Biochem. 1999;975: 966–975.

158. Thelen DG, Won Choi K, Schmitz AM. Co-simulation of neuromuscular dynamics and knee mechanics during human walking. J Biomech Eng. 2014;136: 21033.

159. Winby CR, Lloyd DG, Besier TF, Kirk TB. Muscle and external load contribution to knee joint contact loads during normal gait. J Biomech. Elsevier; 2009;42: 2294–300.

160. Flanigan DC, Harris JD, Trinh TQ, Siston RA, Brophy RH. Prevalence of chondral defects in Athletes' Knees: A systematic review. Med Sci Sports Exerc. 2010;42: 1795–1801.

161. Arøen A, Løken S, Heir S, Alvik E, Ekeland A, Granlund OG EL. Articular Cartilage Lesions in 993 Consecutive Knee Arthroscopies. Am J Sports Med. 2004;32: 211–215.

162. Stefanik JJ, Guermazi A, Roemer FW, Peat G, Niu J, Segal NA, et al. Changes in patellofemoral and tibiofemoral joint cartilage damage and bone marrow lesions over 7 years: The Multicenter Osteoarthritis Study. Osteoarthr Cartil. Elsevier Ltd; 2016;24: 1160–1166.

163. Kvist J, Gillquist J. Sagittal plane knee translation and electromyographic activity during closed and open kinetic chain exercises in anterior cruciate ligament-deficient patients and control subjects. Am J Sports Med. 2001;29: 72–82.

164. Norouzi S, Esfandiarpour F, Shakourirad A, Salehi R, Akbar M, Farahmand F. Rehabilitation after ACL injury: A fluoroscopic study on the effects of type of exercise on the knee sagittal plane arthrokinematics. Biomed Res Int. 2013;2013.

Chapter 9

Dankwoord

Dit was het dan...

Het einde van mijn doctoraatsthesis. Je zou me nu een schouderklopje kunnen geven en zeggen: "*Goed gedaan Sam!*". Maar dit is niet het werk van mij alleen. Integendeel, dit werk is het resultaat van een samenwerking tussen verschillende personen, waarbij iedereen zijn of haar schouderklopje verdient. Daarom zou ik graag een woord van dank richten aan zij die de afgelopen jaren mijn werk van dichtbij en minder dichtbij gevolgd hebben.

Als eerste zou ik graag mijn promotor, Ilse, willen bedanken. Zonder jou zou het aantal pagina's in dit werk sterk gereduceerd geweest zijn. Een welgemeende dankuwel om mij deze kans te geven, mijn werk zo vaak en grondig na te willen lezen (zelfs in de late avonduren of in het weekend), de juiste feedback te geven, om mijn werk steeds naar een hoger niveau te willen tillen, maar ook om steun te geven tijdens de moeilijkere momenten. Dieter bedankt om mij als niet-kinesist toch mee dit project toe te vertrouwen en voor je klinische invalshoek. Benedicte, bedankt voor je kritische blik en feedback op mijn werk en voor het vertrouwen om mij de leuke klusjes in de MALL te laten opknappen. Verder wil ik graag mijn juryleden, Frank Luyten, Wim Dankaerts en Geert Vanderschueren bedanken voor de constructieve feedback doorheen de afgelopen vier jaar. Jullie bijkomende inzichten hebben zeker en vast voor een verhoging van het niveau gezorgd en mee inzichten aangebracht vanuit een ander dan het biomechanische perspectief. Thank you Prof. Caroline Stewart for your critical review, it's an honour to receive such a positive feedback from you and for being present today. Bedankt Prof. Werner Helsen om alles de afgelopen jaren in goede banen te leiden.

Ten tweede wil ik graag alle collega's en ex-collega's van de groep bedanken. Bedankt voor de samenwerking, de leuke en sportieve uitstapjes onder de middag, 's avonds en in het weekend, de gezellige koffie- en middagpauzes, hulp als ik weer eens ergens mee vastzat... Zonder jullie waren de afgelopen vier jaren toch helemaal anders geweest! Secondly, I would like to thank all the colleagues from our group for the collaborations, nice and sportive excursions during lunchtime, in the evening or the weekend, social coffee- and lunchbreaks and help. Without you, the past four years would have been totally different! In tussentijd is de groep zo hard gegroeid dat ik niet iedereen persoonlijk kan opnoemen, maar voor enkelen wil ik een uitzondering maken. Friedl, bedankt voor het gezelschap tijdens de lange loopjes, gezellige kookavonden, serieuze en minder serieuze babbels, extra tips om mijn werk te verbeteren en om af en toe eens een luisterend oor te zijn. Maarten, bedankt voor de toffe loopjes onder de middag, eerste-hulp-bij-matlab-problemen en gezellige babbels. Mariska, bedankt om de rol van promotor over te nemen in de periode dat Ilse in het buitenland zat, je extra hulp bij mijn verschillende projectjes en om mij te verdragen als huisgenoot. Ellen, bedankt voor de toffe momenten en de "lange" fietsritjes naar Rotselaar.

Thank you, colleagues from the Italian Office in which I had the chance to stay the last 1.5 year of my PhD, unfortunately my Italian language skills did not improve much. Thank you Marco for the discussions about graphical issues and the supporting words. Bedankt overbuur Koen voor de babbels en voor de tips. Furthermore, I would like to thank some people from outside our University with who I had the chance to collaborate with. Thank you, Colin, Darryl, Nidal, Cathy, Kate, Robert and Phil. Bedankt Albert om te helpen bij het ontwerpen van mijn kaft. Bedankt aan de zwemmers van baan vier en vijf. De samenstelling is in de afgelopen jaren wat veranderd, maar dankzij jullie waren de zwemtrainingen, of beter gezegd de pauzes tijdens het zwemmen toch nog extra leuk.

Ook wil ik alle mannen en vrouwen van "*Van Overal Wa*" bedanken voor de toffe avonden, interessante gesprekken, leuke weekendjes, sportieve uitstapjes, véél te véél eten en nog zo veel meer! Als je er zo eens over moet nadenken dan besef je pas wat een toffe en geweldige vriendengroep we zijn. Nu ik mijn doctoraat heb afgerond, kan ik ontspannen uitkijken naar al jullie komende verdedigingen. Bedankt Steven voor de stapels wentelteefjes. Vervolgens wil ik mijn trampolineploegje bedanken en ineens al de rest van Wild Gym. Ondanks de vele uren werk blijft het een toffe, lichtjes uit de hand gelopen hobby. Mijn enthousiasme en vreugde als ik iemand iets nieuws heb kunnen leren, is na al die jaren nog steeds niet verminderd. Bedankt aan mijn medetrainster Jante om in mijn laatste periode zoveel trainingen last-minute over te nemen.

Bedankt Bert en Jorine, Inge en Ralf, Myrthe en Hannes om mij – als alweer een Belg – mee in de familie op te nemen. Hopelijk kan ik vanaf nu op de vraag: "*Moet jij weeral zo hard werken?*" negatief antwoorden en wat vaker naar Breda afreizen.

Francine en René, mijn derde oma en opa. Bedankt voor al de gezellige babbels met koffie en taart, voor alle interesse in mij als persoon en in mijn werk.

Oma Tollembeek, Oma en Opa Torhout, sorry dat ik jullie het afgelopen jaar wat minder heb gezien, maar bedankt om toch altijd interesse in mij en in mijn doctoraat te blijven tonen, de bezorgdheid of ik wel genoeg eten had en genoeg sliep. Nonkel Lode en Tante Nathalie, ondanks dat onze drukke agenda's niet altijd goed matchen, waardeer ik de momenten samen en is het fijn om met jullie bij te kunnen babbelen. "*Les amis de la dragée*" bedankt voor de toffe familiefeesten en vanaf nu hoop ik terug mee te kunnen gaan skiën en wat vaker langs de winkel te passeren voor een lekkere pannenkoek!

Tom en Ine, ondanks dat ik jullie oudere broer ben, kan ik altijd bij jullie terecht. Bedankt voor de goeie raad en voor de gezellige momenten als familie samen. Nu ik niet meer thuis woon waardeer ik de momenten met ons vijven of zevenen des te meer. Tom en Lisa, ik hoop dat we nog vaak samen fietstochtjes kunnen maken en leuke dingen zullen ondernemen. Ine, als grote broer heb ik je vaak geholpen bij het studeren en ben nu dan ook super fier om te zien wat voor verpleegster jij aan het worden bent. Weet dat je hier altijd welkom bent om met ons mee te eten. Ik ben oprecht blij dat jullie mijn broer en zus zijn.

Mama en Papa, bedankt om altijd voor mij klaar te staan, mij advies te geven, te steunen in de keuzes die ik maak en om altijd fier te zijn op alles wat ik doe, ook al is het maar iets kleins.

Esther, bedankt om met mij te dromen over mooie reizen, over sportieve uitdagingen en over alles wat de toekomst ons samen nog gaat brengen...

Chapter 10

Appendices

Bijstellingen

Nederlands

- Studies die het effect van specifieke interventies op lange termijn onderzoeken, worden bemoeilijkt door de onzekere duurtijd van doctoraatsfinanciering en het gebrek aan lange termijn financiering binnen het huidige academische milieu.
- Sport en beweging tijdens het werk moet gestimuleerd worden, niet alleen om de negatieve gevolgen van lang stilzitten tegen te gaan, maar evengoed om de productiviteit en het mentale welbevinden te verbeteren.
- Alhoewel er steeds meer wetenschappelijke inzichten rond efficiënt trainen beschikbaar zijn, blijven trainers nog te vaak methodes gebruiken zonder te weten wat de (lange termijn) impact op het lichaam van de atleet is.

English

- Studies that investigate the long-term effect of a certain intervention, are hindered by the uncertain financing duration of PhD-projects and the lack of long-term financing.
- physical activity at work should be promoted, not only to compensate for the sedentary-activity during the day, but also to increase productivity and mental well-being.
- Despite the fact that more insights in evidence-based training are available, trainers keep using training methods without knowing the (long-term) impact on the body of the athlete.

Professional career Sam Van Rossom

Sam Van Rossom was born on March 28^{th}, 1991 in Leuven, Belgium. Sam completed his bachelor's degree *Lichamelijke opvoeding en bewegingswetenschappen* at the KU Leuven in 2012 and his master's degree *Lichamelijke opvoeding en bewegingswetenschappen* at the KU Leuven in 2013. Since 2013 he has been working as a doctoral student affiliated with the human movement biomechanics research group (Department of Kinesiology) at the KU Leuven. This PhD thesis was part of a larger project, title *"Optimalisatie van kraakbeenregeneratie in het tibio-femorale gewricht: de rol van lokale kraakbeenbelasting"*.

Sam also taught the practical sessions on Anatomy to the first year undergraduate students of rehabilitation sciences. Furthermore, Sam coached several master students in rehabilitation sciences during their masterthesis.

List of publications

Articles in internationally reviewed academic journals

1. **Van Rossom, S.,** Smith, C.R., Thelen, D.G., Vanwanseele, B., Van Assche, D., Jonkers, I.(2017) Knee joint loading in healthy adults during functional exercises: implications for rehabilitation guidelines. *Journal of Orthopaedic and Sports Physical Therapy*, accepted for publication.
2. **Van Rossom, S.**, Smith C., Zevenbergen L., Thelen D., Vanwanseele B., Van Assche D., Jonkers I. (2017). Knee Cartilage Thickness, $T1\rho$ and T2 Relaxation Time Are Related to Articular Cartilage Loading in Healthy Adults. *PLoS One*, 12 (1)
3. **Van Rossom, S.,** Wesseling, M., Van Assche, D., Jonkers, I. Topographical variation of human femoral articular cartilage thickness, T1rho and T2 relaxation time is related to local loading during walking. *Cartilage*, in review
4. **Van Rossom, S.,** Wesseling, M., Smith, C.R., Thelen, D.G., Vanwanseele, B., Van Assche, D., Jonkers, I.(2017) The influence of knee joint geometry and alignment on the tibiofemoral load distribution: a computational study. *Journal of Orthopaedic Research*, in review
5. **Van Rossom, S.**, Khatib, N., Van Asssche, D., Holt, C., Jonkers, I. (2017) Medial and lateral tibiofemoral articular cartilage defects do not alter compartmental loading during walking. *Osteoarthritis and Cartilage*, in review
6. Giarmatzis G., Jonkers I., Wesseling M., **Van Rossom S.**, Verschueren S. (2015). Loading of hip measured by hip contact forces at different speeds of walking and running. *Journal of Bone and Mineral Research*, 30 (8), 1431-1440.
7. Falisse A, **Van Rossom S**, Jonkers I, De Groote F. EMG-driven optimal estimation of subject-specific Hill model muscle-tendon parameters of the knee joint actuators. *IEEE Trans Biomed Eng.* 2016;9294: 1–1.
8. Ferreira Meireles S., De Groote F., **Van Rossom S.**, Verschueren S., Jonkers I. (2017). Differences in knee adduction moment between healthy subjects and patients with osteoarthritis depend on the knee axis definition. *Gait & Posture*, 53, 104-109.

9. Dockx, K., Bekkers, E., Devan, S., **Van Rossom, S.**, Huybrechs, D., Verschueren, S., Mirelman, A., Nieuwboer, A. (2017) Recovering from a perturbation: impact of dual tasking in people with mild cognitive impairment. *Gait & Posture*, in review

10. Falisse, A., **Van Rossom, S.**, Gijsbers, J., Steenbrink, F., van Basten, B. J.H., Jonkers, I., van den Bogert A.J., De Groote,F. OpenSim versus Human Body Model: a comparison study for the lower limbs during gait. *Journal of Applied Biomechanics*, in review

11. Bekkers, E.,Dockx, K., Devan, S., **Van Rossom, S.,** Verschueren, S., Bloem, B., Nieuwboer, A. (2017) People with Parkinson's disease and freezing of gait have reduced postural control during dual-tasking. *neurorehabilitation and Neural Repair*, in review

Meeting abstracts, presented at international scientific conferences and symposia, published or not published in proceedings or journals

1. **Van Rossom, S.**, Bosmans, L., Van Campen, A., De Groote, F., De Schutter, J., Jonkers, I. (2014). Effect of Subject-Specific Musculoskeletal Modelling on Kinematics and Dynamics of Jumping in Power Athletes. ESMAC. Rome, 29 September 2014 - 4 Oktober 2014.

2. Giarmatzis, G., Jonkers, I., Wesseling, M., **Van Rossom, S.**, Verschueren, S. (2015). Loading of Hip Measured by Hip Contact Forces at Different Speeds of Walking and Running. International Society of Biomechanics. Glasgow, 12-16 July 2015, Abstract No. ISB 2015-956.

3. **Van Rossom, S.**, Zevenbergen, L., Vanwanseele, B., Van Assche, D., Jonkers, I. (2015). Gait Adaptations Relate to Cartilage Lesion Locations in the Tibiofemoral Joint- Preliminary Results. ICRS World Congress. Chicago, 8 - 11 May 2015.

4. Motte dit Falisse, A., **Van Rossom, S.**, Jonkers, I., De Groote, F. (2015). Estimation of subject-specific muscle-tendon parameters based on dynamic motions using EMG-driven musculoskeletal model and optimal control approach. International Symposium on Computer Simulation in Biomechanics. Edinburgh, 9-11 July 2015.

5. **Van Rossom, S.**, Zevenbergen, L., Smith, C., Thelen, D., Van Assche, D., Vanwanseele, B., Jonkers, I. (2016). Tibiofemoral joint loading during therapeutic exercises and activities of daily living: implications for rehabilitation in OA and cartilage repair surgery. OARSI 2016 World Congress. Amsterdam, March 31 - April 3 2016.

6. **Van Rossom, S.**, Zevenbergen, L., Smith, C., Thelen, D., Van Assche, D., Vanwanseele, B., Jonkers, I. (2016). Cartilage volume and thickness but not biochemical properties relate to joint loading during gait in healthy controls. OARSI 2016 World Congress. Amsterdam, March 31 - April 3 2016.

7. Bruijnes, A., De Groote, F., Afschrift, M., **Van Rossom, S.**, Jonkers, I. (2016) Age-related differences in ADL activity execution. ESMAC. Sevilla, September 26 – October 1 2016.

8. **Van Rossom, S.**, Zevenbergen, L., Smith, C., Thelen, D., Van Assche, D., Vanwanseele, B., Jonkers, I. (2016) Gait adaptations following medial condyle cartilage lesions reduce condyle loading – Preliminary results. ICRS World Congress. Sorrento, September 23 – 27 2016.

9. **Van Rossom, S.**, Khatib, N., Van Assche, D., Holt, C., Jonkers, I. 2017 Medial and lateral tibiofemoral articular cartilage defects do not alter compartmental contact forces and pressures during walking. EORS, Munich, September 13 - 15 2017.

Author affiliations

Corresponding author

Sam Van Rossom
KU Leuven, Department of Kinesiology, Human Movement Biomechanics
Tervuursevest 101 box 1501, B-3001, Leuven, Belgium

Co-authors

Antoine Falisse
KU Leuven, Department of Kinesiology, Human Movement Biomechanics
Tervuursevest 101 box 1501, B-3001, Leuven, Belgium

Benedicte Vanwanseele
KU Leuven, Department of Kinesiology, Human Movement Biomechanics
Tervuursevest 101 box 1501, B-3001, Leuven, Belgium

Ilse Jonkers
KU Leuven, Department of Kinesiology, Human Movement Biomechanics
Tervuursevest 101 box 1501, B-3001, Leuven, Belgium

Lianne W. Zevenbergen
KU Leuven, Department of Kinesiology, Human Movement Biomechanics
Tervuursevest 101 box 1501, B-3001, Leuven, Belgium

Mariska Wesseling
KU Leuven, Department of Kinesiology, Human Movement Biomechanics
Tervuursevest 101 box 1501, B-3001, Leuven, Belgium

Susana F. Meireles
KU Leuven, Department of Kinesiology, Human Movement Biomechanics
Tervuursevest 101 box 1501, B-3001, Leuven, Belgium

Dieter Van Assche
KU Leuven, Department of Rehabilitation Sciences, Musculoskeletal Rehabilitation
Tervuursevest 101 box 1501, B-3001, Leuven, Belgium

Georgios Giarmatzis
KU Leuven, Department of Rehabilitation Sciences, Musculoskeletal Rehabilitation
Tervuursevest 101 box 1501, B-3001, Leuven, Belgium

Sabine Verschueren
KU Leuven, Department of Rehabilitation Sciences, Musculoskeletal Rehabilitation
Tervuursevest 101 box 1501, B-3001, Leuven, Belgium

Colin R. Smith
University of Wisconsin-Madison, Department of mechanical engineering
Mechanical Engineering Building, 1513 University Avenue ,Madison, WI 53706, United States

Darryl G. Thelen
University of Wisconsin-Madison, Department of mechanical engineering
University of Wisconsin-Madison, Department of biomedical engineering
University of Wisconsin-Madison, Department of orthopedics and rehabilitation
Mechanical Engineering Building, 1513 University Avenue ,Madison, WI 53706, United States

Nidal Khatib
Caridf University, Musculoskeletal Biomechanics Research Centre
W/2.45, Queen's Buildings - West Building, 5 The Parade, Newport Road, Cardiff, CF24, United Kingdom

Cathy Holt
Caridf University, Musculoskeletal Biomechanics Research Centre
W/2.45, Queen's Buildings - West Building, 5 The Parade, Newport Road, Cardiff, CF24, United Kingdom

Johannes Gijsbers
Motekforce Link B.V.
Hogehilweg 18C, 1101 CD Amsterdam-Zuidoost, The Netherlands

Frans Steenbrink
Motekforce Link B.V.
Hogehilweg 18C, 1101 CD Amsterdam-Zuidoost, The Netherlands

Ben J.H. Van Basten
Motekforce Link B.V.
Hogehilweg 18C, 1101 CD Amsterdam-Zuidoost, The Netherlands

Antonie J. van den Bogert
Cleveland State University, Department of Mechanical Engineering
H1960 E 24th St, Cleveland, OH 44115, United States

Alice Nieuwboer
KU Leuven, Department of Rehabilitation Sciences, Neuromotor Rehabilitation
Tervuursevest 101 box 1501, B-3001, Leuven, Belgium

Esther Bekkers
KU Leuven, Department of Rehabilitation Sciences, Neuromotor Rehabilitation
Tervuursevest 101 box 1501, B-3001, Leuven, Belgium

Kim Dockx
KU Leuven, Department of Rehabilitation Sciences, Neuromotor Rehabilitation
Tervuursevest 101 box 1501, B-3001, Leuven, Belgium

Surendar Devan
KU Leuven, Department of Rehabilitation Sciences, Neuromotor Rehabilitation
Tervuursevest 101 box 1501, B-3001, Leuven, Belgium

Daan Huybrechs
KU Leuven, Department Computerwetenschappen, Subdivisie Numerieke Analyse en Toegepaste Wiskunde
Celestijnenlaan 200a box2402, B-3001, Leuven, Belgium

Anat Mirelman
Tel Aviv University,4 Department of Neurology, Center for the Study of Movement Cognition and Mobility
13 Henrietta Szold Street, Rehabilitation Building, Tel Aviv, Israel

Bastiaan R Bloem
Radboud University Medical Center, Department of Neurology, Donders Institute for Brain, Cognition & Behaviour
Reinier Postlaan 4, 6525 GC Nijmegen, The Netherlands

List of figures

List of tables

List of abbreviations

ACL	Anterior cruciate ligament
ADL	Activities of daily life
AscSt	Stair ascent
BMI	Body mass index
BW	Bodyweight
COMAK	Concurrent optimization of muscle forces and kinematics algorithm
CF	Contact force
CKC	Closed kinetic chain
DesSt	Stair descent
DoF	Degrees of freedom
FLunge	Forward lunge
FP	First peak
GAG	Glycosaminoglycan
IC	Initial contact
KAM	Knee adduction moment
KCF	Knee contact force
KOOS	Knee osteoarthritis outcome score
LCL	Lateral collateral ligament
MACI	Matrix-enhanced autologous chondrocyte implantation
MCL	Medial collateral ligament
MS	Midstance
OA	Osteoarthritis
OKC	Open kinetic chain
PCL	Posterior cruciate ligament
PF	Patellofemoral
QDL	Quality of life
RMS	Root-mean-square
RoM	Range of motion
SD	Standard deviation
SitD	Sit down
SLH	Single leg hop
SLunge	Sideward lunge
SP	Second peak
Sq	Squat
StUp	Stand up
TF	Tibiofemoral
TO	Toe-off